Cranfield University

Eudoxios Theodoridis

DESIGN AND INVESTIGATION OF A DIESEL ENGINE OPERATED ON PILOT IGNITED LPG

School of Engineering

PhD Thesis

Cranfield University

School of Engineering

PhD Thesis

Academic year 2008-2009

Eudoxios Theodoridis

Design and investigation of a diesel engine operated on pilot ignited LPG

Supervisor: Professor M.F. Harrison

March 2009

This thesis is submitted in partial fulfilment of the requirements for the degree of Doctor in Philosophy

ABSTRACT

This thesis explores the idea of igniting LPG in a compression ignition diesel engine using pilot diesel injection as spark ignition medium. The main advancement in using this technology on current diesel engines is the establishment of a better balance between NOx and PM emissions without losing too much of the CO_2 benefits of diesel.

With the advent of common rail diesel engines, it is now possible to get control of pilot diesel injection and make the LPG and diesel control systems work together.

Combined diesel and LPG operation is a new subject for engine research, so the thesis moves on to consider the results from detailed engine simulation studies that explore the potential benefits of the mix. Subsequent simulations of a modern four cylinder dCi engine suggest that with closer control over the pilot diesel injection, diesel like performance can be obtained, hopefully with less emissions than currently expected from diesel only operation.

A single cylinder variable compression ratio research engine was developed to explore diesel /LPG dual fuel operation. A second generation common rail injection rig was also developed for the engine and for fuel spray characterisation.

Engine experiments proved the concept of using a modest charge of pilot injected diesel for igniting a larger dose of port injected LPG. The experimental work results suggest that combining diesel common rail injection technology with the state of the art LPG injection systems, it is possible to establish a better balance between NOx/ PM emissions without losing too much of the CO_2 benefits from the diesel operation.

ACKNOWLEDGEMENTS

I would like to take this opportunity to thank my supervisor Professor Matthew Harrison for his help, support, tolerance that enabled this research to be carried out. Thank you for making it possible.

Many thanks to all those who helped with this research. In particular thanks to:

Anthony Lawrence for his help and advice on the IDEAS NX software

Tim Lee for making the various components for the E7 engine

Dr Glenn Sherwood for his help with the Shadowgraph measurements

Professor Nick Vaughan and Professor Doug Greenhalgh for supervising the submission of this thesis

Alan Hutchings, Clive Wood, Dave Whittington, Derek Brown, George Lipinski, and all other staff of the DMG Cranfield workshop, for their help and advice

Jaye Engineering Ltd of Ravenstone for the CNC machining of the cylinder head

My fellow PhD candidates for valuable friendship during these years

All others I have not mentioned who helped with this research

Finally I would like to thank my family for their support throughout the years.

CONTENTS

LIST OF FIGURES

LIST OF TABLES

NOMENCLATURE

3D	Three dimensional
AFR	Air fuel ratio
B	Bore
BAT	Battery
BDC	Bottom dead centre
BMEP	Break mean effective power
BNC	Bayonet Neil Concelman
BSFC	Break specific fuel consumption
C	Gain
CA	Crank angle
CAE	Computer aided engineering
CCD	Charge coupled device
C_f	Temperature correction factor
CFD	Computational fluid dynamics
CI	Compression ignition
CNC	Computer numerical controlled
CNG	Compressed natural gas
CO	Carbon monoxide
CO_2	Carbon dioxide
COV	Coefficient of variation
d	Inlet throat diameter
DAQ	Data acquisition
deg	Degrees
DI	Dierct injection

DVM	Digital voltmeter
E	Charge amplifier voltage
E_b	Bias voltage with zero pressure
ECM	Electronic control module
ECU	Electronic control unit
EFI	Electronic fuel injection
EGR	Exhaust gas recirculation
EVO	Exhaust valve open
GDI	Gasoline direct injection
h	Hour
HC	Hydrocarbons
HCCI	Homogeneous compression ignition
IBDC	Inlet bottom dead centre
IDI	Indirect diesel injection
IMEP	Indicated mean effective pressure
ISFC	Indicated specific fuel consumption
IVO	Inlet valve open
K	Kelvin
KW	Kilowatt
L	Engine stroke
LDV	Laser Doppler velocimetry
LPG	Liquefied petroleum gas
MAP	Manifold absolute pressure
mfb	Mass fraction burned
ms	Millisecond
N	Crankshaft speed

NO	Nitrogen monoxide
NO_x	Nitrogen oxide
p_{air}	Specific gravity of air [kg/m^3]
PC	Personal computer
pC	PicoCoulomb
PDPA	Phase Doppler particle analysis
p_f	Fluid pressure [Nm^2]
PIV	Particle image velocimetry
PM	Particulate mater
P_{Nom}	Maximum rated pressure [bar]
ppm	Parts per million
P_r	Power required [W]
ROHR	Rate of heat release
RPM	Revolutions per minute
R_s	Swirl ratio
s	Seconds
SI	Spark ignition
SOC	Start of combustion
SOI	Start of injection
stoich	Stoiciometric
SUV	Sports utility vehicle
TDC	Top dead centre
TTL	Transistor-transistor logic
U_A	Output voltage
U_v	Supply voltage
UV	Ultraviolet

V	Volt
V	Volume
v_g	Mean inlet velocity
X_b	Mass fraction burned
Z	mach index
$\dot{m}_f =$	Fuel mass flow [Kgs^{-1}]
$\dot{m} =$	Air mass flow [Kgs^{-1}]
$n_p =$	Pump speed [rpm]
P_b	Atmospheric pressure measured by a laboratory barometer [mbar]
$\rho_f =$	Fuel density [Kgl^{-1}] for gas oil [$\rho_f = 0.840$]
ρ_{stp}	Air density at standard temperature and pressure, 1.293 [kg/m^3]
P_{stp}	Pressure at standard conditions, 1013.25 [mbar]
T_{stp}	Temperature at standard conditions, 273.15° [K]
T	Inlet temperature [K]
$V_f =$	Fuel volume per pump revolution [ℓ]
m	Wiebe parameter m
α	Wiebe parameter a
γ	Ratio of specific heats
η_f	Fuel conversion efficiency
η_p	Pump efficiency [%]
η_v	Volumetric eficinecy
θ	Crank angle
θ_o	Crank angle
λ	Excess air

μs	Microsecond
π	Pi
φ	Equivalence ratio
ω	Angular velocity

1 INTRODUCTION

1.1 Aims and objectives

This thesis describes the development of a method to operate current common rail diesel engines to run on a unique combination of fuels. The aim of this work is to find a new PM-NOx emissions balance mechanism without losing too much of the CO_2 benefit of diesel in order to establish a bridging technology between Euro emission standards and the Kyoto agreement. This will be achieved by pursuing the following objectives:

- To understand a combined diffusion (diesel) and premixed (propane) flame under high compression ratio.
- To perform accurate cylinder pressure measurements and heat release calculations on a running engine.
- To design and develop new technologies for the dCi diesel and liquid propane injection systems.

1.2 New work contained in this Thesis

The major novelty and the outcome of this thesis is the demonstration of an efficient engine operating on a unique combination of high pressure diesel and liquid phase propane that is highly controllable. This has required the design and the development of a fairly complex single cylinder engine, the development of a high pressure fuel injection rig and the use of a state of art LPG liquid injection system.

The important element in the experimental work is performing accurate indicating measurements on a single cylinder dual fuel variable compression ratio engine which combines the latest developments of the two worlds, CI and SI in a unique way.

1.3 IC engines and emissions legislation

Internal combustion engines are significant contributors to air pollution which has side effects on human health, on the environment and is believed to cause global climate changes. Over the last three decades, environmental concerns have led governments to establish policies in order to control the emission levels from passenger vehicles. As a result national environmental organisations have setup emission control standards. Today the European Community (EC) and the US Environmental Protection Agency (EPA) have the responsibility to pioneer and control standards that specify emission levels for all kinds of vehicles. The emission standards prescribe emission levels for the

pollutant emissions of carbon monoxide (CO), unburned hydrocarbons (HC), oxides of nitrogen (NOx) and particulates (PM).

As the number of vehicles increases, it is expected that there will be a greater increase in the emission levels, not only because of the number of vehicles but also because of a demand for more power. This is caused by a growth in vehicle size in order to accommodate the additional on-board equipment and also by the ready adoption of seven-seater and sports utility vehicles (SUV) as everyday family transport.

Environmental organisations, taking into account projected future pollution levels, revise their standards accordingly in order to keep these levels under control. As a result the continuous change in the emission control standards leads vehicle manufacturers to find new methods of reducing tailpipe emissions from new passenger cars whilst meeting customer demands.

1.4 CO_2

Passenger cars not only emit pollutant emissions but also carbon dioxide (CO_2). Although CO_2 is not directly harmful to human health when in modest quantities, it is the most significant of the greenhouse gases contributing to climate change. The concentration of CO_2 in the atmosphere is higher near urban areas often exceeding acceptable levels.

Surprisingly there are no prescribed specifications for CO_2 emissions in the European emission standards or in the US standards either. The reason is because vehicle CO_2 emissions are mainly controlled by means of fuel consumption /economy targets. If one considers that the catalytic converter converts CO and HC into CO_2 and also the fact that engine operating conditions for minimising pollutant emissions are not the conditions for minimum brake specific fuel consumption, it becomes apparent that the CO_2 emissions can only be regulated by reducing the fuel consumption.

In fact compared to improvements in controlling pollutants, there has been less progress on reducing CO_2 from passenger vehicles. Until recently the average fuel consumption of new cars was similar to that of the mid 1980's (vcacarfueldata, 2003). This happened because while engines became more efficient over this period, the average vehicle mass increased due to the additional features such as power assisted steering and climate control combined with the demand for higher performance. However, there are signs that in the last few years average fuel consumption has begun to drop due to voluntary agreements by vehicle manufacturers in order to reduce CO_2 emissions.

The first driver for CO_2 reduction was the Kyoto Protocol signed in December 1997 by all developed countries to binding targets for greenhouse gas emissions in response to warnings over global climate changes. The result of this was an agreement between the EC and the European Automobile Manufacturers Association in July 1998 that

committed the European car industry to reduce CO_2 emissions from the new passenger cars by over 25% to an average CO_2 emission figure of 140 g/km by 2008 (vcacarfueldata, 2003). This led manufactures to seek new technologies to make new vehicles more fuel efficient in order to satisfy both customer demands for better performance and also obligations to comply with the emission control standards.

From an environmental point of view the use of different fuels has both advantages and disadvantages. Diesel vehicles cause significantly less CO_2 emissions compared to the gasoline vehicles because the diesel engine has greater efficiency in the fuel utilisation. In addition diesel vehicles emit smaller amounts of HC and CO than the equivalent gasoline vehicles. However diesel engines emit greater levels of PM and NOx compared with the new technology gasoline engines.

Both PM and NOx are harmful to health and their control is frequently taken as being mutually exclusive: operating with very lean air fuel mixtures reduces PM but increases NOx whereas operating with a rich mixture has the opposite effect.

One development of note is the rapid growth in the adoption of diesel powered passenger cars in Europe. Ricardo already predicted in 2002 that by 2005, 50% of the passenger car fleet in the UK will be diesel powered (Ricardo, 2002). However, any initiatives aimed at reducing fleet CO_2 levels must be applicable equally to diesel cars and gasoline powered cars if they are to be successful. Such initiatives should also, whenever are practicable, strike a better balance between PM and NOx than is achieved with current diesel engines.

1.5 The need for a better balance

Recently there has been considerable research on dual fuel engines. It is true that diesel engine is one of the most efficient but its major drawback is the high NOx and PM emission levels. On the other hand gaseous fuels such as LPG or CNG in converted gasoline engines have shown significantly better pollutant emissions performance than diesel but higher CO_2 levels. Considering this the following hypothesis was made:

If an alternative fuel is mixed with diesel in a dual fuel engine then perhaps it is possible to establish a better NOx / PM balance mechanism without losing too much of the CO_2 benefits from diesel operation.

Clearly the potential of running diesel engines on dual fuel will play a significant role in the future of engine technology.

This thesis suggests that **with**:

- diesel powered cars constituting 50% or more of the passenger car fleet,

- generally favourable pollutant emissions from the best of the current diesel engines, coupled with relatively favourable CO_2 emissions,

but also with:

- unacceptably high PM and NOx emissions from current diesel engines,
- a pressing need to reduce CO_2 emission levels from the passenger car fleet, but a limit on how much of the fleet can be diesel powered before diesel fuel production saturates,
- no breakthrough technologies anticipated for diesel engines of the future,

a mechanism needs to be found to operate more of the passenger car fleet on diesel type engines (that have favourable pollutant and CO_2 emissions but don't require diesel fuel) whilst reducing PM and NOx emissions.

A mix of diesel and LPG is more favourable as the onboard storage of LPG is less problematic than with CNG and because the LPG retail network is well-developed throughout Europe.

The proposal put forward in this thesis is to investigate the conversion of existing common rail direct injection diesel engines to run on a mix of diesel and LPG. The strategy is simple: to override some inputs to the dCi engine ECM unit to simulate an idle condition (so that less than 2 mg of diesel will be injected to each cylinder per cycle) and to use this pilot injection of diesel as a source of ignition for a much larger charge of LPG. This approach has been described elsewhere as "liquid spark plug".

1.6 Synopsis

Chapter two opens with a review of the current technologies for gasoline, diesel and alternative fuel engines. This discussion reveals the need for a viable means of converting diesel engines to operate on a combination of diesel fuel and LPG (liquid petroleum gas or 'Autogas': being a mix of propane and butane). This need arises from the growing diesel-powered passenger fleet in Europe (and hence the need to convert diesel engines to alternative fuel in order to raise the alternative fuel consumption levels to the point at which they become significant) and the relative availability of LPG and an LPG retail infrastructure.

Chapter three contains a preliminary study. Combined diesel and LPG operation is a new subject for engine research, so the thesis moves on to consider the results from detailed engine simulation studies that explore the potential benefits of the mix. Some preliminary experimental evidence showed that the use of a diesel pilot injection to ignite a larger charge of LPG has promise for passenger car use. Preliminary experiments on a single cylinder engine prove the concept of using a modest charge of diesel pilot to ignite a larger dose of port injected LPG. Subsequent simulations of a

modern four cylinder dCi engine suggest that with closer control over the pilot diesel injection, diesel like performance can be obtained, hopefully with less emissions than currently expected from diesel only operation.

Chapter four contains a description of the engine development. The main objective was to develop a single cylinder dual fuel engine which combines the most up-to-date diesel technology with a state of art liquid propane injection systems. This required the design and the manufacture of a new cylinder head for the Ricardo E6 variable compression ratio research engine incorporating features from the most up-to-date diesel engines. A dedicated high pressure common rail injection system was also developed for the engine and for diesel spray characterisation.

Chapter five describes the experimental work which was undertaken to demonstrate diesel and explore dual fuel engine operation. Experimental work was undertaken to explore and demonstrate the diesel/LPG dual fuel engine operation with particular focus given on engine performance, combustion control and NOx emissions. Dual fuel operation was achieved using a small quantity of diesel pilot to ignite a larger amount of port injected LPG.

Engine measurements were initially carried out to demonstrate typical common rail diesel engine operation focusing on three useful aspects concerning future diesel engine development. These aspects include shorter dwell pilot injections, split main injection and split main injection combined with cool EGR.

Subsequently experiments were undertaken to explore and demonstrate the diesel/LPG dual fuel engine operation with particular focus given on engine performance, combustion control and NOx emissions. Dual fuel operation was achieved using a small quantity of diesel pilot to ignite a larger amount of port injected LPG. Liquid propane injection was achieved through an LPG injector installed on the inlet manifold of the engine.

Chapter six includes the final conclusions and suggestions for future work.

2 LITERATURE REVIEW

2.1 The Best Engine technologies for conventional fuels

Vehicle manufacturers and engine developers put great effort in research and development to make new engines more efficient. Conventional compression ignition (CI) and spark ignition (SI) engines have been developed to a point that it is very hard to find space for further improvements. The development of alternative fuel engines however has been less complete.

The availability of conventional fuels and the unstable fiscal frameworks make vehicle manufacturers rather sceptical to invest in developing engines dedicated for alternative fuels. As a result a considerable number of dual fuel conversion systems became available from the aftermarket manufactures to meet the demand. Although the advantages from these conversion systems are considerable, it can be freely admitted that an engine cannot be optimised to run efficiently on both fuels.

Comparing current technologies and considering the developments of fossil fuels one can realise that it is not viable to switch from the conventional fuels or conventional engine technologies to a cleaner energy source effortlessly. On the other hand the forthcoming emission standards regulations call for immediate emission reductions that are very difficult to achieve even with the modern conventional fuel engines. Of course here there is a big dilemma for the manufacturers on whether to stretch more the conventional engines and continue using the well established conventional fuels or whether it is time to make a great step to the alternative technologies which appear attractive but at the same time rather uncertain.

Notwithstanding this, the advantages of alternative fuels, together with the well established conventional engine technology show that the dual fuel engine is a realistic short term solution. The dual fuel engine can provide two main advantages:

- The conventional fuels stay in the market and vehicles meet the emission standards levels for the near future.
- The real advantages of using alternative fuels are tested in the real world but without having the risks raised as if the change was permanent.

Four of the most advanced forms of conventionally fuelled engines are briefly introduced in the sections that follow. These are deemed to be the most likely candidates for conversion to dual fuel as to accomplish the dual objective of lowering both CO_2 and pollutant emissions including PM.

2.1.1 Lean burn gasoline engines

There is no doubt that there will be a demand at least in the near future for gasoline engines. The enabler for this was the development of the lean burn gasoline engines. The aim of the lean burn is to extend the lean limit for stable combustion by aiding fuel mixing. The primary advantages of lean burn are lower throttling losses since more air is admitted for a given amount of fuel and significantly lower adiabatic flame temperature and hence very much reduced thermal NO (Greenhalgh, 2002). There are several lean burn strategies but only few are currently used.

2.1.2 GDI engine

Inspired perhaps by the diesel engine principle some engine manufacturers developed the gasoline direct injection engine with the main target to improve fuel economy and CO_2 emissions from SI engines. The key features of a typical GDI engine are:

- high pressure direct fuel injection. A specifically designed gasoline injector gives the injected fuel a swirl motion to achieve rapid air fuel mixing.
- upright straight intake port geometry. This kind of port is used to direct the airflow down at the curved-top piston, which redirects the airflow into a strong reverse tumble to assist further fuel injection.
- curved piston crown. The shape of the piston crown is optimised to control the shape of the air-fuel mixture as well as the airflow inside the combustion chamber (Mitsubushi, 2003).
- high pressure fuel pump. This pump feeds the injectors with a pressure of 100 bar circa.

although other designs are emerging all the time.

The GDI engine under part load offers a diesel like operating cycle. Basically the air fuel mixture is located exactly in the centre of the combustion chamber surrounded by air. The GDI engine usually has two operating modes. Under partial load works using heterogeneous charge usually known as stratified charge and in full load changes from late injection to early injection cycle so the charge becomes almost homogeneous.

The primary problem of a lean burn engine is that the flame speed is low due to the very lean mixtures. This results in a poor power output with large torque variations.

2.1.3 HCCI Engine

Homogeneous Charge Compression Ignition (HCCI) is a relatively new combustion concept. The operating principle of the HCCI engine is generally based on having a dilute premixed charge that reacts and burns volumetrically throughout the cylinder as it is compressed by the piston (Epping, Aceves, Bechtold, & Dec, 2002). The combustible

is a mixture of fuel, air and combustion products. The ignition is not assisted using a spark but by compression auto-ignition instead so the temperature of the whole charge has to reach the point of auto-ignition before the end of the compression stroke. This can be achieved by using internal or external EGR or by heating the air in the inlet. HCCI engines can operate at very lean mixtures down to φ=0.1. This extremely lean combustion produces very low emissions and virtually no CO or NOx. Because the combustion process occurs throughout the volume rather than in a flame front very low combustion temperatures occur and this is one reason low NOx.

Although there is great potential from the HCCI engine in terms of emissions and fuel economy there are major problems which have to be solved before this technology becomes widely accepted. The most significant problems with the HCCI engine are:

- low engine output performance
- detonation at high speed, high load
- difficult to achieve ignition timing control under various operating conditions
- cold start issues.

Although there are many problems the potential of the HCCI technology is considerable and is widely researched. There is an opinion that HCCI might be commercialised in light duty passenger vehicles by 2012.

2.1.4 The dCi engine

Generally the diesel engine is the most efficient of all known types of internal combustion engines. Because of its high efficiency diesel engines offer the environmental benefit of low greenhouse gas emissions. A rough comparison shows 20% less CO_2 emissions than a modern gasoline engine (Amorese, De Matthaeis, De Mitchele, & Satriano, 2004). In addition to that CO and HC emissions are also low due to the lean burn combustion and high temperatures but because of the same reasons NOx emissions are considerable (Amorese, De Matthaeis, De Mitchele, & Satriano, 2004),(Heywood, 1988). However the diesel engine is a significant contributor to PM concentration in the atmosphere. Diesel PM is mainly the result of the heterogeneous nature of diesel combustion. The process of PM formation is initiated in fuel-rich regions inside the combustion chamber which leads to pyrolysis of the fuel and the formation of carbonaceous soot particles. Finally these particles stick together (agglomerate) to create visible smoke (Greenhalgh, 2002), (Lilly, 1986).

The diesel is always s operated in lean mode with λ>1. The air/fuel ratio is primarily defined by parameters including (Bosch, 2002):

- injection pressure

- injection duration
- spray characteristics (direction and number of jets,)
- air motion
- injection timing
- air mass.

All the above parameters strongly affect the emissions and also the fuel consumption of the engine.

High combustion temperature and high oxygen concentration leads to NOx generation. On the other hand poor mixture formation generates soot emissions. It is obvious then that a very careful strategy is required in order to make all the above variables to interact efficiently in order to achieve the advantages of diesel operation. In particular, the PM/ NOx balance is hard to achieve.

The advent of common rail injection systems gave a better control of all the above parameters which define also the combustion performance of the diesel engine. The basic differences from a previous DI mechanically controlled diesel engine are:

- Higher injection pressure (1000-2000 bar, depending on the system).
- The pumping process is separated from the injection process.
- Electronic control of injectors allowing close fuel control and more than one fuel injection event per cylinder per cycle.

All of the above help with the PM/ NOx balance but the end result is still not ideal.

2.2 The best engine technologies for alternative fuels

The majority of the current alternative fuel vehicles are running on LPG and fewer on CNG. These vehicles are usually converted from gasoline fuelled vehicles by the original manufacturers or by an aftermarket converter. Usually the result of a modern conversion is a dual fuelled engine that can run on gasoline or on gaseous fuel depending on the demand and fuel availability. In terms of emission levels the LPG vehicle tends to emit less CO and HC compared with an equivalent gasoline vehicle. The CO_2 levels caused by an LPG vehicle are midway between the levels from modern diesel and gasoline vehicles. In comparison to most hydrocarbons, LPG has a low carbon to hydrogen ratio, which means that it generates lower amounts of carbon dioxide per amount of heat produced. In the UK, the LPG used for motor vehicles typically comprises of 96% propane with the rest 14% being mainly butane and propylene with smaller quantities of ethane and methane. Using these percentages for 96% C_3H_8 and 4% $C_4H_{10,}$ the total carbon content by mass can be calculated 82%.

CNG as an alternative fuel has also the potential to contribute to reducing air pollution in urban areas. However the CNG market in the UK is at the very early stages at the moment. Also a technical problem of the CNG is that the HC emissions of CNG combustion contain more than 80% of methane which is very difficult to be oxidized because methane is a very stable hydrocarbon component (Amorese, De Matthaeis, De Mitchele, & Satriano, 2004). So in order to meet the emission standards the CNG vehicles must have high precious metal loadings in their after-treatment components. Another problem is the great variation in emission levels as a result of on the quality of the conversion. The difficulty in achieving a successful conversion especially through an aftermarket system is that most of the vehicle engines are originally optimised to run as mono-fuel.

All the positive aspects from the use of the alternative fuels can make the reader question why governments do not cease the production of conventional fuels and use only alternatives since they give many benefits. It is easy to answer such a question when one considers the following.

- Generally the use of the alternative fuels means certain degree of vehicle modification (engine, exhaust after-treatment devices, fuel delivery system, and electronic control units) which lead to additional vehicle cost.
- The refuelling infrastructure is limited to specific fuels and it would not be realistic to say it is painless to adapt it to the new fuel requirements.
- Since the hardware required in adapting the alternative fuels (including vehicles and the refuelling infrastructure) is premature it might require additional maintenance work.

In some European countries the idea of converting or buying alternative fuel vehicles is being encouraged by governmental support. For example in the UK the government introduced a taxation scheme where the tax payable is a function of the car value and the tank-to-wheel CO_2 emissions, which includes a special reduction for vehicles converted to LPG. Similar examples can be found in Germany where the government have frozen the fuel tax applied to natural gas at a very low level until 2020 (Boisen, July 2002). Also the Swedish government has a similar to the UK system which assured to stay in force at least until 2006.

After all it seems that the future of the automotive sector will be formed based on a development of a mixture of technologies and fuels. This becomes apparent if one considers the increasingly strict emission control standards and also the current trends in the alternative fuels market. It is required then from governments to establish more stable fiscal frameworks in order to generate the initiatives.

Most of the alternative fuelled fleet comprises vehicles fitted with converted spark ignition (SI) engines. Such engines will be introduced in the sections that follow,

leading to a fuel comparison between SI CNG and SI LPG engines and future trends for SI alternative fuelled engines. Thereafter the emerging subject of alternative fuelled diesel engines will be introduced.

2.2.1 SI CNG option

The first alternative fuel engine conversions were implemented on carburetted gasoline engines. The CNG fuel was stored in a tank at pressure 20 to 200 bar and delivered to a mechanical reducer. The mechanical reducer had several functions: to reduce the tank pressure, evaporate the fuel, control the gas flow and also prevent the fuel from freezing. The CNG was supplied to the engine by the means of vacuum through the inlet manifold using a mixer which was usually placed before the venturi. This simple system is been used extensively in some countries especially to covert taxi vehicles. Similar systems have been adapted gradually to the modern EFI (electronic fuel injection) gasoline engines. The better conversion systems had an additional adjuster for sensing the manifold air pressure in order to correct the fuel supply according to engine load.

In the modern CNG system for a gasoline engine, the fuel is stored in a similar manner with the previous generation systems. The CNG is supplied to the engine via electronically controlled injectors from the ECU. The quantity of the injected CNG is a function of throttle position, engine speed, manifold air pressure, air temperature and finally lambda sensor signal. This system needs two sets of injectors one set for gasoline and one set for CNG. Of course this is a typical modern CNG system as there are variations depending on the manufacturer.

The main problem with CNG is its very low density. This has a negative impact on engine's volumetric efficiency and on vehicle autonomy.

2.2.2 SI LPG option

OEM's but also aftermarket companies have developed systems to convert modern gasoline engines to LPG. In parallel with the revolution in CNG technology, LPG conversion systems have been developed to improve the emission levels of the gasoline engine. Although both technologies have similar components they have certain differences. An LPG system offers the option of gaseous or liquid injection. The gaseous injection consists of the LPG tank, the shutoff valve, the pressure regulator-vaporizer and the injectors. The operating pressure of the tank is about 8 bar, which is relatively low compared to the CNG. The fuel is supplied to the pressure regulator which reduces the pressure to 1.5 bar and also converts the liquid LPG to gas phase. The fuel then is delivered to the injectors.

The liquid injection is similar to the gaseous system but it uses an extra electric feed pump inside the LPG tank, also a back flow valve and a rail pressure sensor

(Vouorenkoski, 2004). In this system it is important to have a return line to the LPG tank in order to establish a constant pressure in the fuel rail and also to prevent any fuel evaporation inside the rail.

2.2.3 SI LPG versus SI CNG

Using either LPG or CNG in SI engines reduces the pollutant CO and HC emissions. This happens because at ambient pressure and temperature both fuels are in gaseous phase. This improves air/ fuel mixing and therefore promotes combustion quality due to the gas fuel mixing with air more rapidly. Finally the superior H/C ratio helps to reduce CO_2 emissions. A comparison is shown in Table 2-1.

Emissions Performance			
LPG versus…	**CO_2**	**NOx**	**PM**
A similar gasoline engine	↓10-15%	↑up to 5%	-
A similar diesel engine	↑10-20%	↓75-85%	↓95%
High efficiency CNG engine versus	**CO_2**	**NOx**	**PM**
A similar gasoline engine	↓20 - 30%	Roughly the same	↓95%
A similar diesel engine	↓up to 5%	↓75-85%	↓95%

Table 2-1 LPG CNG emission performance comparison (www.transportenergy.org.uk, 2004)

In terms of emissions performance, it seems that CNG has lower CO_2 emissions even than a diesel engine. Both fuels CNG and LPG have almost the same performance in terms of NOx and PM with LPG having slightly higher NOx levels owing to its higher combustion temperature (Plynt & Martyr, 1999).

From the emissions point of view it is clear that CNG is wining versus LPG but there are other things that one has to consider.

CNG due to its low density needs to be stored under higher pressure approximately 200 bar in density about 140kg/m3@273K in order to give a satisfactory autonomy. It is clear then that this extra energy required to compress the gas increases its CO2 footprint. Therefore expensive and also bulkier storage tanks are required. The size of the tanks is also a reason why CNG conversions are more common for lorries or trucks rather than passenger cars. On the other hand LPG is stored at a much lower pressure but the main

advantage is that when it is injected in the liquid phase, it can give performance equal to that of gasoline.

As it is mentioned earlier the gaseous injection tends to lower the power output of the engine. Recent experimental results have shown that vapour phase injection of both LPG and CNG results in 10% loss due to loss of volumetric efficiency (Jermy, Harrison, Vuorenkoski, Kaparis, & Macarthney, 2004). Using liquid sequential port injection for LPG it is possible to recover much of the lost torque. Since the LPG is kept liquefied until the tip of the injector near the inlet port it evaporates only partially giving better volumetric efficiency than gaseous injection (Jermy, Harrison, Vuorenkoski, Kaparis, & Macarthney, 2004). Also the partial evaporation process before the inlet port cools the air and the mass of the mixture induced per cycle increases and then engine torque increases. This is known as charge cooling effect.

Summarising the comparison of the two systems:

CNG

- lower emissions than gasoline, diesel and LPG engines
- lower price.

But:

- greater fuel storage size and weight
- engine performance loss
- limited infrastructure (in some countries).

LPG

- engine performance close or very similar to gasoline
- better emissions performance than gasoline and diesel engines (except of CO_2)
- greater autonomy respect to CNG
- good infrastructure (in some countries)

But:

- variability in the composition of the fuel (Heywood, 1988)
- higher HC emissions than CNG/gasoline engine.

Considering the above it is obvious that there are many positive outcomes from both CNG and LPG gasoline conversions. However each system fits better to different

applications. CNG conversions are more suitable for heavy duty vehicles whilst LPG is better for the passenger car and medium van markets.

2.2.4 LPG GDI option

The GDI engine is the most recent innovation in the SI technology field. On the other hand alternative fuel conversions are only available for port injected SI engines. The reason for this is because the GDI technology is very new and according to the manufacturer's claims it will be capable to meet the future emission standards. Nevertheless researchers and perhaps some manufacturers examine the feasibility of a clean direct-injected engine operating with alternative fuels. An example, shown in Table 2-2, shows some predicted results for CO_2 emissions of a direct injection LPG engine. The predicted results are based on experimental investigations of the current technologies. The results shown that the level of CO_2 reduction can be equal or little better than the current diesel technology.

Engine technology	% Improvement in CO_2 From each measurement
Current Gasoline Port Injection	≈0%
Change to LPG fuel	≈10%
Stratified Charge Spray-guided Direct Injection	≈10%
Raised Compression ratio +Optimised Spark Timing	≈2%
Introduction of Automatic Stop –Start	≈5%
Total CO_2 Reduction	≈27%

Table 2-2 Predicted results from a Direct Injection LPG engine (source: modified from a confidential client report)

2.2.5 Alternative fuels for CI engines

Although there are many alternative fuel conversion systems for petrol engines there are not many for diesel engines. The idea to use an alternative fuel to improve engine efficiency is not new. In Dr. Rudolf Diesel's U.S patent No.673,160, dated April 30, 1901 the following is stated: "The method of regulating the combustion in internal-combustion engines which consists in producing a mixture of air or oxygen and a

combustible, compressing the mixture to a temperature lower than the igniting point of the combustible, and introducing under excess of pressure into the mixture a secondary combustible, the igniting point of which is equal to or below the temperature due to the compression, sustainability as described". Nevertheless it is not very clear if somebody ever achieved the above.

According to Boyer (Boyer, 1949) the first attempt to compress the mixture of air and gas to ignite it as described by Diesel was performed by J.Jones of the National Gas and Oil Engine Co., Ltd. of England in 1939. The conclusion of his experiments was that the sensitivity of gas-air mixtures to compression pressures is a matter of gas-air ratio.

Some researchers have tried different fuels in diesel engines in order to reduce primarily the NOx and the PM emissions. Natural gas (Agarwal & Assanis, 2000), dimethyl-ether (Kajitani, Chen, Kommo, & Rhee, 1997), methanol, and Fisher-Tropsch diesel fuel (Ishida, Ueki, Sakaguchi, & Imaji, 2004) have been utilised as alternative fuels for low emission diesel engines (Ishida, Tagai, Ueki, & Sakaguchi, 2004). According to (Ishida, Tagai, Ueki, & Sakaguchi, 2004), (Gokhale, 2004), and (Rassweiler & Withrow, 1938) a better way to control the ignition in an HCCI dual fuel engine despite requiring two fuels supply systems is to use natural gas/diesel or natural gas/dimethyl ether . In an experimental study described in (Ishida, Tagai, Ueki, & Sakaguchi, 2004) the combustion behaviour of a dual fuel engine running on either CNG/diesel or methanol/diesel has been investigated. The CNG was supplied trough the inlet manifold for obtaining complete mixing of CNG, exhaust gas recirculation (EGR) and air. On the other hand the methanol was port injected using gasoline injectors.

From the results and the discussions of (Ishida, Tagai, Ueki, & Sakaguchi, 2004), the ignition in a dual fuel diesel engine running on CNG commences after the diesel pilot injection and is little affected by the amount of diesel. The same happens with the methanol but there the ignition happens long after injection and this is probably due to the low intake temperature. Also it is obvious as the quantity of pilot injected diesel decreases the ignition delay increases clearly because of the decrease in temperature of the methanol pre-mixture due to the latent heat of evaporation.

2.2.6 Current knowledge and understanding

Gasoline LPG conversions have been common place for over 20 years, experience showing that the loss of energy density can be offset to some extend by an increase in compression ratio to 13/1, reductions in level of and range of spark advance, and replacement of spark plugs of higher heat tolerance to offset the hotter running.

LPG, a mixture of gaseous hydrocarbons produced from natural gas and oil extraction as well as oil refining, has three physical properties that are particularly relevant to its carbon footprint:

- In comparison to most hydrocarbons, LPG has a low carbon to hydrogen ratio, which means that it generates lower amounts of carbon dioxide per amount of heat produced.

- While there is a degree of natural variation in heating values due to the specific proportions of butane and propane within a particular sample of LPG, it nevertheless has a comparably high heating value, meaning it contains more energy per kilogram than most competing fuels.

- According to the United Nations International Panel on Climate Change (IPCC), LPG is not a greenhouse gas, meaning it is assigned a global warming potential (GWP) factor of zero. The IPCC lists the GWP factor of CO2 as 1 and methane as 25 (Atlantic Consulting 2009)

Road transport is responsible for approximately 17% of EU Greenhouse Gas emissions. LPG is currently Europe's most widely used alternative fuel, accounting for roughly 2% of the road transport fuel mix in the European Union. Studies consistently demonstrate that LPG generates fewer carbon emissions than gasoline (petrol) and broadly equivalent emissions to diesel (Atlantic Consulting 2009).

The majority of the current alternative fuel vehicles are running on LPG and fewer on CNG. These vehicles are usually converted from gasoline fuelled vehicles by the original manufacturers or by an aftermarket converter. Although there are many conversion systems for gasoline engines and the benefits are fairly well understood, there are only very few for diesel engines. Diesel engines were traditionally more problematic to the conversion due to the limited control of the mechanical systems. However, with the advent of the common rail injection systems, the pressure generation was separated from the injection process and it is now possible to get control of pilot diesel injection and make the LPG and diesel control systems work together

In UK appears an application of LPG to diesel engines that is unusual in view of the poor ignitability. The use of LPG has been reported in at least three different types of compression ignition mixture formation systems.

The most conventional method to ignite LPG fuel in a compression ignition engine is to inject a small amount of diesel fuel to the combustion chamber to initiate the combustion (Bilcan et al, 2001). The type of system where diesel fuel is used as a pilot fuel is commonly called the dual-fuel system. The major drawback of this system is the need for two fuel supply systems.

Another method is to use cetane enhancing additives mixed with the LPG, and also adding aliphatic hydrocarbon and lubricating additives to enable the use of LPG in compression ignition engine with only minor changes to the injection system (Sugiyama

et al, 2003). The cetane enhanced LPG fuel is commonly called the LPG Blended Fuel (LBF).

Also, the use of LBF in Homogeneous Charge Compression Ignition (HCCI) engines has been reported (Chen et al, 2001).

This thesis explores the idea of operating a current production common rail diesel engine on LPG using pilot diesel injection as spark ignition medium. The main advancement in using this technology on current diesel engines is the establishment of a better balance between NOx and PM emissions without losing too much of the CO_2 benefits of diesel. This method has the advantage of using the existing common rail injection technology combined with the state of the art LPG liquid phase injection systems in a unique way.

3 PRELIMINARY STUDIES

3.1 Introduction

This chapter contains the results of an early experimental study exploring the potential of running a historic Ricardo E6 variable compression ratio research engine on a mix of diesel and LPG. Subsequent engine simulations show the potential of converting and running a dCi engine on a mix of diesel and LPG but using only a small quantity of diesel pilot as ignition medium. This preliminary study proves the concept of using a modest charge of diesel pilot injection to ignite a larger dose of LPG.

3.2 Preliminary experimental studies

Running an engine on a mix of diesel and LPG is a challenging task. The engine requires a high compression ratio if the diesel charge is to be ignited effectively and despite the relatively high knock resistance of LPG, the combustion is likely to be rapid and potentially uncontrolled.

Results from an early study, carried out at Cranfield engine laboratories showed the potential of running successfully the diesel version of a Ricardo E6 variable compression ratio research engine on a mix of diesel and LPG (Theodoridis, 2003). Although the design of this engine is historic, it has the considerable advantages of the variable compression ratio and a particularly durable design. The Ricardo E6 has the reputation of being able to withstand prolonged periods of uncontrollable combustion. The particular E6 used in this case was fitted with an American Bosch diesel pump, a pintle type fuel injector and an indirect injection cylinder head with the Ricardo Comet Mark V combustion chamber (Figure 3.1).

With low speed operation (less than 2000 $remin^{-1}$), two valve design and a near flat piston crown and cylinder head, the turbulence levels inside the combustion chamber are low. In addition to the diesel equipment the engine was fitted with gaseous phase LPG fuelling system. This comprised of a conventional LPG fuel tank for automotive applications leading to a conventional vaporiser with the rate of fuel delivered being measured using a rotameter and controlled by using a high precision valve.

A series of simple experiments were undertaken using this engine. At the outset there was doubt over whether would be possible to ignite the LPG charge with a dose of diesel and whether any subsequent combustion would be controllable. These two doubts were dispelled quite quickly. Figure 3.2 shows the pressure time histories for the engine running both on diesel and with the mix of diesel and LPG. In the diesel only operation the diesel pump was set to achieve mixture richer than the modern diesel engines, with compression ratio of 17.5:1 and at operating speed 1400 RPM. These operating

conditions are chosen because they resulted in smooth running. The strategy for the dual fuel operation was to progressively reduce the diesel fuelling whilst increasing LPG fuelling, with the aim of maintaining the power output of the engine whilst minimising combustion knock.

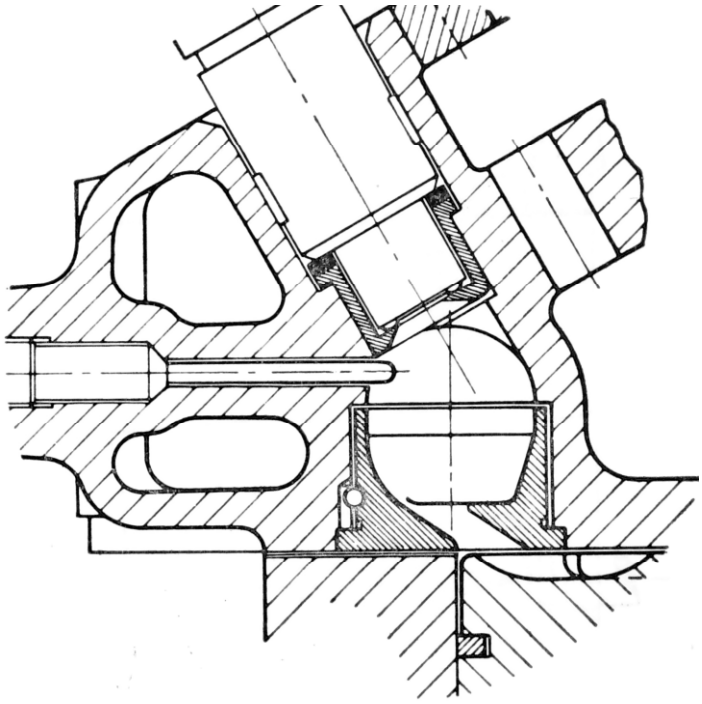

Figure 3.1 Ricardo Comet Mark V combustion chamber (Ricardo H. R., 1968)

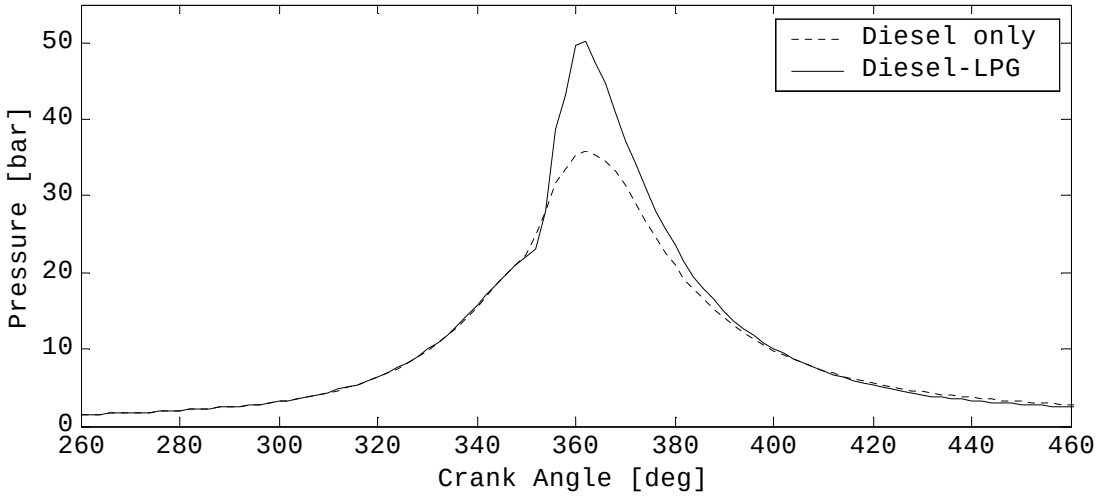

Figure 3.2 E6 pressure time histories. compression ratio 17.5:1, 1400 RPM

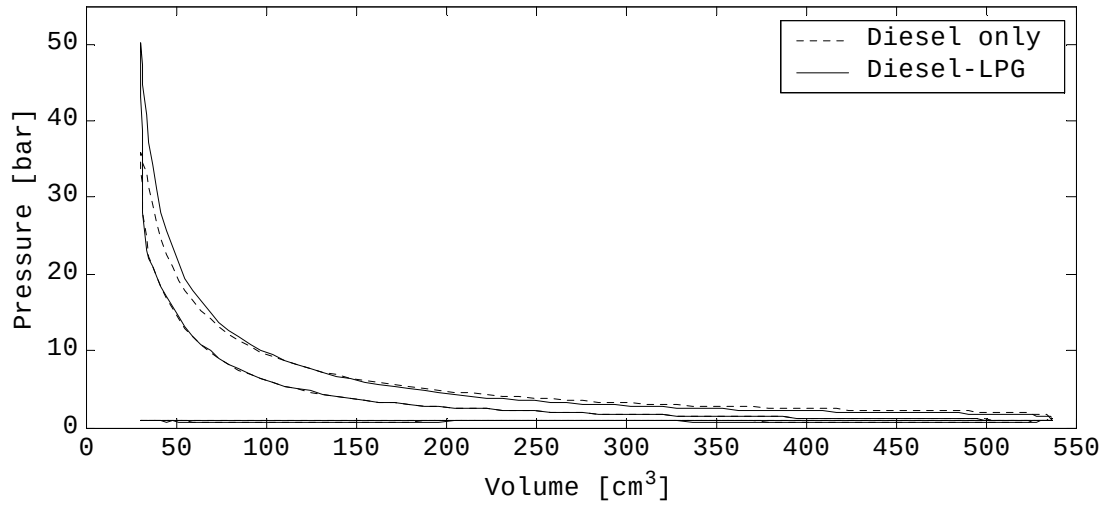

Figure 3.3 E6 pressure volume diagram, compression ratio 17.5:1, 1400 RPM

Thus the results in Figure 3.3 represent conditions where the engine produces almost identical power output but with different fuelling strategies. Inspection of Figure 3.2 and the corresponding PV diagram in Figure 3.3 reveals that under dual fuel operation the combustion occurs rather quickly resulting higher pressure around TDC but lower pressures later on in the combustion stroke.

The results in Figure 3.2 and Figure 3.3 demonstrate the feasibility of using a reduced charge of diesel to ignite a larger charge of LPG within a diesel engine. The diesel pilot ignition concept is therefore proven to be a possibility even in a historic engine fitted with a diesel injection system with rather low pressure (150 bar).

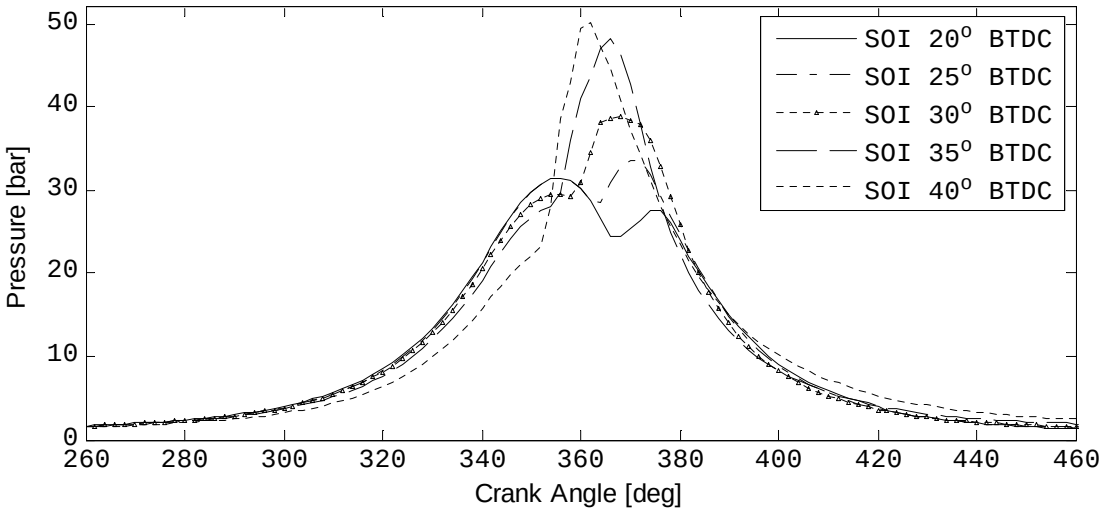

Figure 3.4 E6 dual fuel mode, compression ratio 17.5:1, 1400 RPM

A further step was to investigate how controllable this fuelling strategy could be. Figure 3.4 shows the effect of maintaining the balance between the diesel and the LPG whilst altering the injection timing of the diesel charge. Figure 3.4 readily shows that the

injection timing has a significant effect on the cycle pressure time history and hence on the combustion performance of the engine. It is reassuring to note that the engine operating under the diesel pilot ignition concept can be readily controlled using injection timing alone.

As a final step in the experimental investigation the flexibility of the diesel pilot ignition concept was explored. Figure 3.5 shows the effect of operating the engine within a range of compression ratios. It is comforting to note that the dual fuel operation could be achieved at all the compression ratios commonly encountered with diesel engines (in the range 17-27:1). It is interesting to note that the relative performance e benefits of dual fuel operation are seen mostly with lower compression ratios. This would seen to reflect the more rapid constant volume combustion encountered with the dual fuel operation.

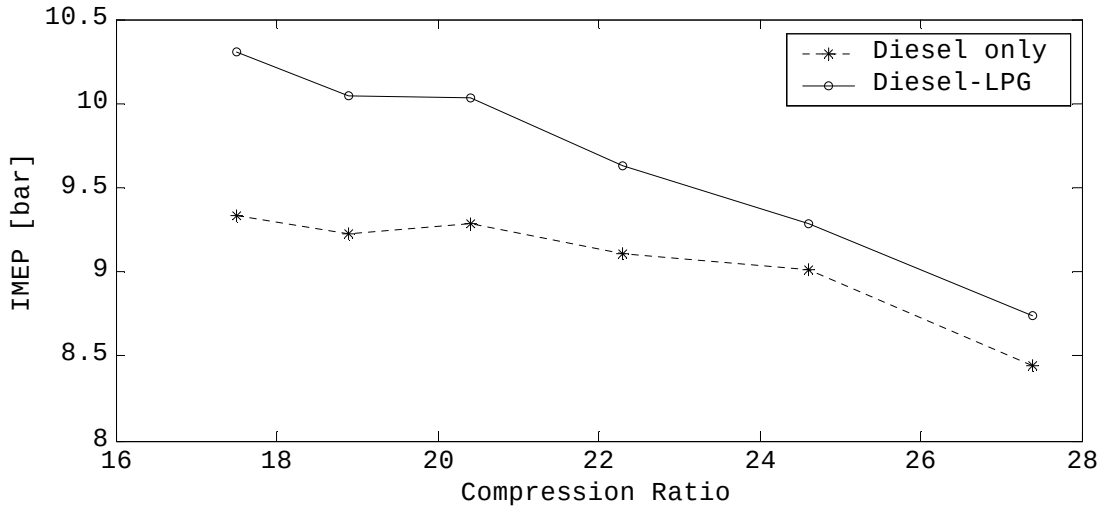

Figure 3.5 E6 IMEP for various compression ratios

3.3 Engine Simulation

The preliminary experiments described in section 3.2 demonstrated that it is possible achieve controllable combustion dual fuel diesel and LPG operation at a range of compression ratios. Successful operation was achieved in an engine that did not benefit from modern fuel injection or high turbulence combustion chamber design. Before committing (and potentially damaging) a modern common rail high speed diesel engine to dual fuel operation, a series of engine simulation studies have been performed in order to quantify the potential benefits of the diesel pilot ignition concept in modern diesel engines.

The simulation studies are not straightforward due to a number of uncertainties relating to the nature of the dual fuel combustion process. In particular, the early inflammation of LPG caused by a distributed (Heywood, 1988) heat source such as a burst of diesel

spray is likely to be different from the early inflammation caused by a compact spark (which itself is fairly well understood) (Vouorenkoski, 2004).

As flame propagating through a premixed charge, in a simple combustion chamber has to travel up to 75% of the chamber radius before consuming 10% of the charge (Campbell, 1979) it was felt that the uncertainty over early flame development is less significant than the uncertainty over the late flame propagation. Therefore, although nothing simple could be done to address the uncertainties over early flame development, a method of predicting the rate of the heat release from an LPG charge at high compression ratio was devised. This presented an opportunity to investigate the diesel pilot ignition concept by simulation with a reasonable degree of confidence in the realism of the simulations.

The AVL BOOST engine cycle and gas exchange simulation software was used for the study. Combustion modelling is based on the simple approach of directly specifying the rate of the heat release using the Wiebe function. Wiebe function describes the mass fraction burned versus crank angle and it is defined by the start of the combustion, the combustion duration, the shape parameter m and the Wiebe parameter a. These parameters must be specified in the combustion inputs of the simulation.

The Wiebe function is given from (Heywood, 1988):

$$X_b = 1 - \exp\left[\left(\frac{\theta - \theta_0}{\Delta\theta}\right)^{m+1}\right] \tag{3.1}$$

For the combined diesel-LPG engine cycle simulation, a double Wiebe function is used in order to better describe the combined diesel-LPG combustion process. Specifying the first Wiebe to be the fraction of fuel energy released from the diesel pilot injection and the second Wiebe to be the fraction of fuel energy released from the combustion of the LPG, the superposition of the two functions is used to approximate the total heat release of the combined diesel-LPG operation.

The method devised for predicting the rate of the heat release by premixed LPG charge at high compression ratios has distinct steps because the simulation code used has no in-build provision for simulating dual fuel operation.

The first step is to devise a realistic simulation model for a naturally aspirated spark ignited engine running on a premixed LPG charge at a standard compression ratio (9.5:1 here). This was achieved using well known Wiebe parameters for gasoline fuels which were corrected for LPG using the measured results from spark ignited LPG engine operation from (Vouorenkoski, 2004). The correction reduces the combustion duration for LPG by 4.4% compared to that of gasoline.

With a realistic simulation model of a 9.5:1 LPG SI engine, the peak gas temperature was found for the idealised case of constant volume combustion. The compression ratio in the model was then raised to 19:1 and the peak gas temperature found once more. The ratio of these two temperatures was found to be 0.955.

It was postulated that, to a first degree of accuracy, the rate of flame propagation (and hence heat release) would be directly proportional to burned gas temperature only. This clearly neglects the influence of the increase turbulence caused by a raised compression ratio, but as BOOST simulation is zero dimensional the approach was adopted. Therefore, the rate of heat release curve adopted for LPG combustion at 19:1 compression ratio was altered so that the combustion duration at 19:1 would be shorter by a factor equal to 0.955.

Figure 3.6 shows the mass fraction burned versus crank angle curves for premixed LPG combustion at 9.5:1 and 19:1 devised using this method.

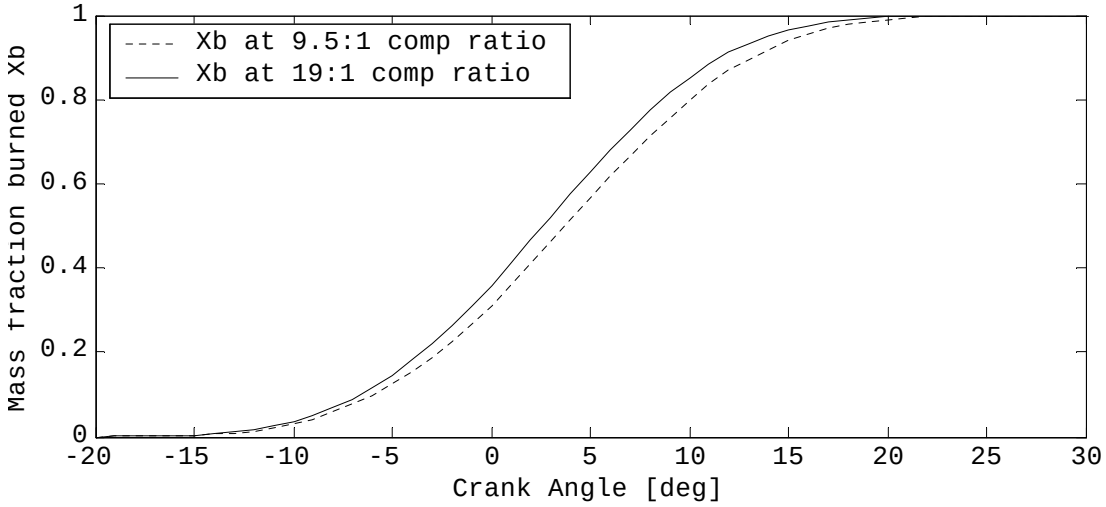

Figure 3.6 Mass fraction burned curves

With reasonable estimate of the shape of the heat release curve, the simulations could be undertaken once the quantities of diesel and LPG were defined. Simulations were undertaken using the geometry of a modern 4 cylinder, 19:1 compression ratio dCi engine. The BMEP feature of the BOOST code was used to find the quantity of spark-ignited LPG required to achieve the same BMEP as with the diesel only compression ignition operation. For the LPG operation, a 10% restriction in the hydraulic diameter of the intake ports was introduced in order to account for the loss of volumetric efficiency commonly encountered when operating on gaseous phase LPG (Theodoridis, 2003).

The step described above, revealed the mass of LPG required to achieve the same engine performance (in terms of BMEP) as with diesel only operation. This mass of LPG was converted to an equivalent mass of diesel fuel and the simulation run again with compression ignition. 10% of this equivalent mass of diesel fuel was assigned to

the pilot phase of a double Wiebe combustion model. Figure 3.7 shows the rates of the heat release predicted from the pilot diesel igniting a much larger premixed charge.

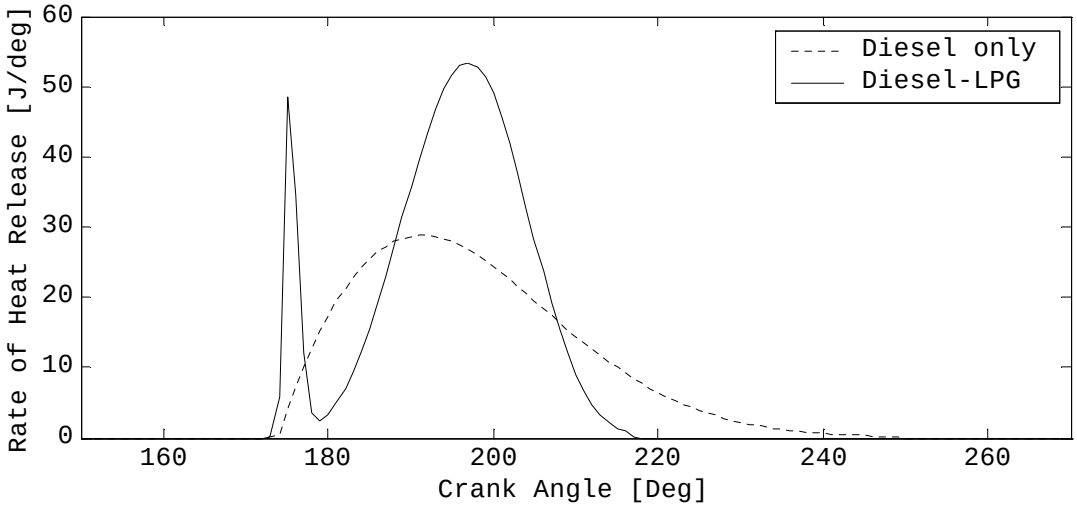

Figure 3.7 Rate of heat release curves for diesel only and diesel/LPG operation

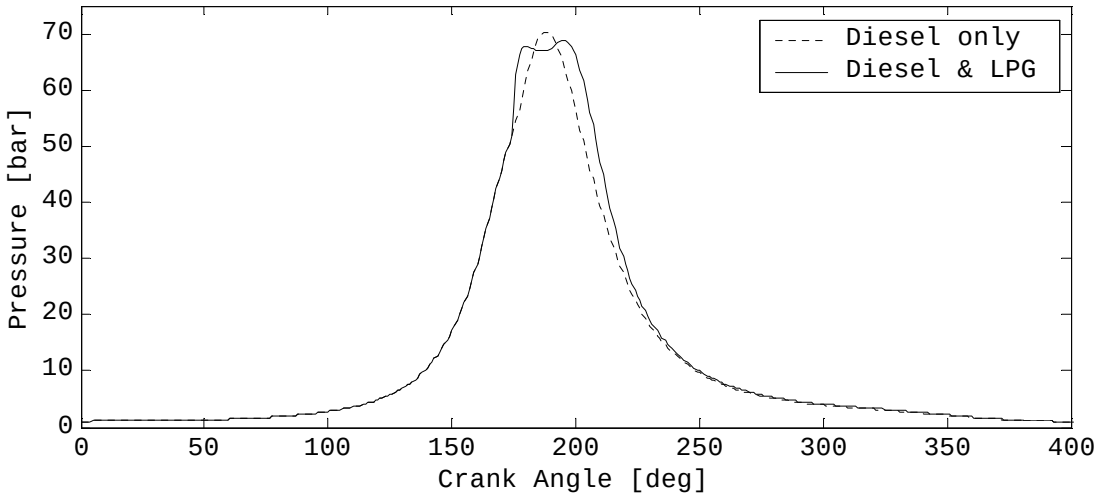

Figure 3.8 Pressure versus crank angle

Figure 3.8 and Figure 3.9 show simulated results for the operation of the 19:1 compression ratio, 4-cylinder dCi engine running on diesel only and with dual fuelling. Figure 3.8 shows that with dCi dual fuel operation, the maximum cylinder pressure differs little from that encountered with diesel only operation. This is a comforting outcome as the diesel engine will have been designed for such pressures. This is in sharp contrast to the experimental results achieved on the Ricardo E6 engine where Figure 3.2 shows the dual fuel operation to produce much higher cylinder pressures than the diesel only operation. This is not unexpected as the Ricardo E6 engine used a considerable charge of diesel to ignite the LPG whereas the dCi simulation called for only a very small diesel pilot.

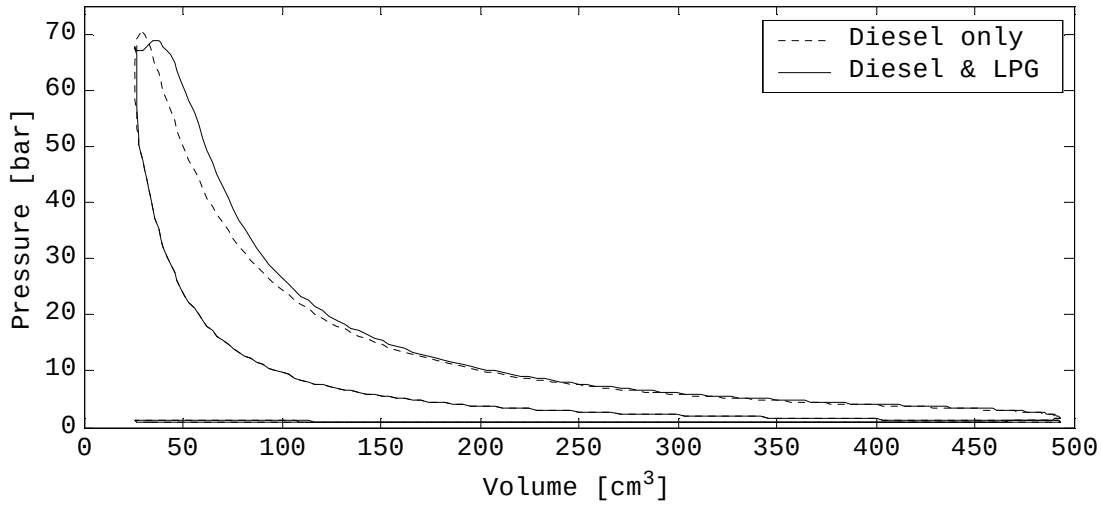

Figure 3.9 Indicator diagram

Figure 3.9 shows the work produced by the dual fuel engine to be slightly superior to that of the diesel only operation. This increase in engine efficiency is a welcome attribute of the diesel pilot ignition dual fuel concept.

An improvement in engine efficiency should result in a lowering of CO_2 emissions for the dual fuel operated engine. In addition, a reduction in the consumption of diesel, in conjunction with similar cylinder pressures (and hence temperatures) should reduce PM without increasing NOx. These simulation results are encouraging and provide a case to support the development of a dual fuel diesel/ LPG dCi engine.

3.4 Conclusions

This preliminary study introduced the notion of a dual fuel diesel and LPG engine as a potential means of achieving diesel like levels of fuel efficiency (and CO_2 emissions) and a more favourable balance between PM and NOx emissions. Preliminary experiments on a single cylinder proved the concept of using a modest charge of diesel pilot to ignite a larger dose of LPG. Subsequent simulations of a modern four cylinder dCi engine suggest that with closer control over the pilot diesel injection, diesel like performance can be obtained, with less emissions expected than currently found with diesel only operation.

4 TEST RIG DEVELOPMENT

4.1 Introduction

The results from dual fuel engine simulation suggested that operating a dCi dual fuel engine with close control over pilot diesel injection, diesel like performance can be obtained, with less emissions expected than currently found with the diesel only operation.

From the preliminary study, the method devised for predicting the rate of heat released by igniting a premixed LPG charge at high compression ratio using diesel pilot injection had many uncertainties. These uncertainties concern the early inflammation and subsequently the burning velocity when pilot diesel is used to ignite a larger premixed charge of LPG and air (surface ignition) in a running engine.

At this stage, a test rig was developed in order to investigate the above uncertainties and demonstrate the dual fuel dCi engine concept.

This chapter contains a brief description of the design and the development of the experimental rig. The main objective was to develop a single cylinder dual fuel engine which combines the most up-to-date diesel engine technology with a state of the art liquid propane injection system.

4.2 Engine considerations

At the outset a production dCi engine was considered as the most appropriate candidate for the experimental work. However, considering that this was a more fundamental combustion study, it was decided to carry out experimental work on a single cylinder engine.

The Ricardo E6 of Cranfield University shown in Figure 4.1 is a single cylinder variable compression ratio research engine mounted on a common test-bed with an electrical dynamometer. The choice of the particular engine was due to the variable compression ratio capability but most important due to the particularly robust design.

Although the E6 engine has these advantages, its IDI cylinder head design together with the low pressure American Bosch diesel injection system was posing a major drawback. The experimental work demanded high quality results from modern DI diesel engines fitted with common rail injection system. Obviously this would have not been achieved using the original diesel E6 version. Therefore it was decided to develop the E6 engine to be representative of the dCi engine.

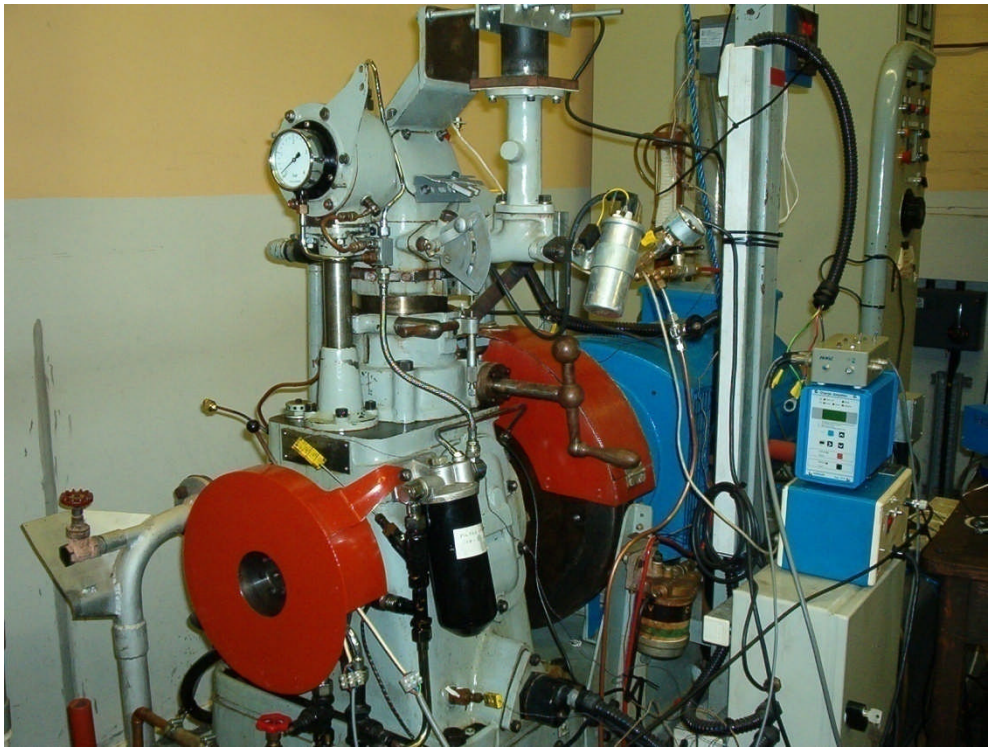

Figure 4.1 The Cranfield E6 single cylinder variable compression ratio research engine on its original form

This required significant engine modifications and the design and manufacture a number of fairly complex parts. The major development was the design and the manufacture of a new cylinder head with features from the most up-to-date diesel engines. A dedicated common rail injection system was also developed using components from a production Bosch second generation common rail injection system.

The E6 single cylinder engine was developed incorporating features from the latest production dCi engines. Table 4-1 shows the main differences between the old and the new E6 design which will be referred as E7 from now on in this thesis.

Ricardo E6 engine features	E7 engine features (new E6)
• Cast iron cylinder head with directional inlet port (low swirl)	• Aluminium cylinder head with helical inlet port (high swirl)
• Indirect fuel injection	• Direct fuel injection
• Fuel injection pressure 130 bar	• Fuel injection pressure 1600 bar
• Fuel pump engine driven	• CR fuel pump separately driven
• Pintle type mechanical injector	• CR solenoid multihole injector
• Prechamber on cylinder head	• Toroidal bowl on piston combustion chamber
• 2 valve overhead camshaft gear driven	• 2 valve overhead camshaft belt driven

Table 4-1 Ricardo E6 and E7 engine features

Figure 4.2 shows the new E7 engine fully developed and instrumented.

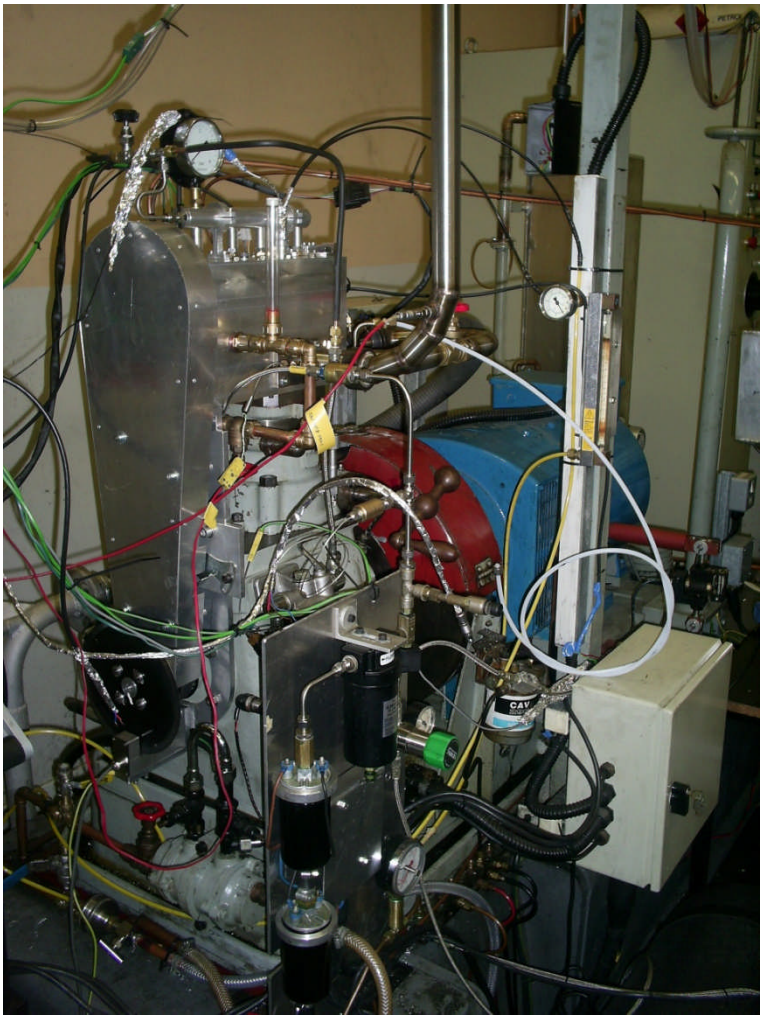

Figure 4.2 E7 engine

4.3 High pressure injection rig development

A high pressure diesel injection system was specifically developed for the E7 engine and for injection spray characterisation measurements. This system is based on second generation diesel common rail injection technology which is typical of medium and heavy duty vehicles. The fuel pressure is generated from a high pressure common rail pump driven by an electric motor.

Figure 4.3 shows a photograph of the high pressure injection rig fully developed. The system consists of the following components which are mounted on a common aluminium plate:

- Aluminium fuel tank
- Electric feed pump
- Fuel filter
- High pressure rotary pump

- Electric motor
- Electronic inverter
- Fuel accumulator
- High pressure fuel line
- Fuel return lines

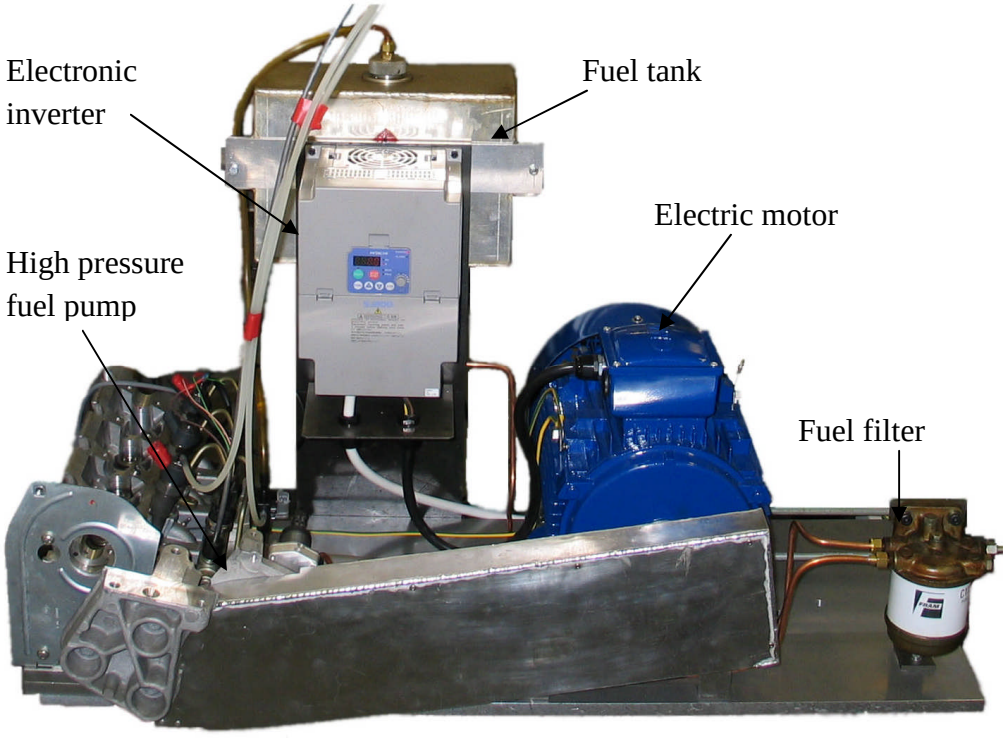

Figure 4.3 High pressure fuel injection rig

4.3.1 Common rail pump

The high injection pressure is generated from a Bosch CP3 pump. The CP3 is a fuel lubricated high pressure pump with suction-side fuel delivery control by means of a metering unit Figure 4.4. Three pump elements are arranged radially with respect to the central shaft and offset by 120°. The eccenter fitted to the driveshaft forces the pump plunger to move up and down providing the pumping. The transverse forces arising from the movement of the eccenter drive roller are removed by using buckets on the housing wall (Bauer, 2004). The pump then has greater stability under load and is capable of withstanding higher pressures. The monoblock housing design reduces the number of leak points in the high pressure section and permits a higher delivery rate.

A gear pump is flanged onto the high pressure pump and driven from the main shaft, pressurises the fuel up to 7 bar (delivery rate up to 400L/h) before it enters into the plunger. This serves two purposes: prevents cavitations, which can be caused from air bubbles formed into the system and adjusts the fuel flow inside the pump housing providing lubrication and cooling.

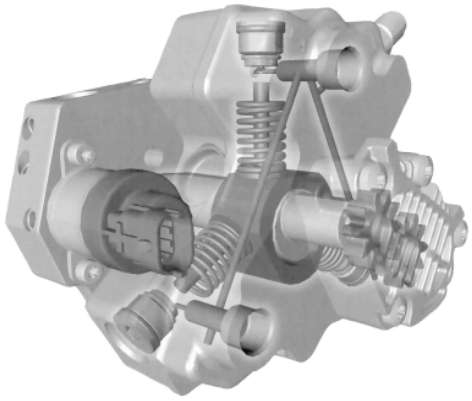

Figure 4.4 Bosch high pressure pump CP3 (Bauer, 2004)

4.3.2 Electric motor

A three phase 7.5KW electric motor and a matched electronic inverter were obtained to drive the high pressure pump.

According to (Bauer, 2004), on a 2-liter engine, the high pressure pump draws a power of 3.8 KW at nominal speed and a pressure of 1350 bar in the fuel rail (at a mechanical efficiency of approximately 90%). This is a considerable amount of power contributing to engine parasitic losses and it must be taken carefully into account if such a system is to be driven from the engine. Considering this, the reason of having the fuel pump independently driven from the experimental engine becomes obvious.

The power required to drive the fuel pump was estimated based on the following requirements

- Fuel pump rated speed 2000 RPM
- Fuel pump rated fuel pressure 1600 bar

To calculate the fuel pump power, the fuel delivery rate must be known. Since this information was not available, the maximum fuel flow was found experimentally. Initially the total fuel flow of pump was measured using a glass tube with precise volume graduations. Operating the fuel pump manually at low speeds, the average fuel quantity was measured for 20 pump revolutions. The fuel flow was measured 1ml per pump revolution. The same experiment was repeated three times to eliminate measurement error.

Then the fuel mass flow was calculated for maximum dCi engine operating conditions. Since the particular pump was taken from a production dCi engine the following parameters were used:

- Engine speed: 4500 RPM

- Maximum pump speed: 2250 RPM (when the pump is fitted on the vehicle the driving ratio is 2:1).

The mass flow for maximum pump speed is given by:

$$\dot{m}_f = V_f \times \rho_f \times n_p \tag{4.1}$$

Where:

$\dot{m}_f$ = Fuel mass flow [Kgs^{-1}]

V_f = Fuel volume per pump revolution [ℓ]

ρ_f = Fuel density [Kgl^{-1}] for gas oil [$\rho_f = 0.840$]

n_p = Pump speed [RPM]

The power required was calculated using the fluid power equation:

$$P_r = \dot{m}_f \times p_f \times \eta_p \tag{4.2}$$

Where:

P_r= power required [W]

p_f= fluid pressure [Nm^2]

η_p= pump efficiency [%]

A 20% excess was added to the final required power to prevent the electric motor and the inverter from overloading and also to account for the friction losses of the driving system.

Therefore a three phase 7.5KW electric motor together with an electronic inverter was chosen to drive the high pressure pump. The electric motor has 4 poles and is suitable for operation with 415 Volt three phase variable frequency drive. The maximum operating speed is 1800 RPM.

The inverter features “intelligent sensorless vector control” as it is stated by HITACHI which is specifically designed for high starting torques and changing load applications.

The power is transmitted from the motor to the pump via a tooth-belt and a pair of tooth-pulleys with a gear ratio 1:1. Although the rig was designed for maximum speed

of 2250 RPM, the 1:1 gear ratio limits this to the maximum speed of the electric motor. This was due to the availability of a pair of standard size tooth-pulleys and since the 1800 RPM is sufficient to deliver more than enough fuel flow for the particular engine.

4.3.3 Solenoid fuel injector

The fuel injector is a Bosch (Ref 0 445 110 021) solenoid valve type with a five-hole injection nozzle shown in Figure 4.5. Unlike the mechanical injectors, here the injection timing and the fuel quantity are controlled by an electric trigger which energises the electromagnetic solenoid valve.

The injector can be subdivided into three main elements:

- The injection nozzle
- The main body including the hydraulic mechanism
- The solenoid valve

Figure 4.5 Bosch (Ref 0 445 110 021) common rail solenoid injector

4.3.4 High pressure fuel lines

Because length, diameter and wall thickness all affect the injection process, prescribed line dimensions are defined (Bauer, 2004). For instance, line length affects the rate of injection discharge dependent on speed whether internal line diameter is related to throttling losses and compression effects influencing the injected fuel quantity

A bespoke high pressure fuel line was used between the high pressure fuel pump and the rail as well as between the rail and the injector. This high pressure pipe was made by Giro Engineering ltd® which is a specialist company producing high pressure fuel lines for naval applications. The pipe was made of extruded steel and it is capable to withstand pressures up to 2000 bar. During manufacturing process, the fuel line was

subjected to pressures up to 3800 bar in order to improve the strength of the inner walls. The sealing cone and union nut connection fittings were made according to DIN 73 365.

4.3.5 Rig operation/schematic

With the presence of the high pressure pump the rig has a capacity to generate a continuous pressure equal to 1600 bar. The inverter allows to smooth start the electric motor and to set the required operational speed. The speed can be interpreted on the inverter display showing frequency using the following formula:

$$Speed\ in\ rpm^{-1} = \frac{Frequency \times 60}{Pairs\ of\ poles} = \frac{Frequency \times 120}{Number\ of\ poles} \tag{4.3}$$

The theoretical speed for the motor is 1800 RPM. However, the motor cannot create torque unless its shaft rotates at slightly different speed. This difference is called slip and so the maximum rated speed of the particular motor is 1750 RPM.

Figure 4.6 shows a schematic of the high pressure fuel injection rig. The fuel is supplied from the fuel tank to the electric feed pump by gravity via a water separator (trap). The feed pump delivers the fuel to the high pressure pump via a fuel filter. An adjustable valve on the feed pump allows the pressure to be set when the rig is operating so any fuel excess returns into the fuel tank by means of a return line. The high pressure pump pressurises the fuel up to 1600 bar into the fuel rail. The fuel pressure is constantly monitored by a piezoresistive pressure transducer, which is installed on the rail. From the rail the fuel flows via the high pressure line to the fuel injector. Finally, another return line carries any fuel excess from the injector back to the fuel tank. This fuel excess is caused either from the internal leaks of injector or from the fuel that has not been injected during the engine cycle.

The fuel pressure in the rail is controlled by means of a metering unit on the high pressure pump and also by a pressure limiting valve on the rail. The purpose of the metering unit is to adjust the fuel quantity flowing into the pump and maintain the pressure in the fuel rail whereas the pressure limiting valve limits the pressure in the rail by releasing a drain hole when pressure exceeds the 1600 bar.

It is clear then that the functions of pressure generation and fuel injection are separate on the rig. Thus, the fuel pressure inside the rail is independent of engine speed and injection events. In addition, driving the rig by means of an electric motor instead of the engine gives the advantage of using it as a stand-alone facility for injector testing.

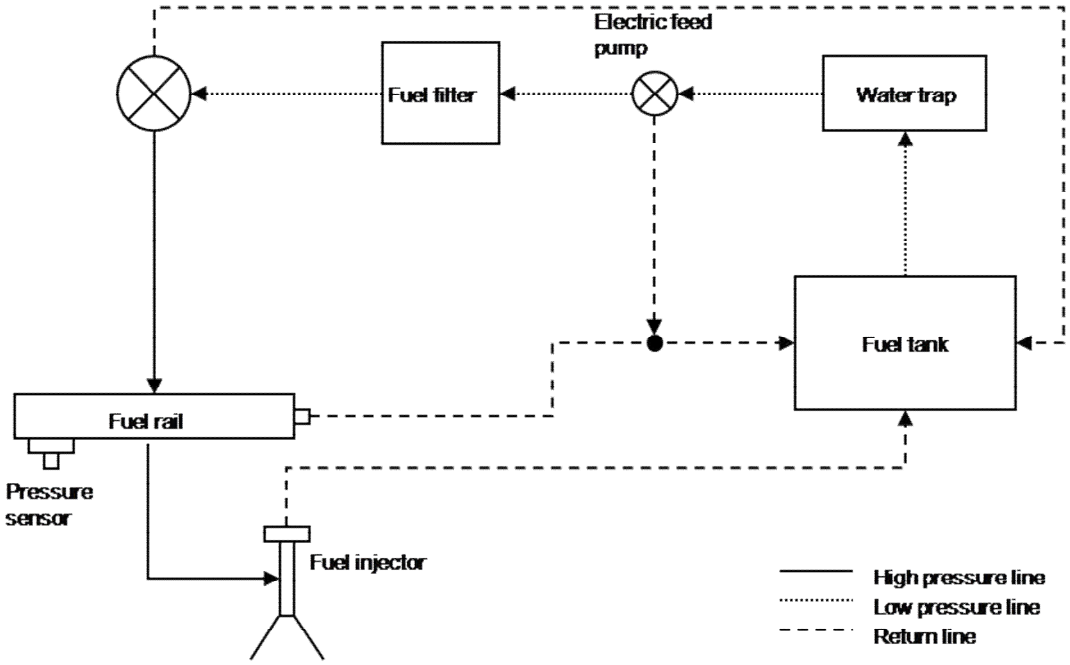

Figure 4.6 High pressure fuel injection rig

4.3.6 Fuel pressure measurement

A Bosch piezoresistive type sensor was used for measuring fuel pressure in the rail. Pressure measurement results from the bending of a thin steel diaphragm on which are attached polysilicon strain gauges connected in the form of the Wheatstone bridge. This permits high signal utilisation and good temperature compensation (Robert Bosch GmbH, 2001). An evaluation IC within the sensor housing amplifies the measurement signal counting offset, sensitivity and temperature compensation.

Using the following formula the characteristic curve of the particular pressure transducer is obtained (Figure 4.7). The characteristic equation of the transducer is:

$$U_{\mathrm{A}} = (0.8\,p / p_{Nom.} + 0.1)U_V \tag{4.4}$$

Where:

U_A output voltage [V]
U_V supply voltage [V]
p pressure [bar]
p_{Nom} maximum rated pressure [bar]

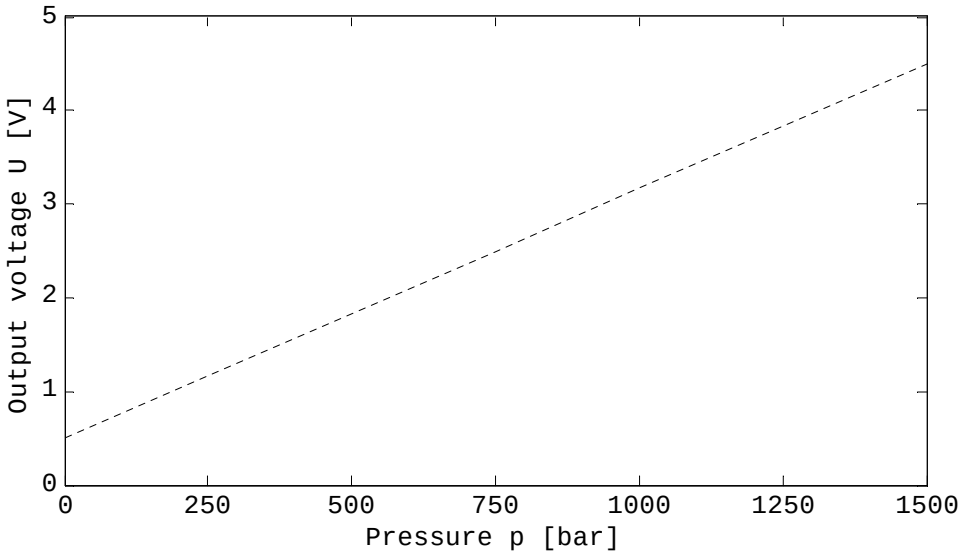

Figure 4.7 Fuel pressure transducer characteristic curve

4.4 Diesel ECM development

4.4.1 ECM requirements

Combustion on diesel engines is highly depended upon the injection process. In the second generation common rail injection systems precise injection control is achieved using fast response low impedance solenoid injectors driven by high current electronic drivers. The advantage of using low impedance injectors is a shorter triggering time. This is a very important feature for diesel injectors because it can dramatically improve the split injection quality. The injector driving units are usually implemented within the engine's ECU.

For the current study, the injector presented in Figure 4.5 was already available but an appropriate electronic driver was required.

Therefore an electronic control module (ECM) was developed. The main design specifications are summarised in the following:

- The electronic driver should be capable to operate the injector consistently at maximum fuel pressure 1600 bar and at engine speeds up to 3000RPM.
- The driver should constantly acquire the combustion TDC signal as well as the crank angle signal from the engine sensors in order to provide the correct triggering signal to the injector.
- The user should be able to set injection duration and timing in terms of engine crank angle through a PC interface whilst engine is running. It should be possible to split the injection into a pilot and a main and furthermore split the main injection. The majority of modern common rail injection systems (second generation onwards) aids split injection. The solenoid valve used to operate the injector can be activated several times within one engine cycle, allowing more than one injection event per time. Splitting the injection into multiple injections helps reducing exhaust emissions and combustion noise.
- The electronic driver should operate the injector solenoid fast enough during the opening phase for minimising the premixed diesel combustion and rapid closing for reducing soot formation.
- The high current produced from the driver should not damage the low impedance injector solenoid and the inductive fly-back currents from the injector solenoid will not damage the injector driver electronics.

4.4.2 Vehicle calibration testing

Although setting the main requirements for the ECM was a fairly simple task, providing the correct electric signals to the solenoid injector was challenging. Usually manufacturers give very limited information on the injection systems and detailed information on electric/electronic signals is always kept confidential.

Therefore a reverse engineering method was devised in order to obtain the exact type of electric signals required for the particular injector. It is important to mention here that modern diesel fuel injectors are highly optimised for the particular application. Hence choosing an appropriate injector for the single cylinder engine that would allow substantial flexibility was another aspect of the design to consider.

At the outset of this project a Vauxhall Vivaro series van vehicle was acquired in order to use its common rail injection system components (high pressure pump and injectors) to build the injection system for the Ricardo E7 engine. The particular vehicle was fitted with a 1.9 turbocharged dCi diesel engine which is exactly the focus of this study. While the injection system was still on the vehicle, its operation was studied by recording and analysing the vehicle's ECU signals to the solenoid injectors at various engine operating conditions.

The vehicle was instrumented with current probes connected to a portable data acquisition system from National Instruments as it is shown in Figure 4.8. The engine TDC signal was taken from the TDC sensor on the camshaft and provides a reference frame for the injection data acquired. The wiring for the current probe is shown in Figure 4.9.

Subsequently engine TDC signal and injector solenoid current signals were record simultaneously under various engine operating conditions at 10 kHz acquisition frequency. Although a large amount of data were captured during vehicle testing, only a particular subset of data is presented on this thesis due to confidentiality reasons.

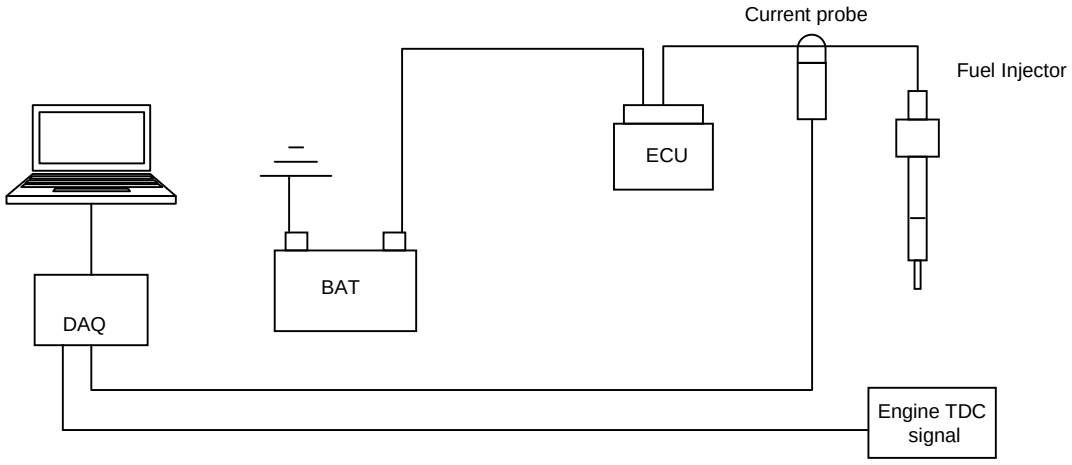

Figure 4.8 Schematic showing the method of measuring the current signals of the injectors

Figure 4.9 Vauxhall Vivaro injector currents measured with current probes

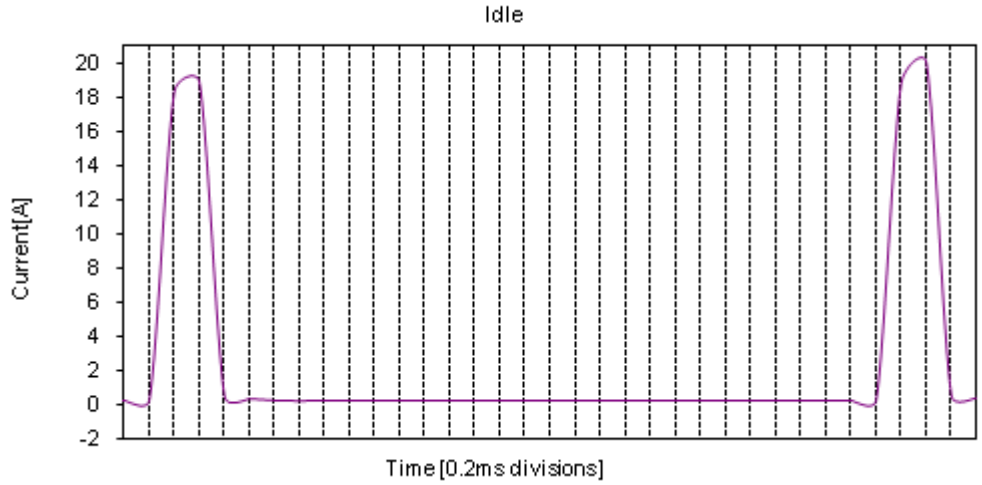

Figure 4.10 Injector current signals at idle engine operation (vehicle stationary)

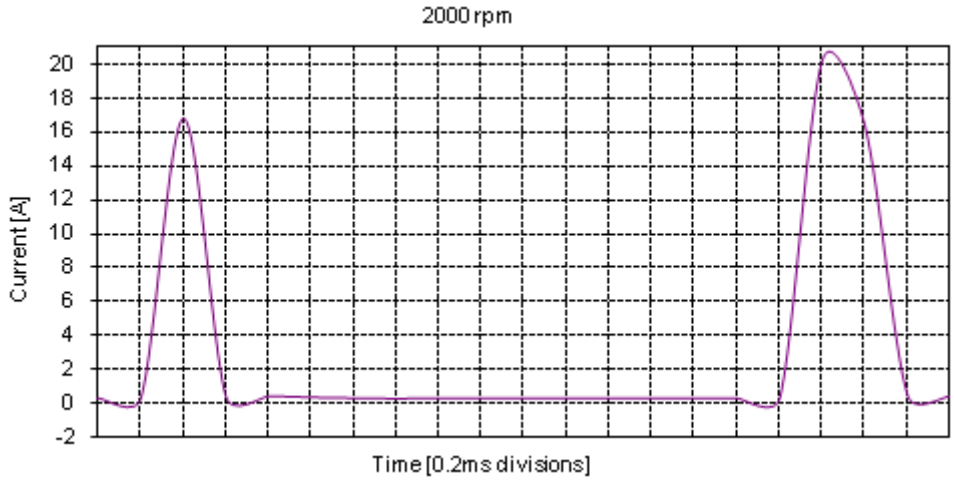

Figure 4.11 Injector current signals at full load and 2000 RPM

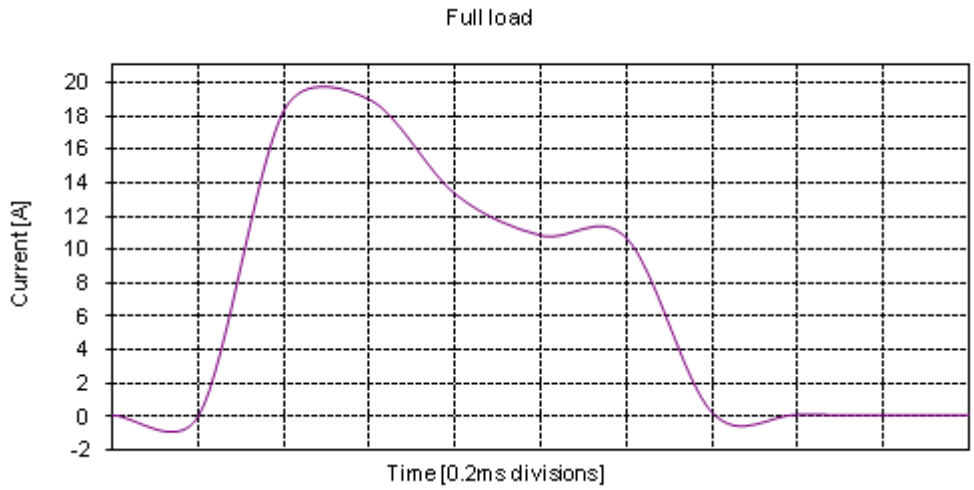

Figure 4.12 Injector current signals at full load and 3000

At zero current the injector's solenoid valve is closed. Fuel is injected only when current passes on the solenoid valve. Figure 4.10 shows that when the engine runs at idle speed (approx. 600 RPM) there are two injection events per engine cycle: pilot and main injection. Both injection events have approximately the same duration 0.6ms. The time between the two events is approximately 5.6ms. As the engine speed increased from idle to 2000 RPM (Figure 4.11), pilot injection duration becomes shorter than that of the idle operation and also the peak current slightly drops. Furthermore the time interval between the pilot and main injection becomes shorter. It becomes obvious that that the time interval between pilot and main injections varies according to engine speed.

Figure 4.12 illustrates the solenoid current signal with the engine operated at full load and 3000 RPM. As can be seen there is only one injection event per cycle but with considerably longer duration than previously (approx. 1.2 ms). In addition the shape of the signal is different. Whereas at low engine speed the signal shape consist of two steep ramps (rise and fall) which are the opening and closing phase of the solenoid , at full load -high speed the signal has an additional holding-current phase. After the steep ramp which is the opening of the solenoid valve, the current drops to approx. 11Amps. This design has been possibly made in order to reduce the power loss in the ECU and the injector itself.

The results captured during all measurement were presented to R2G2 Controls Ltd®, a correspondence company based in the United Kingdom. The company supplies diesel engine management systems as well as fuel injection system control units for defence applications.

A prototype ECM was developed for the E7 engine. Figure 4.13shows a photograph of the R2G2 ECM with the top cover removed.

The ECM is trigged by a crankshaft encoder attached on the E7 engine providing two TTL signals corresponding to crank angle and to engine TDC. An additional shaft encoder attached on the engines camshaft provides the combustion TDC flag to the device.

The output of the ECM is totally configurable through a PC interface called R2Scope shown in Figure 4.14. R2Scope is a software package that interfaces with the R2G2 ECM which enables monitoring and editing of controller parameters along with logging and graphing capabilities. The start of the injection the injection duration and the number of injections are few of the parameters that can be controlled via the interface in real time.

Figure 4.13 R2G2 diesel ECM (electronic control module)

The following software ECM description was adapted from (Adatia, 2006):

Software was developed as an interface between the control unit and the user. In order to "simplify" the up-front calibration process a few restrictions were incorporated within the software. The left-hand side of the screen serves as a display screen to provide critical information about the engine and controller.

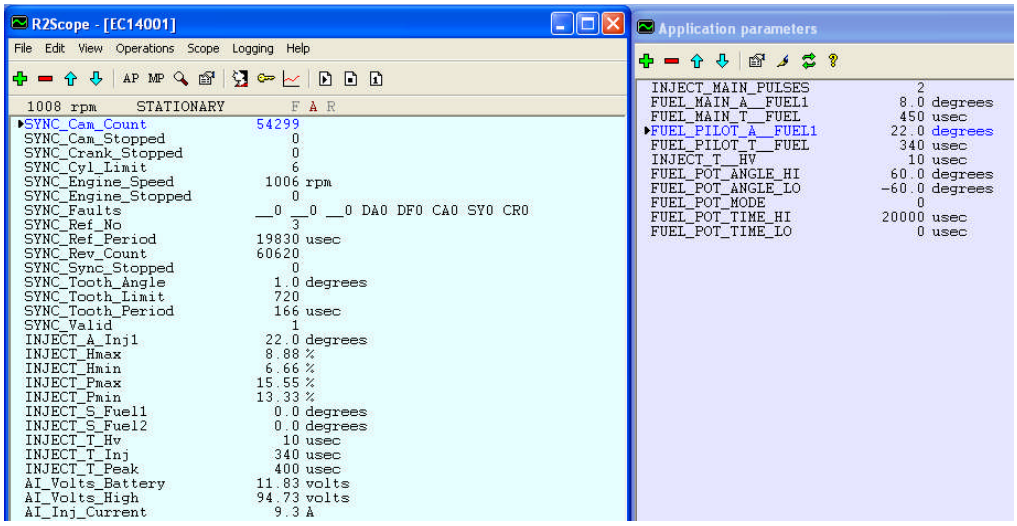

Figure 4.14 Diesel ECM software interface

For example, it displays the engine speed and high voltage supplied to the injector. The red switch, on the front panel controls the high voltage. As one of the restrictions, only the pilot injection can be supplied with a high voltage around 95 [V]. The right hand

side of the screen is the “input” screen where the different application parameters can be modified. For the scope of this project, only the main parameters used for calibration purposes are displayed. “INJECT_MAIN_PULSES” is the first parameter listed. The controller encompasses the capability of having up to four main injection pulses. Each injection pulse is then equally divided by the indicated injection duration (“FUEL_MAIN_T_FUEL”), which is specified in micro-seconds. The start of the main injection pulse is controlled by “FUEL_MAIN_A_FUEL1”. The software was set-up so that 8.0 degrees indicates 8.0 degrees before top dead centre (BTDC). The next parameter listed “FUEL_PILOT_A_FUEL1” controls the start of the pilot injection BTDC. “INJECT_T_HV” is a parameter to specify the duration the high voltage should be applied to the pilot injection in order for it to open rapidly. The high voltage is only necessary for about 10 [μs] to initially open the injector. However, once the needle has been lifted, only 12 [V] is supplied for the remainder of the injection duration to keep the injector open. It is important to note that the pilot injection cannot be split up into a series of pulses. The pilot injection always has to precede the main injection, or in other words, the main injection pulses cannot occur before the pilot. By setting the pilot duration to zero, the main pulses can be injected as a series of pulses, but the drawback is the high voltage supply is only configured for the pilot injection. If the main injection was set before the pilot, the pilot injection takes precedence and the main injection would not inject until the pilot injection was completed. The black knob outlined in Figure 4.13 is known as the “pot controller”. Based on the number entered as the “FUEL_POT_MODE” parameter, the knob provides a means of manually controlling any of the parameters listed (Gunner, 2006).

4.5 Diesel spray characterisation

4.5.1 Introduction

DCi engines generally have injectors with hole-type nozzles with 4-10 injection orifices arranged as centrally as possible. The injection direction is very precisely matched to the combustion chamber design. Divergences of the order of only 2 degrees from the optimum injection direction lead to a detectable increase in black smoke emission and fuel consumption (Bauer, 2004). Therefore fuel injector nozzles are designed exclusively for the specific engine type and the injection system in which they are to be used.

Many quantitative as well as qualitative diagnostic methods are utilised to study the diesel spray process. Optical techniques are generally the best choice since they are relatively non- intrusive. PIV (particle image velocimetry), PDPA (phase Doppler particle analyser), LDV (laser Doppler velocimetry) and photographic imaging are few examples. Among these techniques direct photographic imaging is particularly suitable for quantification of the global characteristics of fuel spray throughout the injection period (J.Shao, 2002).

The main reason for undertaking this work was to understand and quantify the solenoid injector spray geometric characteristics in order to design the new cylinder head and the combustion chamber for the E7 engine. Although the diesel injector was chosen from a production engine, its spray characteristics were not available. These characteristics include spray tip penetration, the various spray cone angles and the injector inclination angle as they are defined in Figure 4.15. All these parameters are critical in determining the precise position of the injector spray relative to the engine combustion chamber.

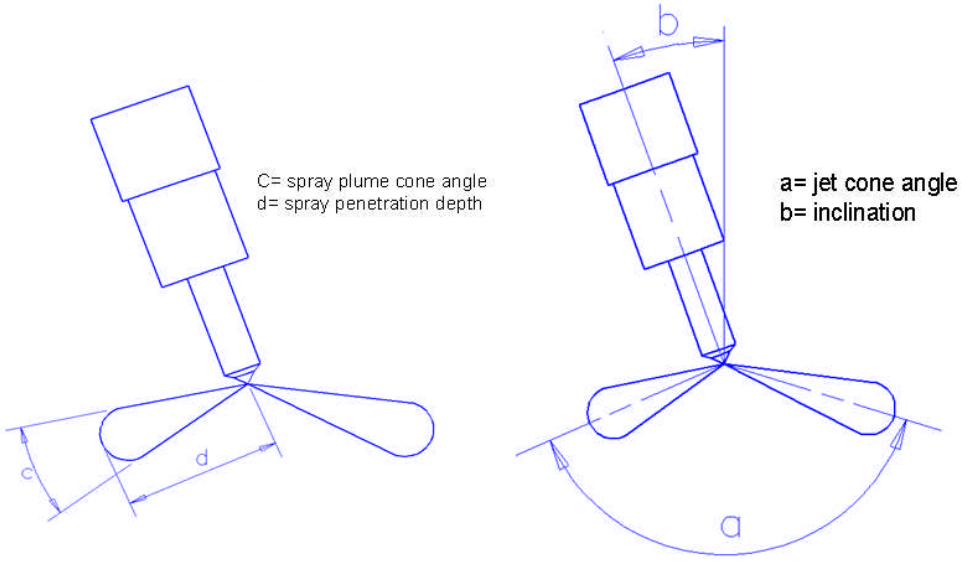

Figure 4.15 Definition of spray parameters

After a brief investigation on available methods and techniques commonly used to characterise sprays, the shadowgraph technique was found to be the most technically appropriate for this study.

4.5.2 Shadowgraph system setup

Figure 4.16 shows the shadowgraph rig and Figure 4.17 a schematic of the experimental arrangement. The diesel common rail rig which was developed for the E7 engine was used to produce a constant injection pressure of 1500 bar. All the experiments were carried out in an optically accessible bomb (constant volume chamber) for atmospheric and for pressurised conditions. The fuel injector was mounted on the top of the bomb using a special adaptor which allowed injector rotation around its axis.

The Cranfield bomb is made out of steel and it has thick circular quartz windows which give excellent optical access and at the same time withstand high pressures. A high intensity flash source was used to back-illuminate the injection spray. A white paper sheet was placed between the flash light and the bomb window to diffuse the. Digital images were captured using a CCD Flowmaster 3 industrial camera which was operated by the Lavision PC. Care was taken with the selection of the camera positioning and the choice of a 105mm UV lens so that clear images were produced close to the injector tip. A master pulse generator was used for triggering the injector and through a fixed delay box the LaVision PC.

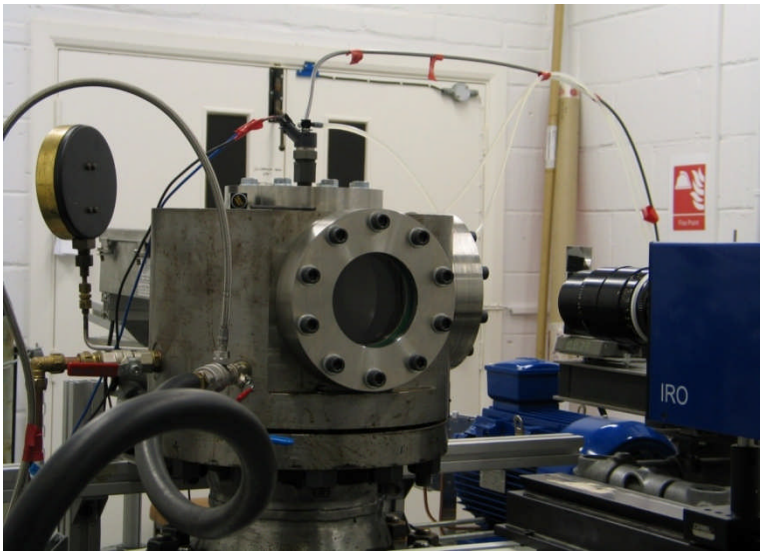

Figure 4.16 Photograph of the shadowgraph set-up

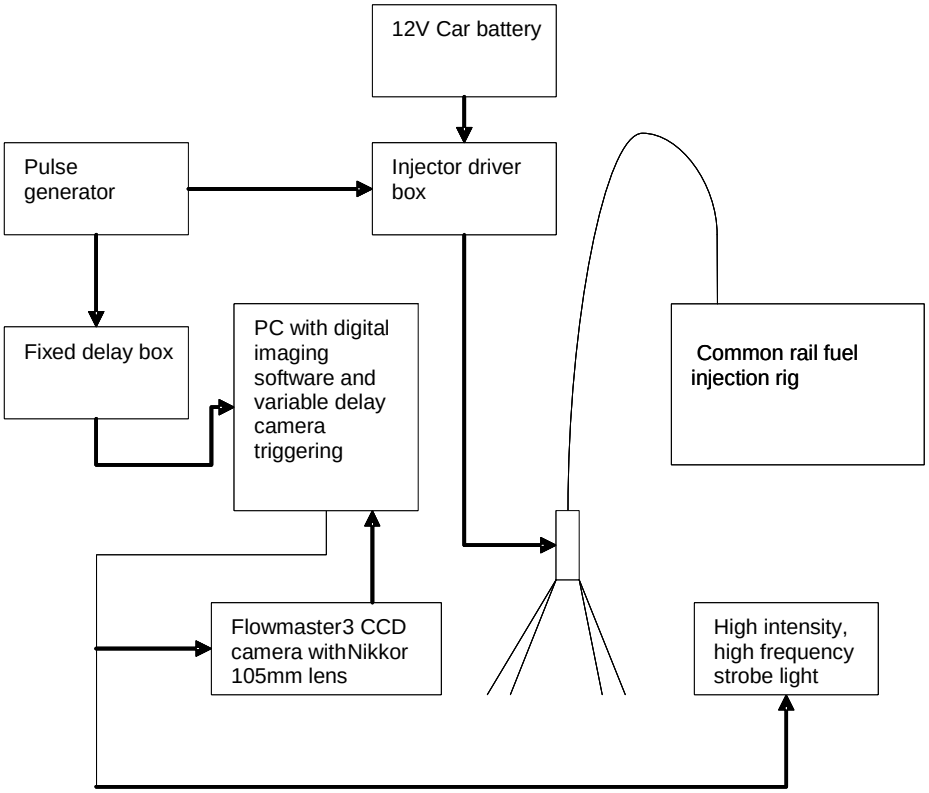

Figure 4.17 Schematic of the shadowgraph setup

4.5.3 Shadowgraph measurements

The injection orifices are usually equally spaced around the cladding of the nozzle cone but at different angles in order to allow injector inclination and accurate spray pattern for the combustion chamber. The injector inclination is a common practice in small engines where the limited space makes difficult to place the injector in the combustion chamber centre.

Initially a few shadowgraph images were taken from below the injector to examine the exact orifice locations on the injector nozzle with respect to injector body orientation. For this measurement one side window of the three was removed from the bomb and the injector was placed in a special holder made out of sandblasted Perspex which allowed the flash light to illuminate the spray from its top side. The CCD camera was placed at the opposite side of the bomb as it is shown in Figure 4.18.

For each test the injector was held open for 2ms at a time. The current passing to the injector solenoid was monitored in an oscilloscope using a current probe. Every image represents an average of 10 single-shot images with a resolution of 1280X1024 pixels.

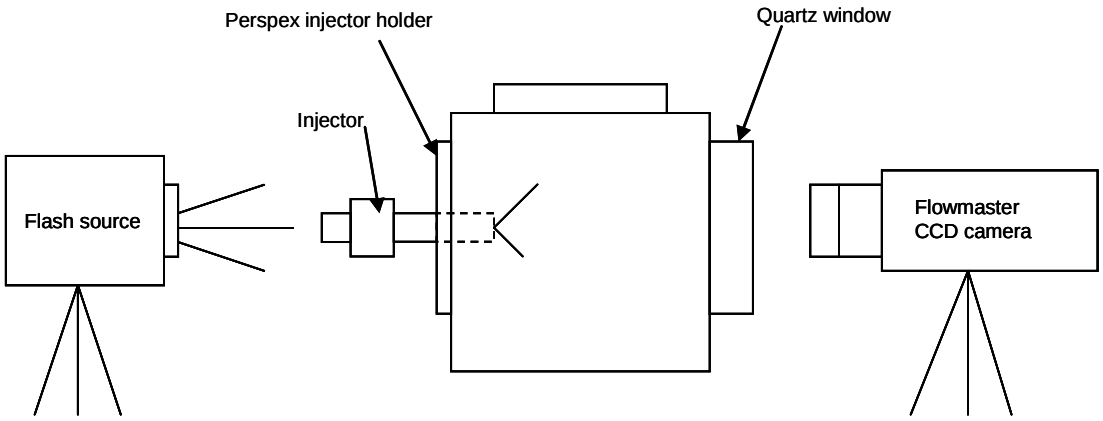

Figure 4.18 Schematic of the shadowgraph setup for the below spray images

Figure 4.19 and Figure 4.20 show average shadowgraph images from below of the fuel injector captured at 2ms after the start of the triggering signal at different flash light angles. Subsequently the two images were combined using the LaVision digital image processing software as it is shown in Figure 4.21. This technique was used in order to remove the unavoidable injector body shadow.

The images taken from the below the injector verified that the five orifices are equally spaced around the circumference of the injector nozzle tip.

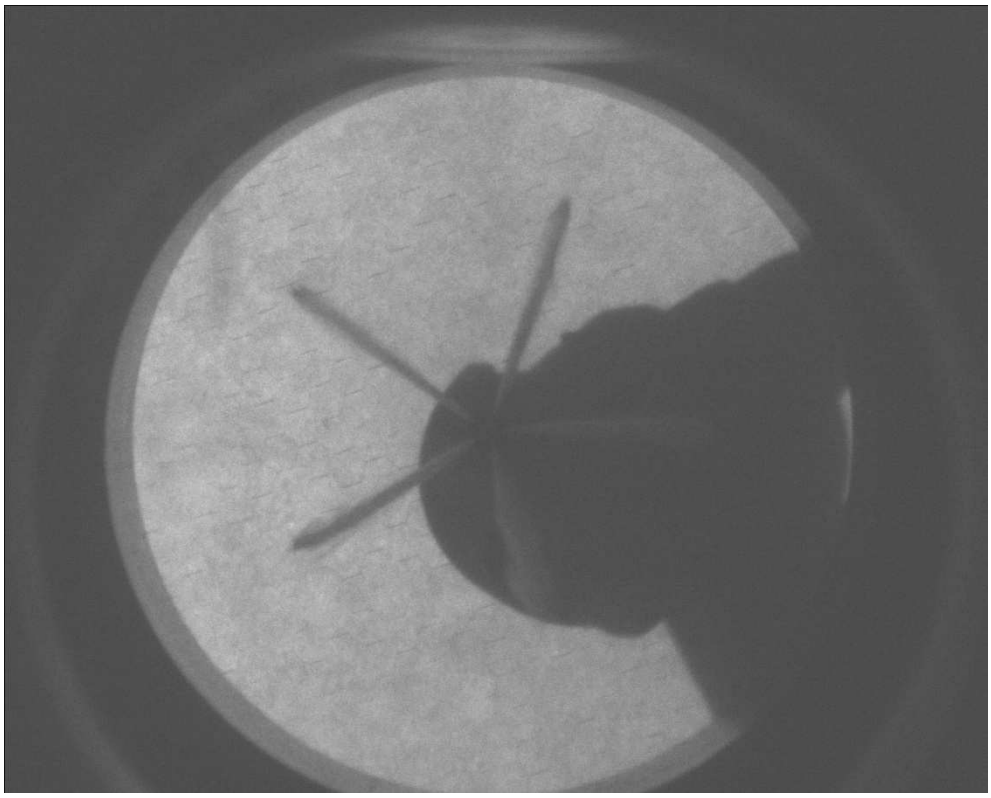

Figure 4.19 Spray image from the below after 2ms from the injection signal. Bomb pressure: atmospheric, fuel pressure 1500bar

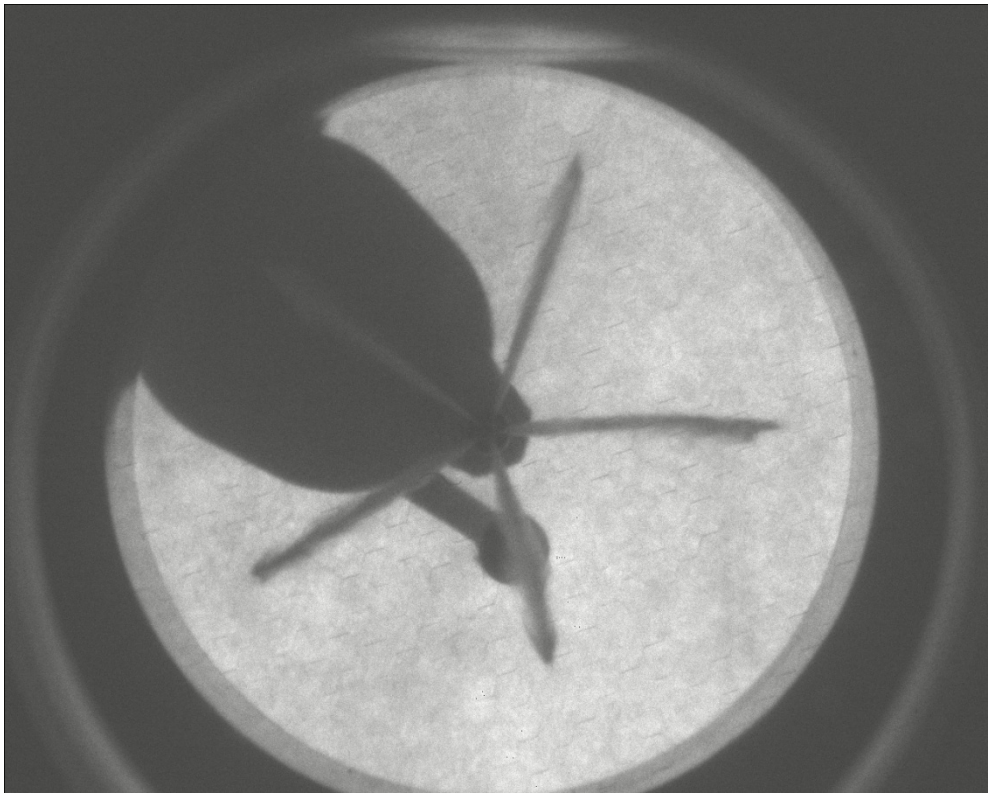

Figure 4.20 Spray image from the below after 2ms from the injection signal. Bomb pressure: atmospheric, fuel pressure 1500bar

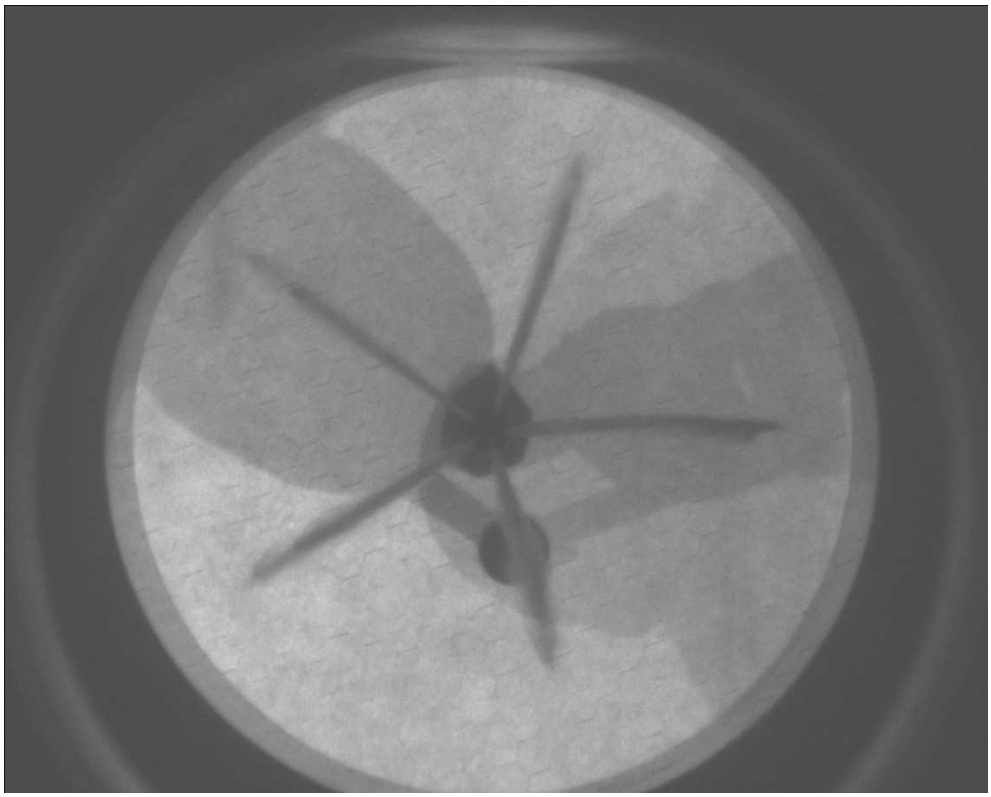

Figure 4.21 Combined shadowgraph images from Figure 4.19 and Figure 4.20using LaVision image processing software

Normally tip penetration measurements can be performed from images taken from below the injector spray if the nozzle orifice angles are known. Since this information was not available, an alternative way of measuring tip penetrations accurately was by capturing spray images from the side of the injector. The schematic in Figure 4.22 show how this was achieved.

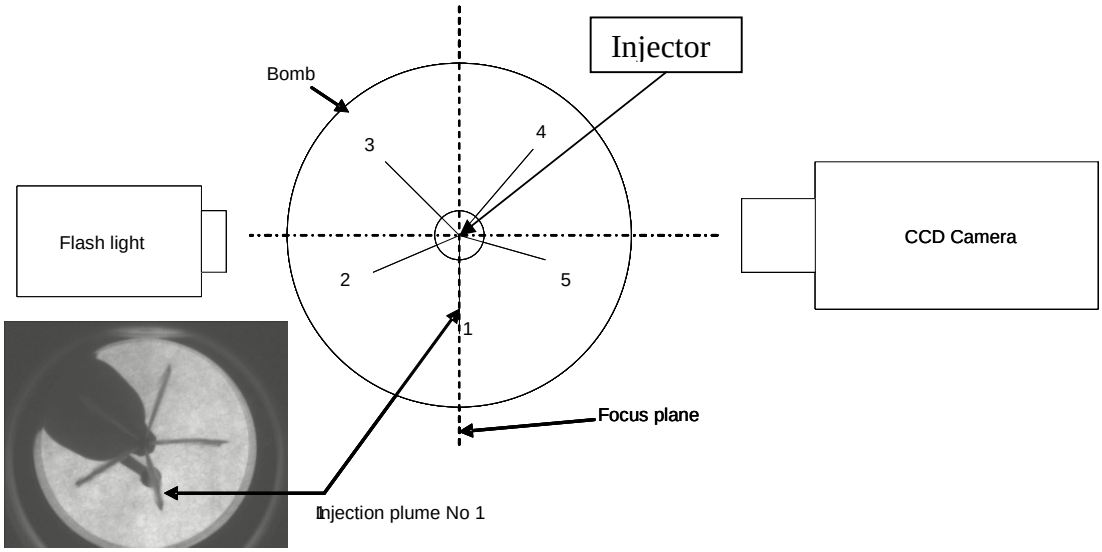

Figure 4.22 Schematic of shadowgraph setup for tip penetrations

A stainless steel adaptor was initially fabricated in order to mount the injector on the top the bomb. The adaptor allows injector rotation at five different positions. At each position a corresponding orifice coincides with the camera focusing plane. This gives the advantage to study each plume separately. However for nozzles with six or more orifices this technique might not be applicable.

Figure 4.23 Injector bomb adaptor

The fuel injector was placed in the bomb as it is shown in Figure 4.23 and the CCD camera was focused on injection plume No1 as this is defined in the schematic in Figure 4.22. Fuel was delivered at constant pressure 1500 bar and the injection duration was set

to 2ms for all measurements. Digital images were captured at atmospheric conditions from 3 spray plumes at three steps 0.5, 0.8 and 0.9ms after the triggering signal. Spray plume No 4 is symmetrical with plume No 3 and plume No5 is symmetrical with plume 2 (defined in Figure 4.22).

Subsequently the bomb was pressurised with oxygen free nitrogen at 40 bar and the same measurements were repeated. As an extra precaution, a vacuum pump was used to remove any excess of oxygen before pressurising the bomb. All measurements were performed at room temperatures approximately 20º C.

Images from Figure 4.26 to Figure 4.37 show the shadowgraph measurements taken for spray plume No1 under atmospheric and pressurised conditions at 0.5, 0.8, 09, 1, 1.5,2 and 2.5ms after the triggering pulse. The development and subsequent decay of the spray is readily seen and assessed using the dimensioned x and y axes.

These image sets have been used to calculate the penetration depth of each spray with respect to time as shown in Figure 4.25. The spray penetration depths have been measured using LaVision software. For the avoidance of doubt, the term 'penetration depth' is taken to mean the distance between the spray front and the injector tip measured along the centre line of the plume cone.

The measurement of the spray penetration depths will be used initially to establish a relationship between solenoid energising times (usually in μs) and spray penetration depths in the optical bomb. This information will be used for determining the exact geometry of the newly developed combustion chamber as it will be seen later on in section 4.6.3 and also for developing and setting the safety limitations on the ECM output signals when the ECM will be driving the injector on the running engine.

For calibration (image pixel to actual length conversion) a shadowgraph image of a reference grid shown in Figure 4.24 was used. Each square within the grid represents one millimetre.

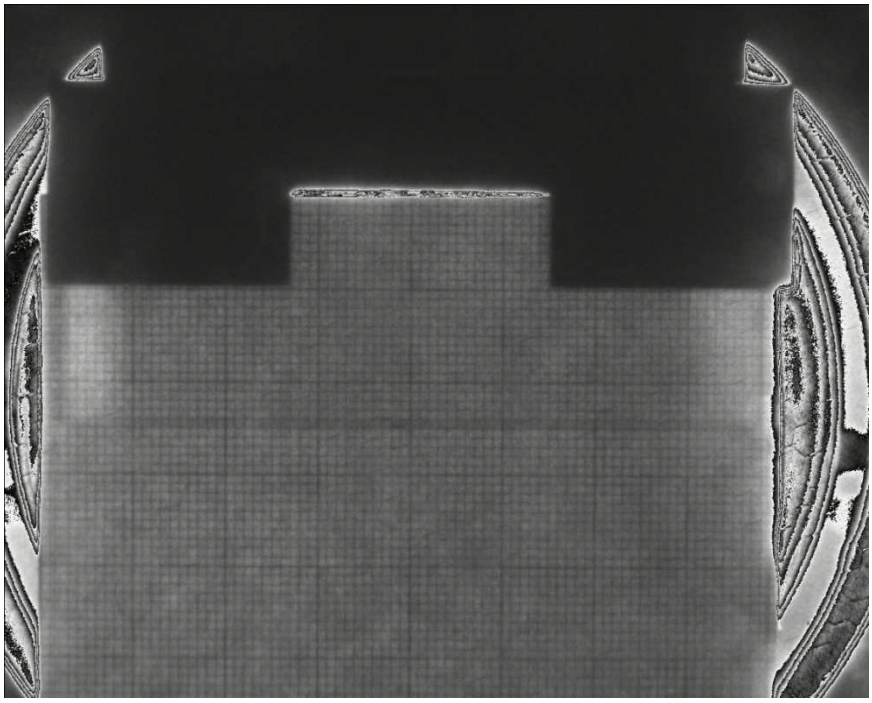

Figure 4.24 Calibration grid

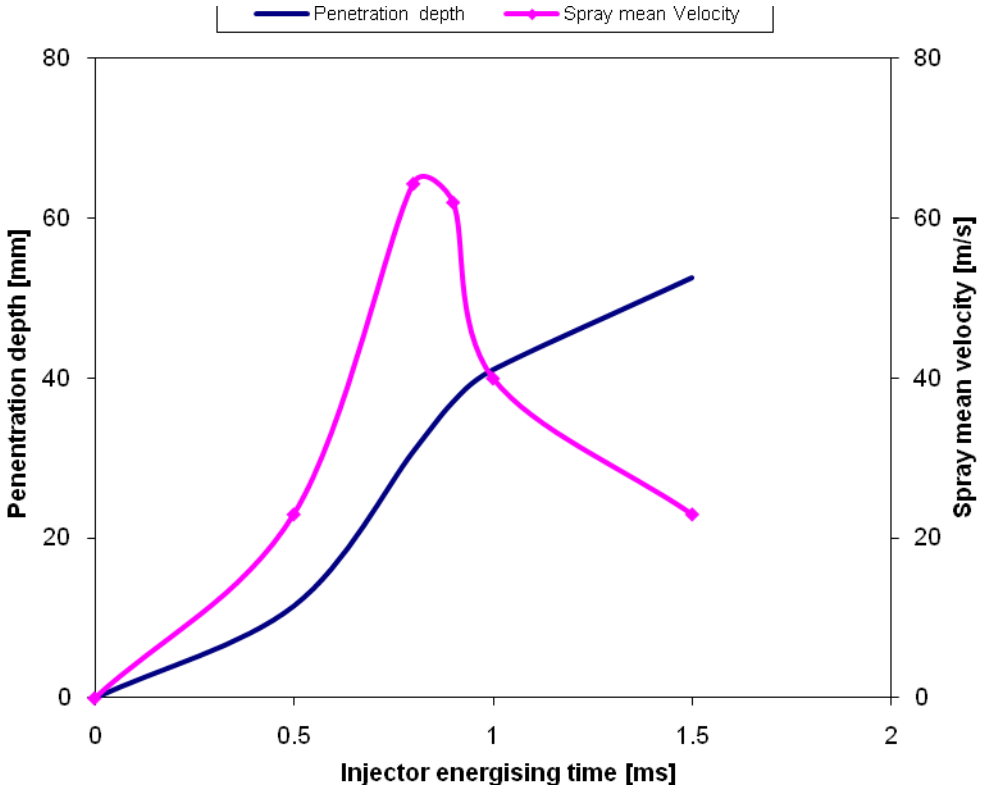

Figure 4.25 Spray tip penetrations for spray plume No 1

All shadowgraph images shown are the average of 10 separate single shot images. Although the spatial resolution of the image is compromised in this way (the images appear blurred in the outer edges) the averaging technique allows for the measurement of the spray cone angle with certainty. Table 4-2 shows the plume direction angles measured from these images. The spray direction angles have been measured using LaVision software. The same procedure was repeated for injection plumes 2 and 3.

Spray plume No	Spray direction angle
1	53°
2	66°
3	93°

Table 4-2 Injector spray direction angle for plume No1

4.5.4 Conclusions

The results presented have demonstrated the use of the shadowgraph digital imaging technique to quantify and analyse important characteristics of the diesel spray.

The results obtained have shown that the tip penetration under a lower bomb pressure is longer than that under atmospheric bomb pressure for the same injection pressure. The reason is that under high pressure the ambient density increases therefore the spray has to overcome higher resistance during penetration. The tip penetration appears to be linear with the time in the earlier stages of the injection process. Also the plume cone angles are greater under higher bomb pressures.

The injector plumes do not seem symmetric when viewed from the side because the correct orientation of the injector should consist of a 20º offset. Spray plume N1 has a unique angle. Spray plume No 3 is symmetrical with plume No 4 and plume No2 is symmetrical with plume 5 (definition is given in Figure 4.22).

Figure 4.26 Injector plume 1, bomb pressure: atmospheric, fuel pressure 1500bar, time: 0.5ms

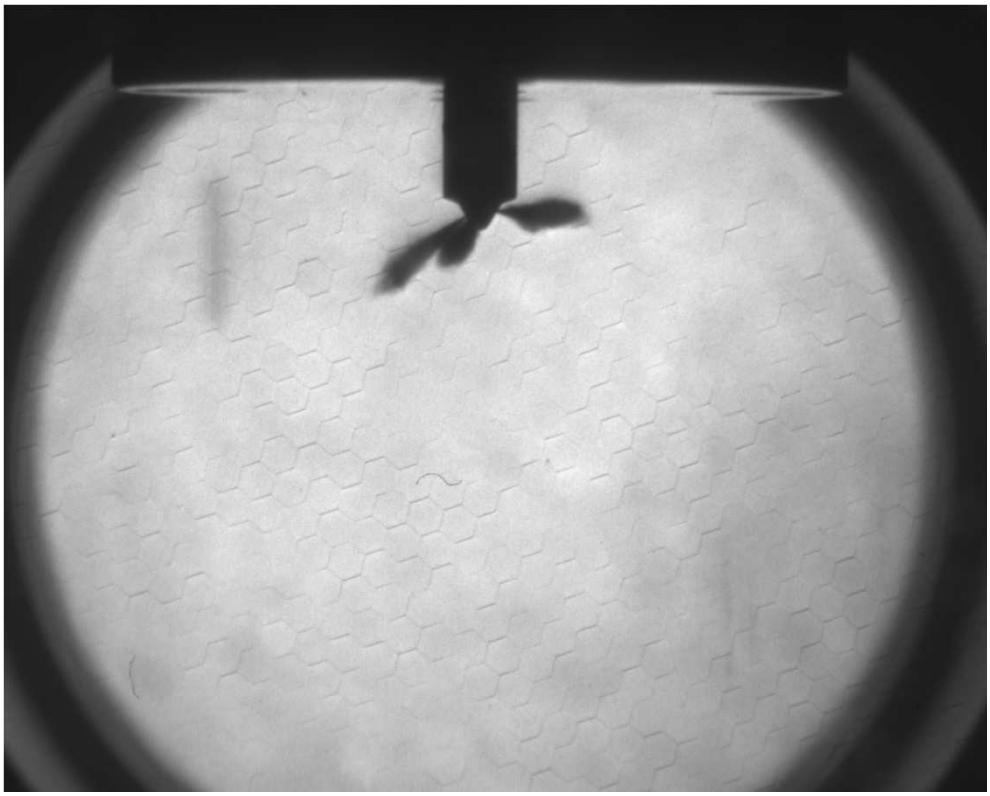

Figure 4.27 Injector plume 1, bomb pressure: 40bar, fuel pressure 1500bar, time: 0.5ms

Figure 4.28 Injector plume 1, bomb pressure: atmospheric, fuel pressure 1500bar, time: 0.8ms

Figure 4.29 Injector plume 1, bomb pressure: 40bar, fuel pressure 1500bar, time: 0.8ms

Figure 4.30 Injector plume 1, bomb pressure: atmospheric, fuel pressure 1500bar, time: 0.9ms

Figure 4.31 Injector plume 1, bomb pressure: 40bar, fuel pressure 1500bar, time: 0.9ms

Figure 4.32 Injector plume 1, bomb pressure: atmospheric, fuel pressure 1500bar, time: 1ms

Figure 4.33 Injector plume 1, bomb pressure: 40bar, fuel pressure 1500bar, time: 1ms

Figure 4.34 Injector plume 1, bomb pressure: atmospheric, fuel pressure 1500bar, time: 1.5ms

Figure 4.35 Injector plume 1, bomb pressure: 40bar, fuel pressure 1500bar, time: 1.5ms

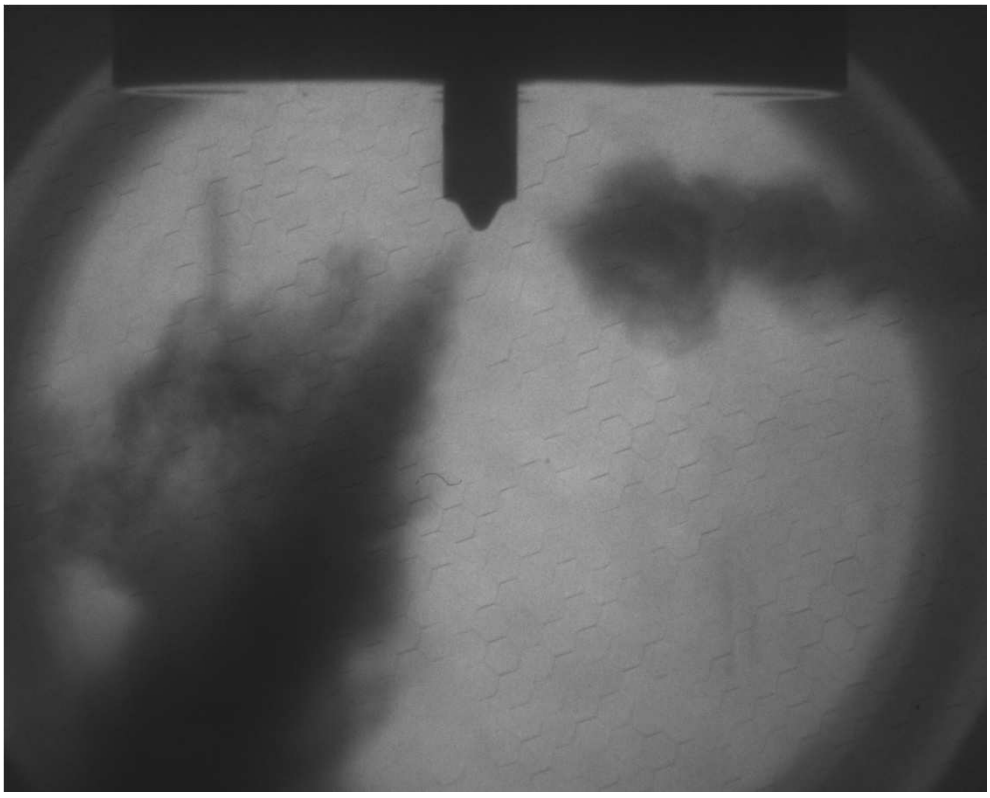

Figure 4.36 Injector plume 1, bomb pressure: atmospheric, fuel pressure 1500bar, time: 2ms

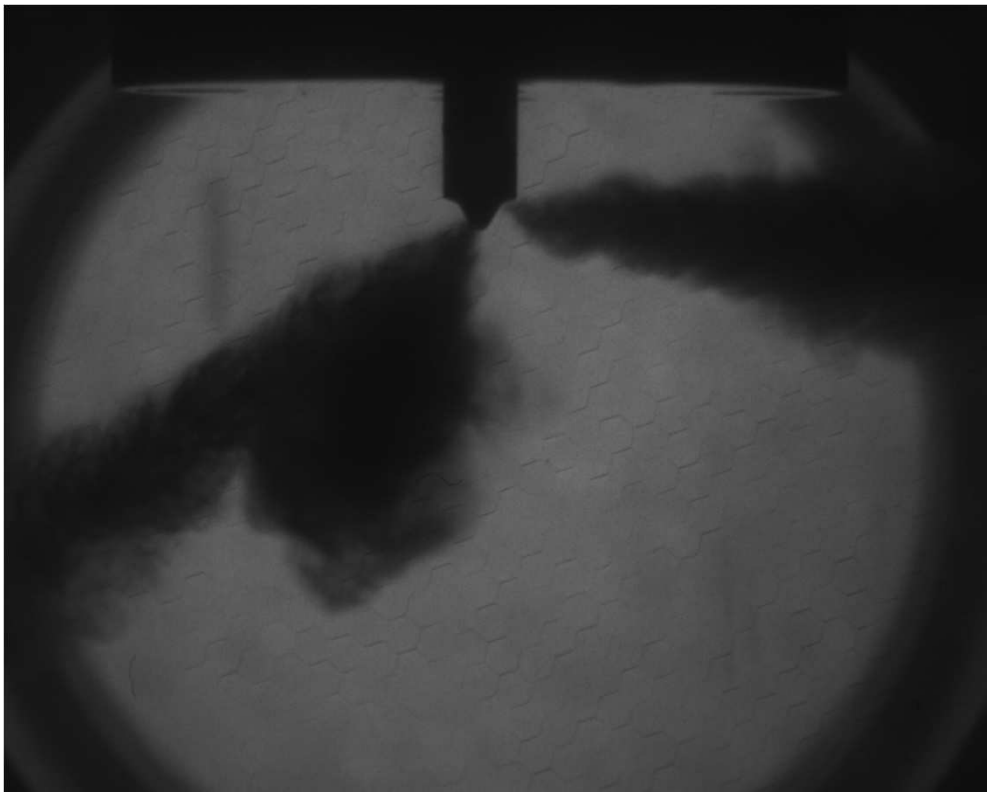

Figure 4.37 Injector plume 1, bomb pressure: 40bar, fuel pressure 1500bar, time: 2ms

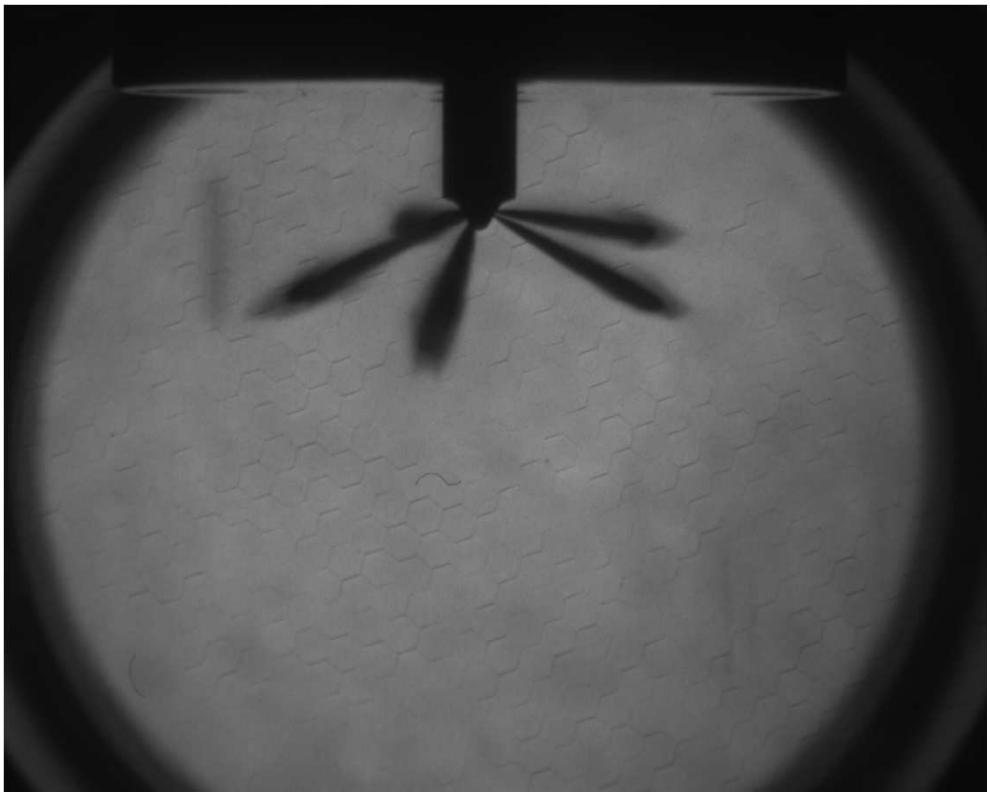

Figure 4.38 Injector plume 2, bomb pressure: atmospheric, fuel pressure 1500bar, time: 0.5ms

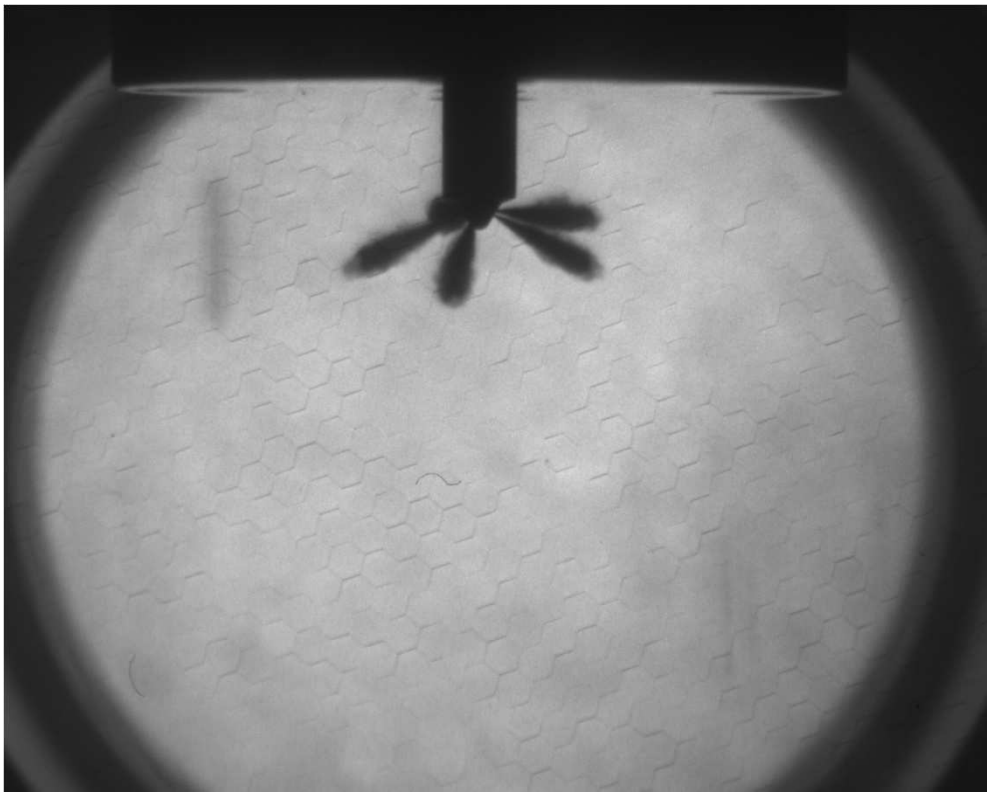

Figure 4.39 Injector plume 2, bomb pressure: 40bar, fuel pressure 1500bar, time: 0.5ms

Figure 4.40 Injector plume 2, bomb pressure: atmospheric, fuel pressure 1500bar, time: 0.8ms

Figure 4.41 Injector plume 2, bomb pressure: 40bar, fuel pressure 1500bar, time: 0.8ms

Figure 4.42 Injector plume 2, bomb pressure: atmospheric, fuel pressure 1500bar, time: 0.9ms

Figure 4.43 Injector plume 2, bomb pressure: 40bar, fuel pressure 1500bar, time: 0.9ms

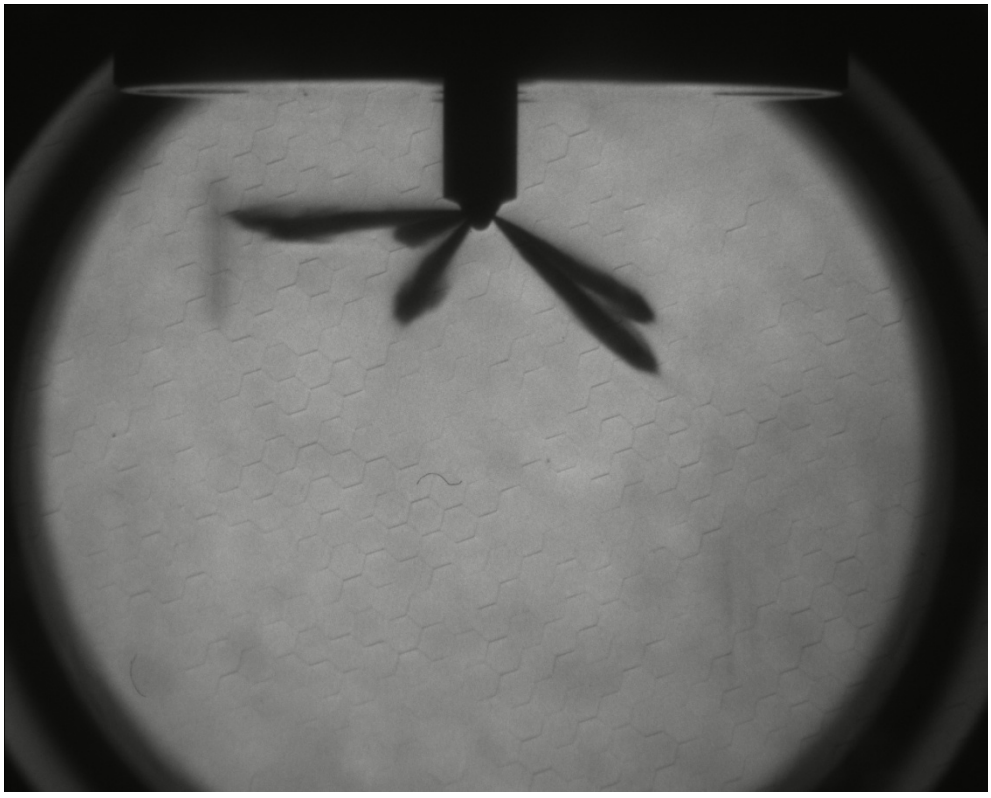

Figure 4.44 Injector plume 3, bomb pressure: atmospheric, fuel pressure 1500bar, time: 0.5ms

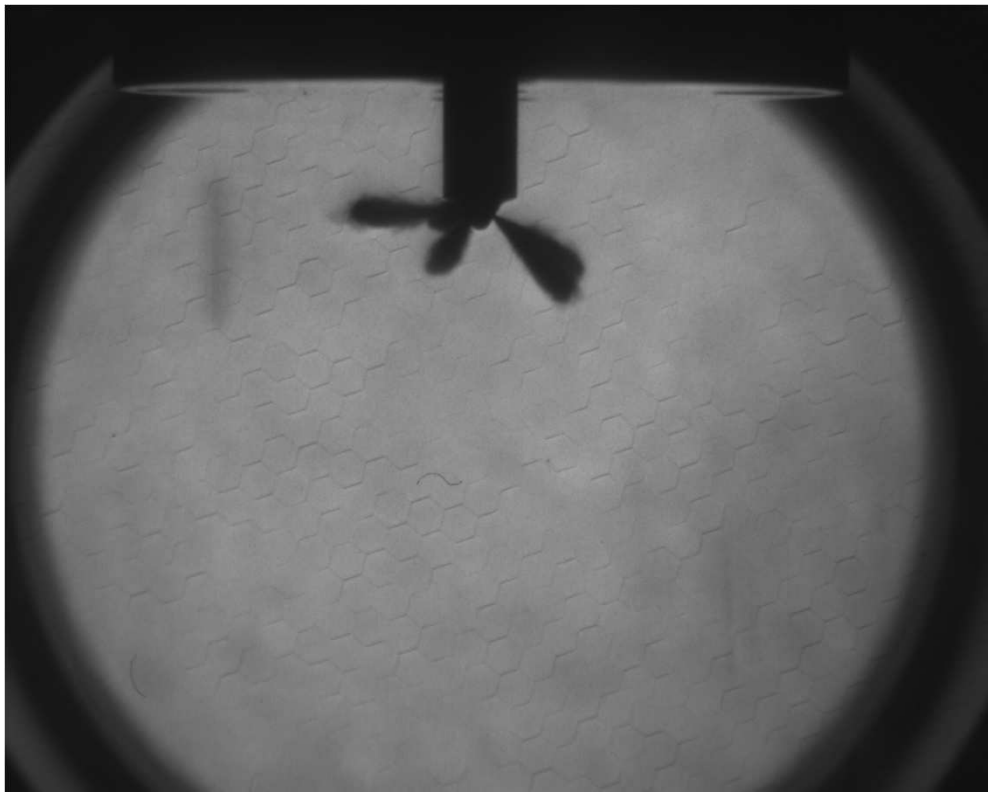

Figure 4.45 Injector plume 3, bomb pressure: 40bar, fuel pressure 1500bar, time: 0.5ms

Figure 4.46 Injector plume 3, bomb pressure: atmospheric, fuel pressure 1500bar, time: 0.8ms

Figure 4.47 Injector plume 3, bomb pressure: 40bar, fuel pressure 1500bar, time: 0.8ms

Figure 4.48 Injector plume 3, bomb pressure: atmospheric, fuel pressure 1500bar, time: 0.9ms

Figure 4.49 Injector plume 3, bomb pressure: 40bar, fuel pressure 1500bar, time: 0.9ms

4.6 Cylinder head design and development

One of the most challenging tasks of this thesis was the design and the development of a direct injection cylinder head for the Ricardo E6 research engine. This involved the extensive use of various CAE tools and the combination of various types of knowledge. The design was made on I-DEAS NX 3D CAE software (release: 11m2). Three dimensional modelling software is a very powerful tool for designing complex parts but its real advantage is the parametric modelling capability. 3D CAD tools can solve geometrical problems which are complicated and time consuming to solve by hand.

Some important considerations concerning the new design were the following:

- Ricardo E6 cylinder geometry
- New combustion chamber geometry
- Injector spray location
- Location of the cylinder head bolts
- Valve sizes
- Shape and dimensions of inlet and exhaust ports
- Valve-train system
- Instrumentation (pressure transducer,)
- Lubrication
- Cooling
- Manufacturing costs

4.6.1 Design methodology

The first step of the design was to create a general 3D model of the existing E6 base engine. Figure 4.50 shows an isometric view of the Ricardo E6 base engine designed on I-DEAS NX. The existing cylinder bore together with the location of the cylinder head studs and the cooling channels were the primary constrains which they had to be considered for the design of the new cylinder head. Since the cylinder-barrel is the interface between the base engine and the cylinder head, is was critical to have a precise 3D drawing of the exact location of the cylinder head studs and the various water and oil channels. Figure 4.51 shows the cylinder-barrel assembly of the E6.

With the physical constrains identified, the design of the cylinder head was based upon intention and level of importance of each feature. The overall cylinder head design was constantly revised during development. Improving one aspect of the cylinder head design had immediate impact on others so constant revision was necessary in order to eliminate design compromise.

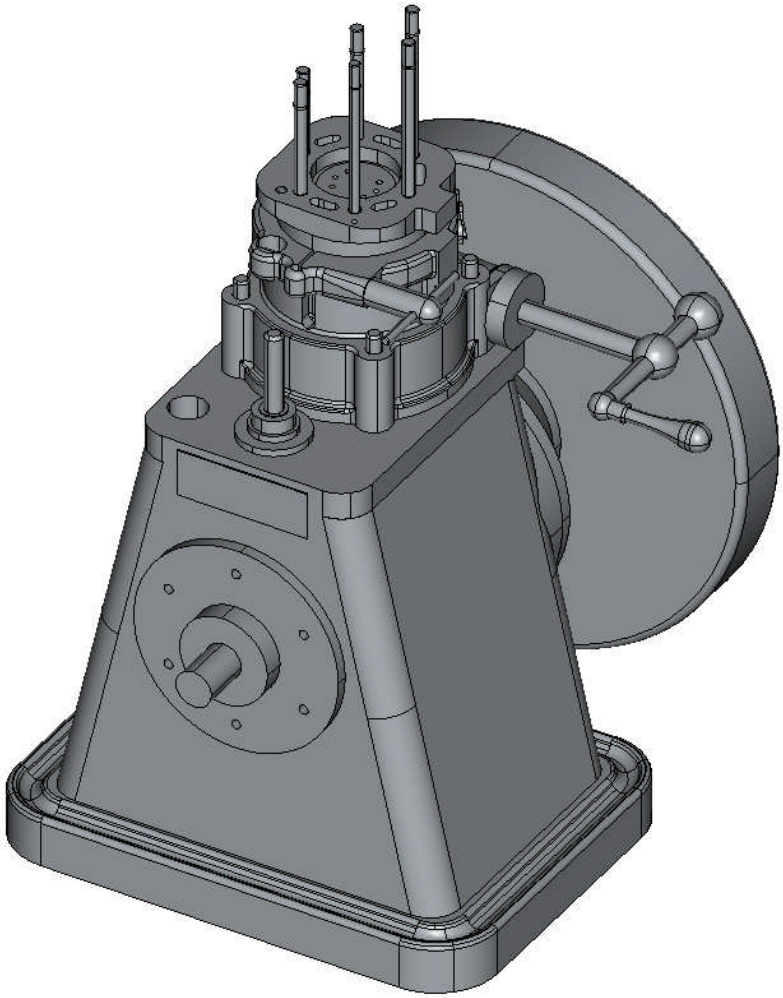

Figure 4.50 The Ricardo E6 base engine with the variable compression ratio mechanism

Figure 4.51 The Ricardo E6 cylinder barrel

4.6.2 Combustion chamber design

Combustion chamber design is one of the most important aspects concerning diesel engine performance. Over the years, various designs and ideas have been proposed and tested in order to improve the combustion chamber geometry. The most common type found in small to medium high speed engines is the deep bowl-in-piston type. As engine size decreases and maximum speed rises, higher amount of swirl is required to obtain better air-fuel mixing rates. The swirl is generated by suitably shaped inlet ports and it is amplified during compression by forcing the air toward the cylinder axis into the deep bowl-to-piston combustion chamber (Heywood, 1988).

The combustion chamber of the Ricardo E7 was designed according to the dCi engine bowl-in-piston combustion chamber but with slightly different offsets from the centre of the cylinder. These offsets were necessary for packaging the injector in the cylinder head. Initially a mould was taken of the original shape of the dCi combustion chamber and precisely measured. Subsequently a 3D model of the chamber was generated on IDEAS-NX. Figure 4.52 shows the 3D solid model of the new combustion chamber.

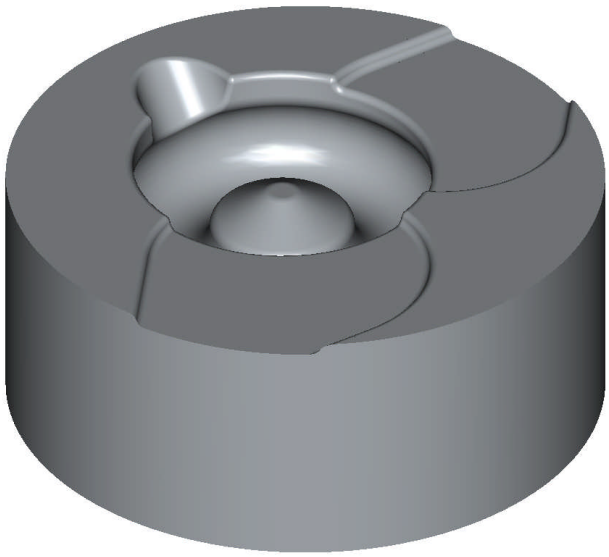

Figure 4.52 E7 newly designed combustion chamber

A new piston crown was manufactured from aluminium alloy according to the 3D drawings. The part was made in two pieces to allow machining. The deep bowl-in-piston combustion chamber required a longer piston crown resulting to an increased piston top land area and to a heavier piston assembly. The new piston crown was bolted on the top of the original E6 piston using six M6 Allen screws and lock-tight. Figure 4.53 and Figure 4.54 show photographs of the piston assembly. Details on the design can be found in the Appendix.

Figure 4.53 Piston assembly parts

Figure 4.54 Piston assembly

The necessity of having bowl-in-piston combustion chamber resulted to a heavier piston crown design, which influenced the original engine balancing mechanisms due to the additional reciprocating mass.

4.6.3 Injector spray position

An important parameter in combustion chamber design is the location of the fuel spray in the combustion space. Divergences of the order of only 2 degrees from the optimum injection direction lead to a detectable increase in black smoke emission and fuel consumption (Bauer, 2004). Thus fuel injector nozzles are designed and optimised exclusively for a specific engine. During engine development extensive experimental work is required in order to match injector spray pattern with combustion chamber geometry.

As a general rule, it is ideal to have the injection fuel spray settled within the toroidal radius of the combustion chamber. Then the injection strategy can be adjusted to prevent the injected fuel from coming into contact with the cylinder wall, which would increase the smoke, HC and CO emission levels.

The results from diesel spray characterisation measurements from chapter 4.5 were used in order to determine the best injector spray position. Initially the spray pattern of the diesel multihole injector was modelled on IDEAS NX. Then the cone angles and tip penetration depths were carefully matched to the shadowgraph results obtained from the pressurised bomb. The pressurised results were chosen as they are closer to the actual engine compression conations. Consequently the spray geometry was modelled for each penetration depth.

Using the results from spray modelling, the location of the injector relative to cylinder head was defined. Figure 4.56 shows a cutaway of the cylinder head with the injector located at 20° angle.

The injector inclination angle was precisely determined. Hence, when the injector is positioned at an angle of 20° measured from perpendicular axis, all injection plumes have the same distance from the toroidal combustion chamber surface.

The results also suggest that fuel spray will be settled within the toroidal radius of the combustion chamber if the injection durations are kept below 500μs. However this is only a general guidance and the injection duration depends on engine operating conditions.

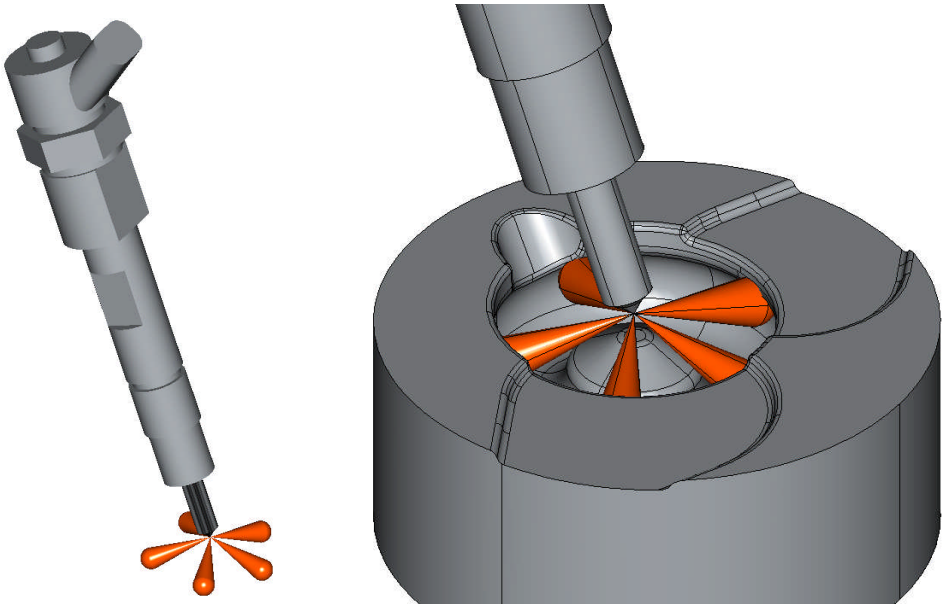

Figure 4.55 Matching diesel spray to combustion chamber

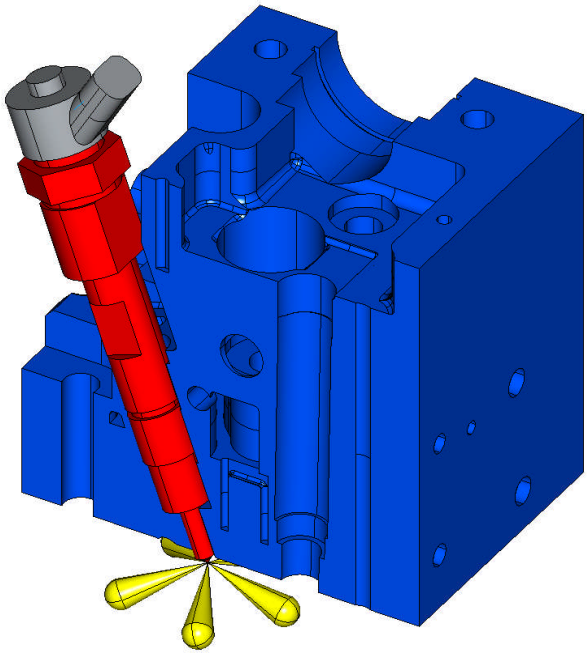

Figure 4.56 Injector position

4.6.4 Valve sizes

Two valve single overhead camshaft design was adopted in order to allocate space for the injector and the combustion instrumentation. The next task was to decide the largest valve sizes that could be accommodated within the cylinder bore radius whilst maintaining adequate cooling between them and also providing sufficient space for the injector to be positioned as centrally in the cylinder as possible. Clearly the design intension here was to optimise injector spray position whilst maintain good engine breathing.

For two vertical valves operating within a cylinder bore B without interference, the maximum inlet port diameter i.e. inner seat diameter is from 0.43-0.46B diameter and the corresponding exhaust port size 0.35-0.37B diameter (Challen & Baranescu, 1999). Exhaust vales are usually made slightly smaller in diameter than the inlet ones since a higher pressure drop is permissible without penalising engine breathing.

One way of checking whether the engine is choked due to insufficient inlet valve size is by using the Match index as it is described by(Taylor, 1999) . This can be defined as the ratio of the speed which the gas moves through the port to the speed of sound in the gas. Experimental work has shown that to maintain good volumetric efficiency the value of Z (Mach index) should not exceed 0.6 with a preferred value of 0.4 and minimum value of 0.25 for rated engine conditions (Challen & Baranescu, 1999).

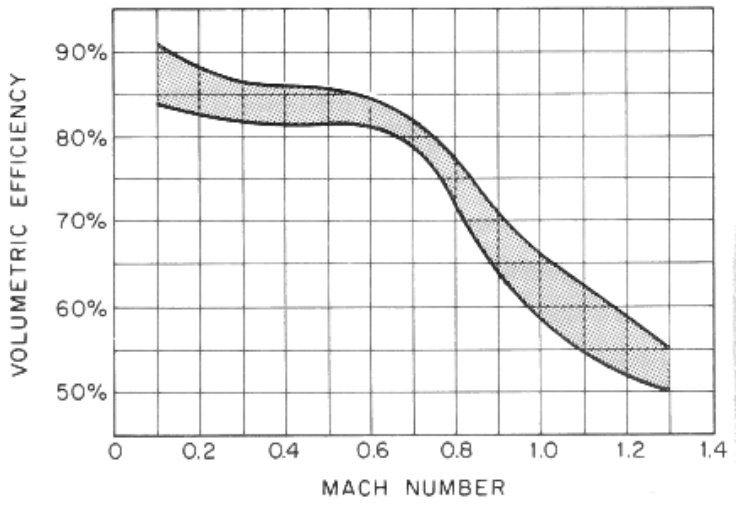

Figure 4.57 Relationship between volumetric efficiency of intake valve port area and Mach number (TRW Valve division, Thompson, Ramo, Wooldridge, Inc.) (Crouse, 1970)

In the particular design the maximum size of the inlet port was constrained from the engine bore and the injector position.

The valves were positioned 8 mm offset from the engine centre line in order to place the injector tip closer to the centre of the cylinder. Hence the valve head diameters were slightly reduced to accommodate this arrangement. This was expected to have a small

influence on engine performance because the engine breathing was already restricted from the intake system of the Ricardo engine.

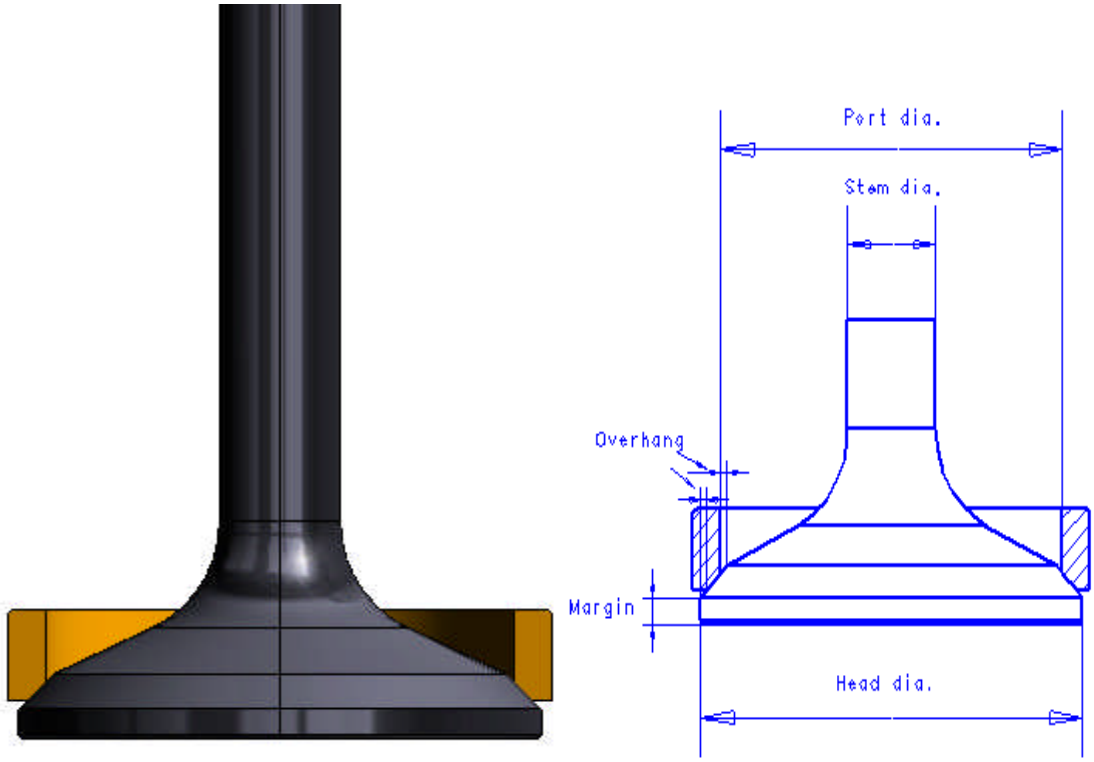

Figure 4.58 Valve and valve seat 3D detail and 2D drawing showing valve head margin and overhang definitions

The valve seat contact areas were carefully designed in order to provide good valve seal. The contact area of the exhaust valve is slightly larger in the exhaust valve in order to provide adequate cooling. However this area should not be too large to cause thermal losses.
Both inlet and exhaust valve face angles were chosen to be 45°. A low angle improves gas flow at low valve lifts but a high face angle is desirable for high seating pressure and good valve seating. Also using 45° face angle, simplifies the manufacturing procedures since it is very common on most passenger cars

Therefore the maximum valve head diameters after taking into account all the constrains and considerations were determined:

- Inlet:……..34.6 mm
- Exhaust :…30 mm

Finally the mean inlet gas velocity at maximum engine operating speed was approximately calculated using the following equation:

$$\upsilon_g = 2LN\left(\frac{B}{d}\right)^2 \text{ m/s} \quad (4.5)$$

were:

υ_g = mean inlet gas velocity [m/s]

L = engine stroke [m]

N = crankshaft speed [rev/s]

B = cylinder bore diameter [m]

d = inlet throat diameter [m]

At 3000 RPM (maximum operating speed of the Ricardo E6) the theoretical mean gas in the inlet port stem area is calculated 54 ms^{-1}. Typical values at maximum power output are 76 m/s for automotive types and up to 52 m/s for the largest stationary engines (Challen & Baranescu, 1999).

To obtain a more realistic result, the mean gas velocity was divided by an estimated mean flow coefficient of 0.383 and divided by the speed of sound in the air in the intake port. For 20 °C the speed of sound for dry air is 330ms^{-1} Hence the Mach number value is equal to 0.43.

Therefore according to the relationship between Mach number and engine volumetric efficiency given in Figure 4.57, the volumetric efficiency of the new valve/port design expected to be between 80 and 85%. This is an acceptable design for the E7 engine considering space imitations as a result of the injector spray location and the combustion instrumentation.

4.6.5 Cylinder port design

The design of inlet and exhaust ports depends mainly on the overall engine design. Detailed shape proportions and critical design areas of typical inlet and exhaust valves and ports are provided from Barne-Moss (Heywood, 1988) and also (Challen & Baranescu, 1999).

A helical inlet port was designed to generate swirl. Swirl is used in direct injection engines to promote good combustion by aiding strong air motion around the fuel injection spray jets. High swirl was a more important on the older diesel engines as injection pressures were much lower. In the modern common rail engines a medium swirl ratio is preferred as mixing is mainly achieved with the high injection pressures. Nevertheless swirl is still beneficial for increasing combustion quality especially at low engine speeds and loads.

Swirl it is defined as the organised rotation of the charge about a cylindrical axis but for IC engines swirl ratio is normally used which is defined as the angular velocity of a solid body rotating flow ω_s, which has the equal angular momentum to the actual flow, divided by the crankshaft angular rotational speed (Heywood, 1988):

$$R_s = \frac{\omega_s}{2\pi N} \tag{4.6}$$

There are other methods of generating swirl for example the use of masked valves or the use of directed ports. Using a masked valve to generate swirl requires greater pressure drops for air and penalised volumetric efficiency. On the other hand a directed port could have been a better solution than the masked valve but the position of the studs on the Ricardo E6 cylinder barrel did not allowed a proper design. Hence using a helical port design was found to be the best means of generating swirl on the particular engine because helical ports are less sensitive to position displacement (whilst position is very critical for the directed ports) since swirl depends on the port geometry above the valve and not on the position of the port relative to the cylinder axis.

Designing a swirl producing helical port is a rather challenging task. Although there are general rules and case studies suggesting good design practices, the most accurate way to assess the swirling ability of the port is still by building and testing prototypes. In addition to that the geometry itself is particularly difficult to model. Even with the help of sophisticated CAD systems available, great effort is still required from the designer.

Several considerations have been made to develop an appropriate helical port for the E7 cylinder head. The most important were:

- Design suggestions from literature
- Engine physical constrains (engine water passages, studs locations)
- The shape of the helical pot from a production dCi engine.

Combining all the above information but above all using good judgement for the shape, several helical port designs were made on IDEAS-NX. The final design of the cylinder head had some impact on the final shape of the helical port due to space limitations. The inlet and the exhaust ports were formed on the cylinder head by machining-out material. Figure 4.59 shows the final shape of the helical port (right) compared to an earlier design (left).

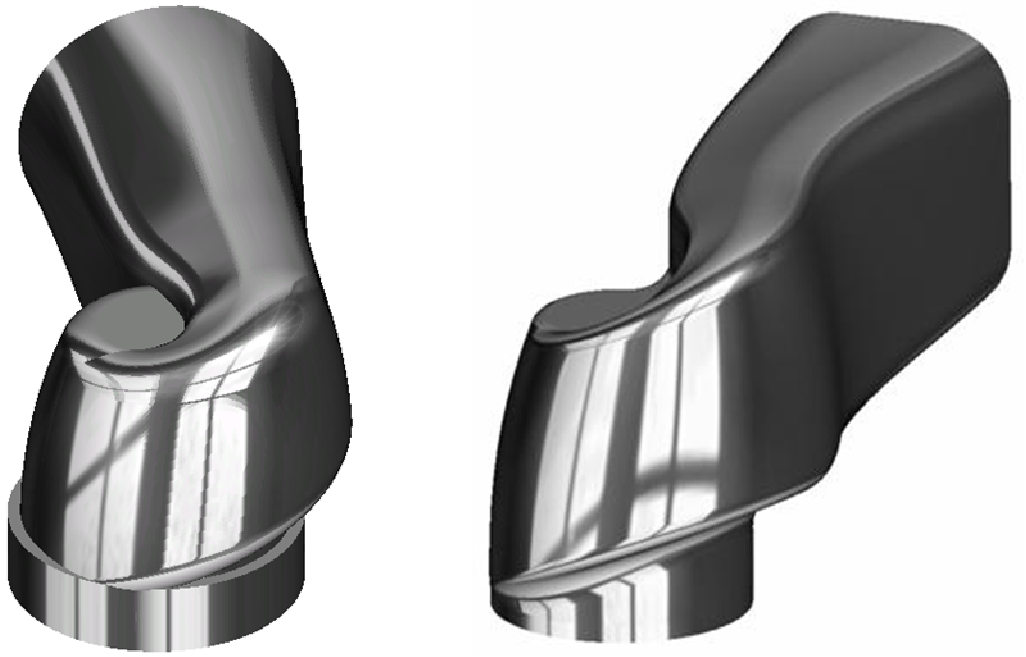

Figure 4.59 Helical port core (left hand: initial design, right hand: final design)

4.6.6 CFD Simulation

CFD simulation was performed to assess the swirling ability of the port. The most common way to assess a port design is done experimentally. Building a full scale equivalent model of the cylinder head, air is blown through the inlet port-inlet valve assembly and the swirl intensity is measured using a swirl impulse torque meter for different valve lifts. A description of this device is given by (Heywood, 1988) and also (Challen & Baranescu, 1999). This method gives the most reliable results and it is used by almost all engine manufactures prior to building a prototype engine.

To assess the helical port design, CFD simulation was chosen due to availability of CAE software and as more time affordable method within the scope of this research.

The Cranfield University Fluent CFD simulation suite was used to perform the flow analysis. Fluent is a CFD software that solves fluid flow problems based on Navier-Stokes equations which define any single-phase fluid flow.

The simulation was performed for maximum valve lift so losses are maximised due the port design mainly.

Pre-processing model preparation

The first step was to create the 3D geometry as it shown in Figure 4.60. The 3D geometry was made as one solid part including the inlet port, the cylinder volume and

the inlet valve cut. At this stage all sharp edges were removed in order to make meshing process easier. Then the solid was exported from I-DEAS NX as STEP file

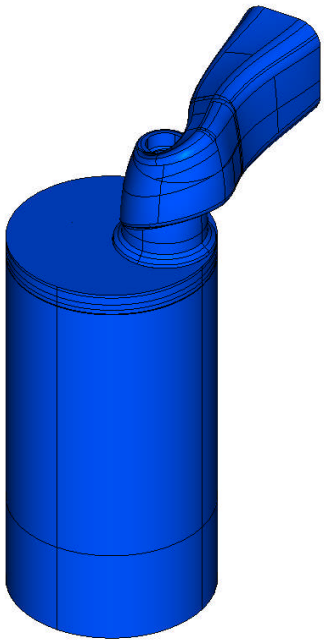

Figure 4.60 CAD model prepared and exported for CFD analysis

Meshing

The STEP file was imported to GAMBIT which is the FLUENT pre-processor and all surfaces were checked.

The grid was constructed in three steps:

- Edge meshing: Each edge was meshed using different node spacing. The spacing depends on the importance on the meshed area. A fine mesh was used near the valve areas and the helical port in order to define the flow accurately. A coarser mesh was utilised for the upper part of the port and the bottom part of the cylinder.
- Surface meshing: surface meshing was automatically generated according to edge meshing.
- Volume meshing: an unstructured mesh with 1mm spacing Tet/Hybrid elements were used for the volume mesh. The final grid had a total of 5,000,000 elements approximately.

Figure 4.61 shows the TGrid generated on Gambit.

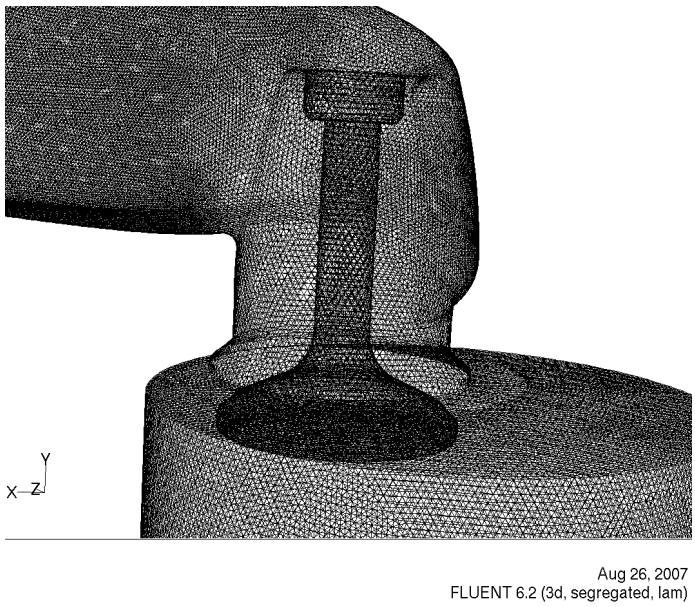

Figure 4.61 T-Grid generated in Gambit

Boundary conditions

The boundary conditions were set up by applying pressure differential between the inlet and the outlet. The outlet was taken as the lower side of the cylinder. Values for the pressure differential were obtained from previous work in the original Ricardo E6 engine (Theodoridis, 2003). Although those values were from the old cylinder head, it was the best estimation that could be made for the time. The only way to obtain the exact pressure differential values would have been by testing the new cylinder head in a flow bench. However this would require making a rapid prototype model of the cylinder head. Since neither a flow-bench nor a rapid prototype facility was available at the time the best estimated values were used to define the boundary conditions.

Turbulence model

Turbulence modelling is an important parameter when simulating complex geometries. In the particular case a steady state calculation was performed which represents the flow bench cylinder head testing where steady sate flow of air is blown though the cylinder head with fixed intake valve lift.

The k-ε turbulent model was chosen since it was the most recommended from literature for its accuracy and computer time saving. The under relaxation factors of the turbulent model were set to default.

Fluent Results

The model was solved using Fluent 3D solver. The 10^{-03} convergence criterion was met after 1000 iterations. Figure 4.62 shows the residuals convergence using the default relaxation factors after 6000 iterations on an attempt to meet the 10^{-4} criterion.

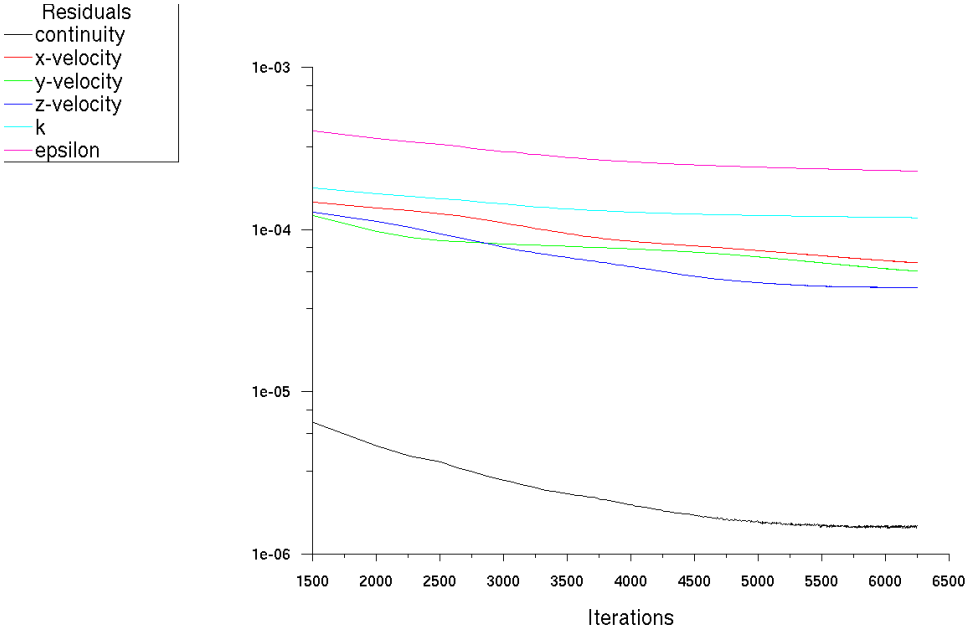

Figure 4.62 Residuals

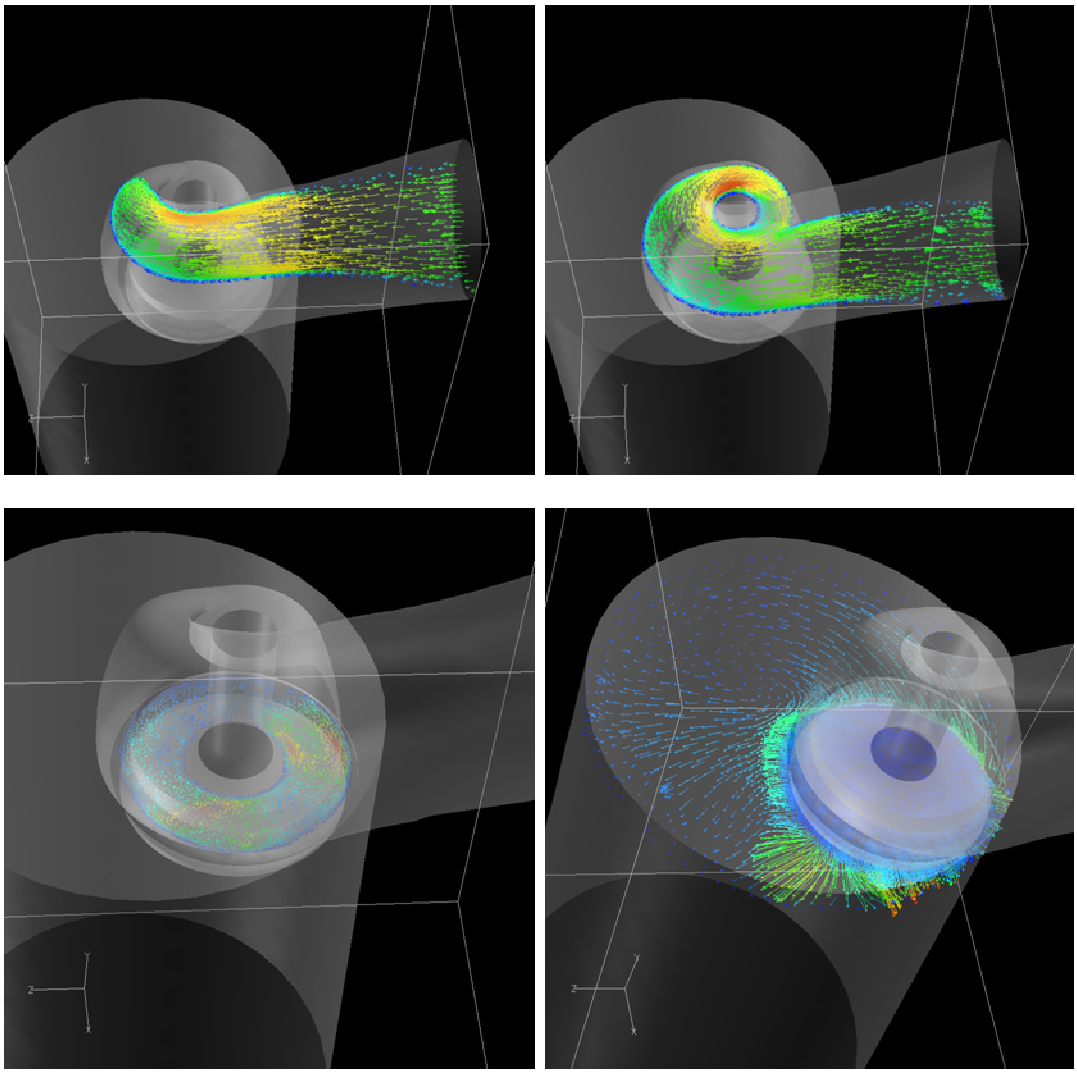

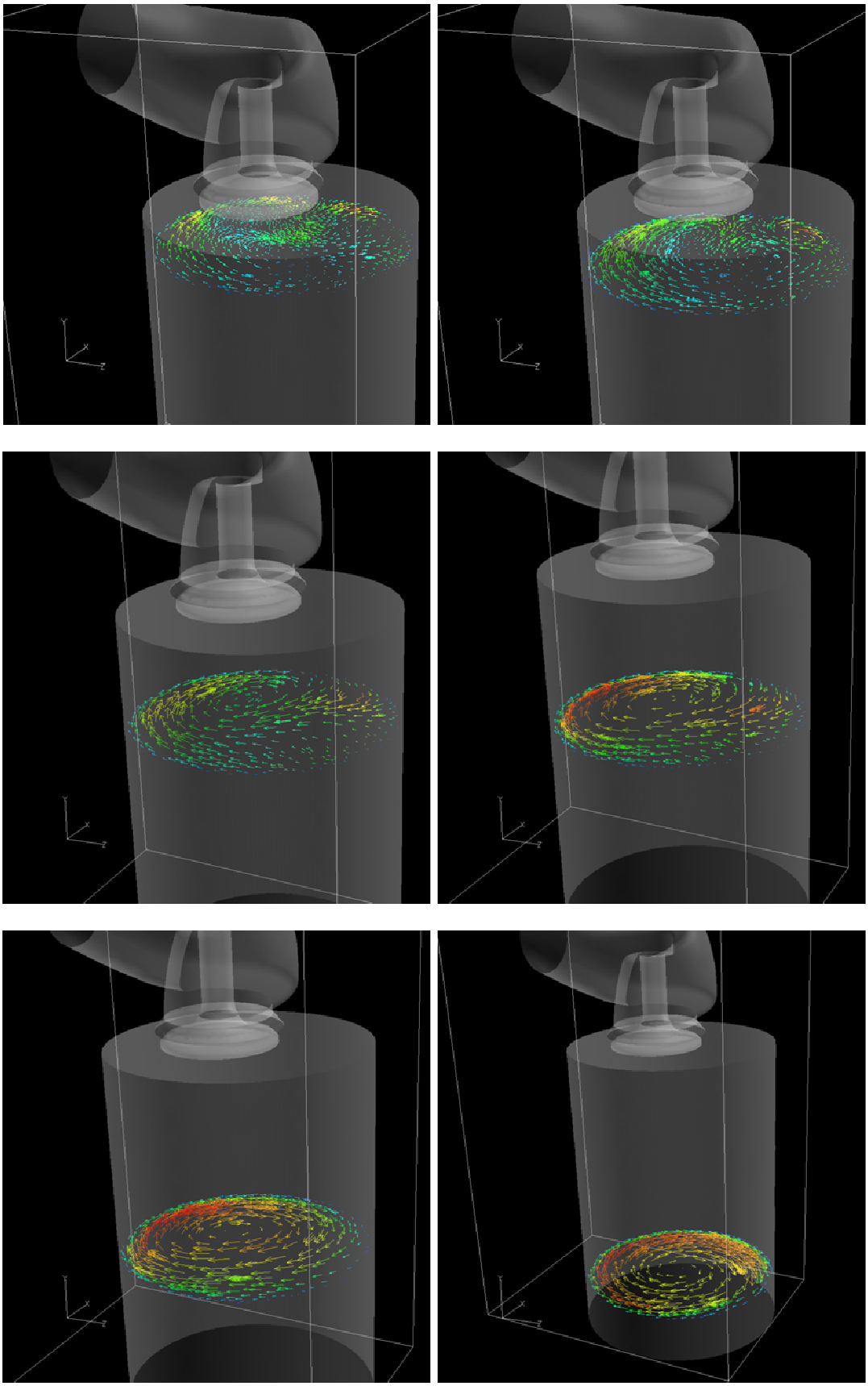

Figure 4.63 Fluent results visualised with FieldView

The Fluent results were visualised using Field-View visualiser. The velocity vectors at different planes clearly show the flow direction from the inlet port opening through the valve and toward the cylinder lower surface. As air enters through the inlet port, it gets a rotating momentum before enters into the cylinder through the valve opening due to the shape of the helix. The air enters the cylinder having the momentum from the helical port and as it travels downwards a more uniform swirl is generated.

The last picture in Figure 4.63 shows the velocity vectors of the flow at the lower part of the cylinder. This plane corresponds to the piston actual position in the cylinder at BDC. Fluent suggested $15ms^{-1}$ average maximum velocity at 19mm radius when piston is at BDC.

The simulation represents an engine running at 1800 RPM.Using equation (4.6), the swirl ratio at the end of the induction stroke (near BDC) was calculated 2.3. This value is not low considering the low engine speed which the velocity boundary conditions were set at.

This simple simulation has demonstrated that the helical port design is producing adequate swirl for even for a low volumetric efficiency naturally aspirated engine. However the CFD results are not accurate enough without validation but this is a time consuming process and well out of the scope of the current thesis. Therefore the CFD stopped at this point and the results were only used to demonstrate the effect of the helical port as part of the cylinder head development process.

4.6.7 Valvetrain

The new cylinder head has a flat combustion face with one inlet and one exhaust valve. These are operated by a direct acting overhead camshaft with inverted, bucket-type followers. The advantage of the overhead camshaft valve actuating mechanism is the increased rigidity compared with the more flexible push rod and rocker arm mechanism. A more precise control of the opening and closing of the valve periods, improves the scavenging and the filling of the cylinder and therefore smaller valve overlaps can be chosen to improve exhaust emissions without sacrificing performance.

Figure 4.64 shows a cross section of the cylinder head with the valvetrain of the E7 engine. The camshaft is supported by three bearings: a double row ball bearing, a roller bearing and by a journal bearing placed in the middle to increase shaft's rigidity. The bearing housings are formed between the cylinder head section and the camshaft cover. The roller bearing at the opposite site of the timing pulley allows axial movement in order to take the thermal expansion loads of the camshaft.

The new camshaft has identical cam profiles with the dCi 1.9 litre turbocharged engine but with slightly different timing. Because the E7 is a naturally aspirated engine and it has a different inlet manifold from the production dCi engine, it required slightly longer

overlap for better engine breathing. The valve timing was optimised using AVL Boost engine simulation.

The camshaft was made from mild steel out of four sections carefully joined together using interference fit and lock pins. A large timing pulley attached to the front of the camshaft is connected to the engine crankshaft pulley via a timing belt.

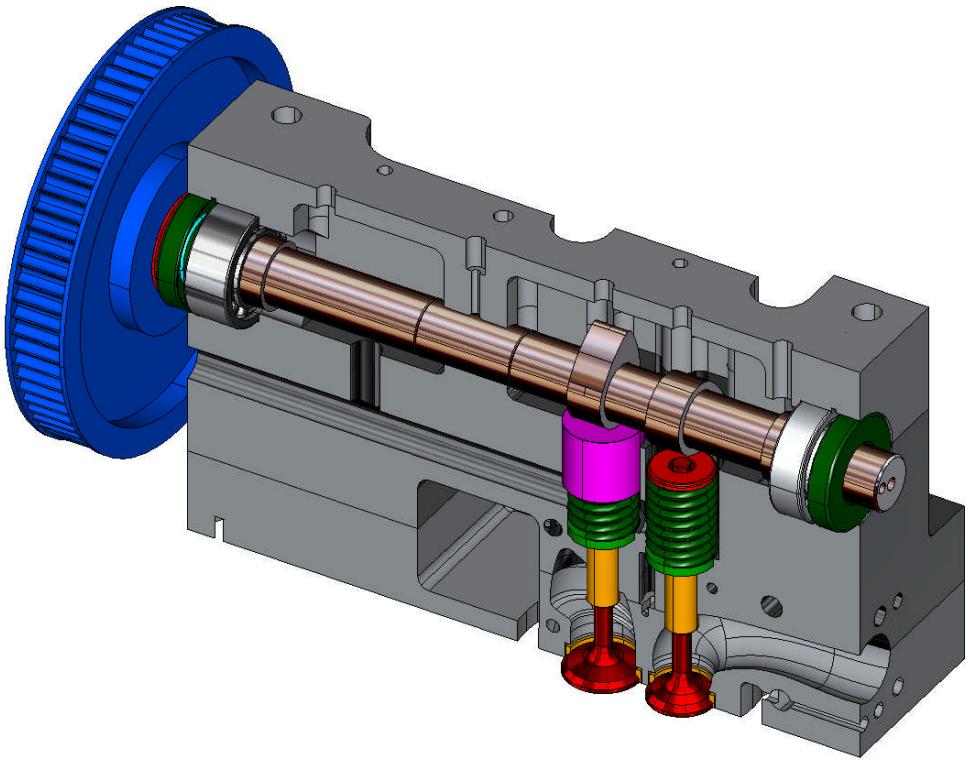

Figure 4.64 E7 valvetrain

The valve guides were made from gunmetal. This martial is preferred than cast iron because it gives a better balance between stiffness and wear.

The valve seats were made from beryllium copper alloy due to the good heat transfer and the superior strength of this material. The seats were initially cooled in liquid nitrogen and then pressed to a preheated cylinder head to achieve a high interference fit. A matched pair of valve springs and valve collets was used with small modifications.

4.6.8 Cooling

In the original Ricardo E6 the cooling is provided in both cylinder barrel and cylinder head. The circulation of water is by a centrifugal pump driven by an electric motor. The water enters into the cylinder barrel from the bottom and then flows through circumferential channels to the cylinder head. Then the water exits from the cylinder

head water outlet, passes through a heat exchanger connected to the man cooling circuit of the laboratory and returns to an open water tank.

For the new cylinder head design the same type of cooling circuit was used but an electric heating element was added in the water tank to provide temperature control.

The cylinder head cooling channels were formed around the cylinder head ports by machining out material using CNC machining. Cross drilling the cylinder head walls, material was removed from below and above the ports in order to facilitate water flow. Then the external holes were closed with plugs. Figure 4.65 shows the cylinder head internal design. The arrows in Figure 4.66 show the cross drilled holes below the inlet and exhaust ports.

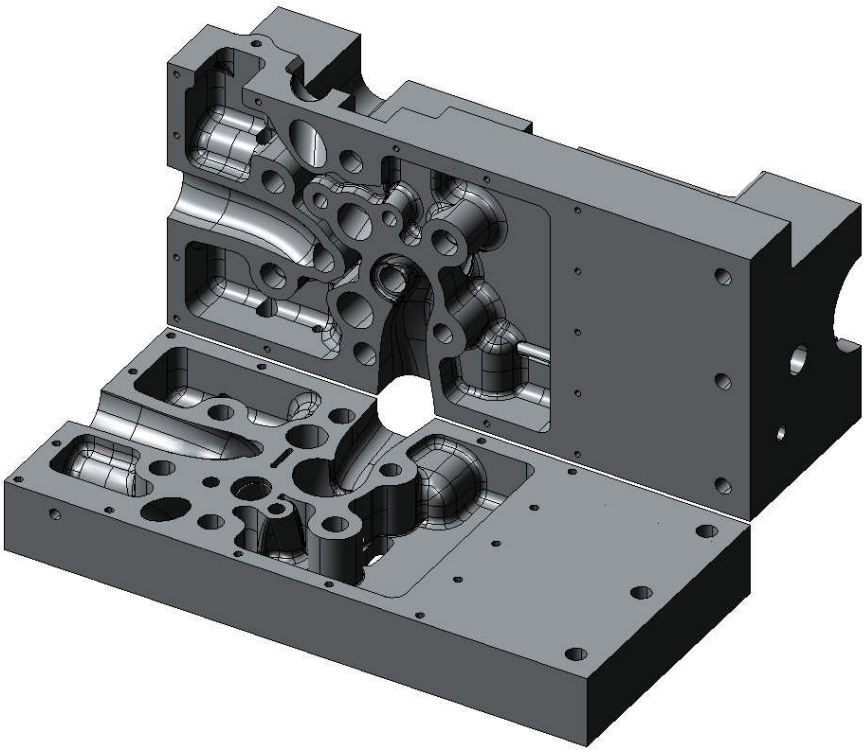

Figure 4.65 Cylinder head section showing cooling channels

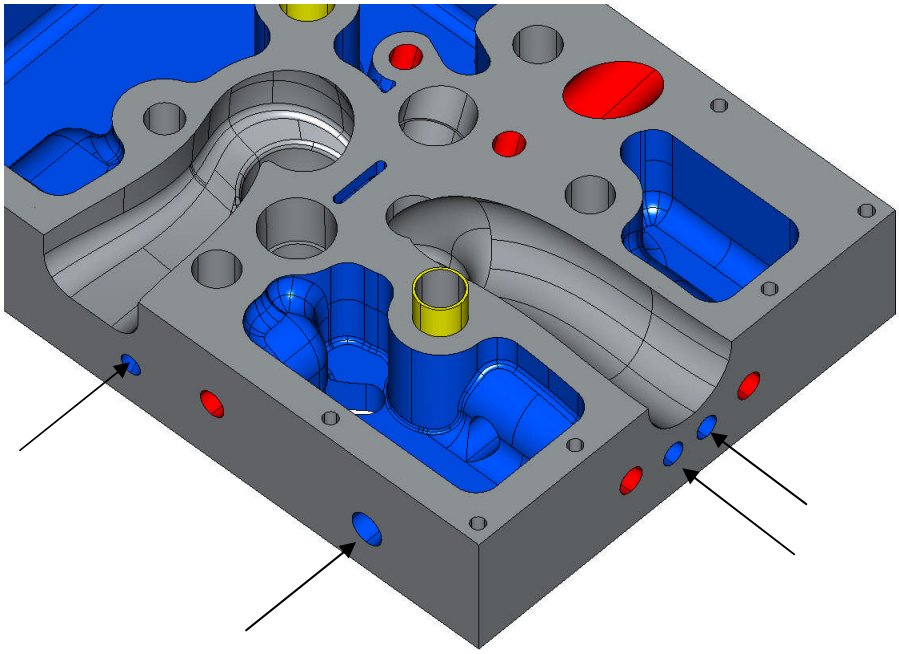

Figure 4.66 Cylinder head cross drilled cooling channels below the exhaust and the inlet port

Using I-DEAS TMG thermal analysis, the performance of the cylinder head block was investigated. Using advanced finite difference control volume technology, TMG makes it easy to model nonlinear and transient heat transfer processes including conduction, radiation, free and forced convection, fluid flow, and phase change [I-DEAS NX 11].

Conduction through the aluminium cylinder head walls was modelled with solid tetrahedral elements. The material property for the elements was specified as aluminium alloy with thermal conductivity 155 $W \cdot m^{-1} \cdot K^{-1}$.

The boundary conditions were specified as follows:

It was assumed that the combustion process produces a steady-state thermal load of 1.7 KW on the cylinder head bottom part on the area exposed to the combustion. A constant temperature of 80 °C was specified on the surfaces of the water channels.

The model was solved using the TMG solver. The results were visualised using I-DEAS post processing and the visualiser.

Figure 4.67 shows the results of an early TMG simulation. The highest thermal load was occurring between inlet and exhaust ports. The maximum temperature at this area according to TMG was 119 °C. Figure 4.69 shows the temperature distribution between the ports. The reason for this was the absence of any water channels to provide cooling in that area. Therefore the size of the exhaust valve was slightly reduced in diameter in order to accommodate a cooling passage between the ports whilst maintaining cylinder head wall minimum thickness. Figure 4.65 shows the added water channel between the ports in the latest cylinder head design. This action was considered sufficient to solve

the problem and due time constrains no further simulation was carried out to investigate the effectiveness of the new design.

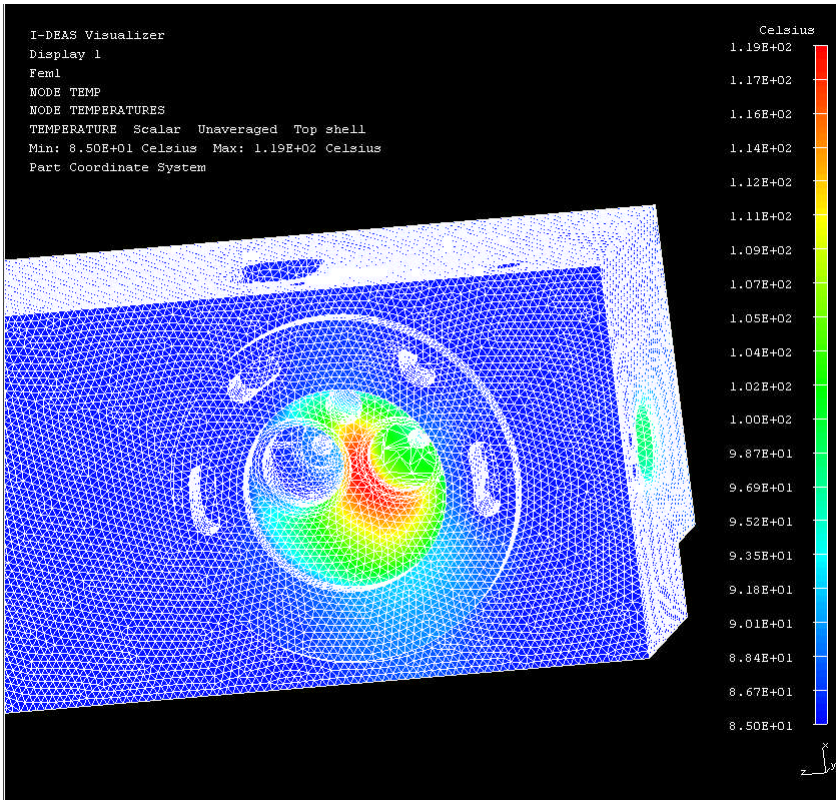

Figure 4.67 Thermal load distribution (grid on)

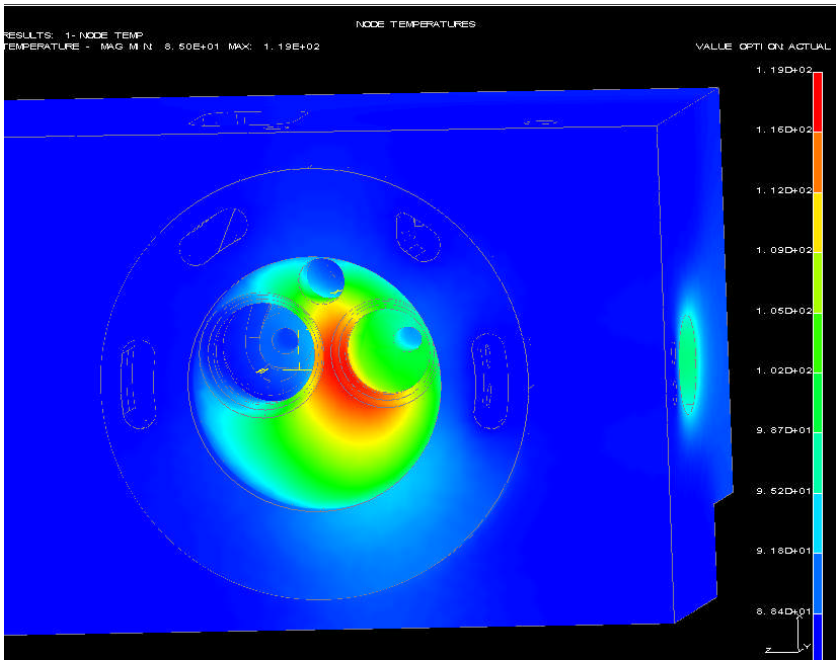

Figure 4.68 Thermal load distribution (grid off)

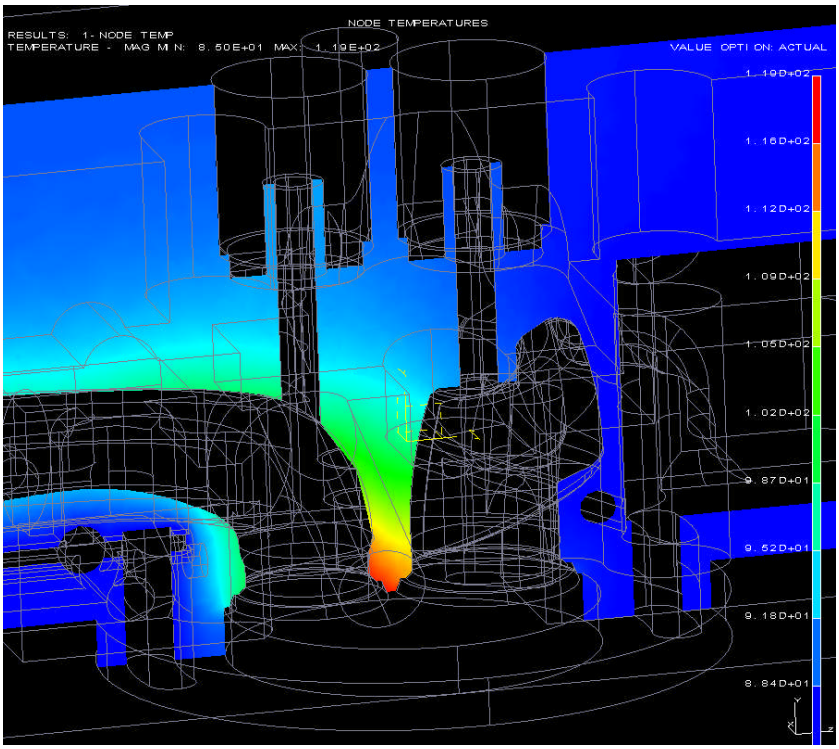

Figure 4.69 Thermal load between valve ports

4.6.9 Lubrication

Engine lubrication is by means of a gear pump which is separately driven by an electric motor. The pump lifts the oil from the engine sump and passes it to a filter via a pressure relief valve. From the filter the oil is distributed to the crankcase and to the cylinder head accumulator via external stainless pipes. The accumulator is a hollow pipe made from aluminium. From the accumulator the oil is delivered to the cylinder head via five restrictors. Oil is injected on the roller bearings and the camshaft lobs through small orifices placed on the tip of each oil restrictor. A larger diameter orifice is used to provide oil to the hydrostatic journal bearing. The oil accumulated in the cam-box upper deck returns into the sump through a return gallery and a large diameter copper pipe. Figure 4.70 shows the cylinder head oil galleries of the E7 engine.

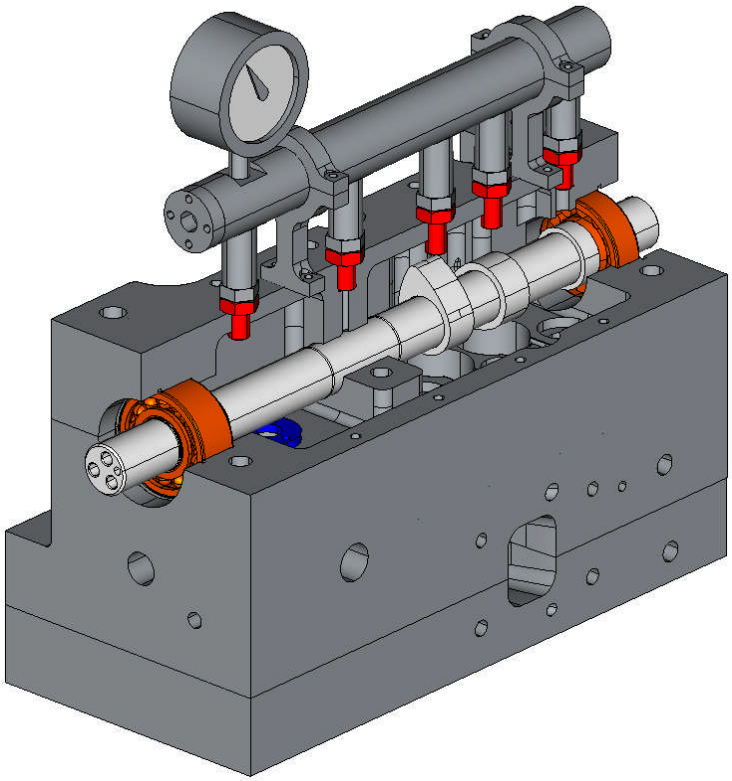

Figure 4.70 Cylinder head lubrication system

4.6.10 Inlet/exhaust manifold

A bespoke inlet manifold was designed for the E7 engine. The aim of the design was to develop an inlet manifold with an integrated port fuel injection system for the dual fuel operation.

The inlet manifold was made of stainless steel tubes and consists of three sections: the primary section, the throttle body and a secondary section. The primary section is a short length duct with variable diameter and shape. The primary purpose of this section was to accommodate the LPG injector and the inlet pressure transducer. Apart from that this section also provides a smooth transition between the circular shape of the intake manifold to the square section of the inlet port.

Although this is diesel cylinder head, a throttle body was placed in the inlet to provide air control. The rest of the rest of the manifold was made out of a bent stainless steel pipe.

The optimum intake manifold length for the E7 engine was found using AVL Boost simulation.

The exhaust manifold was made from steel pipe of diameter equal to the exhaust port. Two steel bosses were welded on the pipe to accommodate a Lambda sensor and a thermocouple.

Figure 4.71 shows a 3D model of the E7 cylinder head with the inlet and he exhaust manifolds attached. Figure 4.72 shows a detail of the inlet primary section.

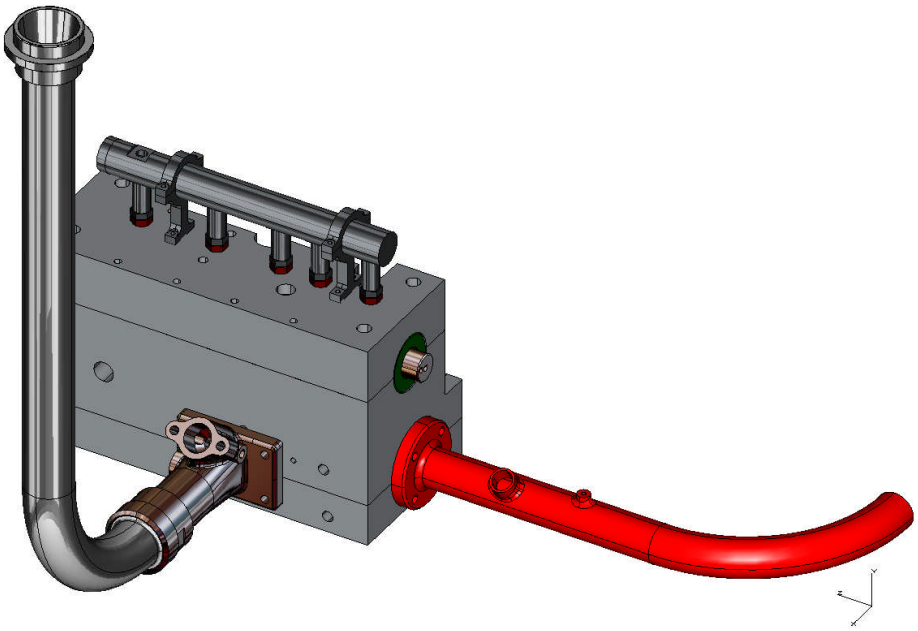

Figure 4.71 Cylinder head with inlet and exhaust manifolds attached

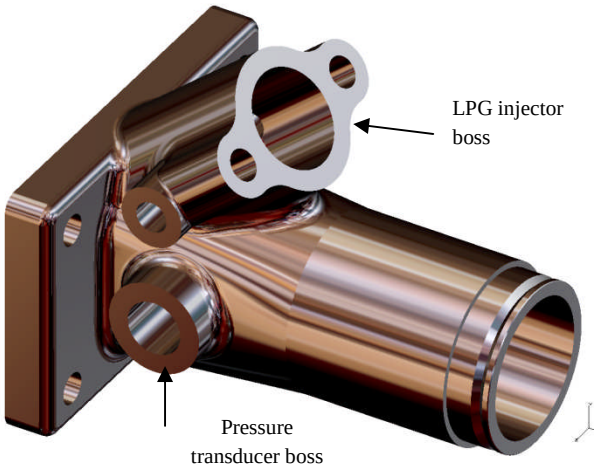

Figure 4.72 Inlet manifold primary section

4.6.11 Manufacturing methods and materials

Cylinder heads are usually cast in one piece using cast iron or aluminium alloy. Although casting is commonly used for mass production of complex parts, it is costly for making one-off prototype. Hence the cylinder head was machined out from a large aluminium alloy billet using 5axis CNC machining. Aluminium alloy was chosen due to its high degree of heat conductivity, high strength and good machinability properties. 3D models and 2D drawings were presented to Jaye Engineering Ltd®, a CNC specialist company based in the United Kingdom. The company manufactures cylinder head parts for F1 racing engines as well as other complex components directly from 3D models. Figure 4.73 shows a photograph taken during cylinder head machining at Jaye Engineering Ltd workshop. Figure 4.74 shows a photograph of the finished cylinder head components at the workshop. Figure 4.76 shows a photograph of all the additional parts for the cylinder head.

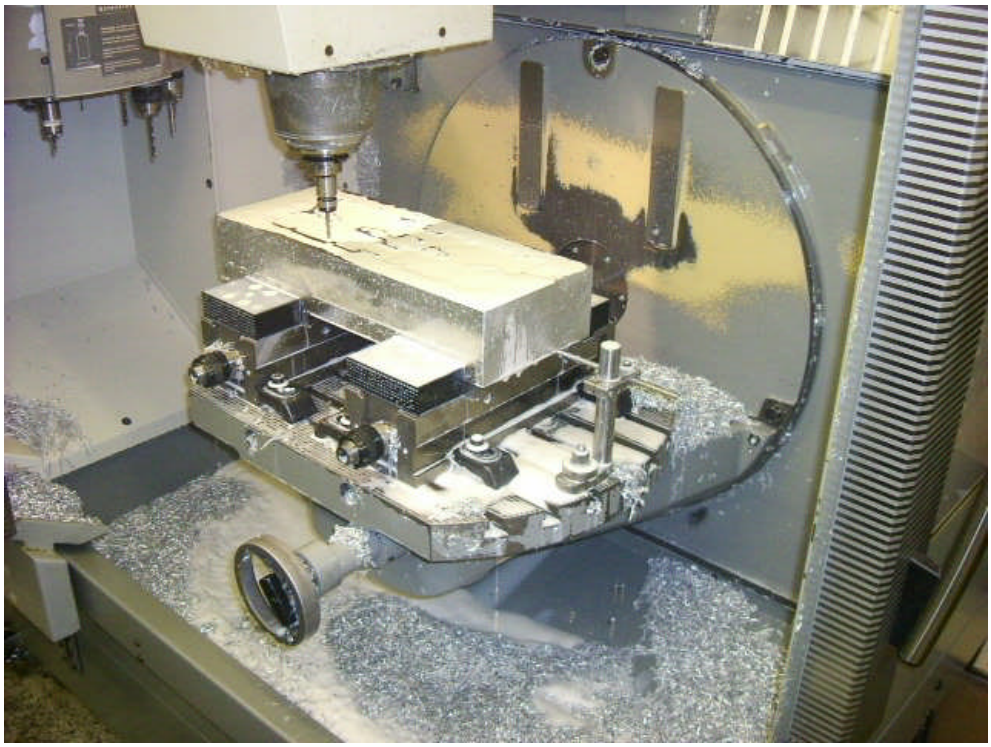

Figure 4.73 CNC cylinder head manufacturing at Jaye Engineering Ltd.

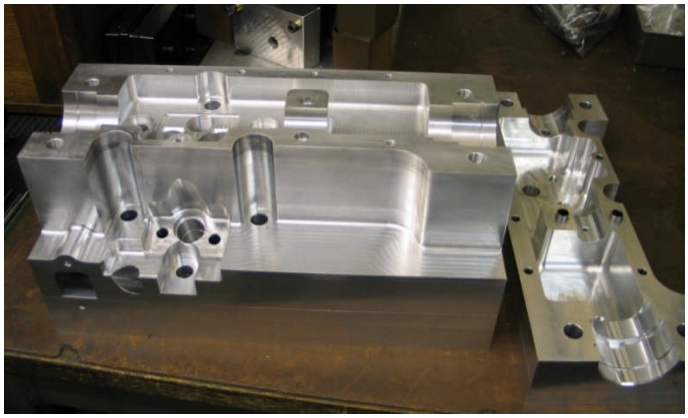

Figure 4.74 Finished cylinder head parts

Figure 4.75 Valve seats and valve guides assembled

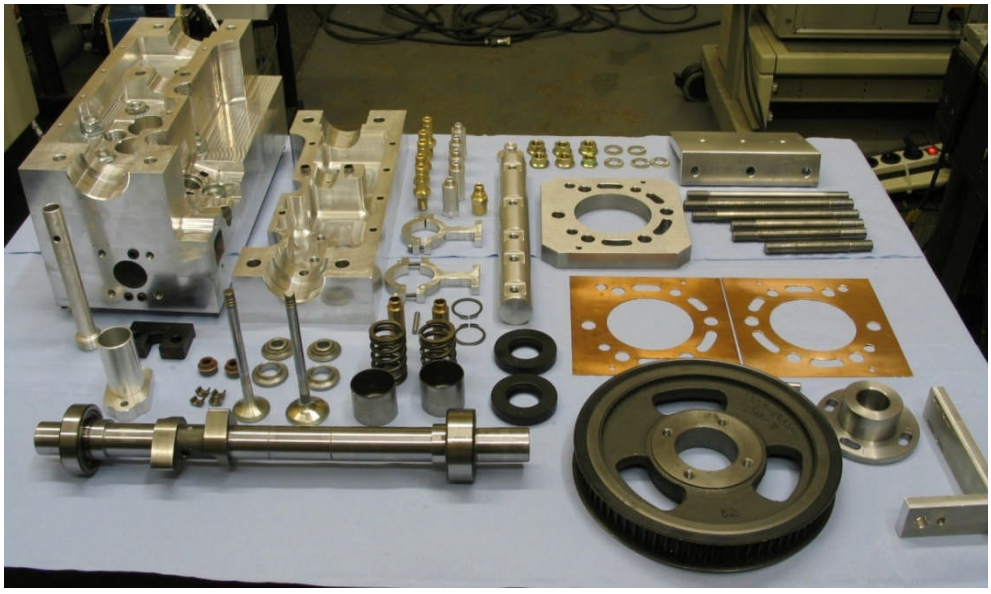

Figure 4.76 E7 bespoke parts awaiting assembly

4.7 LPG injection system

The LPG injection system used in the experimental work, it is a variant of a liquid LPG injection system which has been developed for gasoline engines as part of a PhD thesis in Cranfield University by Dr.A.K.Vouorenkoski (Vouorenkoski, 2004).

The system comprises of an LPG automotive tank, a pressure regulator, two electric pumps, a number of electromagnetic valves, a SIEMENS DEKA gasoline injector and an injector electronic driver.

The LPG tank was placed below the inlet manifold of the E7. An aluminium bracket was fabricated in order to accommodate the electric pumps the LPG filter and the pressure regulator. It is very important for these components to be fixed securely for safety reasons. Figure 4.77 shows a photograph of the LPG system installation arrangement.

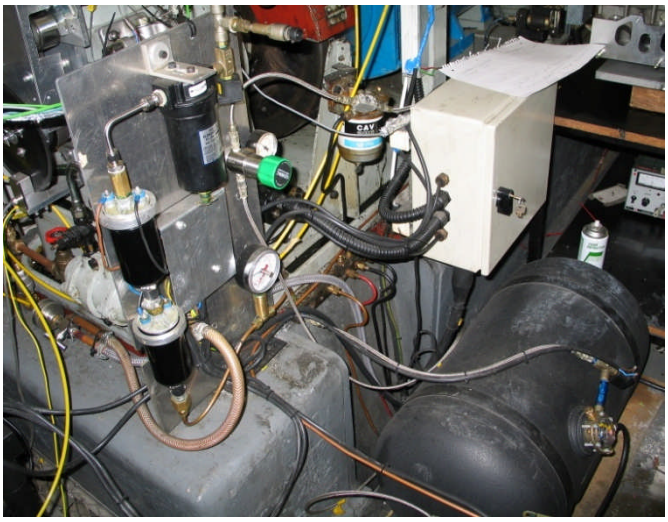

Figure 4.77 E7 LPG injection system

A Siemens Deka side fed injector was installed on the special boss of the inlet manifold as it shown in Figure 4.78 . The injector is operated by an electronic driver which is triggered from the engine's crankshaft TTL signal and the camshaft encoder flag. The start of the injection can be selected from the engine controller and the injection duration can be adjusted from a pulse generator. Figure 4.79 shows a schematic of the LPG injector electronic driver.

LPG is stored in the tank at approximately 8 to 10 bar pressure. LPG is delivered to the electric pumps through a high pressure flexible pipe. Two electric pumps connected in series pressurise the fuel to the injector pod via a filter. The fuel is constantly circulated from the tank to the injector and back to the tank via a return line and a pressure regulator.

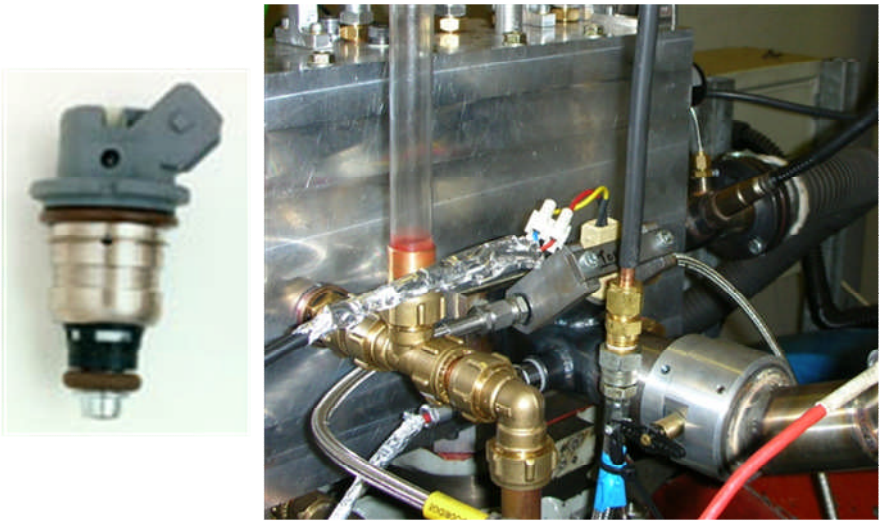

Figure 4.78 LPG injector installed onto the inlet manifold

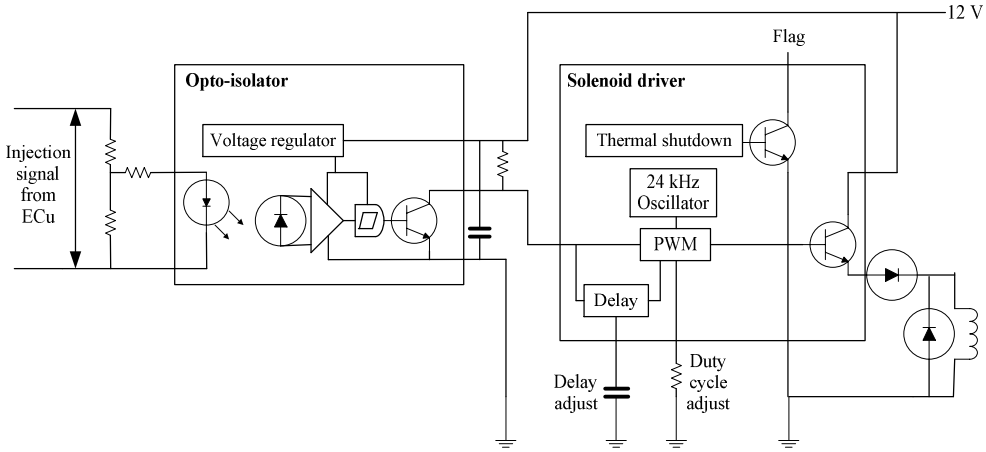

Figure 4.79 Injector actuator circuit (Vouorenkoski, 2004)

The system has three electromagnetic valves for controlling the LPG flow. A main vale is installed on the top of the tank allows LPG to flow from the tank to the system. A second valve is paced after the LPG filter to allow injector removal without the need to empty the entire system. If the system needs to be emptied there is a third valve which releases LPG outside of the lab through a long copper pipe.

Figure 4.80 shows a 3D section of the cylinder head with the LPG and the diesel injectors in place.

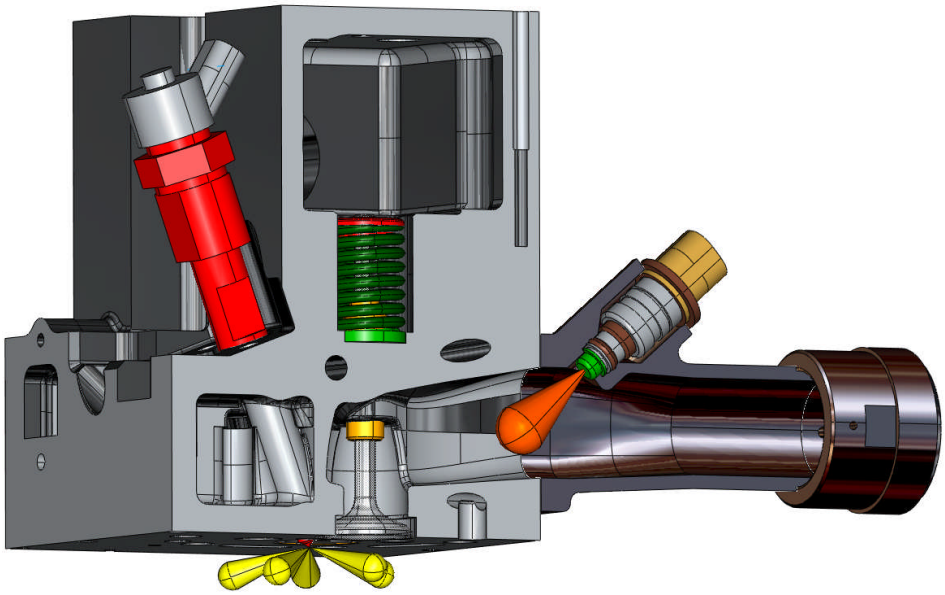

Figure 4.80 The dual fuel injection system of the E7

4.8 Engine instrumentation

This section describes the various engine instrumentation used for the experimental work. Figure 4.81 shows a photograph of the E7 engine controls and the instrumentation.

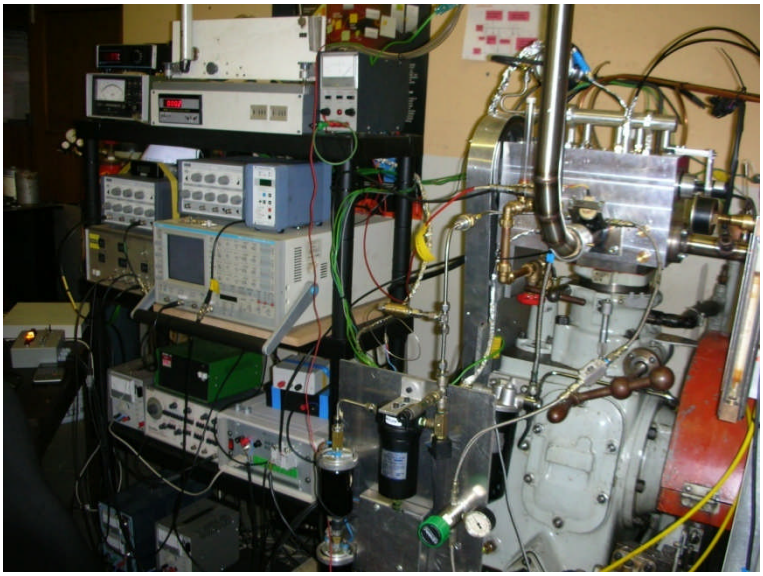

Figure 4.81 Engine controls and instrumentation

4.8.1 Cylinder pressure measurements

When serious thermodynamic analysis is required, water cooled sensors are always preferred to maximise sensitivity and keep thermal shock at minimum levels. Therefore

a water cooled AVL piezoelectric transducer together with a 5011A Kistler charge amplifier were used to measure cylinder pressure. The transducer was flush mounted on the top of the cylinder head wall (provision was made during the design for the particular sensor) as it shown in Figure 4.82. The transducer was tightened at the manufacture's specified torque. Short length-high insulation resistance cables were used to connect to the charge amplifier.

The pressure transducer was calibrated for long constant against a piezoresistive reference sensor on a Budenberg deadweight tester. The charge amplifier output was also tested using a charge calibrator and also zeroed using a precision DVM according to Kistler operating manual.

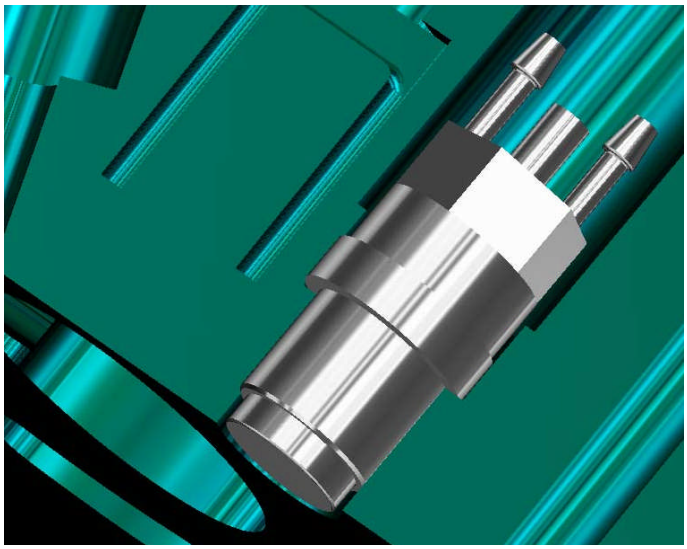

Figure 4.82 AVL water cooled pressure transducer flush mounted on the cylinder head

Water was supplied to the transducer at constant pressure and temperature in order to minimise fluctuations. The water flow was controlled by an ABB rotameter.

The charge amplifier settings were:

- Transducer sensitivity: 38.84[pC/Mechanical Unit]
- Scale: 20 [Mechanical Units/Volt]
- Filter: off (low-Pass)
- Time Constant: short (High-Pass filter)

The output of the charge amplifier was fed into the second analogue channel of the fast data acquisition system through BNC cables. The real time cylinder pressure signal was constantly monitored in a high speed oscilloscope which was connected in parallel using BNC T-connectors.

4.8.2 Cylinder pressure referencing (pegging)

The cylinder pressure at inlet bottom dead centre (IBDC) was referenced to the intake manifold absolute pressure. According to (Ladommatos & Zhao, 2001) this method of referencing is very accurate for untuned intake systems or for tuned intake systems at low speed.

A 4043A Kistler piezoresistive sensor together with a Kistler amplifier was used for measuring the absolute pressure in the intake manifold. The sensor was calibrated using the Budenberg dead weight calibrator. Then it was mounted onto the primer inlet manifold section as it shown in Figure 4.83. The inlet manifold pressure signal was fed into the third analogue channel of the fast data acquisition system.

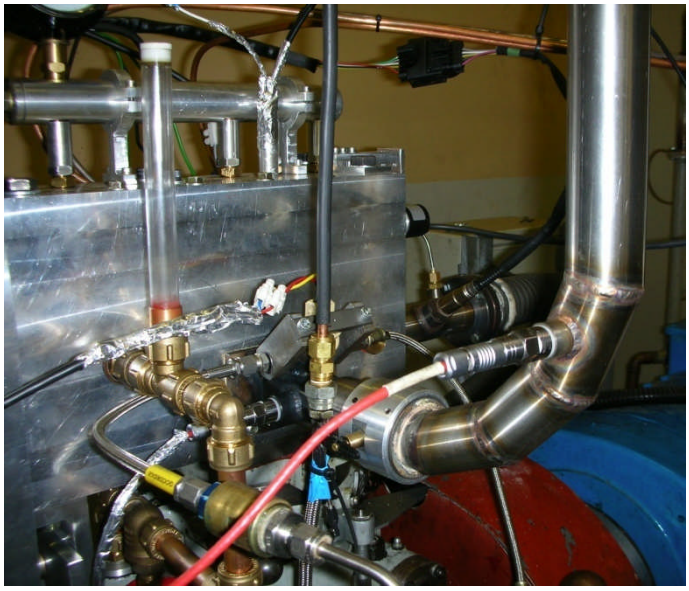

Figure 4.83 Inlet manifold pressure transducer

The output voltage of the charge amplifier at any crank angle is:

$$E(\theta) = \frac{p(\theta)}{C} + E_b \tag{4.7}$$

Where:

E_b = Bias voltage with zero pressure

C = Gain (Mechanical unit/Volt)

Referencing the cylinder pressure at IBDC to manifold absolute pressure (MAP) requires:

$$p_{(IBDC)} = MAP \tag{4.8}$$

Then the absolute pressure determined from charge amplifier output voltage at any crank angle is:

$$p = C \times (E_{(\theta)} - E_{IBDC}) + p_{IBDC} \tag{4.9}$$

Where:

$E_{(\theta)}$ = Charge amplifier output voltage at any crank angle degree

E_{IBDC} = Charge amplifier output voltage at IBDC

C=charge amplifier gain

P_{IBDC}=cylinder pressure at IBDC

In order to minimise the potential of error associated with relying on a single point measurement, an average of five points was taken as reference for the transducer output at IBDC, two CA degrees after and two CA degrees before IBDC.

4.8.3 Air mass flow

The air mass flow was measured using the Ricardo-Alcock viscous air flow meter. Figure 4.84 shows the flow meter installation upstream the intake manifold of the engine. This kind of air flow meter gives sufficient accuracy because it eliminates serious errors which arise when pulsating air flow is measured in the kinetic air meters of the orifice, Venturi and other types.

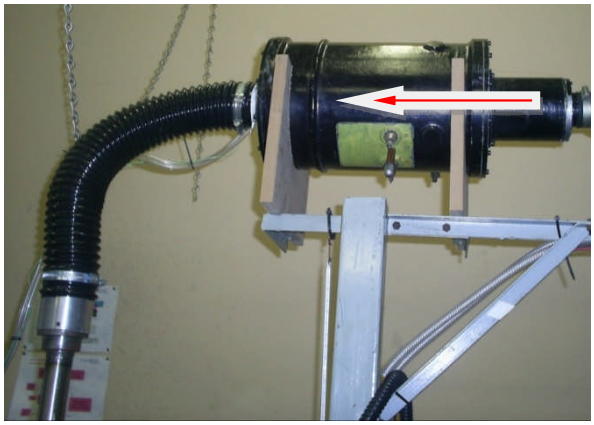

Figure 4.84 The Ricardo-Alcok viscous air flow meter

The operation of viscous flow air meter is based on the fact that the pressure difference across a laminar air flow passage is nearly proportional to the velocity of the flow.

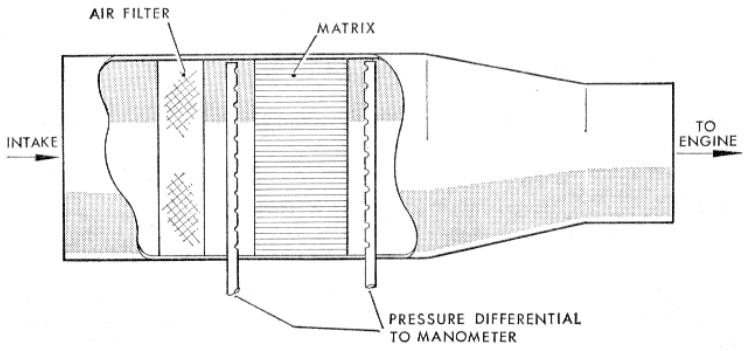

Figure 4.85 Viscous air flow meter schematic

In the viscous air flow meter the measuring element is a honeycomb structure with many small triangular passages of 76mm long and 0.4mm in height. The flow through these passages is laminar and consequently the pressure difference across the element is approximately proportional to the velocity of flow rather than to its square as in the air box orifice plate.

The pressure differential across the air flow meter was recorded by an FCO14 analogue micro manometer shown in Figure 4.86. The electric output of this instrument was connected to the fourth data acquisition channel and corresponds to mmH_2O. A Ricardo multislope manometer was also connected in parallel with the electronic micro manometer as an additional accuracy measure.

Figure 4.86 FCO 14 micromanometer and multislope manometer

The mass flow rate ($\dot{V}$) was calculated from the pressure difference by the following equation:

$$\dot{m} = \textit{flow}\ \text{meter}\ \textit{calibration}\ \text{constant} \times * \Delta P_{mmH_2O} * \rho_{air} * Cf \qquad (4.10)$$

Where:

$\dot{m}$ = Air mass flow [Kgs^{-1}]

ΔP= pressure differential across the flow meter [mmH_2O]

C_f= temperature correction factor

p_{air} = specific gravity of air [kg/m^3]

The specific gravity of air is given by:

$$\rho_{air} = \rho_{stp} \frac{T_{stp} * P_b}{P_{stp} * T} \tag{4.11}$$

Where:

ρ_{stp} = air density at standard temperature and pressure, 1.293 [kg/m^3]

T_{stp} = temperature at standard conditions, 273.15° [K]

P_{stp} = pressure at standard conditions, 1013.25 [mbar]

P_b = atmospheric pressure measured by a laboratory barometer [mbar]

T = inlet temperature [K]

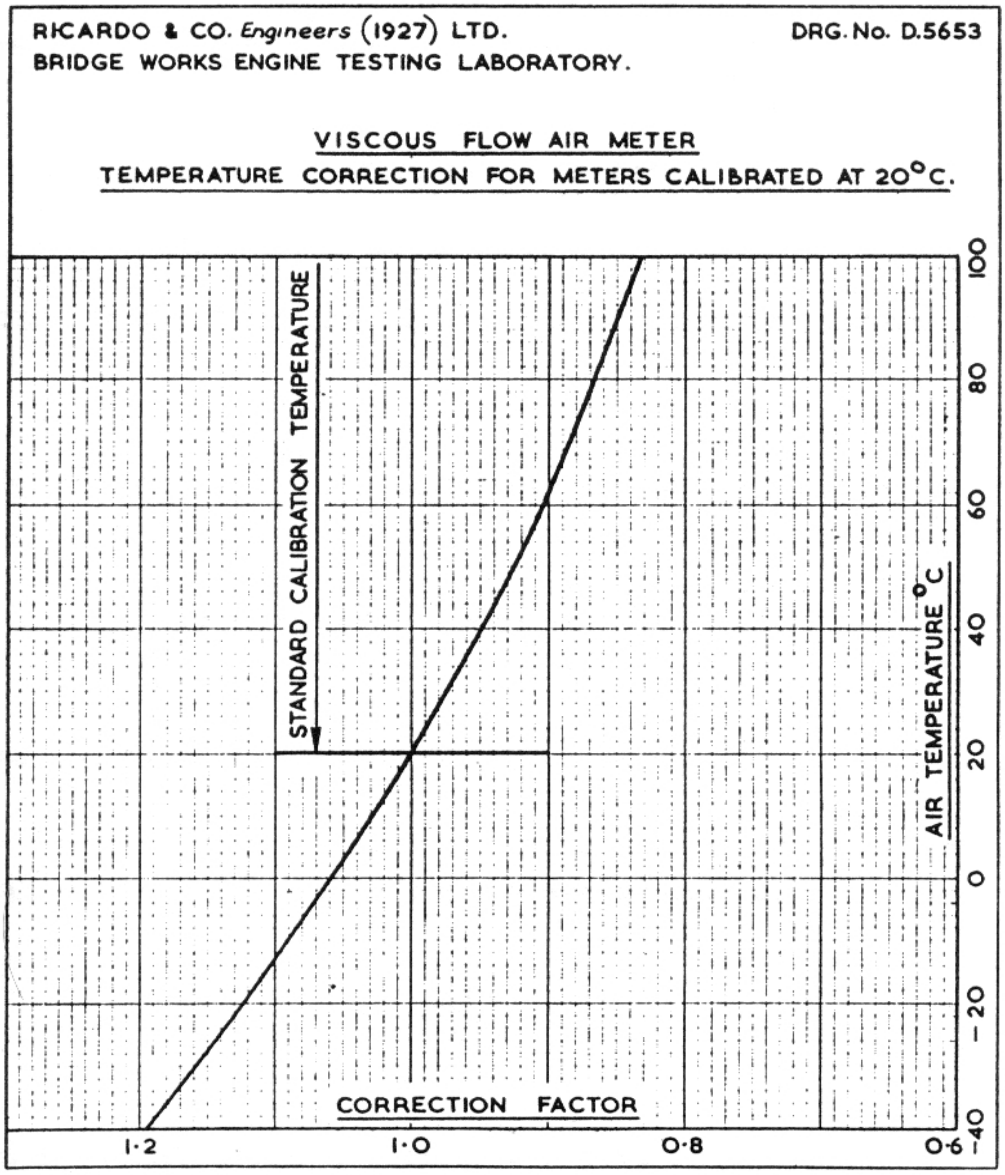

Figure 4.87 Temperature correction factor for the viscous flow meter

4.8.4 Fuel mass flow

A MoTeC wide band Lambda sensor system was utilised for fuel mass flow measurements. The sensor (Bosch LSU Ref: 0 258 006 066) was ideally installed at about 100mm from the exhaust port of the cylinder head as it is shown in Figure 4.88. The signal from the Lambda sensor is acquired, processed and displayed on the MoTeC processing unit shown in Figure 4.89.

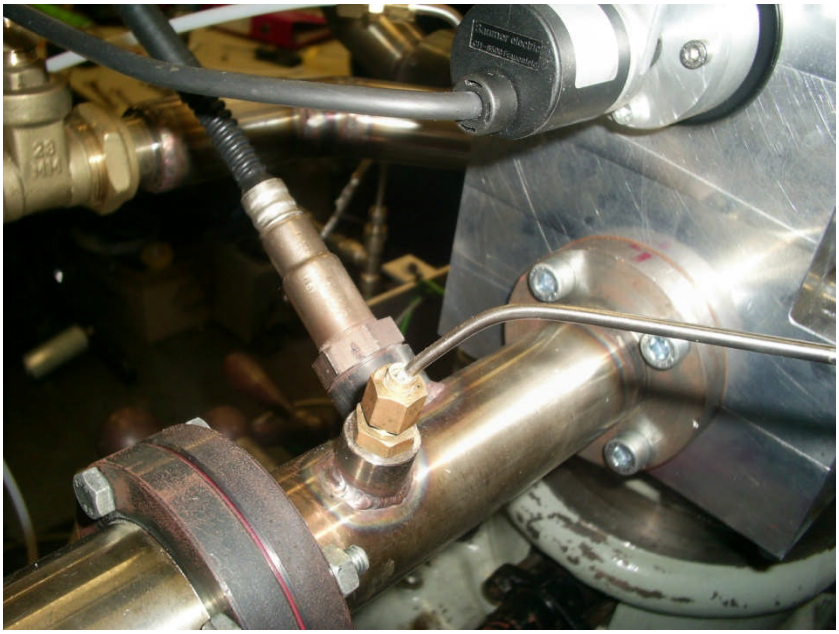

Figure 4.88 Bosch LSU wide band λ sensor

Figure 4.89 MoTeC wide band λ processing/display unit

Measuring the actual λ from the exhaust and the air mass flow from the intake, the fuel mass flow was accurately calculated from the stoichiometric AFR. Thus for mineral diesel fuel:

$$\lambda = \frac{\left(\frac{Air}{Fuel}\right)_{actual}}{\left(\frac{Air}{Fuel}\right)_{stoich}} = \frac{\left(\frac{Air}{Fuel}\right)_{actual}}{14.5} \tag{4.12}$$

Therefore the diesel mass flow was calculated using:

$$\dot{m}_{diesel} = \frac{\dot{m}_{air}}{\lambda \times \left(AFR\right)_{diesel,stoichiometric}} \tag{4.13}$$

For dual fuel operation the mass flow of LPG was derived as follows:

$$\lambda = \frac{\left(\frac{Air}{Fuel}\right)_{actual}}{\left(\frac{Air}{Fuel}\right)_{stoich}} = \frac{\left(\frac{Air}{Fuel}\right)_{actual}}{15.6} \tag{4.14}$$

Then:

$$AFR_{actual} = \frac{\dot{m}_{air}}{\dot{m}_{diesel} + \dot{m}_{LPG}} \tag{4.15}$$

So:

$$AFR_{stoich,total} = AFR_{stoich,diesel} * \frac{\dot{m}_{diesel}}{\dot{m}_{diesel} + \dot{m}_{LPG}} + AFR_{stoich,LPG} * \frac{\dot{m}_{LPG}}{\dot{m}_{diesel} + \dot{m}_{LPG}} \tag{4.16}$$

Then:

$$AFR_{stoich,total} = 14.5 * \frac{\dot{m}_{diesel}}{\dot{m}_{diesel} + \dot{m}_{LPG}} + 15.6 * \frac{\dot{m}_{LPG}}{\dot{m}_{diesel} + \dot{m}_{LPG}} \tag{4.17}$$

Substituting with λ:

$$\lambda = \frac{\dot{m}_{air}}{14.5 * \dot{m}_{diesel} + 15.6 * \dot{m}_{LPG}} \tag{4.18}$$

Therefore the LPG mass flow was calculated using:

$$\dot{m}_{LPG} = \frac{\dot{m}_{air} - \lambda * 14.5 * \dot{m}_{diesel}}{15.6 * \lambda} \tag{4.19}$$

4.8.5 Emission analysers

Figure 4.90 shows a photograph of the Signal NOx analyser which was used for measuring and NOx emissions and Figure 4.91 shows a photograph of a Horiba portable analyser which was used for measuring the CO emissions. During experiments it was found that the response time of the Signal analyser was significantly faster in comparison with the Horiba unit. Emissions were sampled from the exhaust of the E7 via a two meter heated line. The analyses were calibrated before every measurement using reference gases. Detailed information about the installation can be found in (Hitache, 2006).

Figure 4.90 Signal NOx –HC analysers

Figure 4.91 Horiba gas analyser

4.8.6 Data acquisition

When computerised combustion analysis is required, high speed data acquisition system is necessary. The data acquisition system used in the measurements consists of a National Instruments DAQ-6026 PCMCIA card connected to a laptop computer and National Instruments LabVIEW data acquisition software. The analogue signals were acquired by the system via a SCB-2345 carrier block which is shown in Figure 4.92.

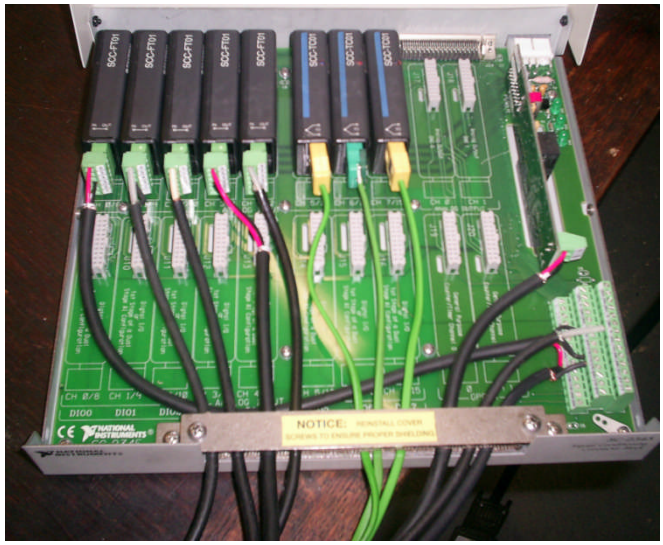

Figure 4.92 SCB-2345 carrier block

FT01 modules were used to connect the analogue voltage signals and TC01 modules for the thermocouple signals.

The high speed data recorded by the order connected to the carrier are:

- Channel 00: engine TDC
- Channel 01: cylinder pressure signal
- Channel03: intake manifold absolute pressure signal
- Channel04: air mass flow
- Channel05: engine torque
- Channel06: intake air temperature
- Channel07: exhaust gas temperature
- Channel08: engine coolant temperature

For true crank angle resolved pressure recordings it was necessary to use an external clock for the data acquisition system because the engine speed is never constant during a combustion cycle.

The acquisition clock was provided from a photoelectric sensor with a black painted steel disc with 360 slots on its circumference attached on the engine's crankshaft. The system designed to provide two TTL outputs: one produces 360 pulses per engine revolution and another producing a single pulse per engine TDC. Therefore high speed crank resolved data at 1° resolution were acquired during all engine experiments. Figure 4.93 shows a photograph of the optical disc attached on the crankshaft.

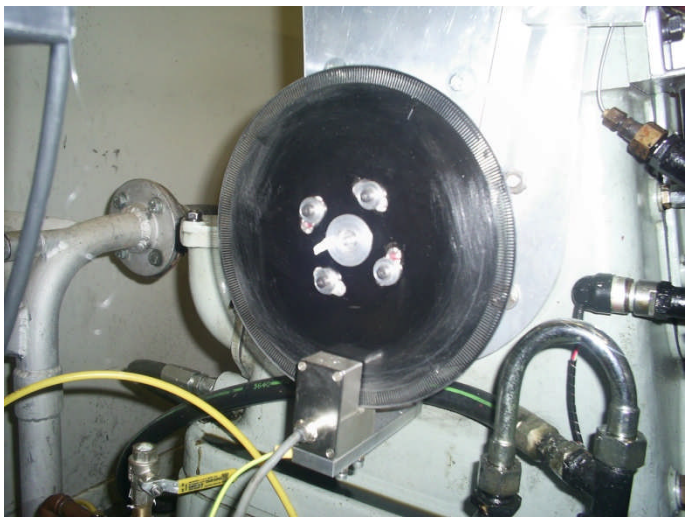

Figure 4.93 Crankshaft optical disc encoder

At the same time averaged values from the following parameters were also recorded:

- Exhaust lambda signals
- Diesel fuel rail pressure
- LPG rail pressure
- LPG rail temperature
- Engine oil temperature

Two Labview VI programs were written to control the acquisition. One provides real time screen of the measured data and the second records a predefined number of engine cycles. When LabView is prompted by the user to begin recording, it records a predefined number of beginning at a TTL high signal from the TDC sensor. The outputs from the crankshaft optical disc were also used to trigger the injection systems. An additional shaft encoder attached at the one end of the camshaft provided the combustion TDC flag. The recorded data were saved in the computer memory as .lvm files.

4.8.7 Data post processing

Matlab code was written to post process the combustion data. The code averages a specified number of combustion cycles and converts the electric signals to physical quantities. It also derives the various engine performance parameters and calculates the heat release and the mass fraction burned per CA from the measured cylinder pressure data. The heat release is calculated from the following equation (Ladommatos & Zhao, 2001):

$$\frac{dQ_n}{d\vartheta} = \frac{\gamma}{\gamma - 1} p \frac{dV}{d\vartheta} + \frac{1}{\gamma - 1} V \frac{dp}{d\theta} \tag{4.20}$$

Where:

γ is the ratio of specific heats $\frac{C_p}{C_v} = 1.3 - 1.35$

p is the instantaneous cylinder pressure

V is the instantaneous cylinder volume

$\frac{dV}{d\theta}$ is the change in cylinder volume per CA

$\frac{dp}{d\theta}$ is the change in cylinder pressure per CA

The mass fraction burned is calculated using the Rassweiler and Withrow method which assumes that the mass fraction burned is in proportion to the fraction of total pressure rise due to combustion. This method does not take into account dissociation, variable gas properties and heat transfer effects and it is commonly used to calculate the mass fraction burned in spark ignition engines (Stone, Armytage, 1987).

The main steps of the Rassweiler and Withrow method are as follows:

1. Obtain the cylinder pressure data versus engine crank angle
2. Determine the pressure rise due to combustion as distinct from the pressure rise attributed to piston motion
3. Normalise the pressure rise data due to combustion and assume that the fraction of total pressure rise is equal to the mass fraction burned. This also assumes that the combustion is complete (Stone, Armytage, 1987).

The choice of the particular method was adopted because of its simplicity and also due to the fact that the pilot ignited operation is similar to a spark ignited operation in principle.

A more detailed description of this method can be found in (Rassweiler & Withrow, 1938).

Some of the derived values are:

- IMEP
- ISFC
- COV
- η_{vol}
- η_f

5 EXPERIMENTATION

5.1 Introduction

The purpose of the experimental work described in this chapter is to demonstrate diesel and explore dual fuel engine operation in order to understand and clarify the ignition characteristics and the combustion process of the diesel/LPG combined operation.

The experimental work is organised in two stages according to engine operating modes. At the first stage the engine is operated in diesel mode in order to demonstrate typical diesel DI engine operation and controllability. Subsequently, using only a small amount of diesel pilot to ignite a larger premixed charge of LPG, the engine is operated in dual fuel mode. A comparison between the two operations reveals the main attractions and drawbacks of operating diesel engines on liquid injected propane.

Regarding to the continuous development in diesel engine technology, a comparison approach based upon three useful aspects concerning future diesel engine development was devised. These aspects include shorter dwell pilot injections, split main injection and split main injection combined with cool EGR.

Late post injections have a soot-oxidizing effect, documented by several authors e.g. (A Helmantel, 2003), which is believed to be due to associated increases in turbulent energy in the late part of the combustion, which enhances the mixing process (Richard Ehleskog, 2007). Therefore as post injections are mainly utilised for exhaust aftertreatment purposes their use was not considered in the present study.

During all the experiments, diesel was supplied at a constant pressure (1600 bar) to the diesel injector from the high pressure common rail injection rig which is described in chapter 4.3.

For the combined diesel/LPG operation, liquid propane injection was achieved through an LPG injector installed on the inlet manifold of the engine. Both diesel and LPG injectors were triggered from the engine shaft encoder signals and controlled via two separate injector driving units.

Important conventions:

It is important at this point to give some definitions adopted during all the experimental work for clarification reasons. These are:

- Injection durations are defined by the injector energising time (in μs) and not by the actual fuel injected quantity. This convention was decided due to the design of the electronic injection system and also as a more common way of describing the injection process.

- The injection strategy was developed based on the assessment of the following parameters:
    - ❖ combustion stability (observed during engine measurements and from COV)
    - ❖ IMEP
    - ❖ ISFC
    - ❖ visible smoke
    - ❖ combustion noise
    - ❖ CO, NOx levels (not always possible due to equipment constrains)
- All experiments were carried out setting the following parameters constant:
    - ❖ Engine speed 1000 $revm^{-1}$
    - ❖ Compression ratio 19:1
- 360° corresponds to engine TDC after the end of the compression stroke.
- Each result represents the average of twenty consecutive combustion cycles.

5.2 Diesel Engine Operation

5.2.1 Introduction

Engine measurements were initially carried out in order to demonstrate typical common rail diesel engine operation. The injection strategy was chosen to be representative of the naturally aspirated dCi engine. Such a strategy, depending on engine operating region (cold, very cold or hot) and load, is generally characterised by a pilot injection followed by a single main and sometimes by a short post injection.

Initially, the effect of pilot injection on engine operation was demonstrated and a basic start of ignition (SOI) timing optimisation was performed. Subsequently using the best-to-date pilot injection, the effect of multiple injections on engine operation was studied by splitting the main injection up to four consecutive sub-injections. In the next step the effect of EGR was investigated for both single and spilt injection. Finally engine part load operation is demonstrated.

5.2.2 Diesel operation with a short pilot and a main injection

A pilot injection results in an increase of thermodynamic conditions within the combustion chamber. The main idea of having pilot injection is to minimise combustion noise by reducing the amount of fuel injected during the diesel combustion delay period. This effectively reduces the premixed combustion duration from which the combustion knock is generated.

Minimum pilot injected quantity was achieved with pilot energising time set to 95μs. It is important to mention here that the very high voltage capability of the diesel ECM was used in order to reduce pilot duration to minimum. Supplying up to 90 Volts to the injector solenoid for the first 20μs of pilot pulse duration enables rapid solenoid operation.

Operating parameters	
Engine speed [RPM]	1000
Pilot SOI [deg]	variable
Pilot duration[μs]	95
Main SOI [μs]	4° (BTDC)
λ	2
Injection pulses	1 pilot +1 main
EGR rate	0%

Table 5-1 engine operating parameters for 1 pilot+1 main operation

Table 5-1 shows the engine operating conditions. At 1000 RPM the pilot injection duration is equivalent to approximately 0.56 crank angle degrees.

Operating the engine with one pilot, a main injection was added at 4° before TDC to achieve λ=2. The value of λ was measured with the MoTeC wide band Lambda sensor system which has been described in paragraph 4.8.4 of chapter four.

Pilot SOI sweeps were performed to determine the optimum timing. λ was kept constant by adjusting the main injection duration for every SOI. Figure 5.3 shows effect of varying the pilot injection SOI on cylinder pressure histories Advancing pilot SOI results to an earlier start of combustion (SOC) and to a 5% increase in peak combustion pressure. Altering SOI timing however does not significantly shift the combustion peak pressure location which seems to occur always at 6° ATDC. The only exception is at fully advanced pilot injection which advances the peak pressure for 1° but this change might be due to the high combustion knock.

Table 5-2 show the effects of pilot SOI on engine performance parameters. The optimum SOI was chosen based on the best compromise between engine performance, exhaust emissions, knock limit and smoke levels. As pilot injection is primarily used to reduce combustion noise, it must be taken as the main driver for the pilot injection optimisation.

Hence the optimum pilot SOI was found at 7° before TDC.

Pilot timing (CA BTDC)	IMEP (bar)	ISFC (g/KWh)	COV (%)	NOx (ppm)	CO (ppm)	Knock	Visible smoke
11°	5.2	204	1.9	968	182	heavy	no
10°	5.2	202	1.4	1120	209	noticeable	no
9°	5.1	208	1.5	1120	160	small	no
8°	5.3	200	2	1106	156	small	no
7°	5.2	201	2.1	1048	135	no	no
6°	5.3	200	1.5	1066	140	small	no

Table 5-2 Influence of pilot timing on engine performance and emissions (start of main injection: 4° BTDC, Rail pressure 1500 bar, λ=2)

Combustion noise, NOx and CO emissions reached a local minimum when pilot SOI was set at 7° BTDC (Figure 5.2). Low CO levels is an indication of good combustion efficiency. Advancing pilot SOI increases combustion noise, becoming heavier at 11° whilst retarding the pilot SOI below 7° has the same effect and below 6° combustion knock becomes severe. This suggests that advancing a small pre-injected quantity beyond a certain limit, has no effect in reducing the ignition delay of the main injection. On the other hand, retarding pilot below a certain point, there is not enough time for the injector needle to close properly and a large quantity of fuel is injected during the

combustion delay period. As a result, a large amount of fuel is premixed with air and when fuel reaction rate reaches the explosive stage, there is a sudden steep pressure rise and combustion noise is generated.

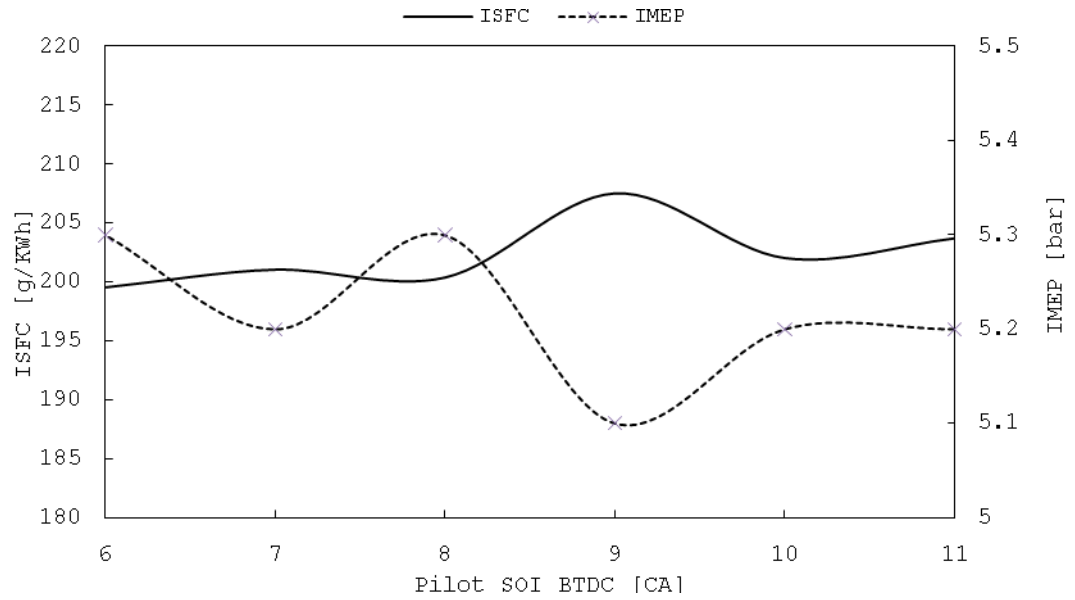

Figure 5.1 Influence of pilot timing on ISFC and IMEP (start of main injection: 4° BTDC –Rail pressure 1500 bar –λ=2)

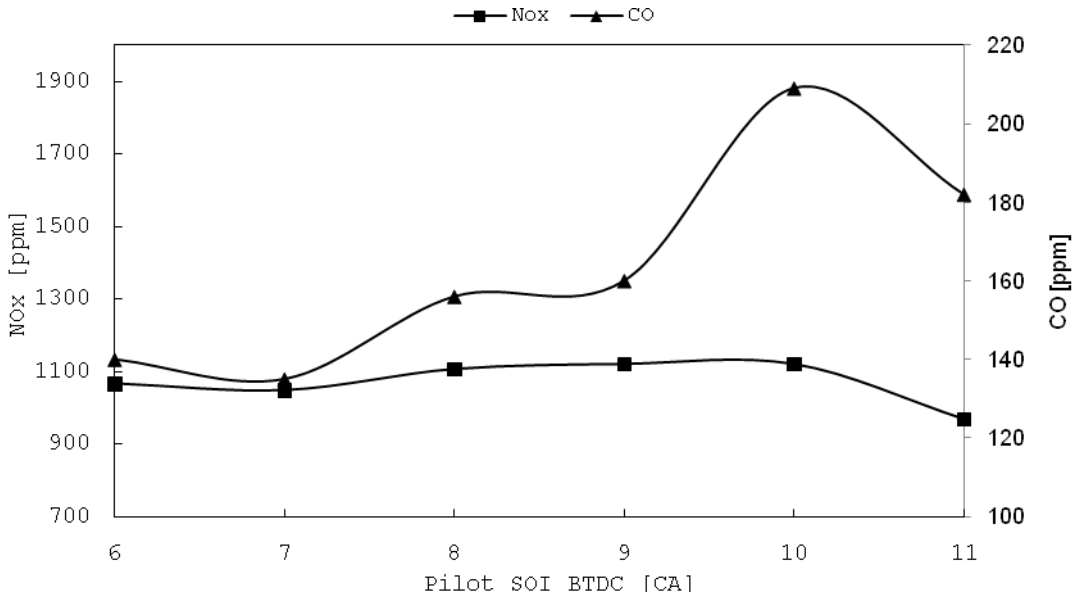

Figure 5.2 Influence of pilot timing NOx and CO emissions (start of main injection: 4° BTDC, Rail pressure 1500 bar, λ=2)

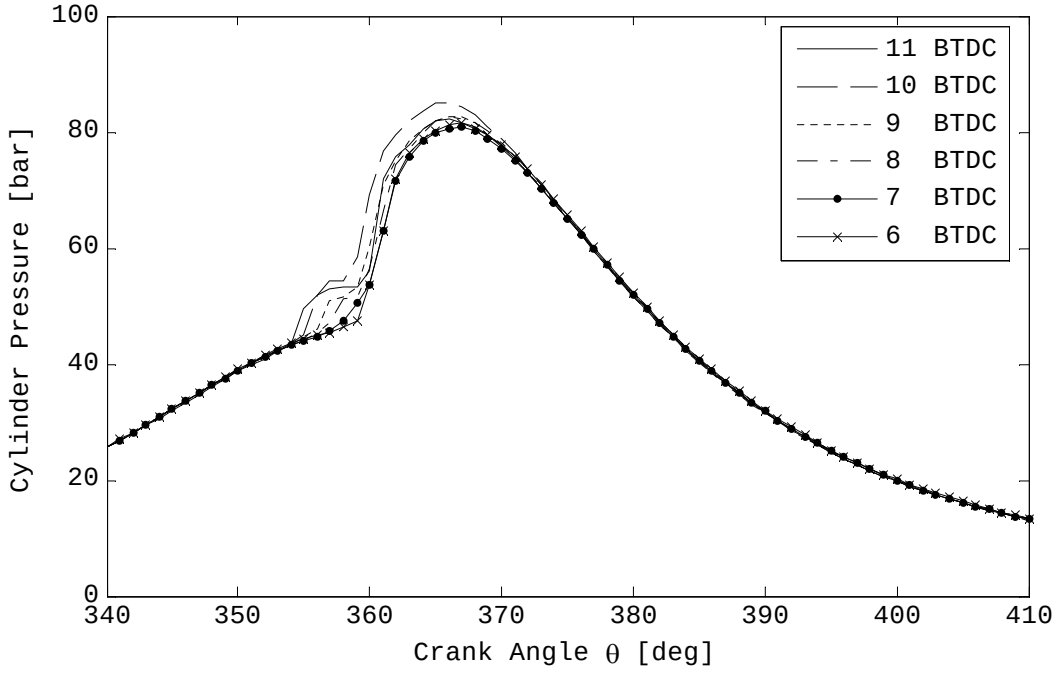

Figure 5.3 Pilot timing sweeps 11…6 ° BTDC, main SOI: 4° BTDC

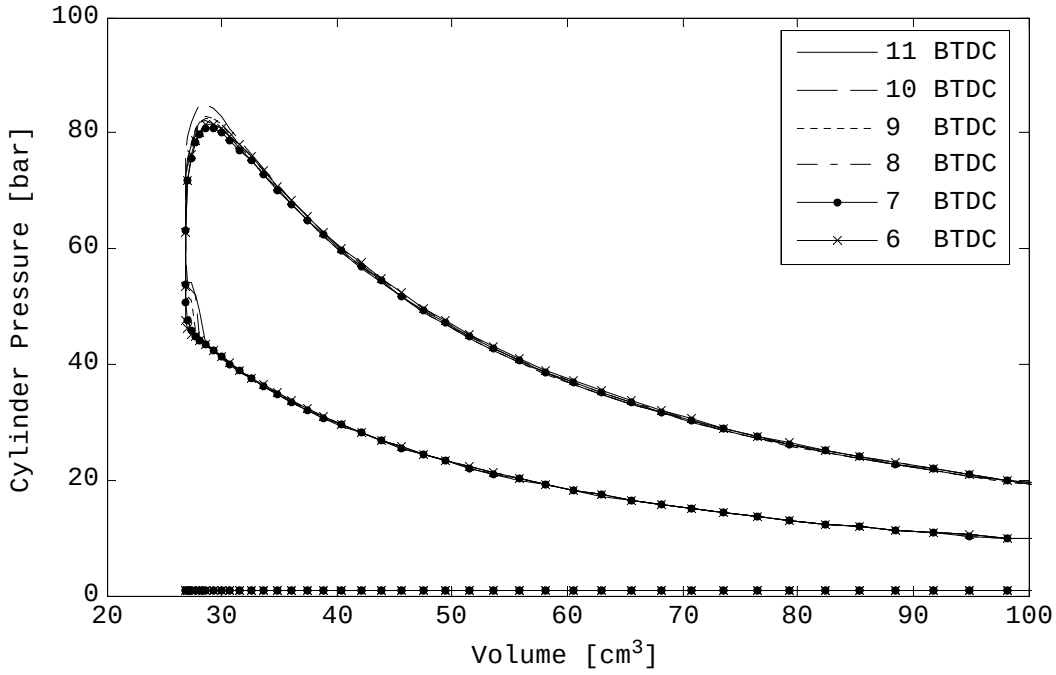

Figure 5.4 Pilot timing sweeps 11…6° BTDC, main SOI: 4° BTDC

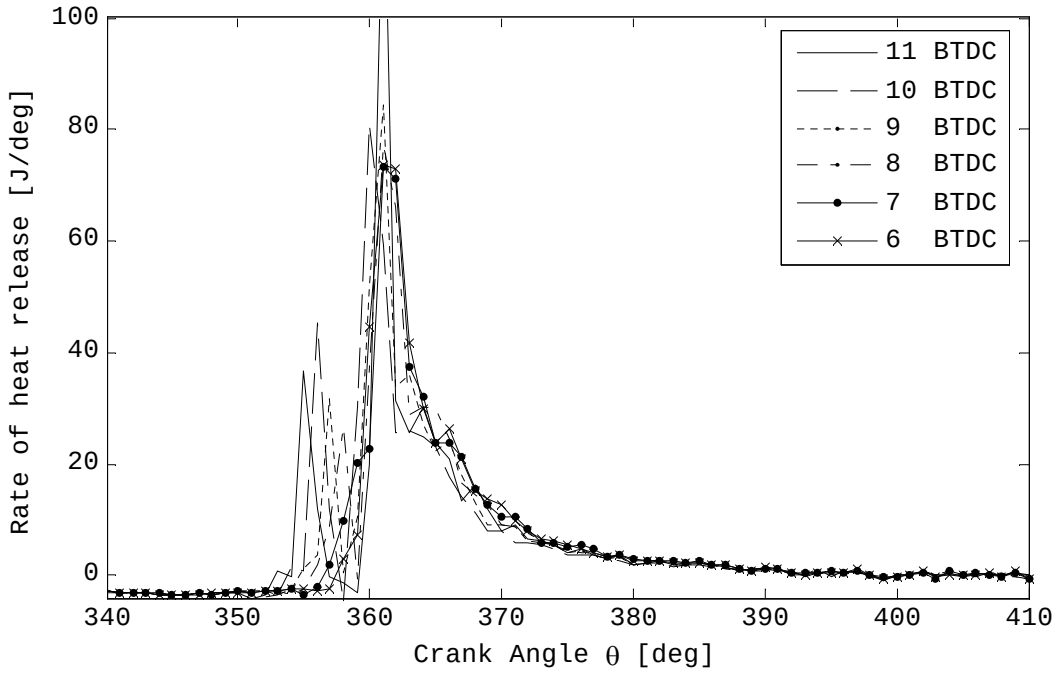

Figure 5.5 Pilot timing sweeps 11…6° BTDC, main SOI: 4° BTDC

Figure 5.5 shows the rate of heat release profiles for various pilot SOIs. Heat release and mass fraction burned calculated from the recorded data give useful information on how the combustion unfolds.

Advancing and retarding pilot injection from optimum point increases combustion noise, although combustion does not unfold in the same way. Combustion noise is the result of the ultra rapid combustion of a large amount of premixed fuel quantity with a high heat release rate. When pilot injection is too short and very advanced from main to influence the combustion delay period, the maximum rate of heat release is generated from the main injection premixed burning phase. On the other hand, when pilot injection is retarded close to the knock limit, noise is generated as a result of pilot grouping with the main injection.

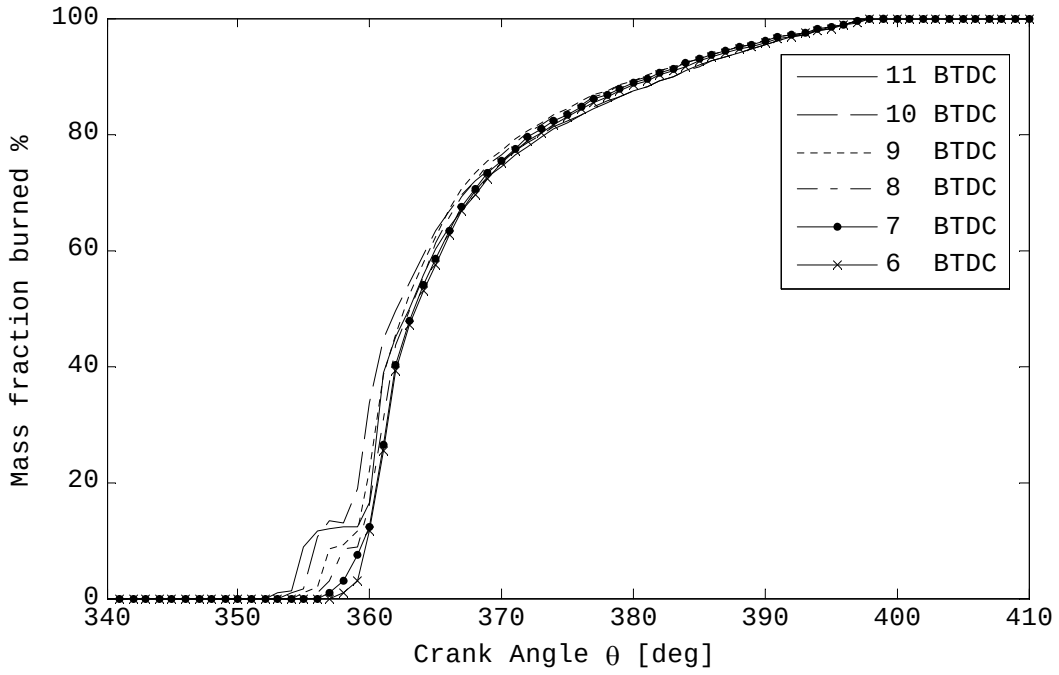

Figure 5.6 Pilot timing sweeps 11…6° BTDC, main SOI: 4° BTDC

Figure 5.6 presents the mass fraction burned derived from the cylinder pressure data using the method of (Rassweiler & Withrow, 1938). The optimum case characterised by the shortest combustion delay and a more progressive slope gradient. This indicates a smooth transition from pilot to main combustion. The combustion of pilot injected quantity is rapid up to 15%CA. After that the burning rate of main injection increases again rapidly until 50% CA of the mass fraction is burned.

From Figure 5.6 and Table 5-3 it is evident that the start of combustion (SOC) is directly depended to SOI timing and advancing the SOI increases the combustion duration. Retarding the SOI increases the burning rate which increases the engine thermal efficiency.

Pilot timing BTDC	**11**	**10**	**9**	**8**	**7**	**6**
SOI [CA]	349	350	351	352	353	354
SOC [CA]	352	353	354	355	356	357
Combustion duration [deg]	46	45	45	44	43	42
Mass fraction burned 02%	2	2	2	2	2	2
Mass fraction burned 05%	2	2	2	2	2	2
Mass fraction burned 10%	3	3	4	4	4	3
Mass fraction burned 50%	11	9	9	8	7	6
Mass fraction burned 90%	31	30	27	26	25	25
Mass fraction burned 95%	37	37	34	33	32	32

Table 5-3 Diesel pilot timing optimisation MFB

The results obtained from optimum pilot injection are presented separately for better clarity (Figure 5.7-Figure 5.10).

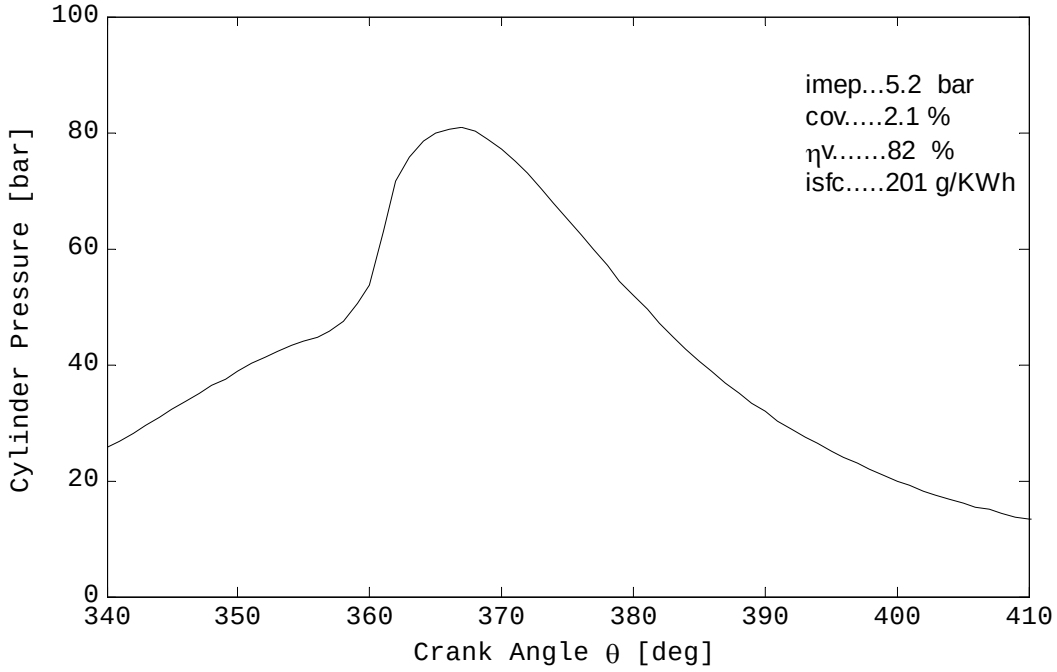

Figure 5.7 Optimum pilot injection timing 7° BTDC –Start of main injection: 4° BTDC

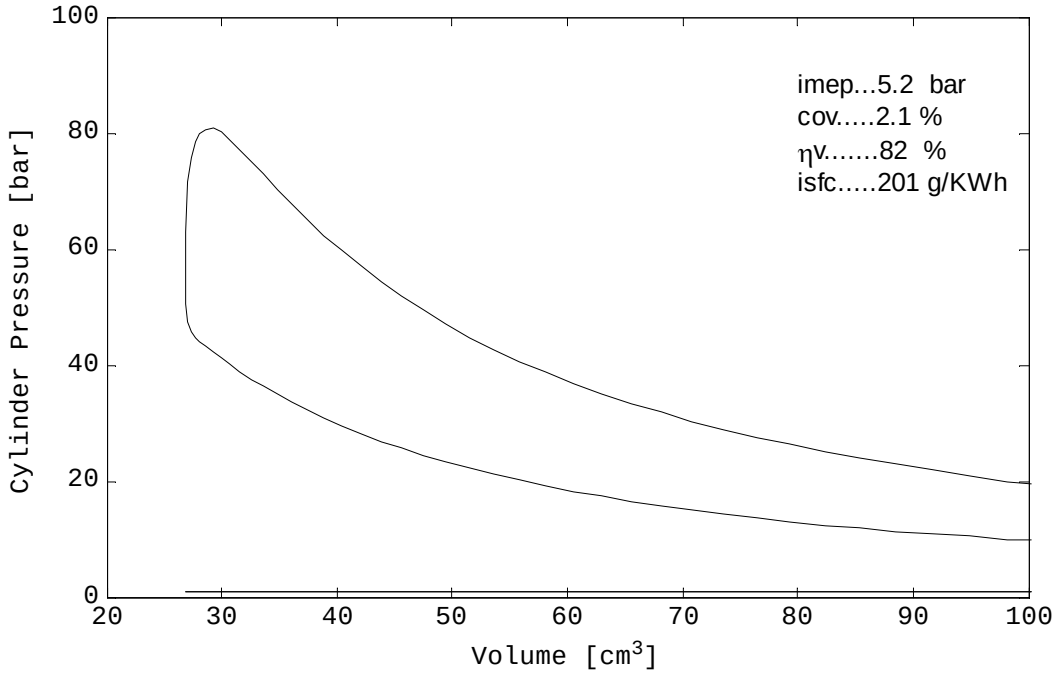

Figure 5.8 Optimum pilot injection timing 7° BTDC –Start of main injection: 4° BTDC

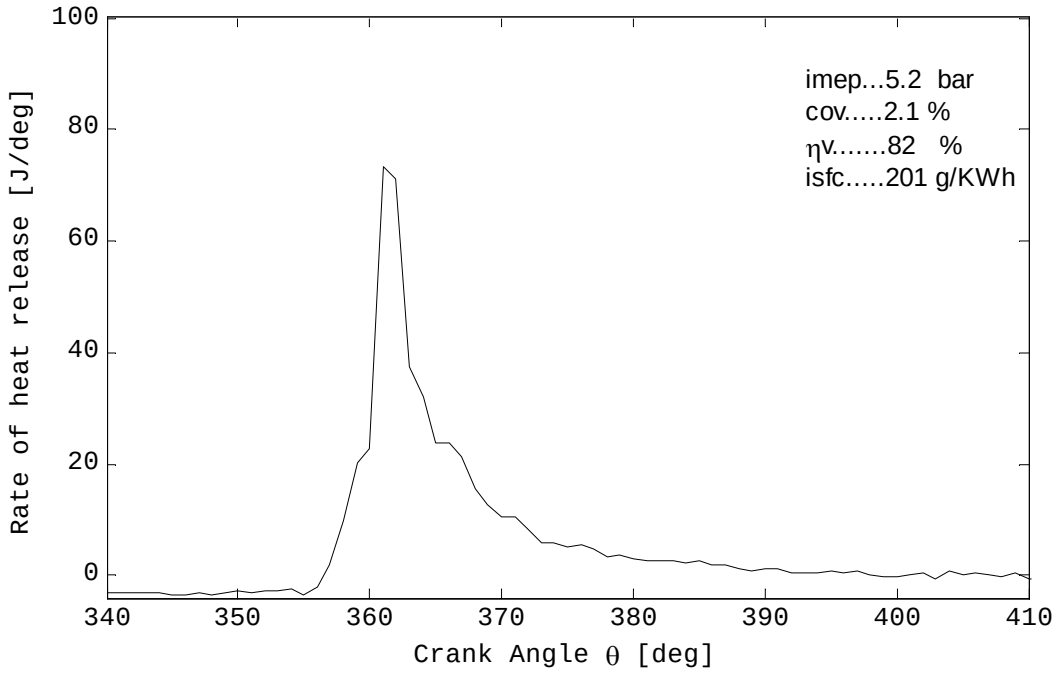

Figure 5.9 Optimum pilot injection timing 7° BTDC –Start of main injection: 4° BTDC

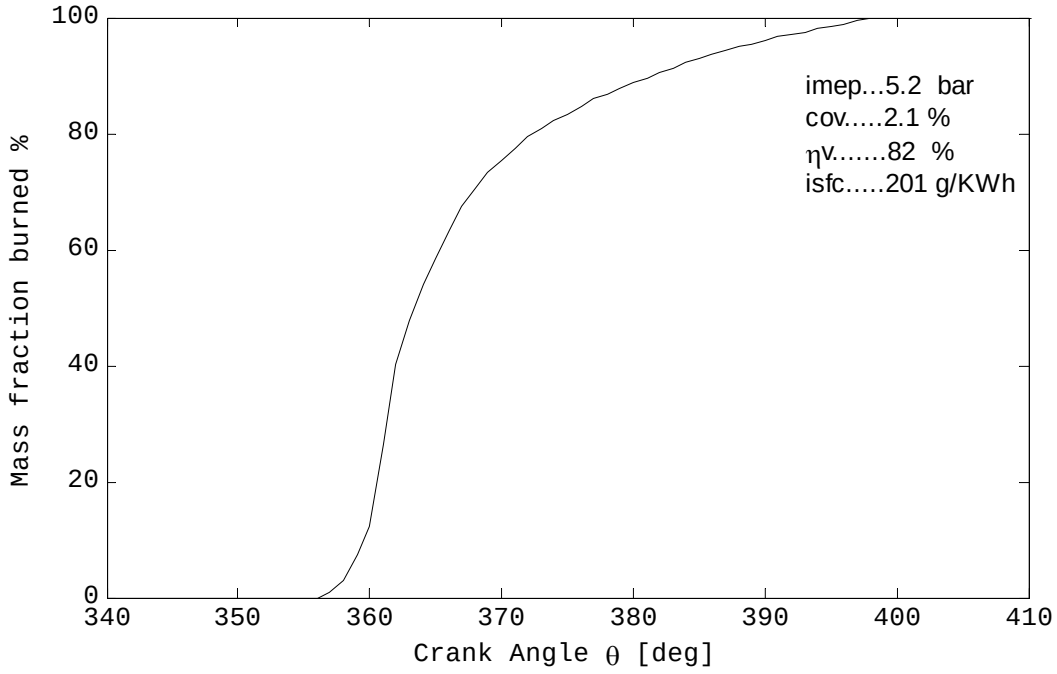

Figure 5.10 Optimum pilot injection timing 7° BTDC –Start of main injection: 4° BTDC

Best pilot MFB	[CA]
SOI	353
SOC	356
Combustion duration	43
Mass fraction burned 02%	2
Mass fraction burned 05%	2
Mass fraction burned 10%	4
Mass fraction burned 50%	7
Mass fraction burned 90%	25
Mass fraction burned 95%	32

Table 5-4 Optimum pilot timing MFB

Overall, a pilot injection reduces the rate of heat release which consequently lowers combustion temperature and therefore NOx levels. As a result combustion noise is also reduced.

Pilot injection results to a lower combustion temperature rise because there is less fuel burned during the combustion delay period.

Pilot injection timing has the most significant effect on diesel combustion noise and it can be used in two different ways: long duration pilot with long dwell times or short duration pilot with short dwell times. Both strategies are effective ways to reduce combustion noise however they both have trade-offs.

The minimum dwell time between pilot and main is limited by the injector hydraulic and electric solenoid performance. Therefore a long duration pilot strategy is more common for solenoid injectors fitted on high speed engines where opening and closing response becomes an issue particularly at high engine speeds. However, long duration pilots are likely to increase engine BSFC due to the inevitably higher amount of heat release occurring before TDC. On the other hand using short pilot durations combined with short dwell times, precise combustion control can be achieved but at the same time good shot-to-shot injection stability is limited by the injector solenoid and needle design.

On in-production engines using solenoid injectors the dwell times between consecutive injections cannot be reduced below a minimum threshold because of electronic/hydraulic response time. With the advent of the new piezoelectric injectors this limitation can be stretched.

Clearly the short dwell time pilots are the most interesting for future diesel engine development for reducing combustion noise without the penalty of increasing BSFC and for improved fuel injection control.

5.2.3 Split injection

Using pilot injection reduces combustion noise and promotes good combustion performance but NOx levels are still considerable. The main reason for this is the high peak combustion temperatures occurring near TDC.

This section explores the idea of splitting the main injection in order to reduce combustion peak pressures and consequently NOx. Thus engine experiments were undertaken using the diesel ECM capability to split the main injection up to a maximum of four sub-injections.

The optimal injection timing with one pilot and one main injection from previous step was used as a baseline (Table 5-1). Then the pilot injection was set at 7° before TDC at constant injection duration (95μs). Subsequently the main injection was split up to a maximum of four small injections of equal duration as it is shown in Figure 5.11. The length of each small injection was adjusted to maintain λ by increasing the total duration of the main injection.

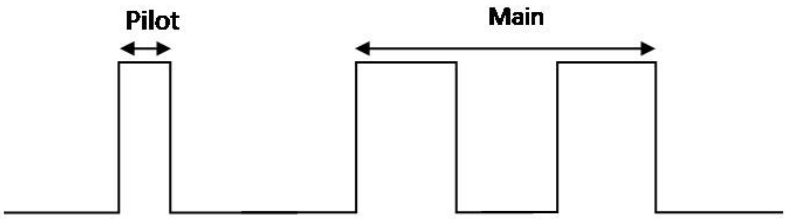

Figure 5.11 Split injection 1 pilot & 2 mains

Using always the same injection timing, cylinder pressure data and emission levels were recorded for the following split injection cases:

- 1 pilot + 1 main (best diesel from previous step)
- 1 pilot + 2 mains
- 1 pilot + 3 mains
- 1 pilot + 4 mains

The engine operating parameters are shown in Table 5-5.

Operating parameters				
Engine speed [rp]	1000	1000	1000	1000
Pilot SOI [deg]	7° (BTDC)	7° (BTDC)	7° (BTDC)	7° (BTDC)
Pilot duration[μs]	95	95	95	95
Main SOI [μs]	4° (BTDC)	4° (BTDC)	4° (BTDC)	4° (BTDC)
Main duration[μs]	470	555	590	582
λ	2	2	2	2
Injection pulses	1pilot+1main	1pilot+2mains	1pilot+3 mains	1pilot+4mains
EGR rate	0%	0%	0%	0%

Table 5-5 Engine operating parameters for split injection testing

Increasing the number of injections has the effect of reducing combustion temperature by lowering the rate of heat release. This results to a significant reduction in NOx levels as it can be seen in Figure 5.12.

The following figures represent the cylinder pressure and the corresponding heat release profiles for double, triple and quadruple main injections. The combustion data for optimum 1 pilot-1 main injection are also plotted for comparison.

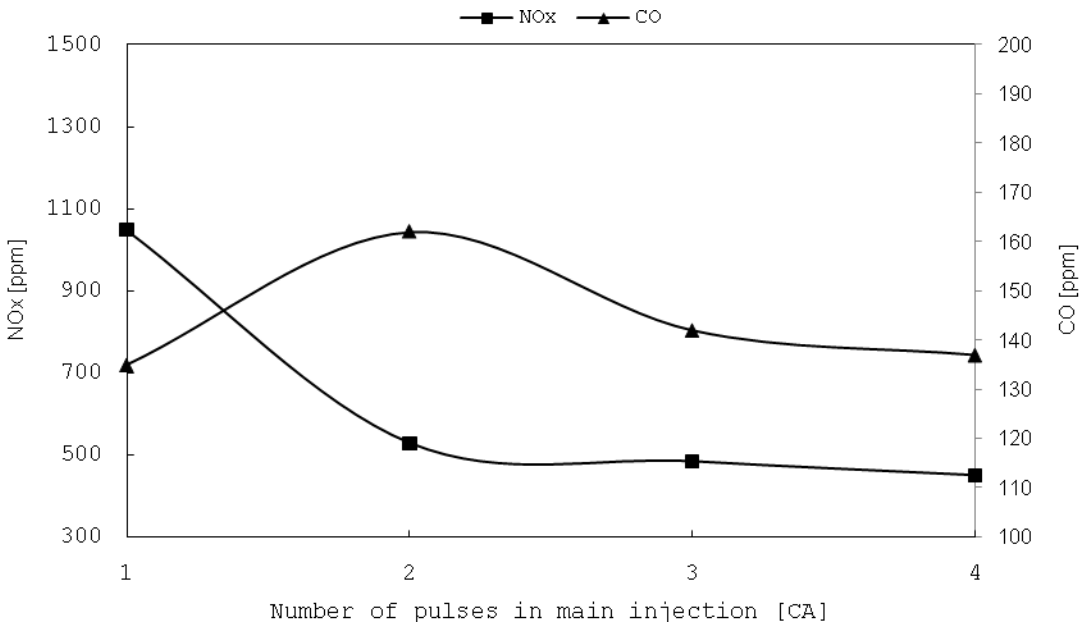

Figure 5.12 Effect of split injection on NOx and CO emissions

The most obvious observation in the cylinder pressure histories is the reduced combustion peak pressure when the main injection is split (Figure 5.13, Figure 5.17, Figure 5.21). The engine produces the same IMEP but with heat release rates significantly lower compared to the single main injection.

The PV diagrams (Figure 5.14, Figure 5.18 and Figure 5.22) show clearly how work is produced in each case, i.e. when single main injection is used, most of the work is produced near TDC whereas with multiple injection activated, large amount of this work is produced later in the expansion stroke.

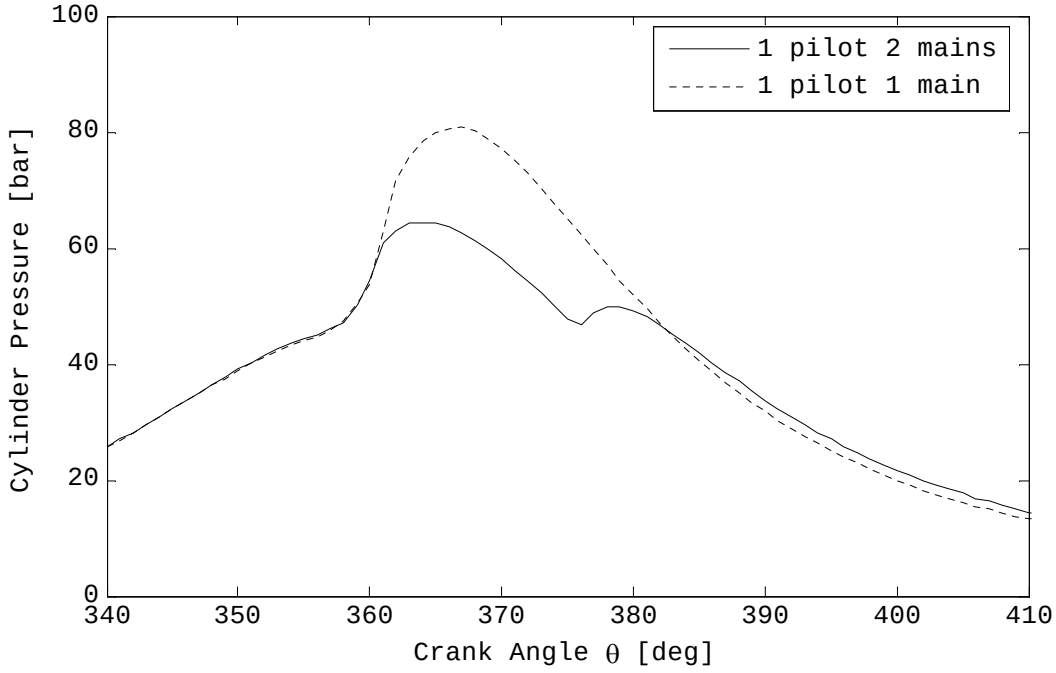

Figure 5.13 PT 1 pilot, 2 mains (pilot SOI: 7° BTDC, main SOI: 4° BTDC, λ=2)

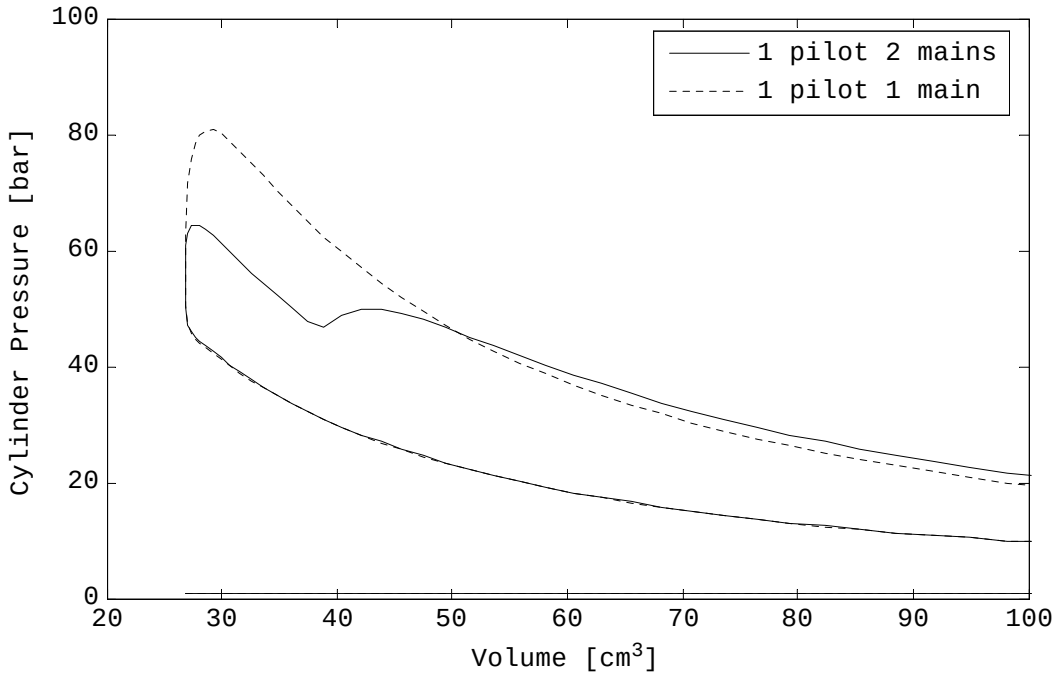

Figure 5.14 PV 1 pilot, 2 mains (pilot SOI: 7° BTDC, main SOI: 4° BTDC, λ=2)

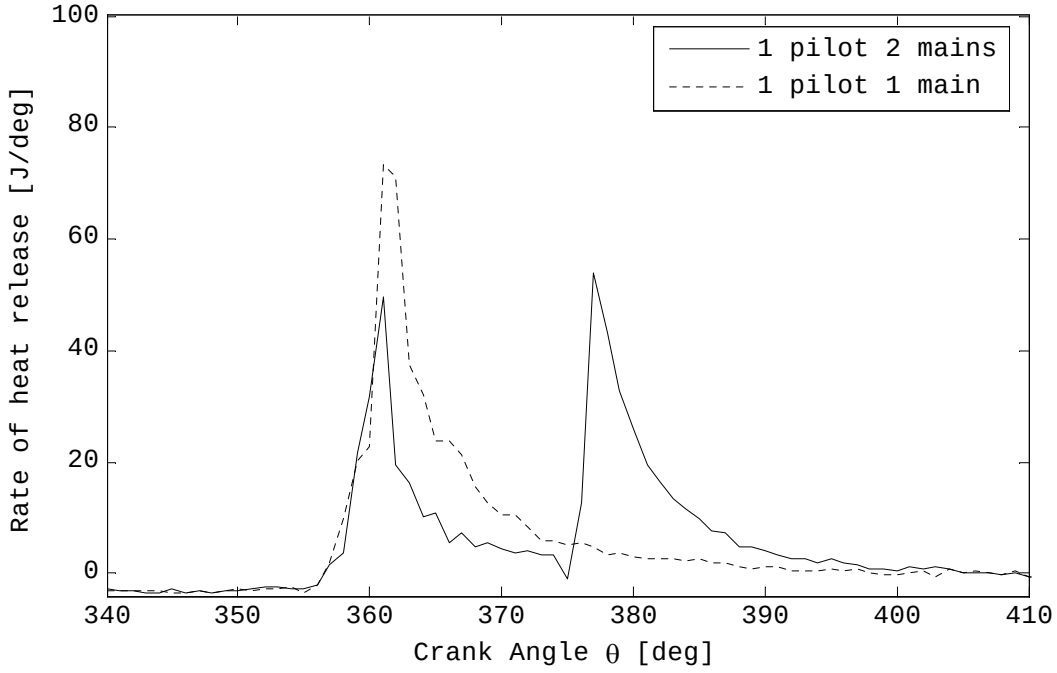

Figure 5.15 ROHR 1 pilot, 2 mains (pilot SOI: 7° BTDC, main SOI: 4° BTDC, λ=2)

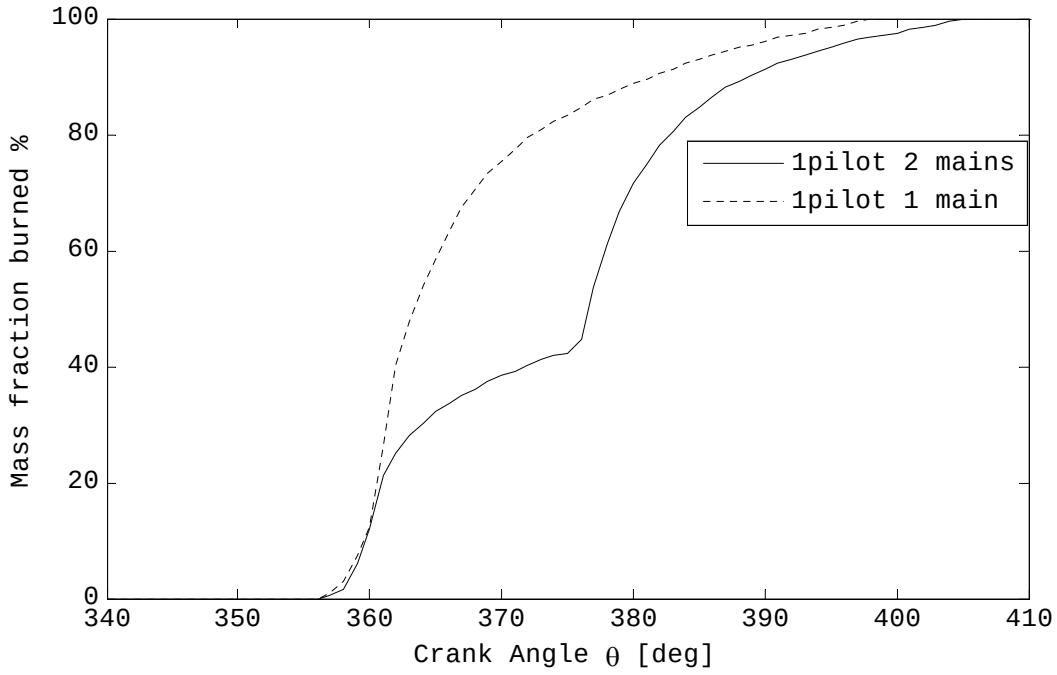

Figure 5.16 MFB 1 pilot, 2 mains (pilot SOI: 7° BTDC, main SOI: 4° BTDC, λ=2)

The number of main injections and the corresponding dwell times have a significant effect on how the energy is released during combustion. All ROHR curves coincide to 4° before TDC as pilot injection and dwell time of the first main are identical in all cases. However after this point the shape of the curves changes with the number of injections. Each individual injection corresponds to a discrete peak on the ROHR

profiles. The dips following the ROHR peaks indicate a decrease in combustion intensity during injector closing period. Also it is apparent that the dip duration becomes shorter as the number of main injections increases but this is due to the way the injector driver divides the main injection.

From Figure 5.15 it is clear that for double main injection the maximum rate of heat release is lowered by 26% which results to a 50% reduction in NOx levels. This is a remarkable result even for non optimised injection dwell times. Introducing another main injection, lowers the ROHR by 37% compared to single main injection (Figure 5.19). This brings NOx down by 54%. Finally, quadruple main has similar result with the triple one: ROHR is 38% lower causing a further reduction in NOx by 57% (Figure 5.23).

There are two mechanisms that influence combustion temperature when splitting the main injection. When a specific quantity of fuel is injected in multiple stages instead of one stage, the energy is released at lower rate causing a drop in peak combustion temperature. The second mechanism is due to the charge cooling effect from fuel evaporation. When fuel is injected in the combustion chamber it initially evaporates absorbing some heat from the surrounding. In the case of single main injection there is only an initial cooling effect from the fuel injection and the combustion progresses until the fuel is burned. In the case of split injection however, the cooling effect occurs more than once causing a progressive reduction in combustion temperature.

The mass fraction burned profiles (Figure 5.15, Figure 5.19 and Figure 5.23) show an identical start of combustion timing for single and split main injections. This is not surprising as pilot injection and first main injection timing are constant. Up to CA10% burning rates are almost identical but they are significantly retarded after CA50% due to the split injection. As the number of injections increases the dwell durations become shorter which results to an advanced CA50. This probably explains why triple and quadruple injections show slightly faster burning rates at CA50% than double main injection.

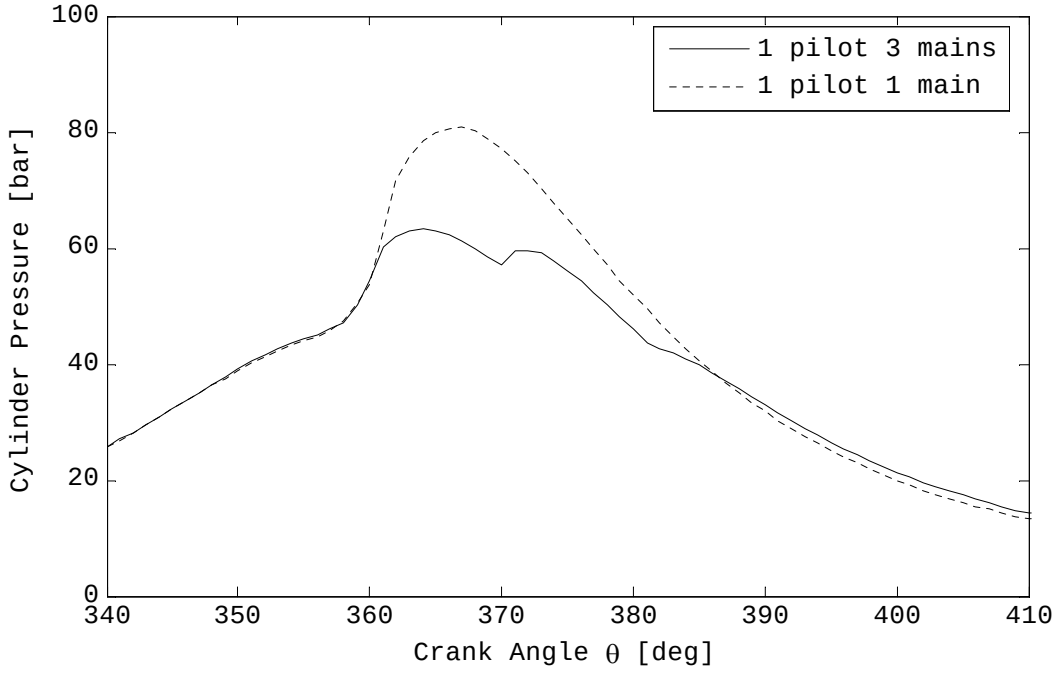

Figure 5.17 PT 1 pilot, 3 mains (pilot: SOI: 7° BTDC, main SOI: 4° BTDC, λ=2)

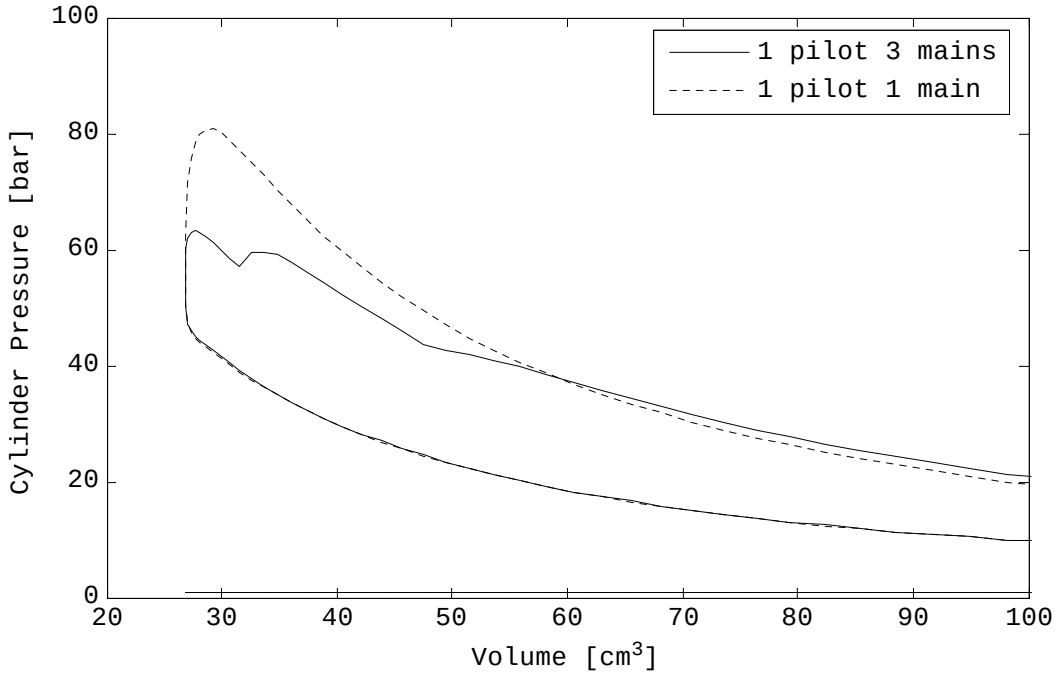

Figure 5.18 PV 1 pilot, 3 mains (pilot: SOI: 7° BTDC, main SOI: 4° BTDC, λ=2)

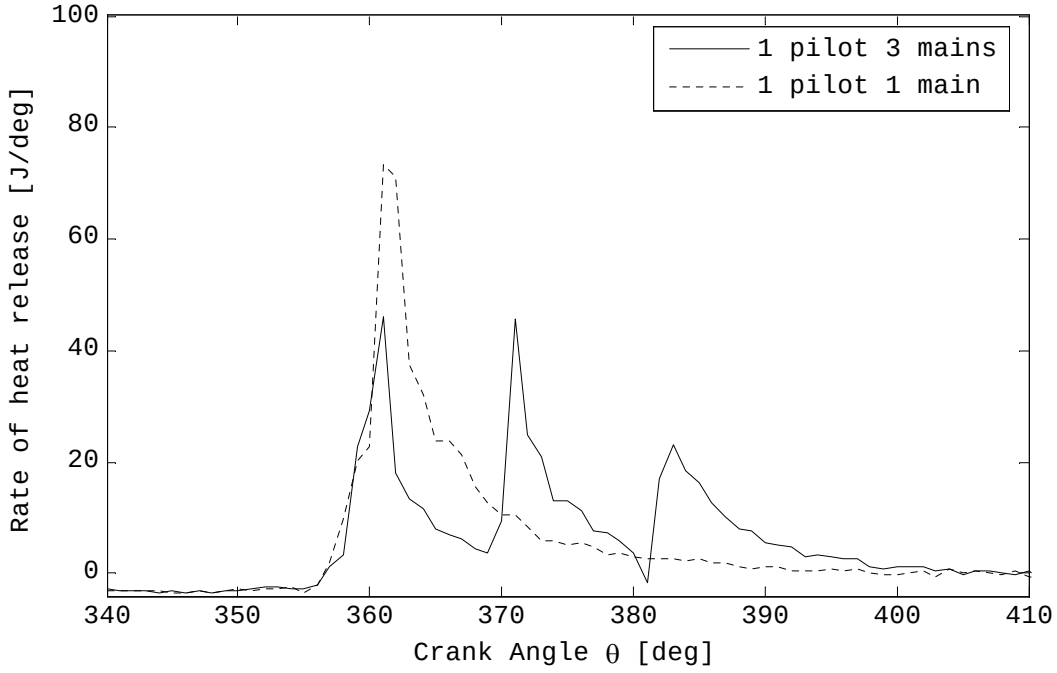

Figure 5.19 ROHR 1 pilot, 3 mains (pilot: SOI: 7° BTDC, main SOI: 4° BTDC, λ=2)

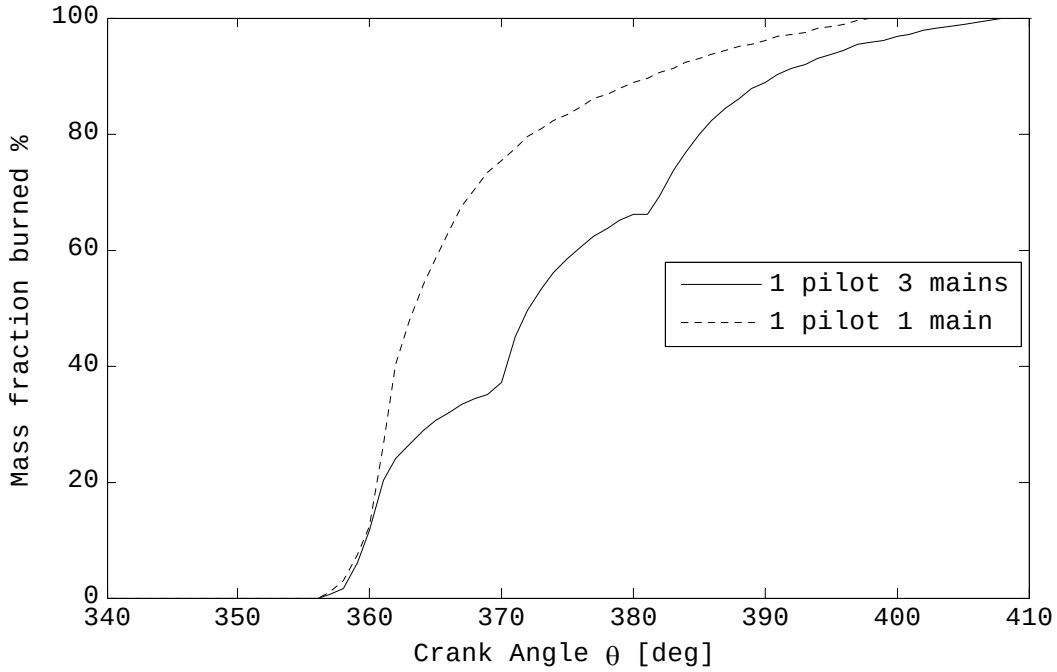

Figure 5.20 MFB 1 pilot, 3 mains (pilot: SOI: 7° BTDC, main SOI: 4° BTDC, λ=2)

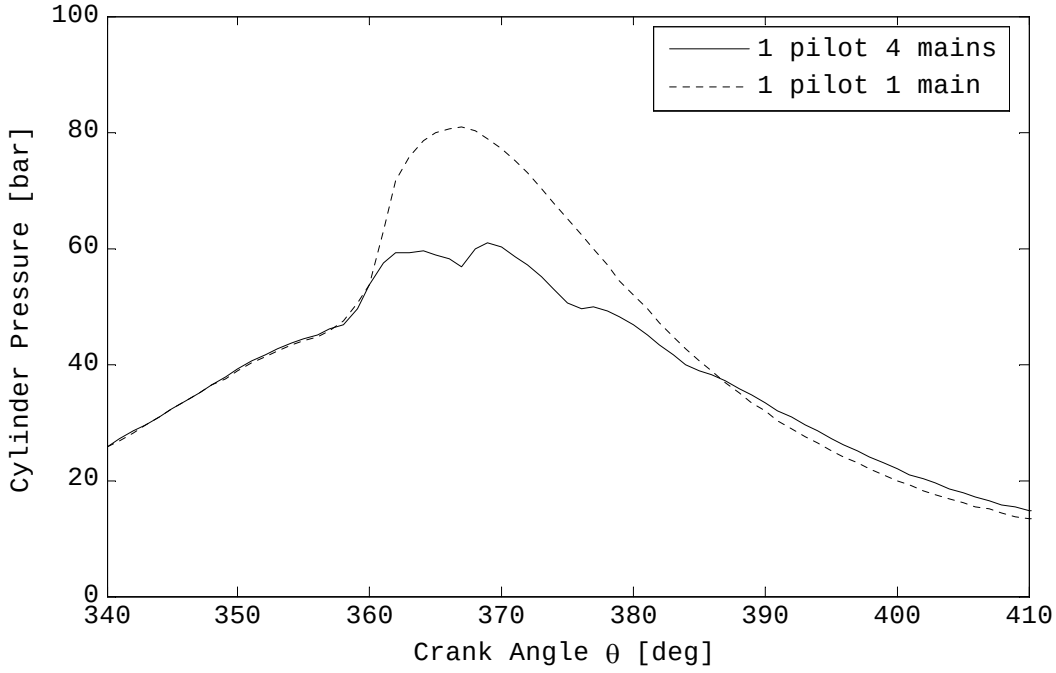

Figure 5.21 1 pilot, 4 mains (pilot: SOI: 7° BTDC, main SOI: 4° BTDC, λ=2)

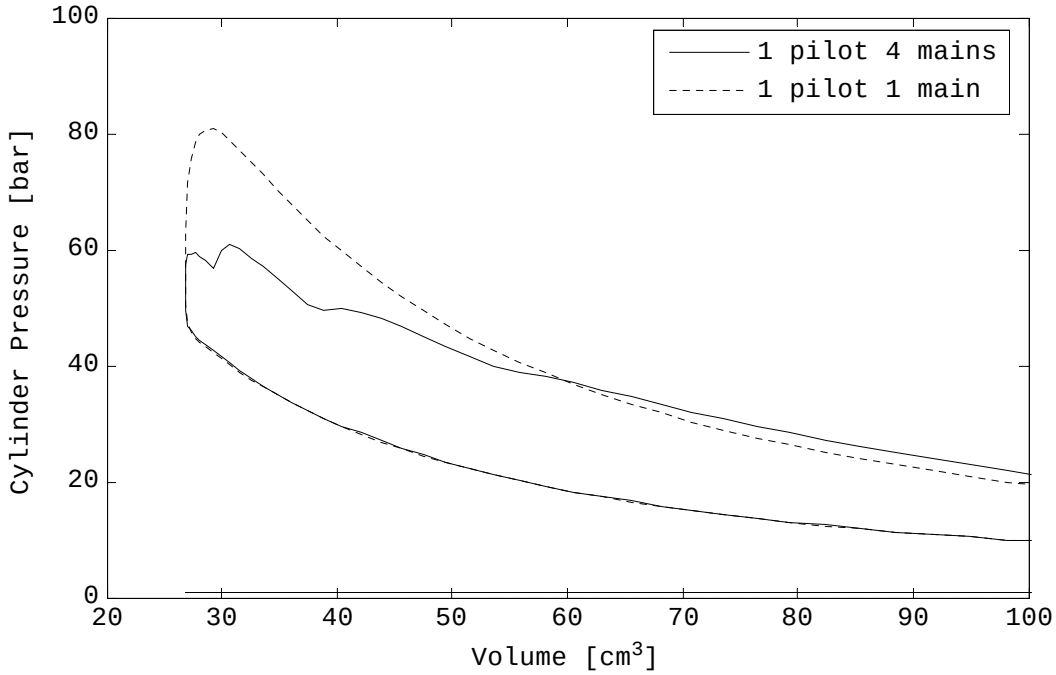

Figure 5.22 1 pilot, 4 mains (pilot: SOI: 7° BTDC, main SOI: 4° BTDC, λ=2)

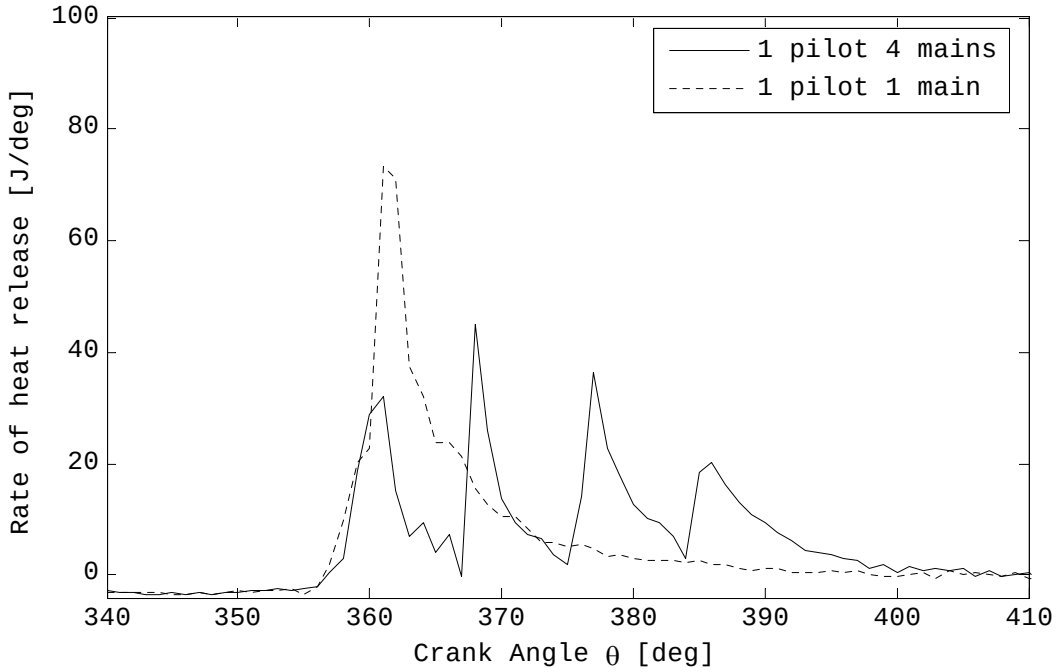

Figure 5.23 1 pilot, 4 mains (pilot: SOI: 7° BTDC, main SOI: 4° BTDC, λ=2)

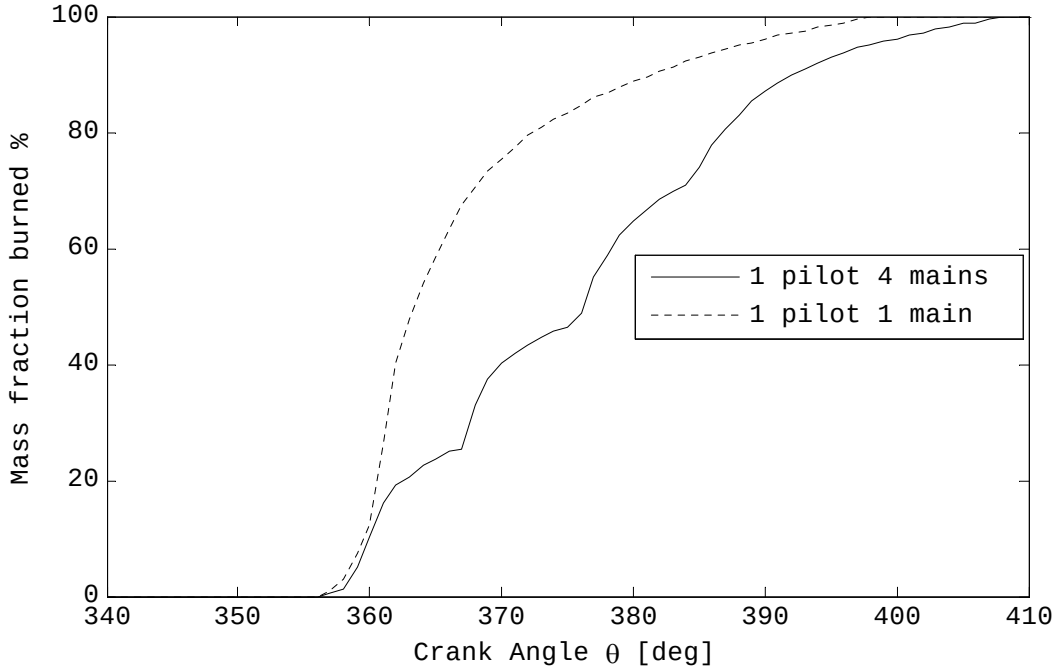

Figure 5.24 1 pilot, 4 mains (pilot: SOI: 7° BTDC, main SOI: 4° BTDC, λ=2)

From Table 5-6 it is obvious that combustion duration increased by increasing the number of injections which explains the small raise of CO levels (Figure 5.12). However it is not very clear whether this increase is directly related to split injection

and is believed to be due to limited capability of the injector to operate at shorter dwell times. This limitation can be probably stretched using piezoelectric injectors.

Number of main injections	**1**	**2**	**3**	**4**
SOI [CA]	353	353	353	353
SOC [CA]	356	356	356	356
Combustion duration [deg]	43	50	53	53
Mass fraction burned 02%	2	2	2	2
Mass fraction burned 05%	2	3	3	3
Mass fraction burned 10%	4	4	4	4
Mass fraction burned 50%	7	21	16	20
Mass fraction burned 90%	25	33	35	36
Mass fraction burned 95%	32	39	41	42

Table 5-6 Effect of split injection on combustion

Splitting the main injection, the rate of injection can be precisely controlled leading to a more progressive combustion. This results to a lower rate of heat release which consequently reduces combustion temperatures and therefore NOx.

Number of main injections	**1**	**2**	**3**	**4**
IMEP [bar]	5.2	5.3	5.2	5.3
ISFC [g/KWh]	201	200	204	201
COV [%]	2.1	2.6	4	2.1
NOx [ppm]	1048	528	483	449
CO [ppm]	135	162	142	137
Visible smoke	No	No	No	No
Knock	No	No	No	No
η_f [%]	41.6	42	41.4	42
η_v [%]	82	82	83	83

Table 5-7 Effect of split injection on engine performance

Using split injection reduced NOx emissions by 57%. However this expected to slightly increase PM due to the lower combustion temperatures.

Combustion noise is considerably lower and the engine operation is quieter compared to the optimum 1 pilot-1main case.

The CO emissions increased slightly for split injection in Figure 5.12. This is probably the consequent reduction in combustion efficiency due to the increased combustion duration and the lower heat release rates. However this CO increase is low enough to be important.

At higher engine speeds and higher load a significantly longer main duration is necessary. By using split injection the fuel is less likely to penetrate against the cylinder wall and more likely to settle within the piston bowl. This would result in lower HC emissions.

5.2.4 EGR

In some engines, a fraction of the exhaust gases is recycled to the intake to dilute the fresh mixture in order to control NOx emissions (Heywood, 1988). This is known as exhaust gas recirculation (EGR). Cooled EGR is a common way to control in–cylinder NOx production in the majority of modern common rail engines. Considering this, it was decided to demonstrate some of the effects of EGR on combustion heat release and NOx emissions.

EGR was achieved by piping a route from the exhaust to the inlet manifold of the E7 using copper pipes and appropriate Y-connectors. The EGR flow rate was controlled via a gate valve placed close to the intake manifold side.

Engine experiments were carried out using best-to-date diesel injection settings from chapter 5.2.2. Pilot and main SOI duration and timing were kept constant in order to demonstrate the effect of EGR.

Operating parameters	
Engine speed [RPM]	1000
SOI pilot [deg]	7° (BTDC)
SOI main [deg]	4° (BTDC)
Pilot duration[μs]	95
λ	2
Injection pulses	1 pilot 1 main
EGR rate	22%

Table 5-8 Engine operating conditions for EGR

Initially the engine was operated using best to-date diesel settings without EGR and data were recorded to be used as reference. Subsequently data were recorded with the 22% of the induced mass replaced by EGR.

When EGR was introduced, λ was reduced from 2 to 1.6 due to the dilution effect. This is the reduction in oxygen fraction in the inlet charge due to the replacement of fresh charge with CO_2 and H_2O which are the main constituents of EGR.

Adding 22% EGR reduced NOx emissions by 55 % (Table 5-11) but increased CO levels.

Subsequently data were recorded with the main injection duration reduced in order to establish λ=2. This lowered the engine IMEP by 1 bar.

From the results it appears that the engine volumetric efficiency has dropped from 83% to 64% after introducing EGR. This difference though is not a throttling effect caused by the EGR but it is due to the method of measuring the volumetric efficiency of the engine. Basically the installation of the engine air flow meter upstream the inlet manifold measures only the air induced from the atmosphere neglecting the EGR flow.

Knowing that a higher inlet charge temperature would have lowered the inlet charge density resulting to a reduced mass flow, cold EGR was used to keep the throttling effect minimum. Therefore the difference in volumetric efficiency corresponds to the EGR mass flow percentage. EGR was cooled by passing the hot gases through a long copper pipe as heat exchanger.

According to other researchers, EGR causes an increase on ignition delay and a shift in the location of the start of the combustion. This effect is very clear on the best to-date diesel operation with 1 pilot and 1 main injection when EGR is introduced. Adding EGR reduced the value of λ from 2 down to 1.6 without any change on IMEP. Figure 5.27 shows the rate of heat release rate for best to-date diesel with 22% EGR with and without fuel compensation. In the non compensated operation (λ=1.6) the IMEP remains unchanged since the same amount of fuel is used. The ignition delay was increased (Table 5-10) and the combustion start was retarded by two degrees of crank. Longer ignition delay causes more fuel to burn in the premixed phase causing a higher ROHR. This is clear on ROHR profiles with EGR in Figure 5.27 showing that a larger quantity of pilot burns in the premixed phase causing a higher ROHR for both pilot and main injections. Since pilot burns faster and main ignition delay increases there is a dip between pilot and main ROHR which distinguishes pilot from main injection.

The ROHR profile for λ=2 has almost identical shape as for λ=1.6 but lower peak values due to the leaner combustion.

In both cases the combustion noise is significantly reduced as a result of the lower ROHR.

As a next step, it was decided to demonstrate the effects of combined EGR with split injection. Using the same engine settings the main injection was initially split into two consecutive injections and λ was kept to 2. Table 5-9 shows the engine operating parameters. Then 22% EGR added and combustion data were recorded. Subsequently the main injection was further split and measurements were taken for triple main injection.

Operating parameters	
Engine speed [RPM]	1000
SOI pilot [deg]	7° (BTDC)
SOI main [deg]	4° (BTDC)
Pilot duration[μs]	95
λ	2
Injection pulses	(a)1 pilot 2 main, (b)1pilot 3mains
EGR rate	22%

Table 5-9 Engine operating parameters for EGR and split injection

Adding double main injection to EGR NOx was reduced by 57% and when main injection was split to three sub-injections the reduction was 62%.Hence the total

reduction in NOx from the combined EGR and triple main injection was 83% lower compared to the diesel only operation. This is a remarkable result even for not fully optimised parameters. Splitting the main injection caused also a small reduction on CO levels. This is probably due to the multiple premixed combustion events during one cycle which promote good combustion efficiency.

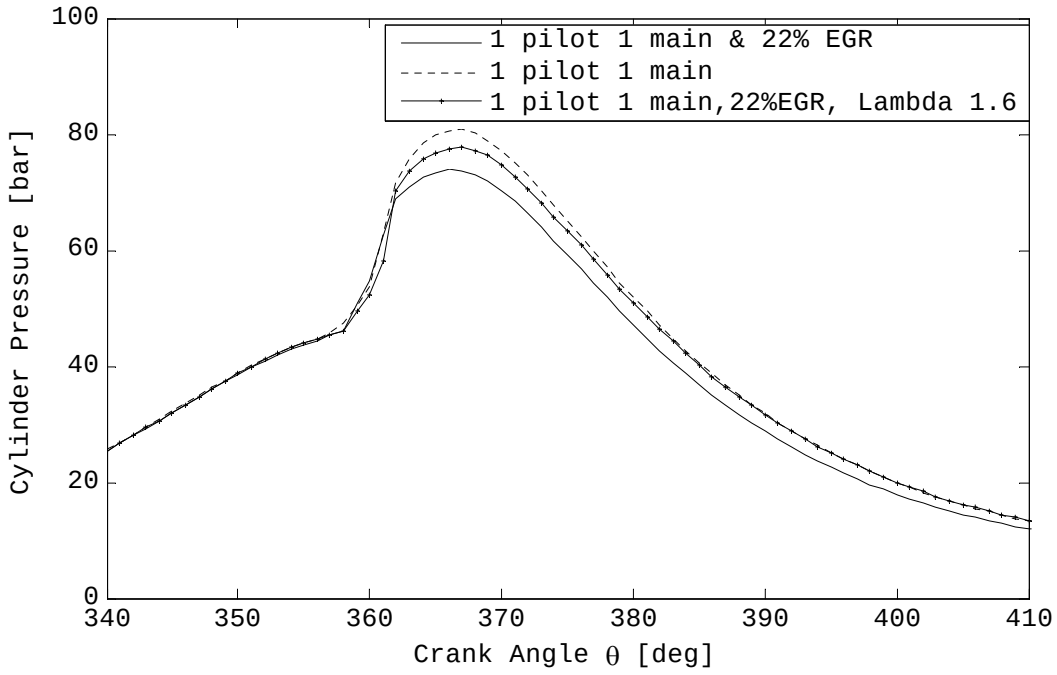

Figure 5.25 1 pilot, 1 main, pilot SOI: 7° BTDC, main SOI: 4° BTDC, λ=2

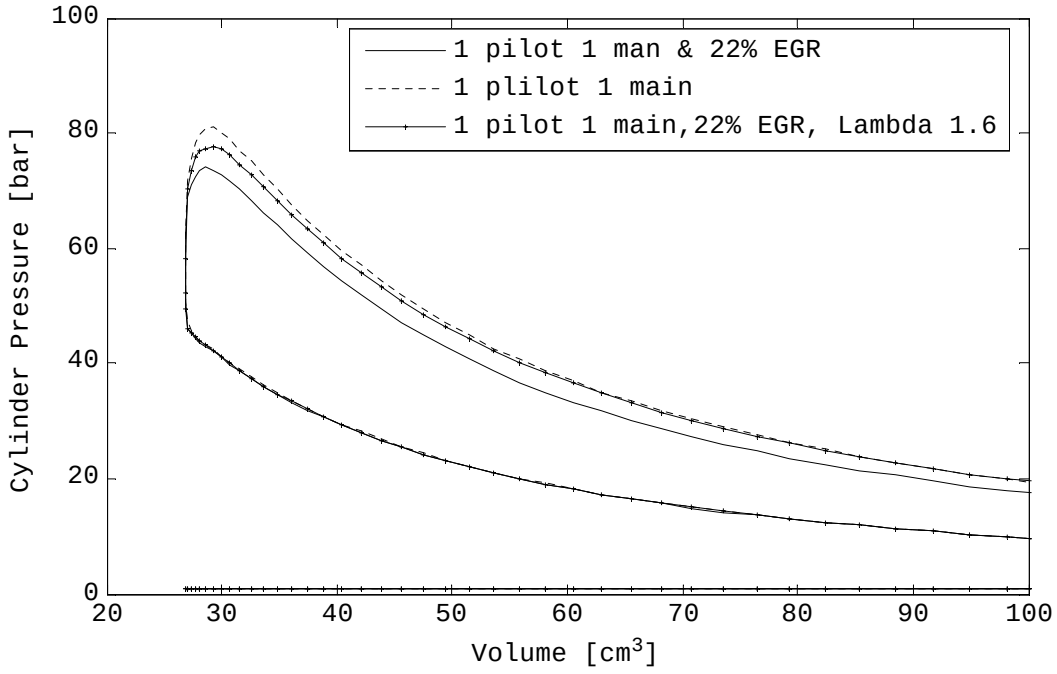

Figure 5.26 1 pilot, 1 main, 22% EGR (pilot: SOI: 7° BTDC, main SOI: 4° BTDC, λ=2)

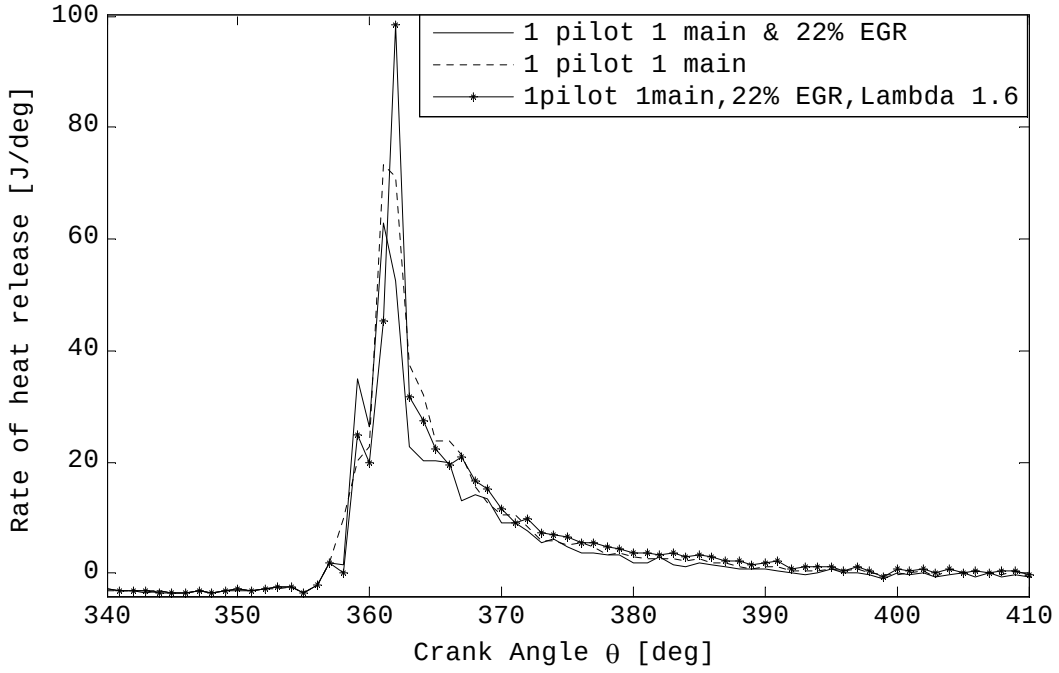

Figure 5.27 1 pilot, 1 main, 22% EGR (pilot: SOI: 7° BTDC, main SOI: 4° BTDC, λ=2)

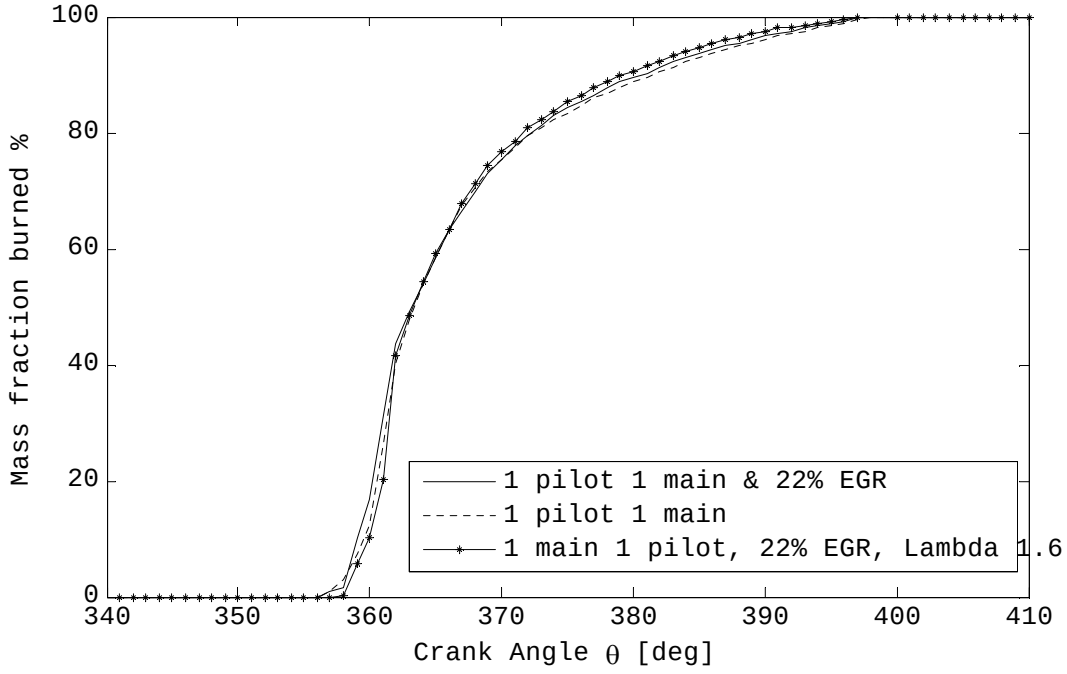

Figure 5.28 1 pilot, 1 main, 22% EGR (pilot: SOI: 7° BTDC, main SOI: 4° BTDC, λ=2)

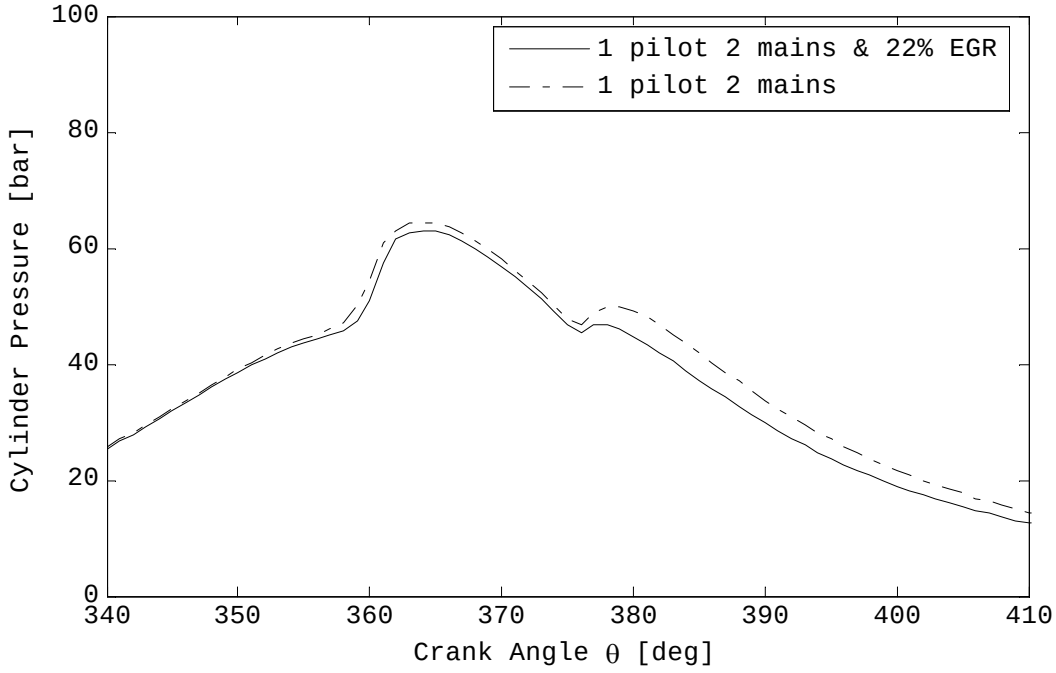

Figure 5.29 1 pilot, 2 mains, 22% EGR (pilot: SOI: 7° BTDC, main SOI: 4° BTDC, λ=2)

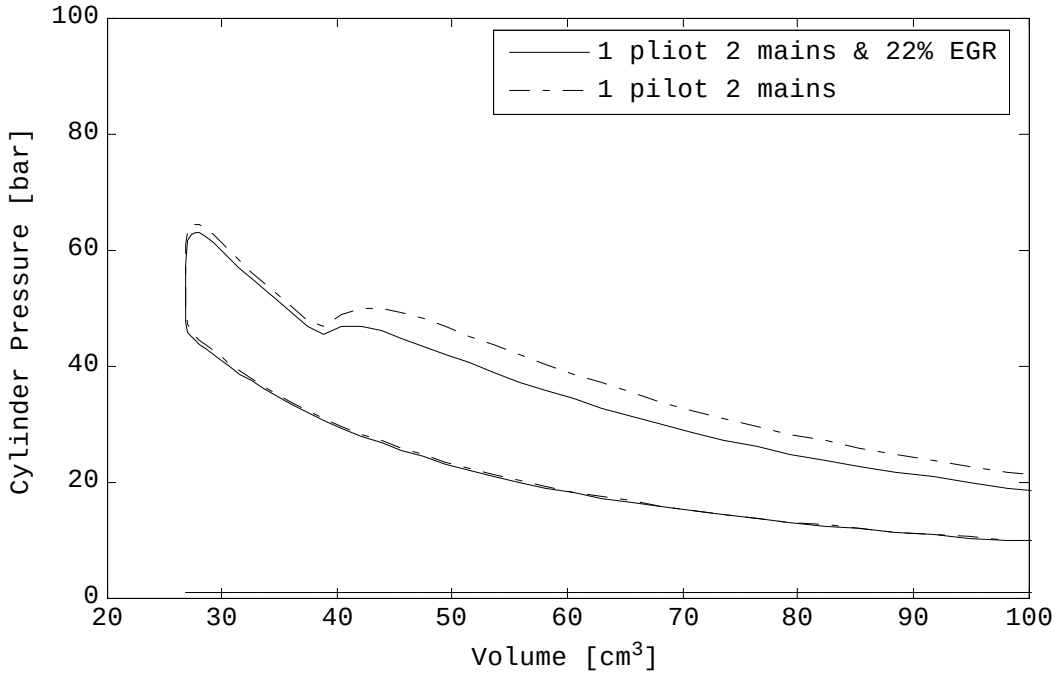

Figure 5.30 1 pilot, 2 mains, 22% EGR (pilot: SOI: 7° BTDC, main SOI: 4° BTDC, λ=2)

Figure 5.31 shows the rate of heat release profiles for double main injection with and without EGR. Splitting the main injection into two consecutive injections reduced the peak ROHR values but it increased combustion duration. Adding EGR increased ignition delay by 2 degrees of crank. As a result the ROHR peak values are higher due to the increased premixed combustion at the beginning of each injection. Although the peak ROHR values appear identical in Figure 5.31, one must consider the lower IMEP (by 1 bar) when EGR is added. The mass fraction burned in Figure 5.32 shows the influence of EGR on double main injection. It is clear that the ignition point is retarded and the burning rates from 0 to 30%CA are increased due to the increased premixed combustion phase. EGR has small influence on the later part of the combustion.

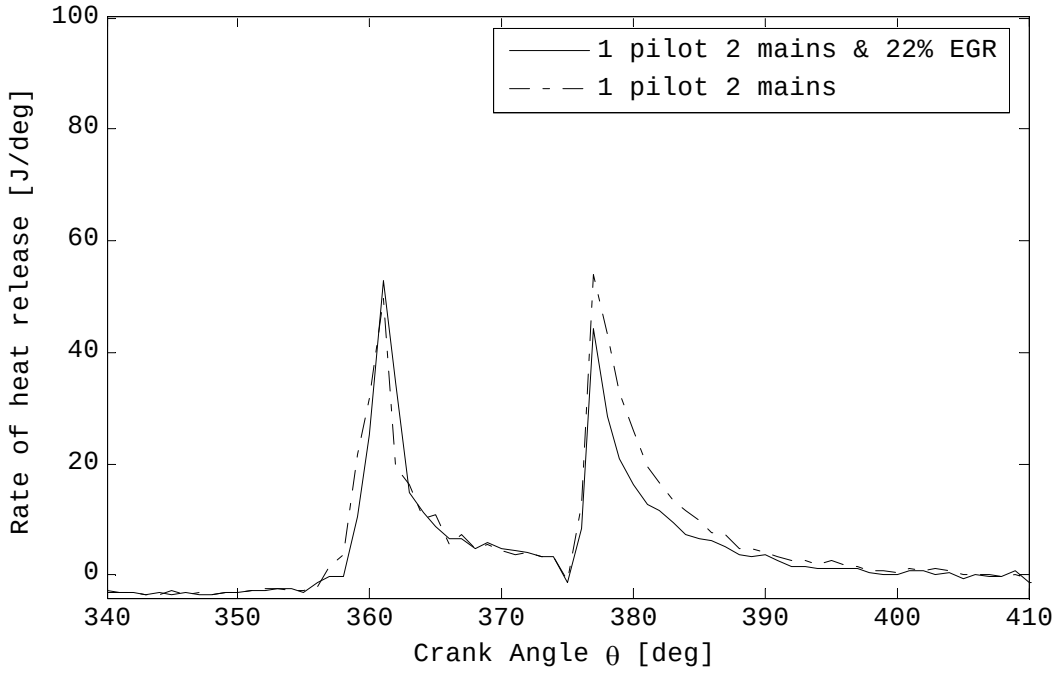

Figure 5.31 1 pilot, 2 mains, 22% EGR (pilot: SOI: 7° BTDC, main SOI: 4° BTDC, λ=2)

Increasing the number of main injections to three reduced the peak ROHR values but the presence of EGR slightly increased the premixed combustion (Figure 5.35).

Adding 22% EGR reduced NOx emissions by 55 % (Table 5-11) but increased CO levels.

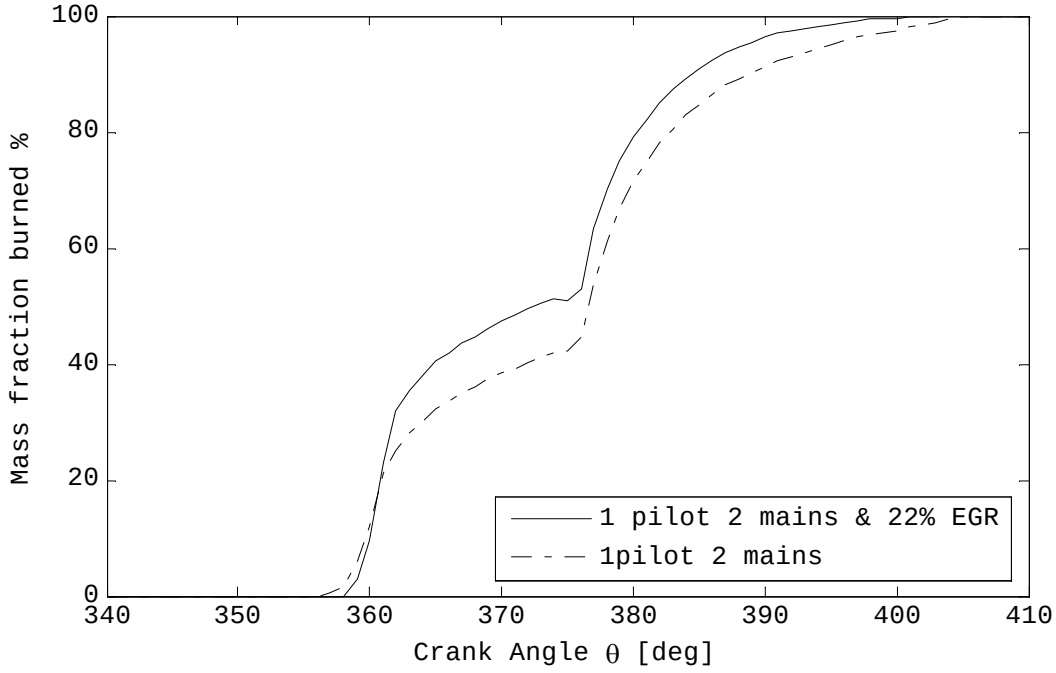

Figure 5.32 1 pilot, 2 mains, 22% EGR (pilot: SOI: 7° BTDC, main SOI: 4° BTDC, λ=2)

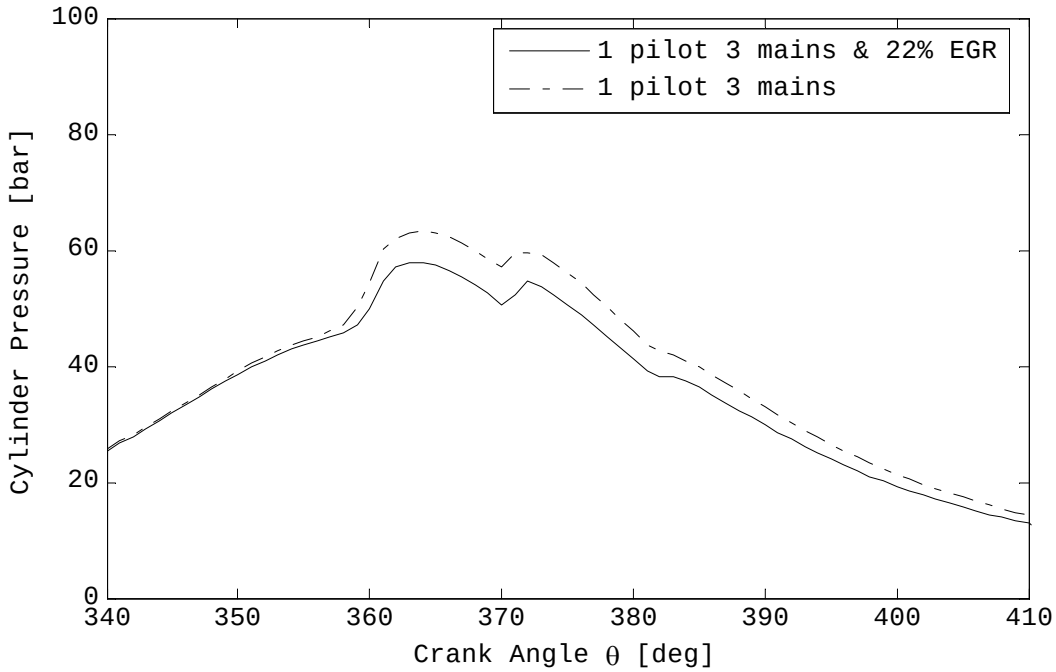

Figure 5.33 1 pilot, 3 mains, 22% EGR (pilot: SOI: 7° BTDC, main SOI: 4° BTDC, λ=2)

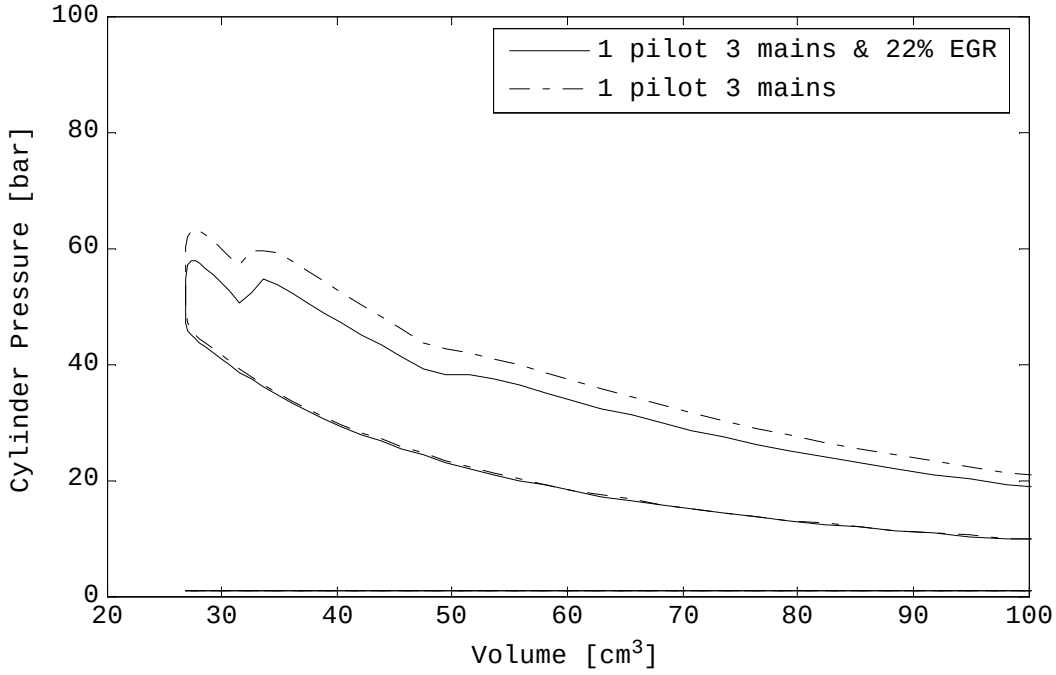

Figure 5.34 1 pilot, 3 mains, 22% EGR (pilot: SOI: 7° BTDC, main SOI: 4° BTDC, λ=2)

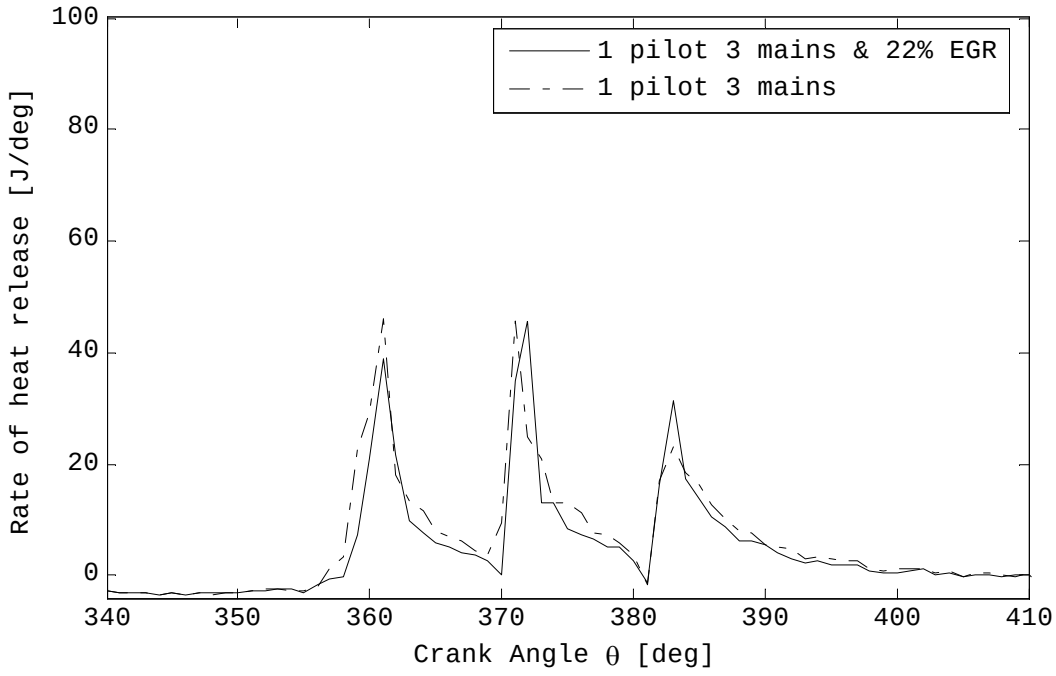

Figure 5.35 1 pilot, 3 mains, 22% EGR (pilot: SOI: 7° BTDC, main SOI: 4° BTDC, λ=2)

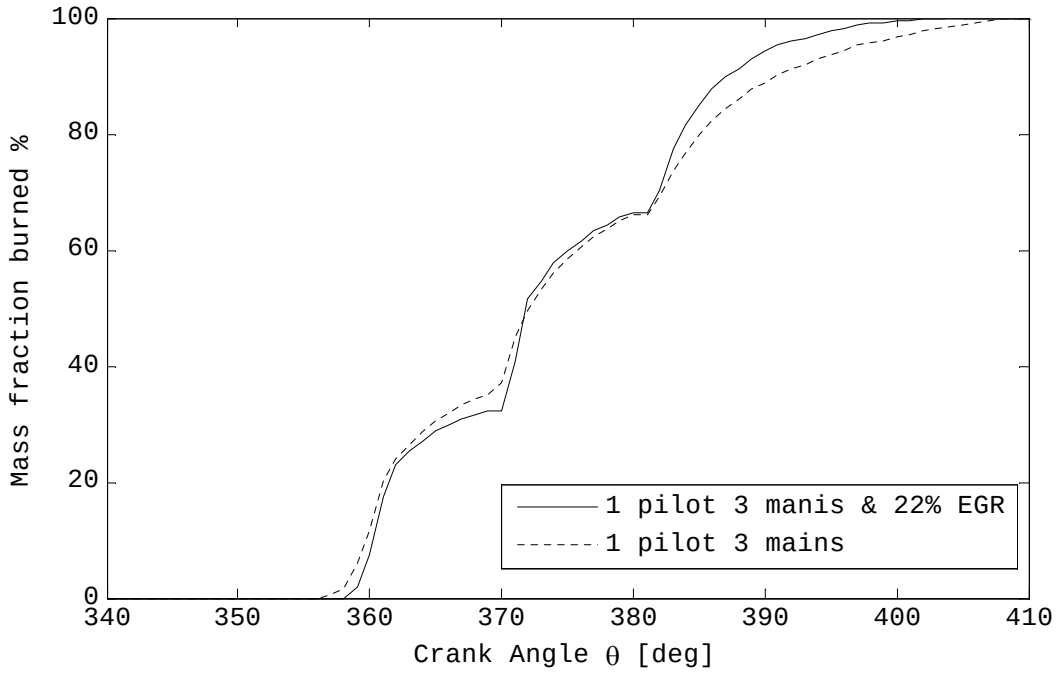

Figure 5.36 1 pilot, 3 mains, 22% EGR (pilot: SOI: 7° BTDC, main SOI: 4° BTDC, λ=2)

N° of main injections	1(0% EGR, λ=2)	1(22%EGR,λ=2)	1(22%EGR,λ=1.6)	2(22%EGR, λ=2)	3(22%EGR, λ=2)
SOI [CA]	353	353	353	353	353
SOC [CA]	356	356	358	358	358
Combustion duration [deg]	43	42	41	47	47
Mass fraction burned 02%	2	2	0	1	1
Mass fraction burned 05%	2	2	1	1	2
Mass fraction burned 10%	4	3	2	2	2
Mass fraction burned 50%	7	7	5	15	14
Mass fraction burned 90%	25	25	21	27	29
Mass fraction burned 95%	32	31	28	31	33

Table 5-10 Effect of EGR

N° of main injections	1(0%EGR λ=2)	1(22%EGR, λ=2)	1(22%EGR,λ=1.6)	2(22%EGR, λ=2)	3(22%EGR, λ=2)
IMEP [bar]	5.2	4.2	5.2	4.2	4.2
ISFC [g/KWh]	201	198	194	200	200
COV [%]	2.1	2.5	3	3	4.5
NOx [ppm]	1048	471	466	198	175
CO [ppm]	135	231	472	320	300
Visible smoke	No	No	Just visible	No	No
Knock	No	No	No	No	No
η_f [%]	41.6	42.4	43	42	42
η_v [%]	82	64	63	65	65

Table 5-11 Eeffect o EGR

5.2.5 Part load operation

In compression ignition engines the torque is varied by varying the amount of fuel injected with the engine air flow unchanged resulting to a lower pumping loses than a conventional PFI gasoline engine. Engine testing was carried out in order to demonstrate engine operation and controllability at part load operation. Initially the best to-date diesel engine operating parameters were used to check repeatability and for reference. Subsequently the main injection duration was reduced in order to lower engine load. To improve combustion stability the pilot injection duration was increased to 100μs and the SOI was tuned. The best operation found with main injection slightly retarded and pilot SOI advanced. Table 5-12shows the injection settings for best part load engine operation.

Operating parameters	
Engine speed [RPM]	1000
SOI pilot [deg]	9° (BTDC)
SOI main [deg]	3° (BTDC)
Pilot duration[μs]	100
λ	4.76
Injection pulses	1 pilot 1 main
EGR rate	0%

Table 5-12 Part load engine operating parameters

Consequently combustion data were recorded from part load operation. Figure 5.37 shows the cylinder pressure curves obtained from part load operation with λ=4.76 compared to optimum diesel with λ=2. At part load the combustion peak pressure is lower and occurs near TDC. The PV diagram in Figure 5.38 shows a significant reduction on net work at part load which corresponds to the lower IMEP.

At part load operation the ISFC increased by 17% (Table 5-13). This is not unexpected if one considers the increased amount of energy input before TDC and the simultaneous reduction of energy input during the expansion stroke. Also the leaner operation causes lower flame speed and hence reduces IMEP. Figure 5.39 clearly shows that the total

amount of energy produced from pilot injection as well as a substantial portion of the main injection energy is released before TDC. This reduces fuel conversion efficiency to 35.5%.

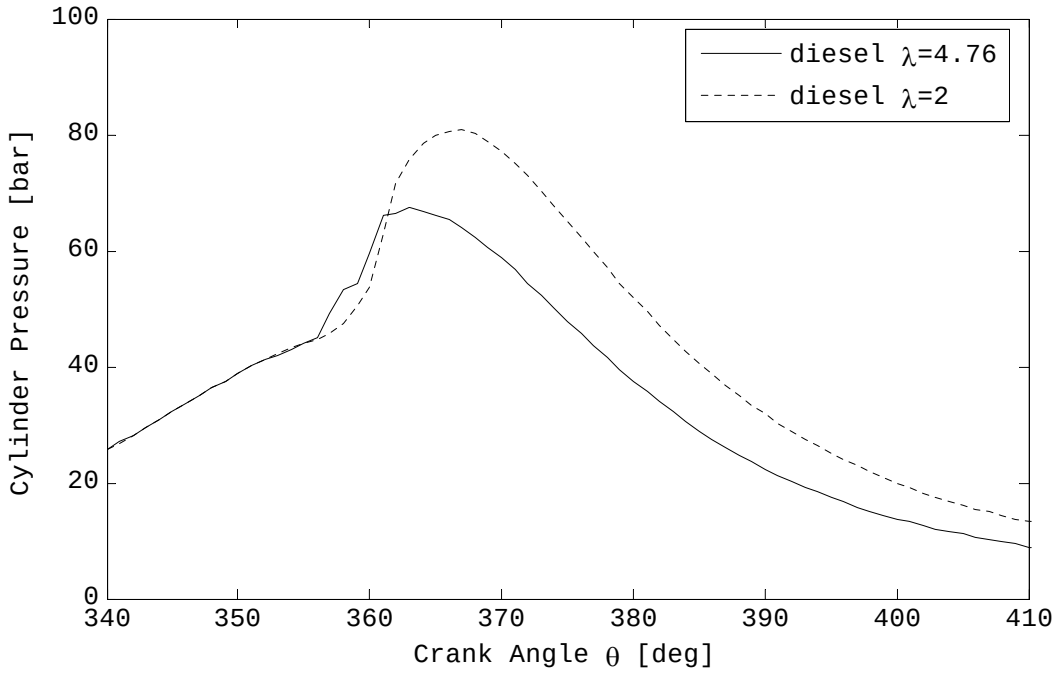

Figure 5.37 Cylinder pressure versus CA at part load

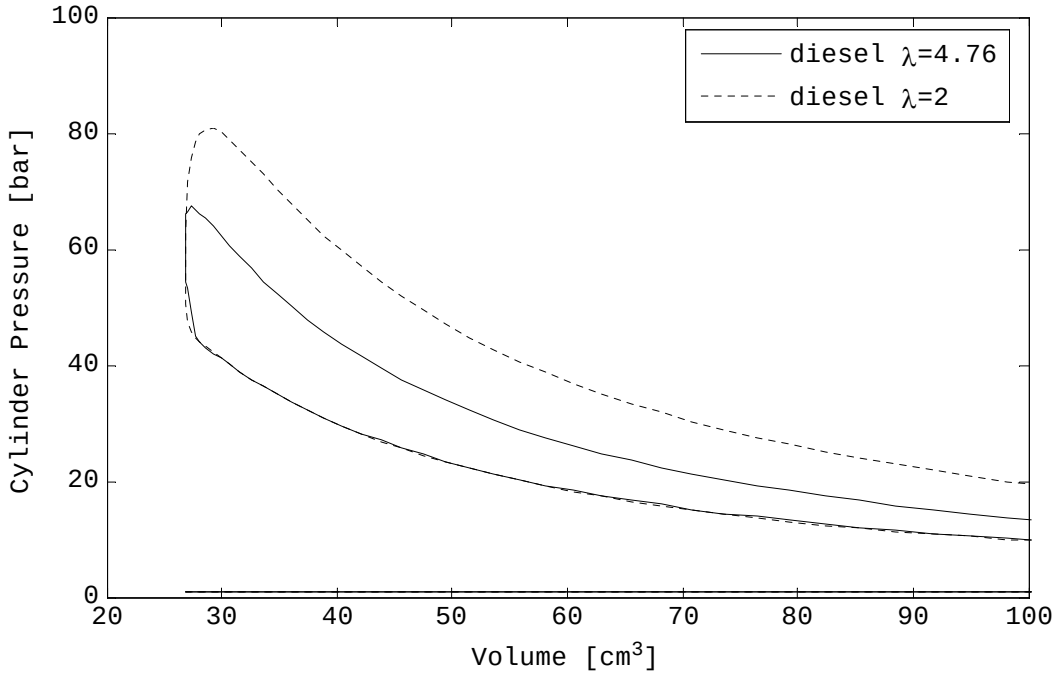

Figure 5.38 Pv diagram at part load

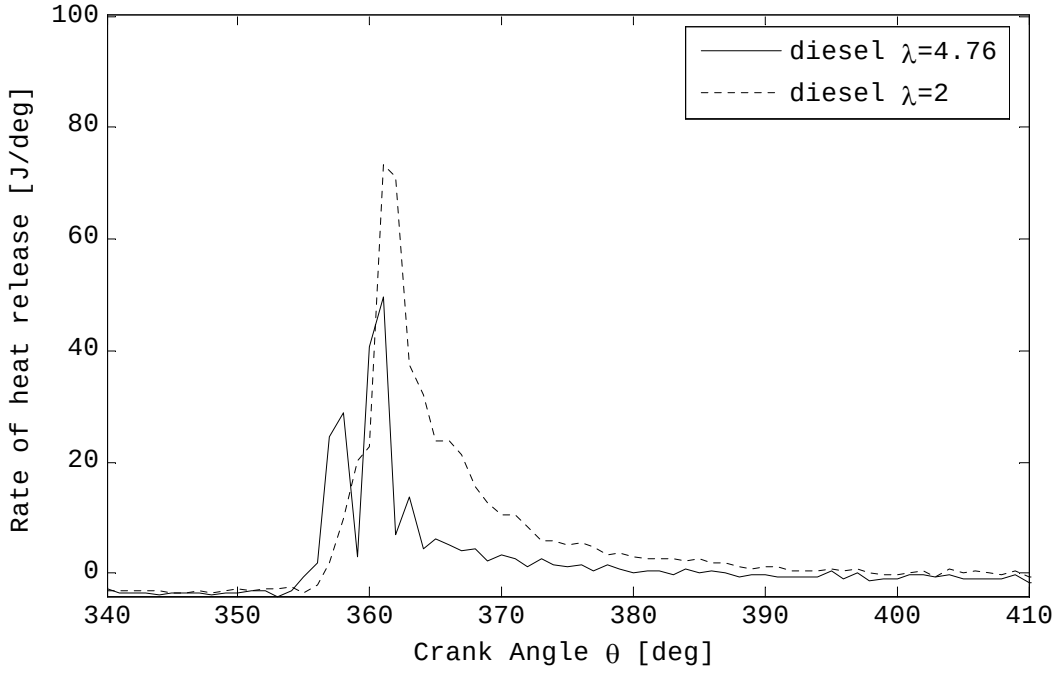

Figure 5.39 Rate of heat release at part load

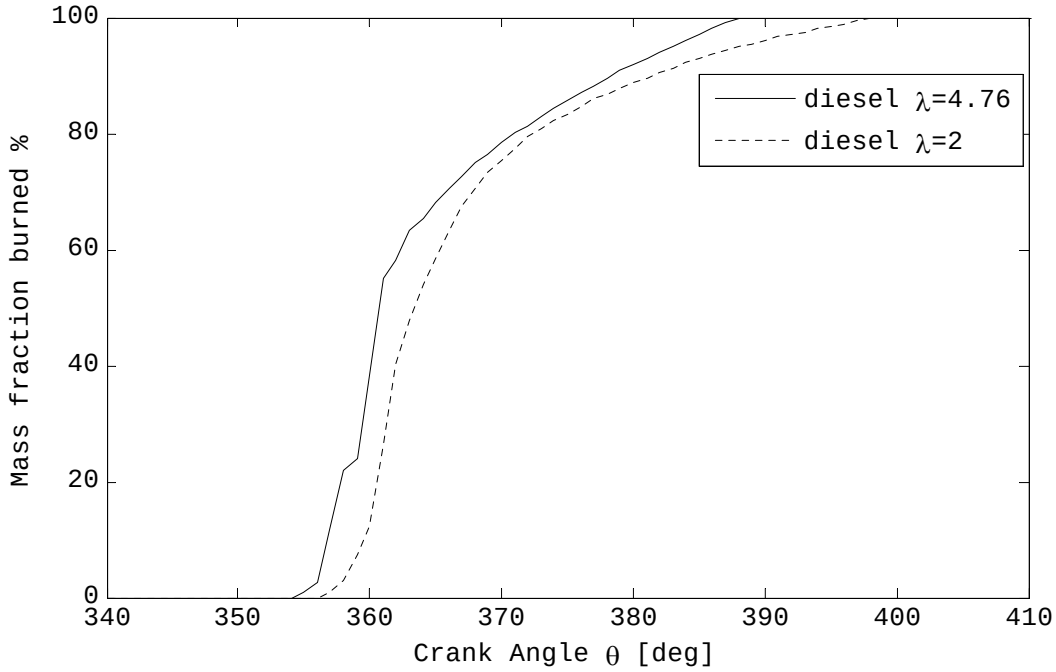

Figure 5.40 Mfb part load

Engine load	**λ=2**	**λ=4.76**
IMEP [bar]	5.2	1.9
ISFC [g/KWh]	201	236
COV [%]	2.1	4.3
NOx [ppm]	1048	----
CO [ppm]	135	----
Visible smoke	No	No
Knock	No	No
η_f [%]	41.6	35.5
η_v [%]	82	83

Table 5-13 Diesel part load

Diesel part load operation	**λ=2**	**λ=4.76**
SOI [CA]	353	351
SOC[CA]	356	354
Combustion duration[deg]	43	34
Mass fraction burned 02%	2	2
Mass fraction burned 05%	2	2
Mass fraction burned 10%	4	3
Mass fraction burned 50%	7	7
Mass fraction burned 90%	25	24
Mass fraction burned 95%	32	29

Table 5-14 Diesel part load combustion characteristics

5.3 Dual fuel operation

5.3.1 Introduction

This section describes the experimental work undertaken to explore and demonstrate the diesel/LPG dual fuel engine operation with particular focus given on engine performance, combustion control and NOx emissions. Dual fuel operation was achieved using a small quantity of diesel pilot to ignite a larger amount of port injected LPG.

At the outset diesel pilot injection was isolated from main combustion and studied separately in order to demonstrate its combustion characteristics.

Then using diesel pilot from the best to-date diesel operating parameters from section 5.2.2, the main diesel injection was replaced by port injected LPG at liquid phase. The first results obtained from the combined diesel/LPG operation were compared to the best to-date diesel operation.

Subsequently a series of experiments were performed in order to find the best SOI for dual fuel operation for λ=2.

The effect of varying the injected amount of LPG was also demonstrated for early and late diesel pilot SOI.

In the next step, stoichiometric dual fuel operation was explored in an attempt to demonstrate a method of achieving SI like operation on a high compression ratio diesel engine.

Finally the section closes by showing dual fuel engine part load control.

5.3.2 Diesel pilot injection as ignition medium

From the best to-date diesel operation (paragraph 5.2.2), the main diesel injection was disabled by setting main injection duration to 000μs. Operating the engine with diesel pilot only, resulted to a very lean combustion λ=12. With the main injection disabled, the injector solenoid was energised to produce only pilot injection. To demonstrate this, cylinder pressure data were captured highlighting the very low energy input per cycle.

Figure 5.41 depicts the pressure time history for this very lean combustion process which is characterised by a low cylinder pressure increase with peak values occurring near TDC. Figure 5.42 shows the amount of work produced from pilot injection in a PV diagram. The IMEP is close to zero which means that the pilot injection supplies a small amount of energy per cycle. The heat release rate diagram shows a small but rapid increase two degrees after the injection set point.

The boost voltage (90V) applied to the solenoid during the first 20μs of the pilot injection signal together with the high injection pressure helped to increase the injection rate for a given pulse duration. Thus pilot burning rates are very high up to 50%CA shown in Figure 5.44.

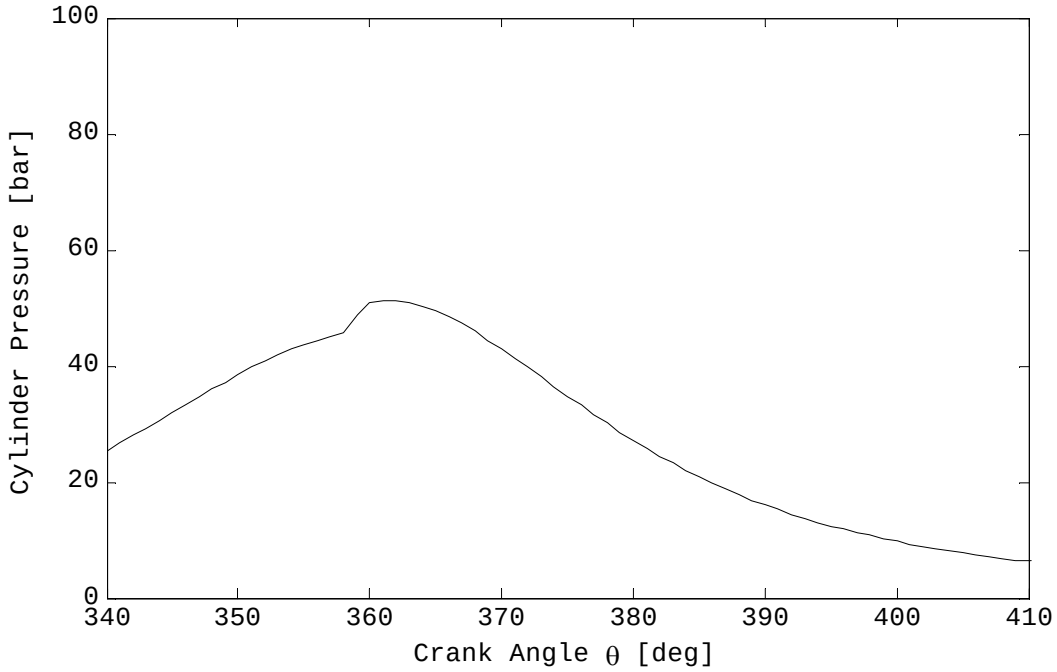

Figure 5.41 Pressure CA of diesel pilot only

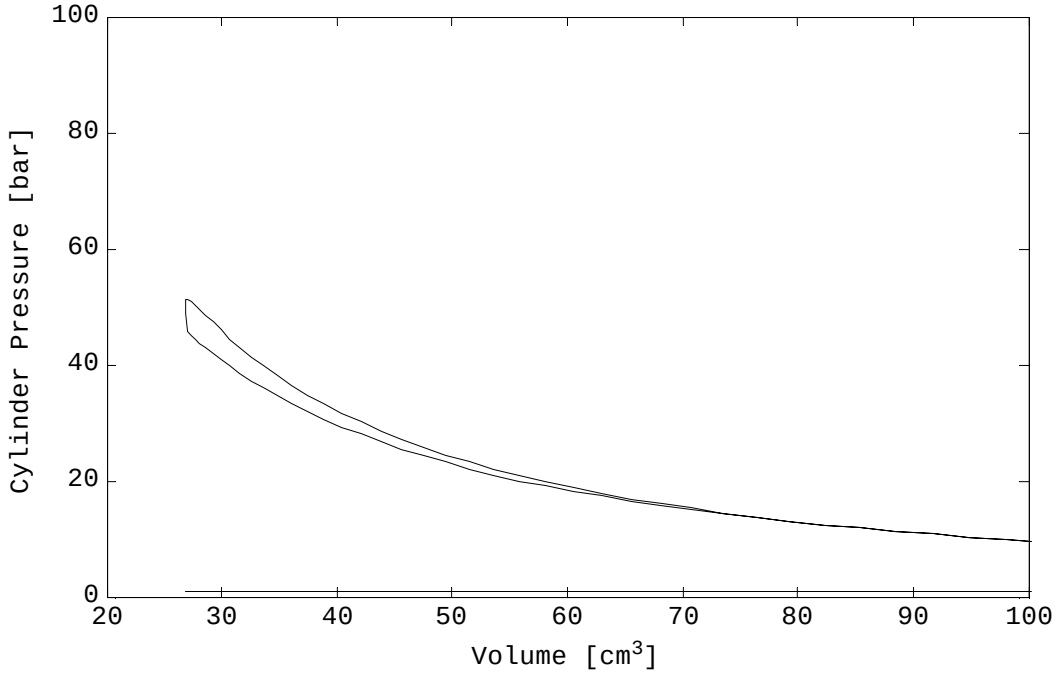

Figure 5.42 PV diagram diesel pilot only

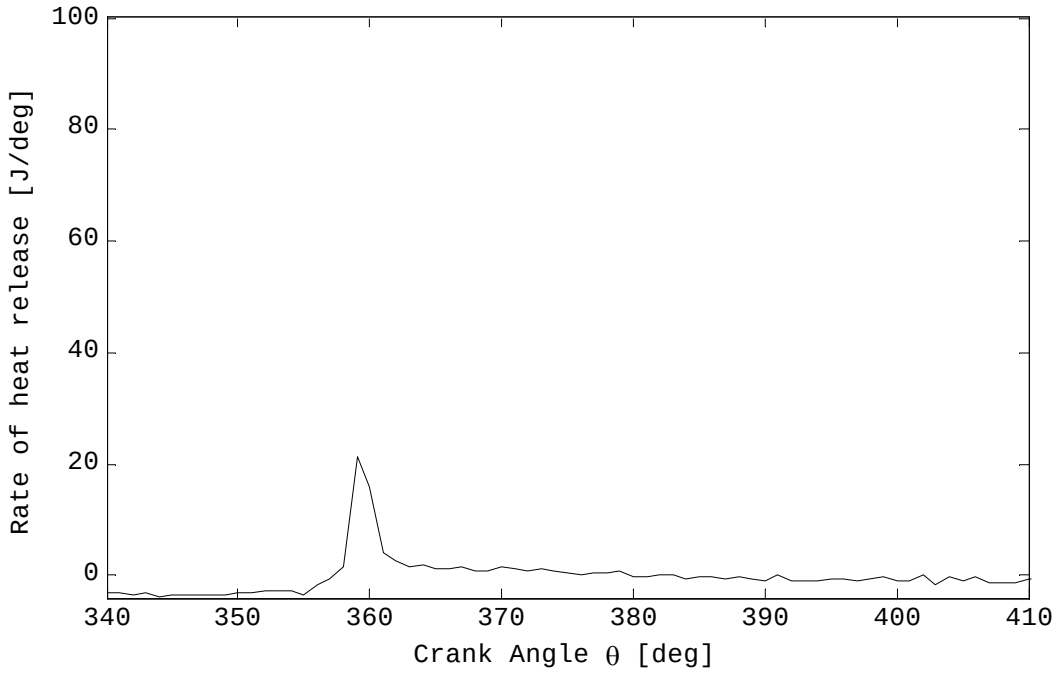

Figure 5.43 ROHR of diesel pilot only

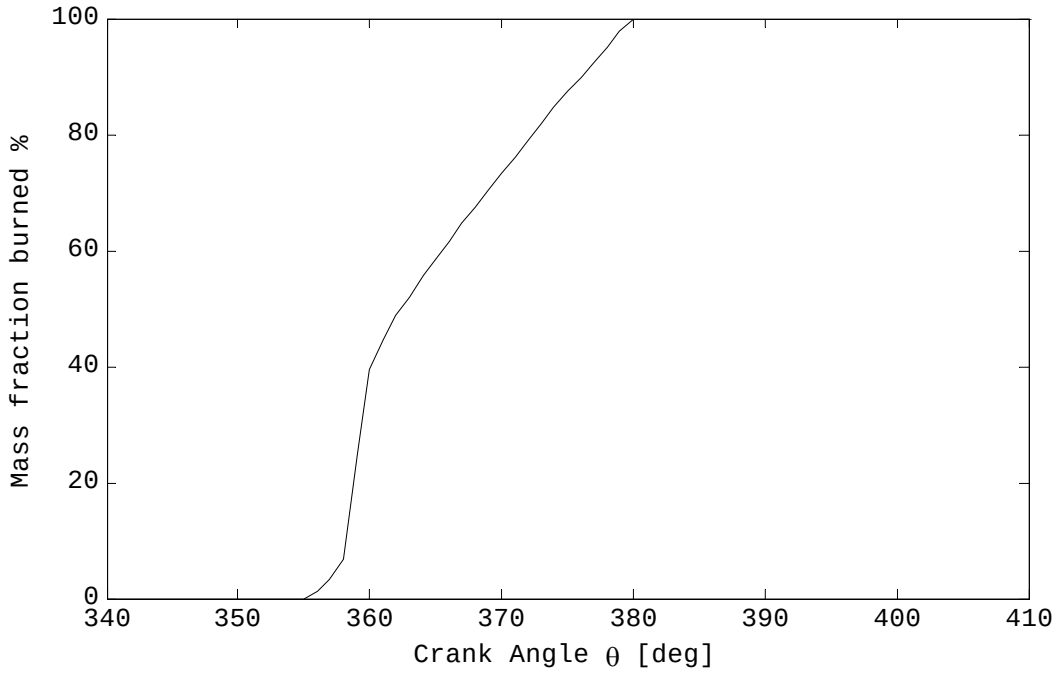

Figure 5.44 Mfb of diesel pilot only

Increasing the rate of injection allows higher energy input per crank angle. This rapid energy release is necessary to reliably and repeatedly ignite the LPG premixture.

The diesel pilot might be the best method to provide ignition on a high compression ratio LPG engines. There are two main reasons for this. First, the majority of modern

diesel engines use common rail systems and therefore diesel pilot is readily available. If a conventional automotive spark ignition system is to be used, more than 50 KV will be required to generate spark across the electrodes for an average turbocharged diesel engine due to its high compression pressures. Although this can be solved by using stronger ignition coils, the higher breakup voltage across the electrodes causes sparkplug fouling and premature failure .This is also a current problem concerning the highly boosted downsized engines which needs further development

Combustion Events	Crank Angle [deg]
SOI	353
SOC	357
Combustion duration	23
Mass fraction burned 02%	1
Mass fraction burned 05%	1
Mass fraction burned 10%	1
Mass fraction burned 50%	3
Mass fraction burned 90%	15
Mass fraction burned 95%	19

Table 5-15 Diesel pilot combustion events

5.3.3 Dual fuel operation

Operating the engine with the best to-date diesel settings, the main diesel injection was disabled and pilot SOI and duration were kept constant (Table 5-16). Subsequently liquid LPG was injected into the inlet manifold at liquid phase during the inlet stroke. Increasing gradually LPG injection duration λ=2 was achieved.

Operating parameters	Best diesel	Dual fuel
Engine speed [RPM]	1000	1000
Pilot SOI [deg]	7 (BTDC)	7 (BTDC)
Pilot duration[μs]	95	95
LPG SOI[deg]	-	TDC (inlet stroke)
λ	2	2
Injection strategy	1pilot+1main	1pilot+83.5% LPG (port injected)

Table 5-16 Engine operating parameters

The dual fuel engine produced the same IMEP with the diesel engine for the same λ value. The engine operation was knock-free and quieter than the best to-date diesel one. Dual fuel ISFC was slightly lower than diesel owing to the higher energy content of LPG. A significant reduction on NOx levels (approximately 69% lower than of those of diesel) was another welcome result from the dual fuel operation (Table 5-18).

Combustion data were captured and compared with best to-date diesel from previous steps. Figure 5.45 shows the in-cylinder pressure from dual fuel and diesel operations. It is obvious that the peak in-cylinder pressure and the rate of pressure rise from dual fuel mode are different in both magnitude and shape. The peak pressure of dual fuel operation is 15% lower and its corresponding crank angle is retarded.

Figure 5.47 shows the corresponding rate of heat release profiles. The dual fuel operation is characterised by two distinctive ROHR peaks. The first peak indicating the diesel pilot combustion has short duration but is very high. This is followed by second peak which is lower in magnitude but with a longer duration corresponding to LPG combustion.

When the two ROHR profiles are compared, it becomes apparent that the ignition delay has increased when LPG was added. For diesel only operation the pilot is injected in a cylinder filled with fresh air and some combustion residues from the previous cycle whereas in the case of dual fuel operation the pilot is injected into a homogeneous mixture of air and LPG. Owing to the larger latent heat of vaporization and the lower boiling point LPG causes a great in-cylinder temperature drop and thus extends pilot ignition delay. This temperature drop is clearly identified as a pressure drop during the compression stroke in Figure 5.45 as well as in the PV diagram in Figure 5.46. If gaseous LPG injection was used the combustion delay would have been shorter but at the expense of causing significant throttling effect.

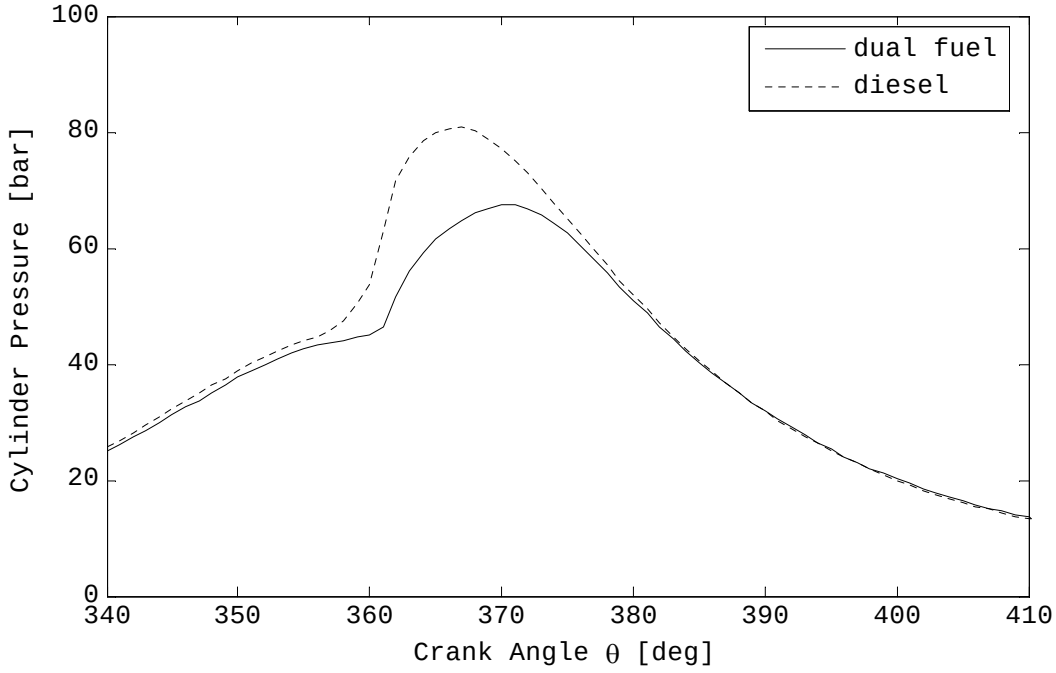

Figure 5.45 Pt diagram from dual fuel operation

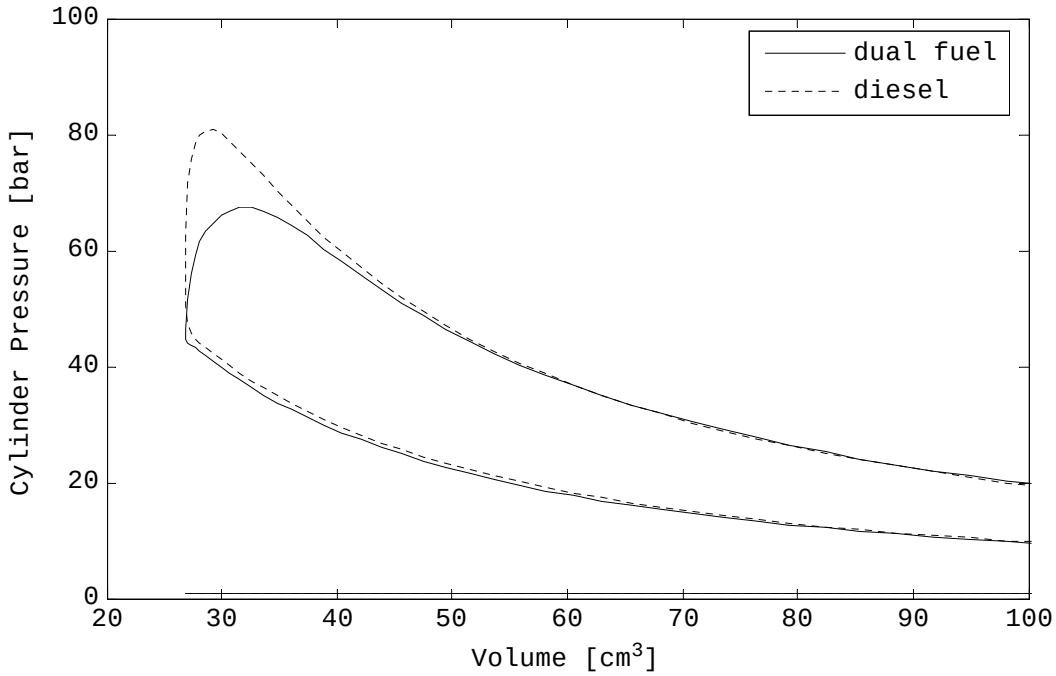

Figure 5.46 Pv diagram from dual fuel operation

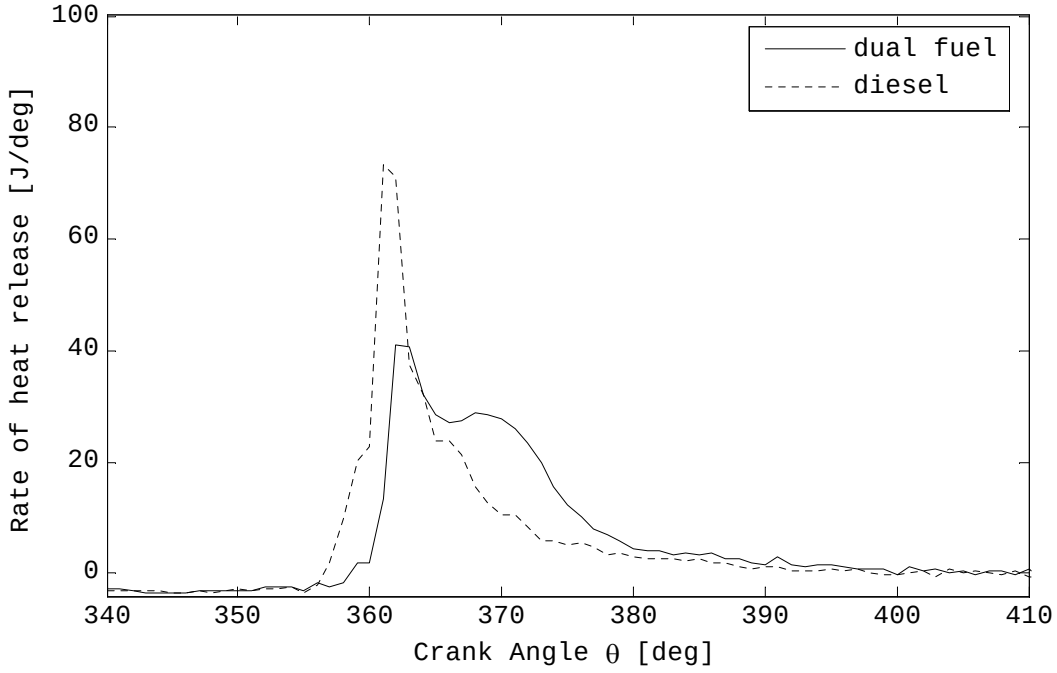

Figure 5.47 ROHR diagram from dual fuel operation

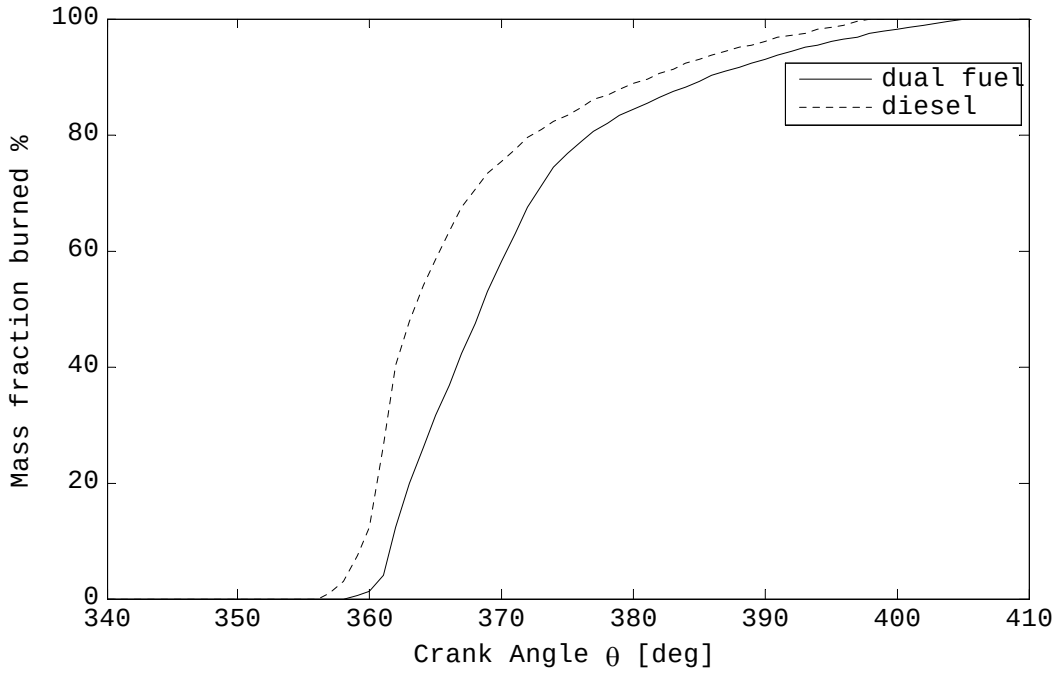

Figure 5.48 Mfb from dual fuel operation

Dilution might be another possible reason contributing to the enlarged ignition delay. It is known that LPG has lower cetane number (<3) and the autoignition temperature is higher than that of diesel. Hence when a small quantity of diesel is injected into a lager LPG charge at high levels of turbulence, it is likely for diesel pilot jet to adopt some of the LPG properties. This phenomenon is likely to occur in the outer regions of pilot

injection at the early stages of injection. However this is only an assumption and there is no clear evidence to prove it.

MFB	Diesel	Dual fuel
SOI [CA]	353	353
SOC [CA]	356	358
Combustion duration [deg]	42	48
Mass fraction burned 02% [deg]	2	2
Mass fraction burned 05% [deg]	2	3
Mass fraction burned 10% [deg]	4	4
Mass fraction burned 50% [deg]	7	10
Mass fraction burned 90% [deg]	25	28
Mass fraction burned 95% [deg]	32	35

Table 5-17 Dual fuel engine mfb

Engine Performance parameters	Diesel	Dual fuel
IMEP [bar]	5.2	5.2
ISFC [g/KWh]	201	194
COV [%]	2.1	1.4
NOx [ppm]	1048	330
Visible smoke	No	No
Knock	No	No
η_f [%]	42	40
η_v[%]	82	83

Table 5-18 Dual fuel engine performance parameters

5.3.4 Effect of SOI on dual fuel operation

Using diesel pilot to ignite LPG causes significant ignition delay with dual fuel operation. This section explores the effect of varying the pilot SOI on dual fuel engine performance for a fixed λ value.

Maintaining pilot duration constant the SOI was varied from 5 to 29 degrees before TDC at one crank angle degree intervals and combustion data were recorded for every case. However data is presented using 5° intervals to simplify the plots. Figure 5.49 shows the effect of SOI on IMEP and COV. Advancing or retarding pilot SOI beyond a certain range results in engine misfire. This is in good agreement with COV percentage showing an increase near the misfire limits. Between 6 and 25 degrees SOI appears to have little effect on IMEP but beyond these points IMEP drops rapidly due to engine misfire. Also when misfire occurs, fuel conversion efficiency is reduced (Table 5-20).

Figure 5.50 shows the effect of pilot SOI on ISFC and NOx. Between 10 to 20 degrees BTDC NOx is approximately constant with a peak value of 450 ppm which is significantly lower compared with diesel operation. This reduction is attributed to LPG prolonged ignition delay which retards combustion resulting to in cylinder temperature drop which subsequently reduces NOx. Near the engine misfire limits NOx levels appear to drop somewhat but this is due to incomplete combustion and the lower combustion rates.

ISFC rapidly increases towards misfire limits but remains almost constant between 10 and 22 degrees BTDC Figure 5.50. Advancing the SOI has a clear effect on the way the combustion unfolds. This is clearly shown in Figure 5.51. Although cylinder pressures show some difference, the combustion quality within this SOI range is good and NOx levels an ISFC are almost the same. This extended range of SOI gives a high level of flexibility to optimise other engine operating parameters making the calibration procedure more forgiving. However this flexibility is highly depended on engine geometry. The Ricardo E7 engine is an undersquare engine and therefore the piston travel relative to crank angle is considerably smaller than that of an oversquare engine. This is a reason why the extended SOI results to similar levels of NOx and ISFC.

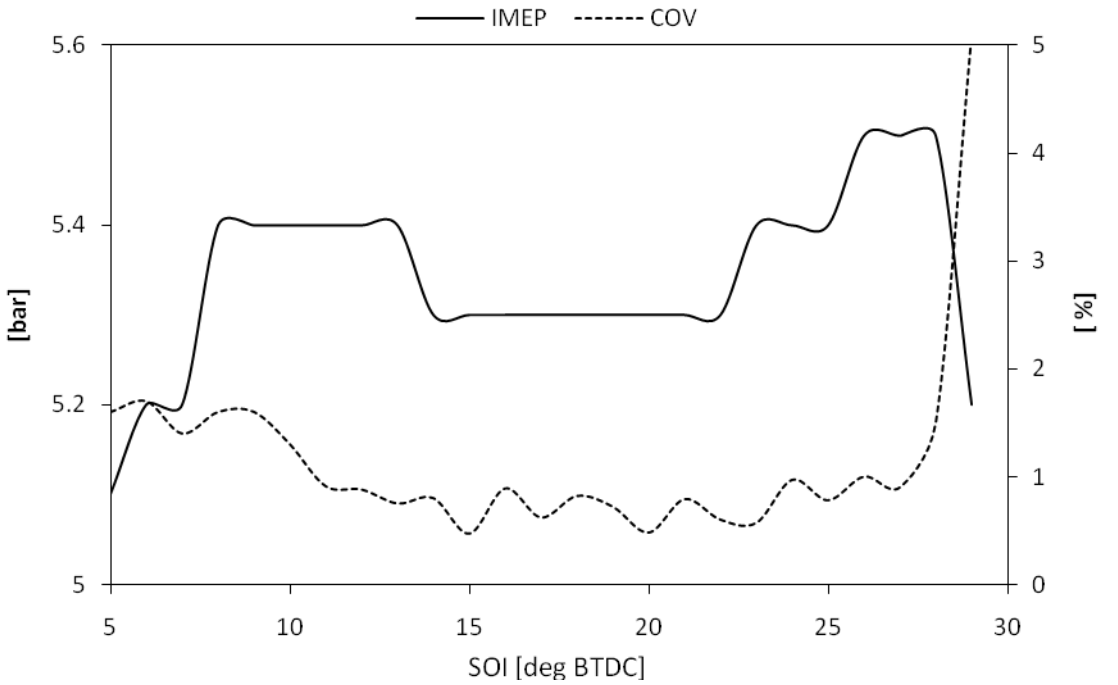

Figure 5.49 Effect of pilot SOI on IMEP and COV (dual fuel operation)

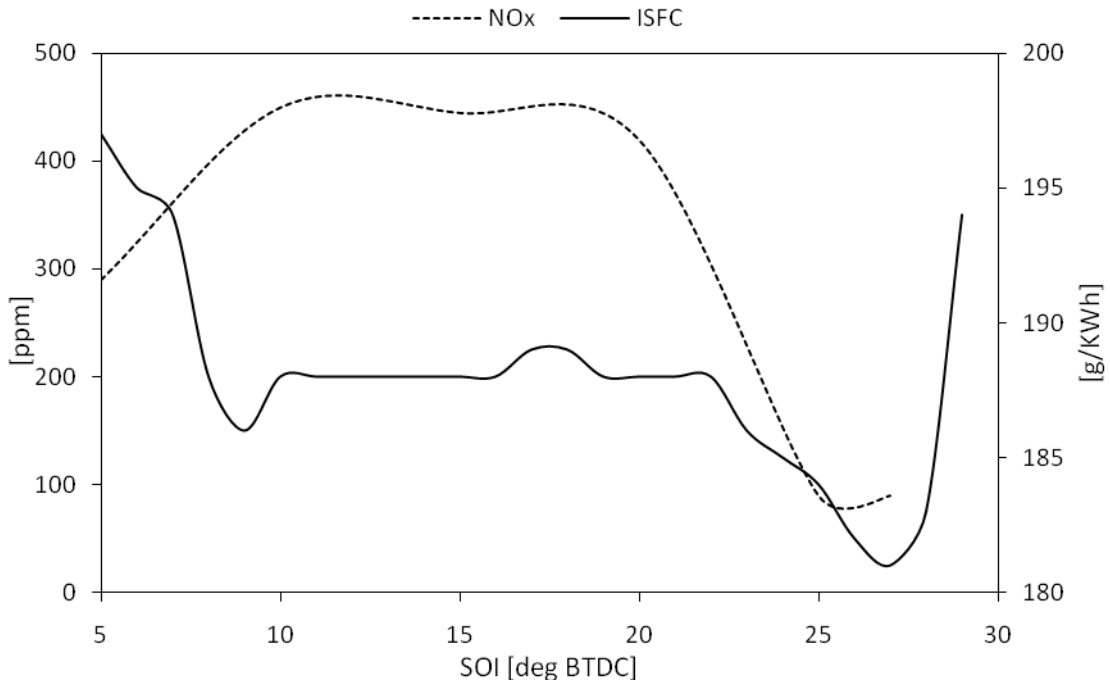

Figure 5.50 Effect of pilot SOI on ISFC and NOx (dual fuel operation)

Figure 5.51 shows the effect of varying pilot SOI on cylinder pressure for dual fuel operation. When engine misfire occurs the combustion peak pressures are significantly lower. The PV diagrams in Figure 5.52 show that the lowest work is produced when a very late or a very early SOI is used.

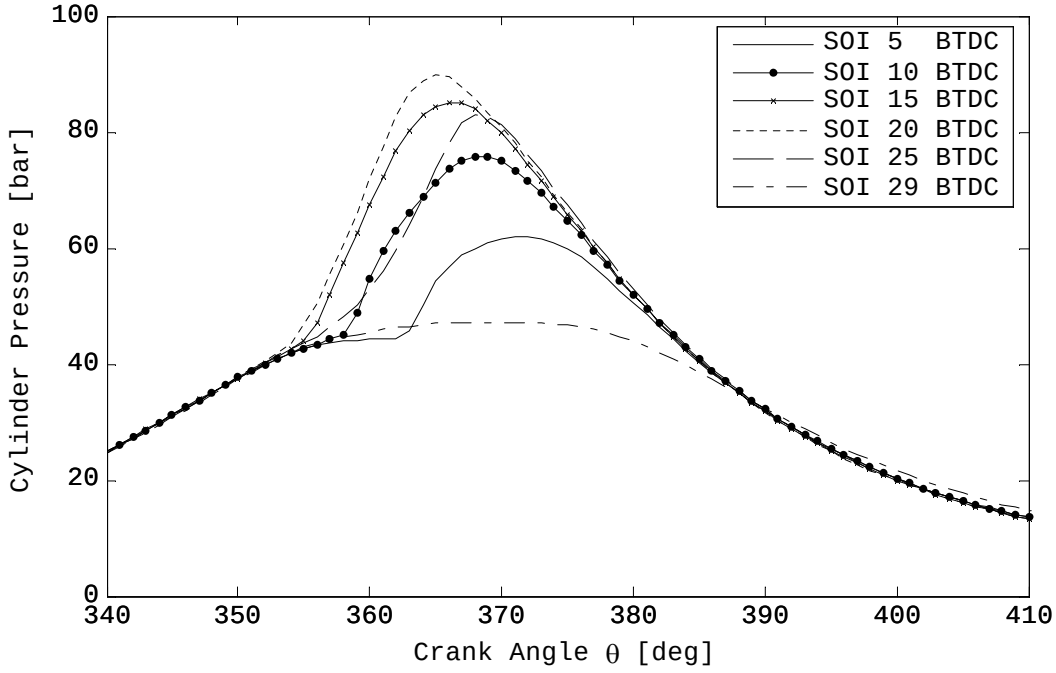

Figure 5.51 Effect of SOI on dual fuel operation cylinder pressure

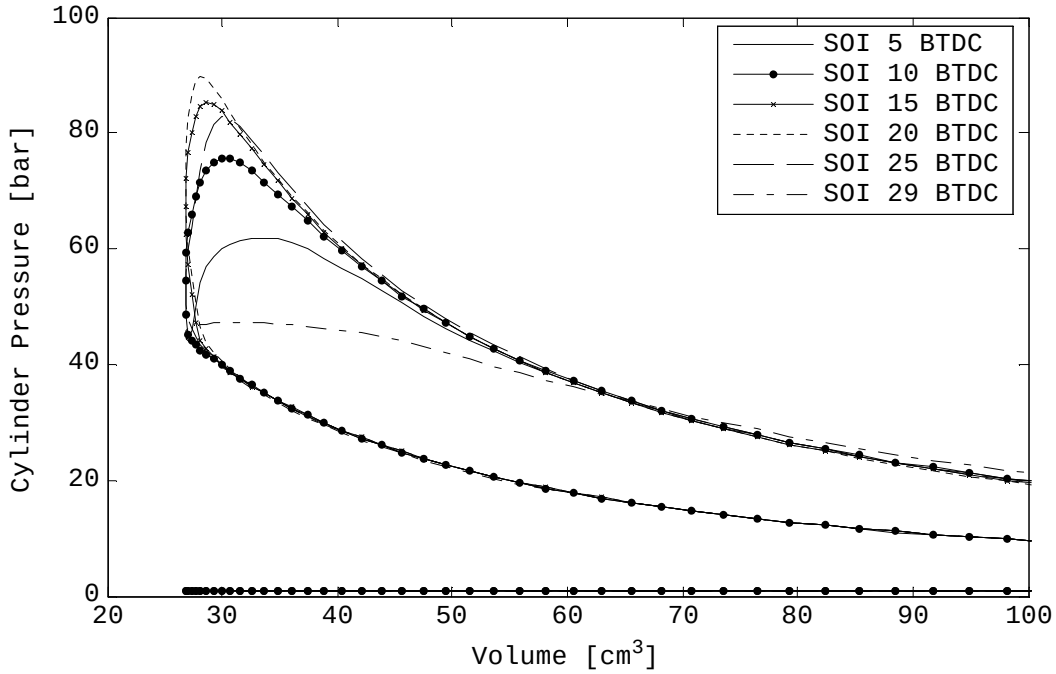

Figure 5.52 Effect of SOI on dual fuel operation PV diagram

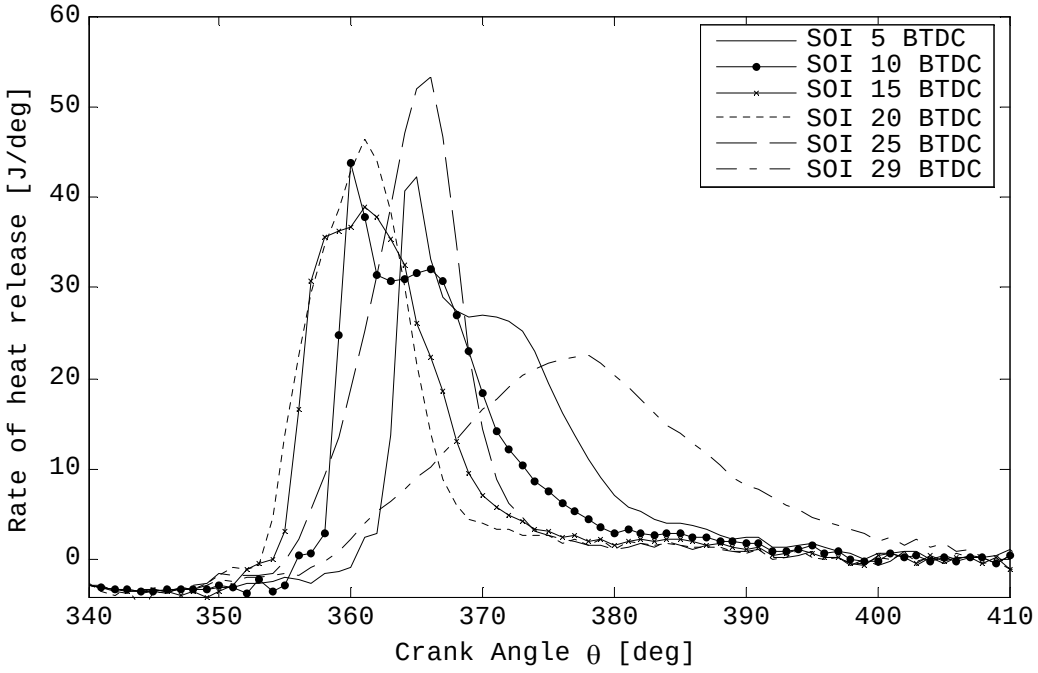

Figure 5.53 Effect of SOI on dual fuel operation ROHR

More comprehensive information regarding the combustion process can be obtained from RHOR profiles in Figure 5.53. An SOI between 5 to10 degrees before TDC produces a double peak ROHR with 5 degrees ignition delay. Advancing the SOI beyond 15 the ignition delay increases to 6 degrees a combined ROHR is produced. By further advancing the SOI the ignition delay increases and the ROHR per crank angle becomes steeper before reaching the engine misfire limit.

Figure 5.54 shows the effect of varying the SOI on the mass fraction burned. When SOI is advanced from 5 to 10 degrees before TDC the start of combustion is directly depended on SOI. Therefore ignition delay is constant. However, advancing SOI beyond 15 degrees BTDC, increases ignition delay and extends combustion duration.

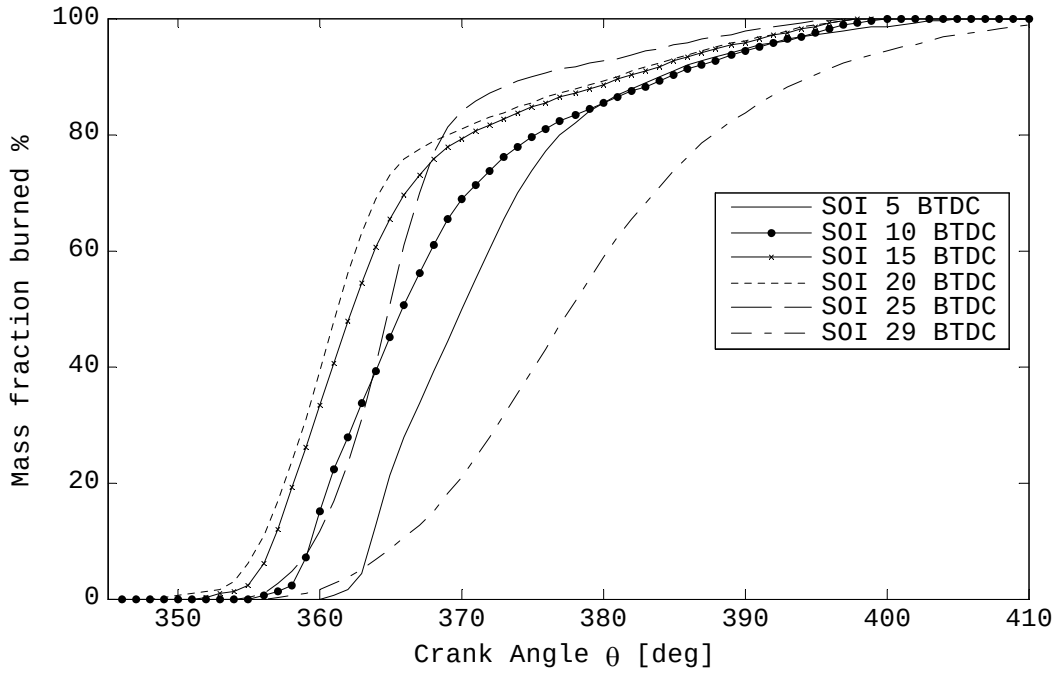

Figure 5.54 Effect of SOI on dual fuel operation MFB

When retarding the pilot SOI below 5° engine misfire is the result of excessive in-cylinder temperature drop from the late LPG charge evaporation. This indicates that under normal operation, the cooling effect continues during combustion.

On the other hand, an early pilot SOI causes engine misfire due to pilot dilution with LPG. Advancing the SOI increases the ignition delay. This is due to the longer residence of injected pilot into the cool LPG charge before autoignition conditions occur in the combustion chamber.

Results readily show that the injection timing has a significant effect on the cycle pressure time history and the hence on the combustion performance of the engine. It is reassuring to note that the engine operating under the diesel pilot ignition concept can be readily controlled using injection timing alone.

SOI (BTDC)	**5**	**10**	**15**	**20**	**25**	**29**
SOI [CA]	355	350	345	340	335	331
SOC [CA]	360	355	351	348	354	356
Combustion duration [deg]	46	45	48	50	44	58
Mass fraction burned 02% [deg]	2	3	4	5	3	5
Mass fraction burned 05% [deg]	3	4	5	7	4	7
Mass fraction burned 10% [deg]	4	4	6	8	6	10
Mass fraction burned 50% [deg]	10	11	11	13	11	22
Mass fraction burned 90% [deg]	24	30	31	33	21	39
Mass fraction burned 95% [deg]	31	36	38	40	30	45

Table 5-19 Combustion events for various SOI

SOI (BTDC)	**5**	**10**	**15**	**20**	**25**	**29**
IMEP [bar]	5.1	5.4	5.3	5.3	5.4	5.2
ISFC [g/KWh]	197	188	188	188	184	194
COV [%]	1.6	1.3	0.47	0.48	0.78	5.1
NOx [ppm]	290	450	445	420	90	-
Visible smoke	No	No	No	No	No	No
Knock	No	No	No	No	No	No
η_t [%]	39	41	41	41	42	39
η_v [%]	84	83	83	83	83	83

Table 5-20 Effect of SOI on dual fuel engine operation

5.3.5 Effect of the quantity of LPG

This section explores the effect of varying the quantity of injected LPG on dual fuel engine operation. Four cases were demonstrated where the proportion of LPG is given as the percentage of total fuel mass injected. Diesel pilot injection was kept constant throughout measurements by adjusting the fuelling. The various LPG concentrations were achieved by gradually reducing port injected LPG whilst compensating with diesel main injection. Therefore the injection strategy consists of: 1 pilot (fixed duration), 1 main (variable duration with fixed SOI point) and 1 port LPG injection (variable duration).

Results from previous steps suggested that good engine operation can be achieved for pilot SOI between 8°-20° before TDC. Two sets of experiments were carried out one for advanced and another for retarded pilot SOI in order to cover a wider engine operating envelope.

Table 5-23 shows the effect of the various LPG percentages on engine performance for SOI 8° before TDC. IMEP is almost constant in all cases. This is normal as the removed energy amount of LPG is compensated by an equivalent amount of diesel. The lowest ISFC occurs with 43% LPG. From the COV it is clear that higher LPG percentages reduce engine cycle variability. This is due to the combustion of the LPG premixture. Indicated fuel conversion efficiency is marginally higher for diesel only operation owing to its lower calorific value than LPG (for the same IMEP).

Due to several problems with the gas analysers and the time constrains NOx emission measurements were not performed. Nevertheless by observing the combustion data, especially the heat release profiles, NOx trends can be identified with a fair degree of confidence.

Similar effects on engine performance from 20° pilot SOI are shown in Table 5-24. IMEP shows a small variation and ISFC is 5% lower than the one of diesel only operation. The advanced SOI has significantly reduced COV for LPG premixtures above 72%.

Figure 5.55 and Figure 5.56 show the effect of injected amount of LPG on time history of combustion in the cases of early and late SOI under knock free condition. In both cases ignition occurs after injection of pilot injection.

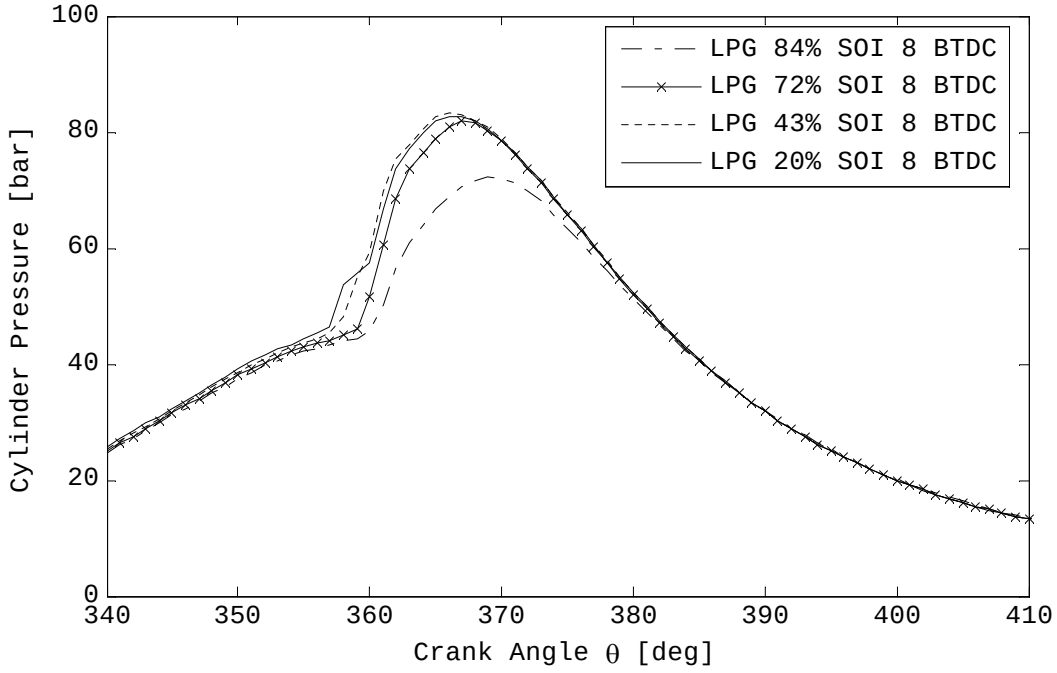

Figure 5.55 Effect of LPG percentage on cylinder pressure

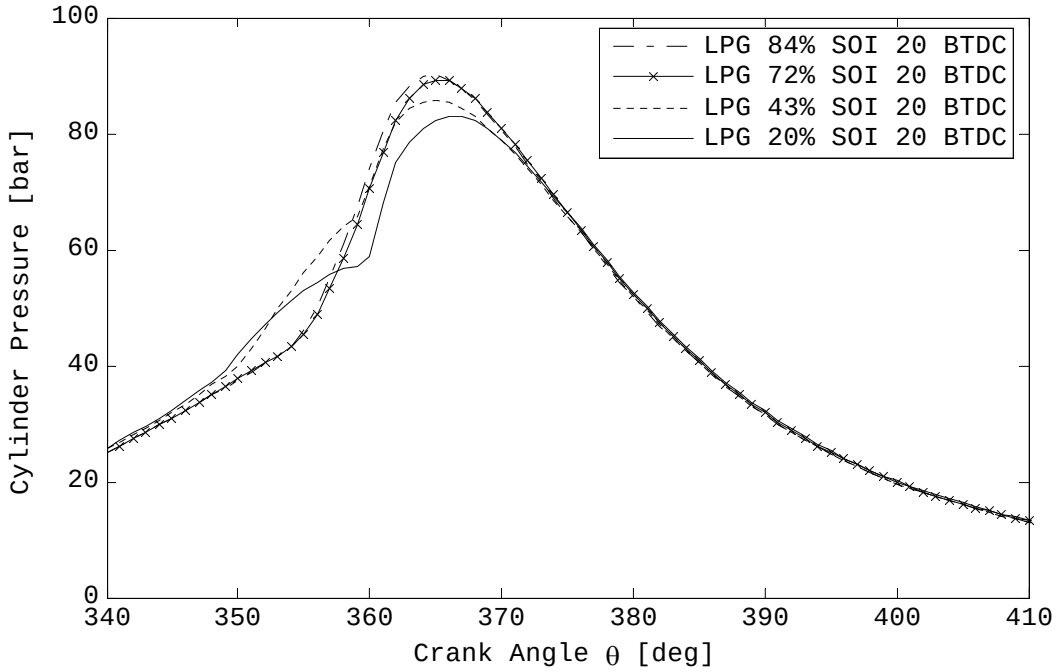

Figure 5.56 Effect of PG percentage on cylinder pressure history

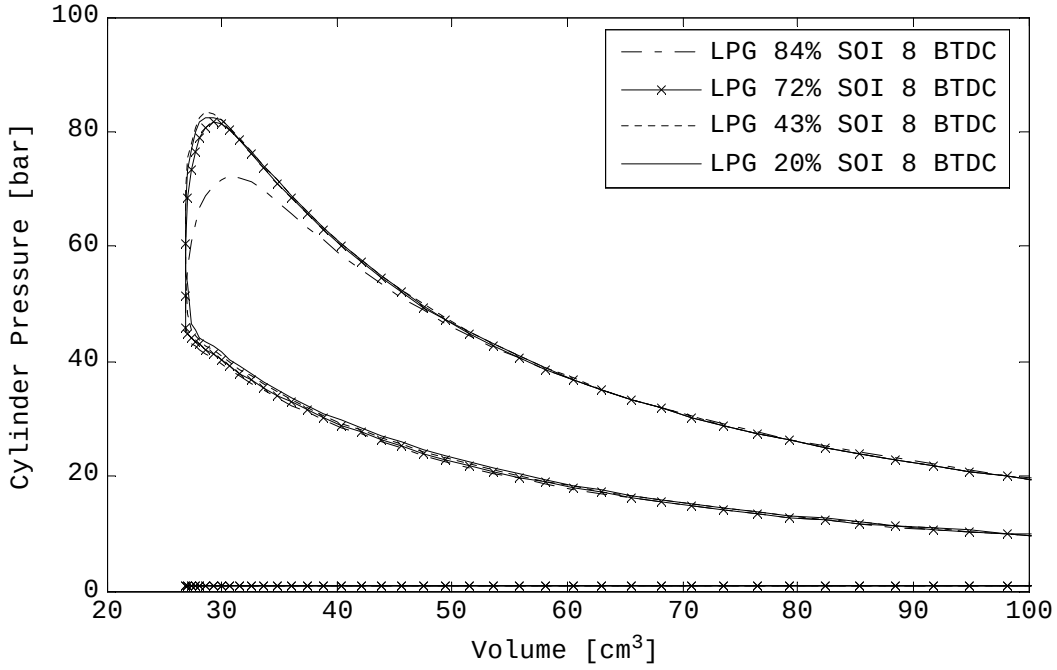

Figure 5.57 Effect of LPG percentage on PV diagram

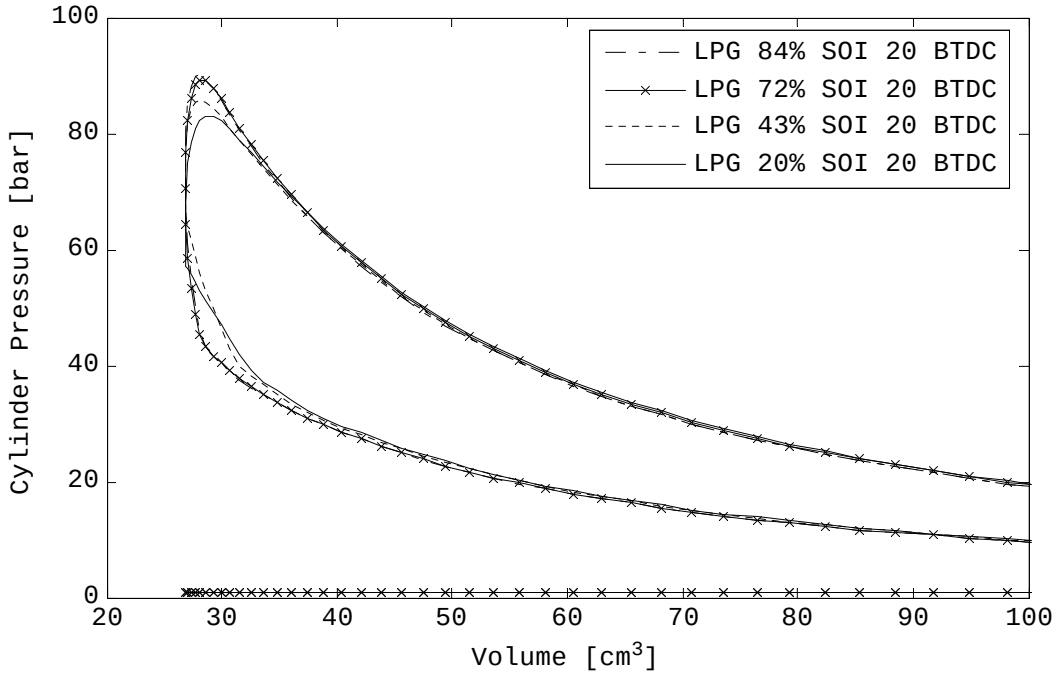

Figure 5.58 Effect of LPG percentage on PV diagram

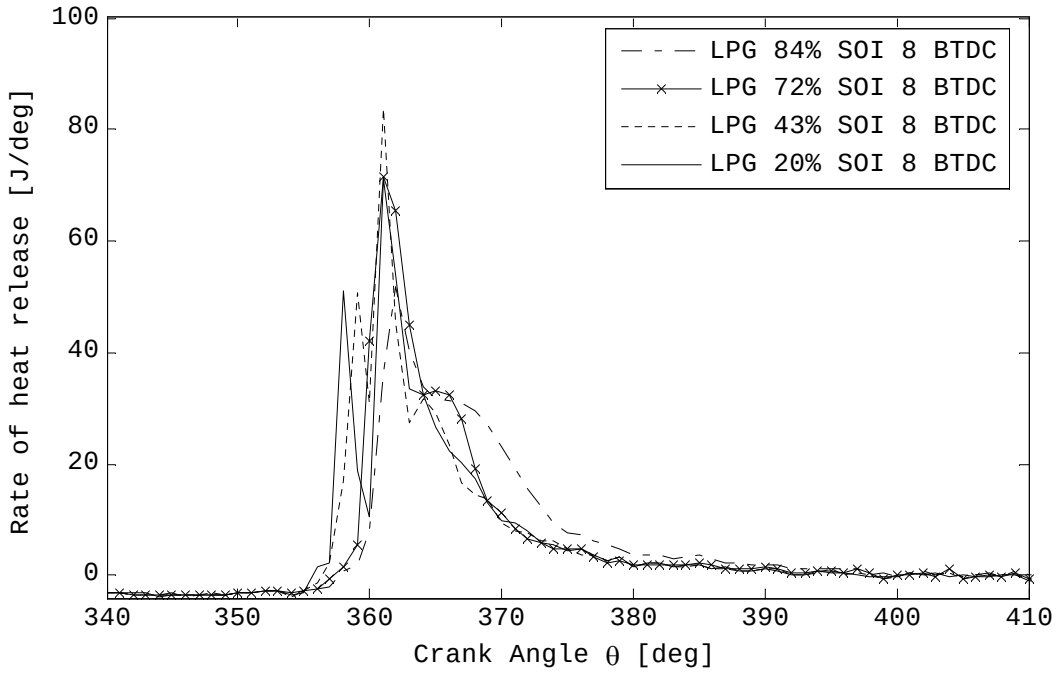

Figure 5.59 Effect of LPG percentage on ROHR

In Figure 5.59 the first peak of the heat release profile is the result of combustion of diesel and the second peak is mainly based on combustion of the premixture. The pilot ROHR peak moves towards and finally joins the ROHR of the premixture as the amount of LPG increases. However the ROHR from pilot combustion is still discernible. Therefore in the case of late pilot SOI, the ignition delay increases slightly as the quantity of LPG increases, resulting from a decrease in temperature of LPG premixture due to latent heat of evaporation. Interestingly, the highest ROHR occurs with 43% LPG. Since ROHR curve shows LPG combustion occurring after the diesel main ignition, a possible reason for the increased ROHR could be the combustion of diesel main injection occurring too early, immediately after the pilot ignition as a result of the increased ignition delay. Figure 5.61 shows MFB curves for various LPG concentrations with late pilot SOI. As the percentage of LPG increases the burning rates decrease after 50%CA.

The corresponding ROHR profiles for 20° SOI under dual fuel operation with various LPG percentages are shown in Figure 5.60. It is evident that the amount of injected LPG has a strong effect on diesel pilot SOC. Combustion delay is relatively small for low to medium LPG quantities but it increases markedly with higher LPG percentages. This is not unexpected because a higher amount of evaporating LPG results in a higher charge cooling. For 72% LPG percentage, diesel pilot, LPG and diesel main combust simultaneously. Therefore the ROHR characterised by a single peak and a reduced maximum value with substantially smooth slopes which is a good indication for smooth engine operation. When the maximum quantity of LPG is added there is a slight increase in burning rates at the early stages of combustion. This is probably due to the

increased mixture homogeneity due to the higher percentage of LPG which increases the premixed combustion phase. This is also indicated from the small increase on the ROHR peak value.

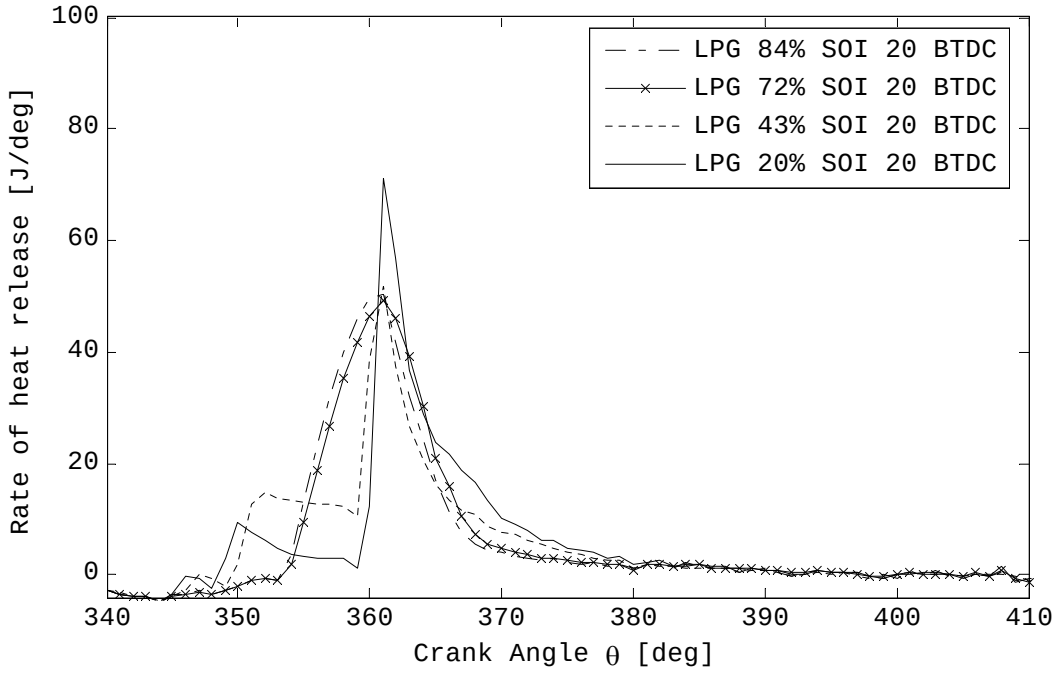

Figure 5.60 Effect of LPG percentage on ROHR

A reduced LPG percentage (below 43%) combined with an early SOI (20° BTDC), results to an uneven engine operation indicated by an increased COV (Table 5-24). This is due to a fairly complex sequence of combustion events: diesel pilot is injected in LPG premixture undergoing evaporation. Then LPG combustion starts almost at the same time with pilot ignition and continues after the end of pilot combustion. Subsequently main diesel is injected and there is another temperature drop caused from diesel injection evaporation. Then diesel main combustion initiates producing a high peak on ROHR increasing the global burning rates. LPG continues burning at a lower rate until the end of the combustion generating a longer ROHR tail.

Advancing the pilot SOI causes a separation of the above events. The ROHR of the intermediate LPG combustion stage between pilot and main diesel strongly depends on local stoichiometry which is determined by pilot SOI. When retarding pilot SOI the intermediate stage leans out due to the higher amount of oxygen which is already consumed from pilot combustion and therefore LPG burning rates increase when approaching stoichiometric conditions.

NOx emissions can be controlled using early SOI for higher quantities of LPG or late SOI with low to medium quantities. This gives the advantage to operate an engine under different fuel proportions.

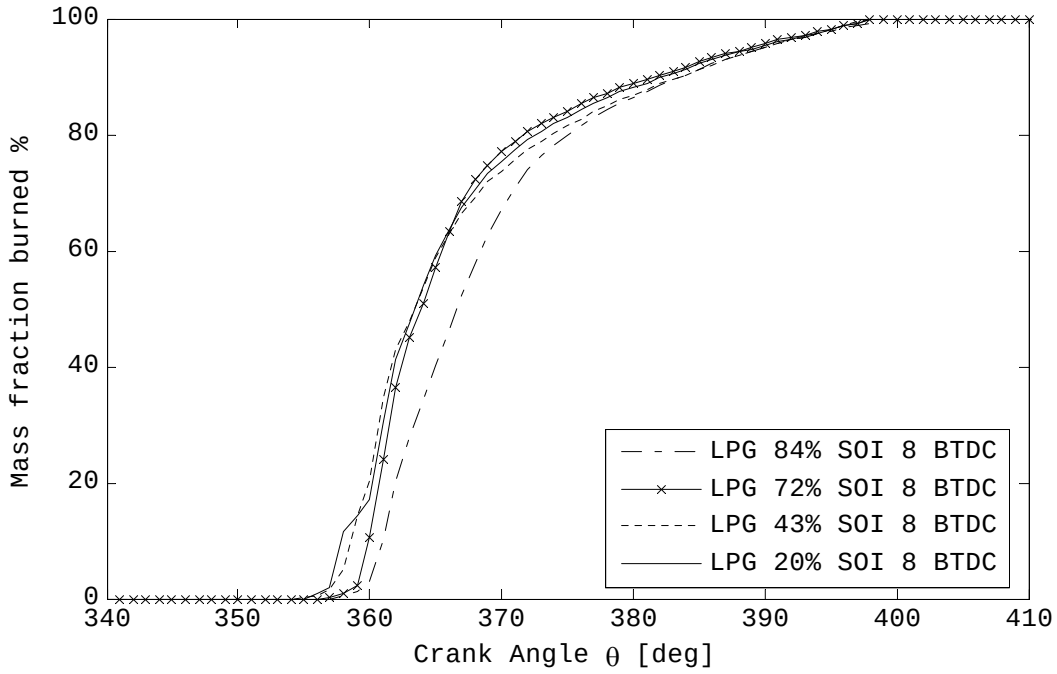

Figure 5.61 Effect of LPG percentage on MFB

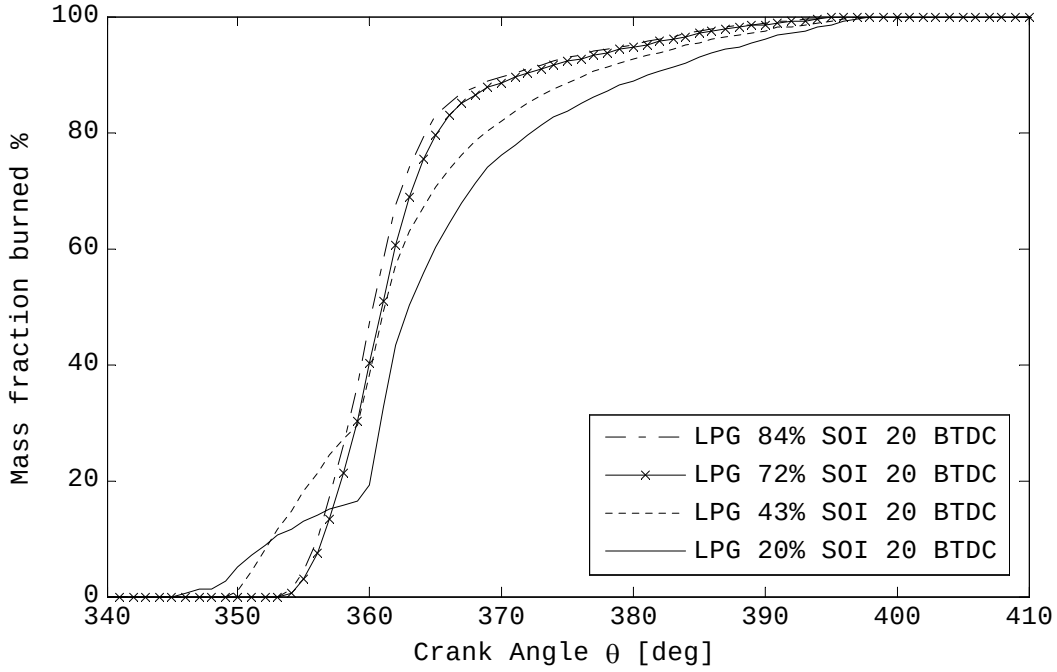

Figure 5.62 Effect of LPG percentage on MFB

LPG percentages (SOI 8 BTDC)	84%	72%	43%	20%	Diesel only
SOI [CA]	352	352	352	352	353
SOC [CA]	357	356	355	355	356
Combustion duration [deg]	45	43	44	44	42
Mass fraction burned 02% [deg]	2	3	2	2	2
Mass fraction burned 05% [deg]	3	3	3	2	2
Mass fraction burned 10% [deg]	4	4	4	3	4
Mass fraction burned 50% [deg]	10	7	8	8	7
Mass fraction burned 90% [deg]	27	24	28	27	25
Mass fraction burned 95% [deg]	33	31	34	34	32

Table 5-21 Effect of LPG percentage on MFB

LPG concentrations (SOI 20 BTDC)	84%	72%	43%	20%	Diesel only
SOI [CA]	340	340	340	340	353
SOC [CA]	353	353	349	345	356
Combustion duration [deg]	44	45	50	53	42
Mass fraction burned 02% [deg]	1	2	1	4	2
Mass fraction burned 05% [deg]	2	2	2	5	2
Mass fraction burned 10% [deg]	3	3	4	8	4
Mass fraction burned 50% [deg]	7	8	12	18	7
Mass fraction burned 90% [deg]	18	18	28	36	25
Mass fraction burned 95% [deg]	27	27	35	43	32

Table 5-22 MFB of various LPG percentages for late SOI

LPG percentages (SOI 8° BTDC)	84%	72%	43%	20%	Diesel only
IMEP [bar]	5.2	5.3	5.3	5.2	5.2
ISFC [g/KWh]	194	192	189	191	201
COV [%]	1.1	1.7	2.2	2.2	2.1
NOx [ppm]	-	-	-	-	1048
Visible smoke	No	No	No	No	No
Knock	No	No	No	No	No
η_t [%]	40	40	41	40	41.6
η_v [%]	84	83	82	82	83

Table 5-23 Effect of LPG percentage on engine performance

LPG percentages (SOI 20° BTDC)	84%	72%	43%	20%	Diesel only
IMEP [bar]	5.2	5.3	5.1	5.2	5.2
ISFC [g/KWh]	193	190	196	190	201
COV [%]	0.64	0.68	3.9	2.6	2.1
NOx [ppm]	-	-	-	-	1048
Visible smoke	No	No	No	No	No
Knock	No	No	No	No	No
η_t [%]	40	41	40	41	41.6
η_v [%]	84	84	82	82	83

Table 5-24 Effect of LPG percentages on engine performance

Volumetric efficiency

Figure 5.63 shows the effect of varying the injected amount of LPG on engine volumetric efficiency with early and late pilot SOI. Injecting more LPG, results to a positive increase in volumetric efficiency. This is due to the partial evaporation of the LPG in the inlet manifold causing a charge cooling effect. The trends are similar for both early and late pilot SOI. For an unthrottled diesel engine a 2% increase in volumetric efficiency is small enough to be considered important. However the importance of mentioning volumetric efficiency here is to signify the advantage of using injected LPG at liquid phase instead of fumigation.

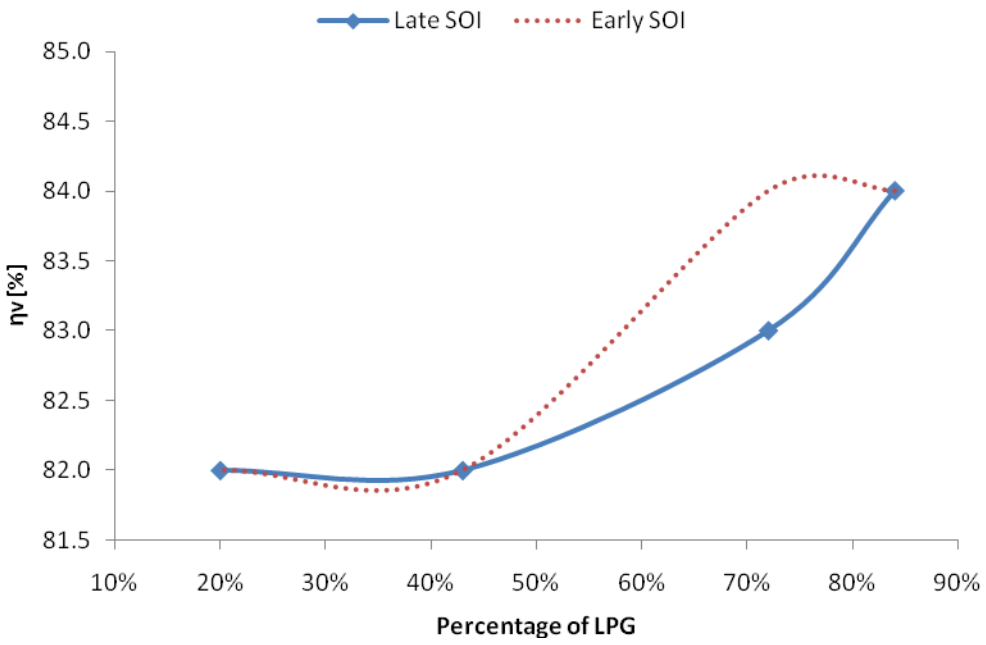

Figure 5.63 Effect of LPG percentage on engine volumetric efficiency

5.3.6 Stoichiometric dual fuel operation λ=1

This section demonstrates stoichiometric dual fuel operation. Diesel engines have been produced with indicated efficiencies approaching 46%. By way of contrast, the indicated efficiency of a typical SI engine is around 35% (Harrison, 2002). The main idea of pursuing this experiment was to demonstrate a method of achieving SI like operation on a high compression ratio diesel engine. This expected to extend the dual fuel operating envelope and also increase engine's thermal efficiency. This is an attempt to get much higher thermal efficiency from an LPG engine and also a way to diversify fuel type.

At the outset of the experimental work, operating the engine on dual fuel below λ=1.9 was generating heavy combustion noise due to the premixed combustion knock limitation. The common way to control the amount of combustion oxygen in SI engines is to restrict inlet air flow. Although a throttle body was already installed on the engine's inlet manifold, it was decided to use EGR to control the air flow. It was thought that using the readily available EGR system instead of a mechanical throttle, it would demonstrate a more realistic method of controlling air flow on diesel engines converted to run on dual fuel. Besides EGR can act as dilutant in order to reduce peak combustion temperatures and hence NOx which are expected to be high for LPG stoichiometric operation.

Replacing 22% of the intake charge with EGR, knock free dual fuel stoichiometric operation was achieved for two different LPG percentages: 80% and 92% respectively.

To achieve stoichiometric operation with only 80% LPG, the main diesel injection was enabled and it was split into two sub-injections in order to compensate the 12% quantiy of LPG. For 92% LPG only diesel pilot was necessary to aid ignition.

Operating parameters	**LPG 92%**	**LPG 80%**
Engine speed [RPM]	1000	1000
Pilot SOI [deg]	8 (BTDC)	8 (BTDC)
Pilot duration[μs]	95	95
LPG SOI[deg]	TDC (inlet start)	TDC (inlet start)
λ	1	1
Injection strategy	1pilot+LPG	1pilot+2 mains +LPG
EGR [%]	22%	22%

Table 5-25 Engine operating parameters for stoichiometric operation

Table 5-26 shows the effect of stoichiometric operation on dual fuel engine performance parameters. The first thing to notice is a significant increase in engine IMEP. It is already known that the torque output of an SI engine is maximum when the flame temperature is at maximum with dissociation, (λ≈0.9) (Harrison, 2002). Therefore the advantages of operating the engine close to stoichiometric are obvious from performance point of view.

Normally ISFC increases as $\lambda>1.1$ due to the effects of incomplete and abnormal combustion. For stoichiometric operation ISFC was reduced due to the increased cycle efficiency owing to the higher value of γ. Therefore fuel conversion efficiency increased by 3.2%.

Running the engine at stoichiometric with EGR resulted in a significantly smoother operation compared to that of diesel only operation. COV was always below 1 which is an indication of stable engine operation.

Increasing the LPG quantity from 80% to 92% resulted to a 7.5% increase in volumetric efficiency for dual fuel stoichiometric operation due to the higher charge cooling effect.

NOx emissions however were somewhat high for the 92% LPG dual fuel operation even with 22% EGR. It is known that when operating an engine at stoichiometric λ, the combustion temperatures are high (highest at $\lambda=0.9$). Therefore the presence of N_2 and O_2 molecules is likely leading to the formation of NOx according the Zeldovich mechanism. Notwithstanding this, the gain on IMEP from dual fuel stoichiometric operation is considerable even for a naturally aspirated single cylinder engine operating at 1000 RPM.

A better NOx -CO_2 balance than dual fuel operation with 92% LPG was achieved using 80% LPG with 20% diesel and 22% EGR. Table 5-26 shows a 58% reduction on NOx levels when LPG quantity is reduced to 80%. This is due to the lower combustion temperature which is the result of LPG combustion lean out (owing to the lower quantity of LPG) and also the result of the simultaneous increase of turbulence and diffusion conditions due to the double main diesel injection combustion. In addition there is a small charge cooling effect from diesel main injection evaporation which contributes on reducing peak combustion temperature in the combustion chamber.

Figure 5.64 shows the combustion pressure histories for stoichiometric operation. Using 92% LPG slightly retards the SOC. The pressure rise during compression is slightly lower than that of the 82% LPG, becoming more obvious near TDC. Due to the larger amount of LPG in the combustion, the charge cooling effect is higher. The same phenomenon increases the ignition delay by 1 degree for 92% LPG and therefore combustion duration which is obvious in the ROHR profiles in Figure 5.66. The ROHR profiles are very similar but the 82% LPG has a lower peak value which is directly associated with the reduced NOx levels.

Figure 5.65 the PV diagram shows a small work increase when 92% LPG is used. The better performance is the result of the better volumetric efficiency due to the charge cooling effect but also due to the increased burning rates of LPG combustion.

Dual fuel operation is clearly a better way to burn LPG than the usual spark ignited gaseous injection way even in a non-optimised engine. The significantly higher IMEP allows potential for engine downsizing.

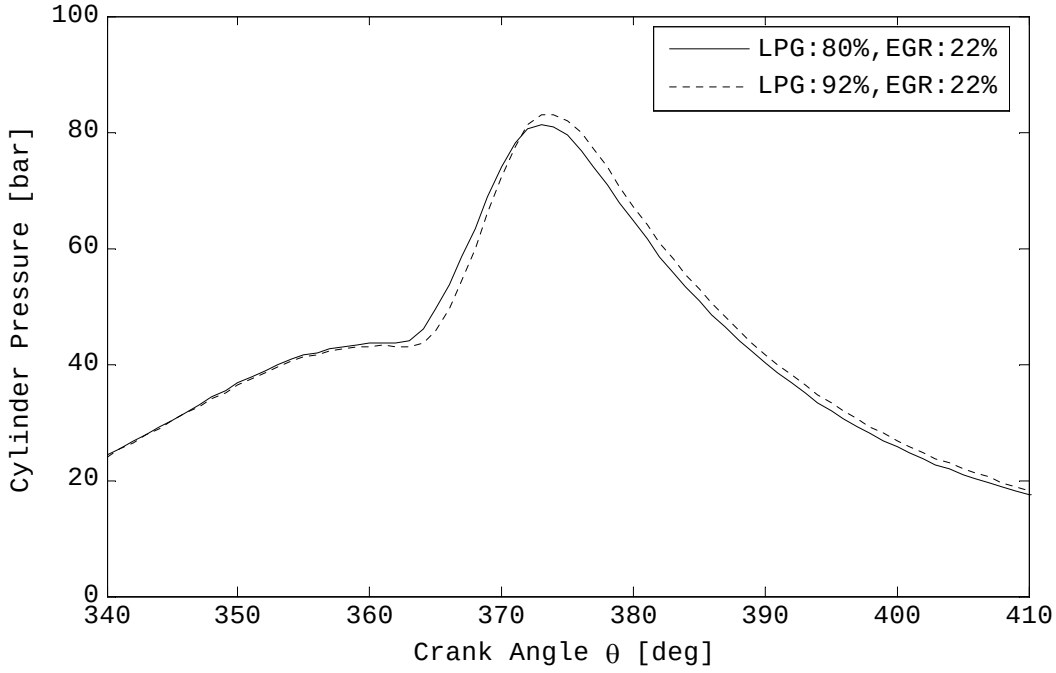

Figure 5.64 Dual fuel stoichiometric operation cylinder pressure histories

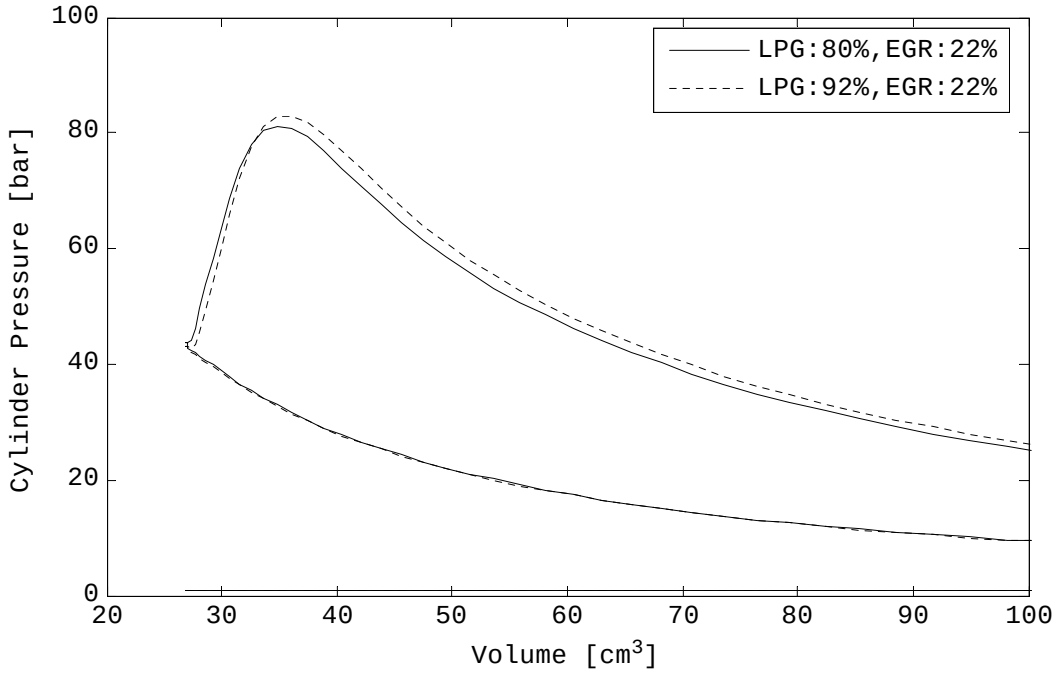

Figure 5.65 Dual fuel stoichiometric operation PV diagram

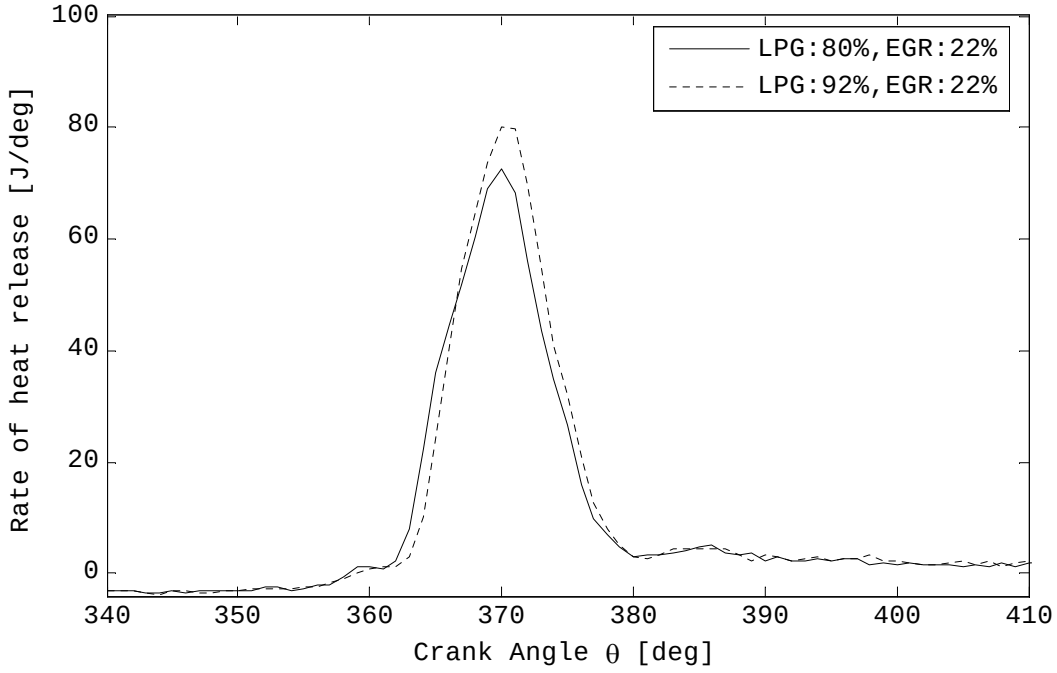

Figure 5.66 Dual fuel stoichiometric operation ROHR profiles

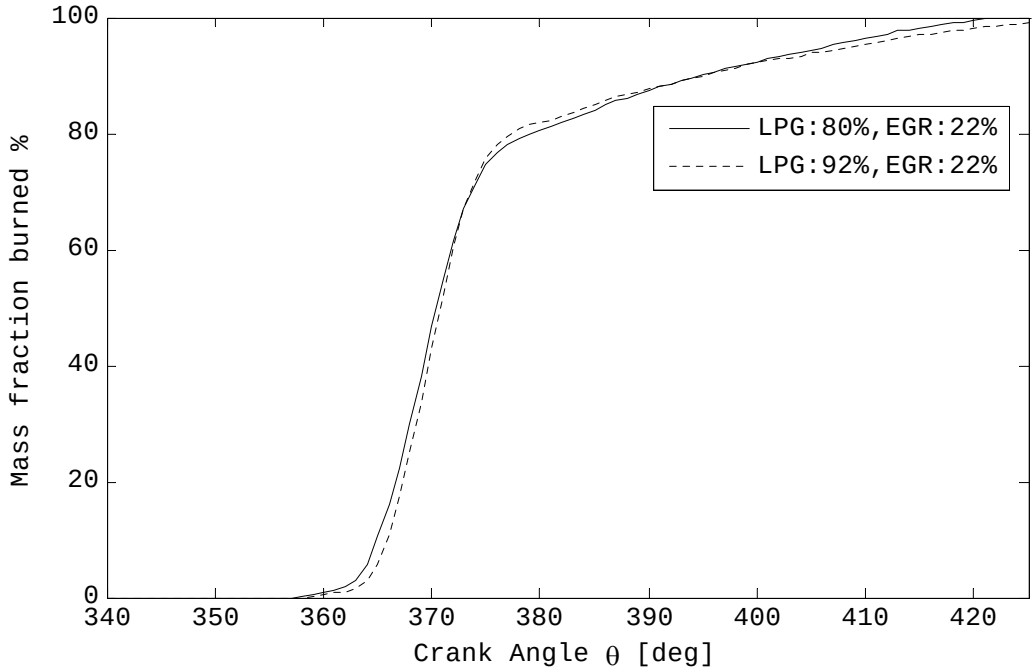

Figure 5.67 Dual fuel operation MFB curves

LPG percentage (λ=1, SOI 8 BTDC) **EGR percentage**	**92%** **22%**	**80%** **22%**
IMEP [bar]	8.8	8.2
ISFC [g/KWh]	179	179
COV [%]	0.65	0.5
NOx [ppm]	1024	433
Visible smoke	No	No
Knock	No	No
η_t [%]	43	43
η_v [%]	66	61

Table 5-26 Dual fuel stoichiometric operation performance

LPG percentage (λ=1, SOI 8 BTDC) **EGR percentage**	**92%** **22%**	**80%** **22%**
SOI [CA]	352	352
SOC [CA]	358	357
Combustion duration [deg]	72	65
Mass fraction burned 02% [deg]	5	5
Mass fraction burned 05% [deg]	7	7
Mass fraction burned 10% [deg]	8	8
Mass fraction burned 50% [deg]	13	13
Mass fraction burned 90% [deg]	37	38
Mass fraction burned 95% [deg]	51	49

Table 5-27 Dual fuel stoichiometric operation MFB rates

5.3.7 Part load operation

This section demonstrates throttle-less part load dual fuel operation. On diesel engines load is controlled by the amount of fuel injected and not by the intake throttle as with the gasoline engine. This un-throttled operation improves part load efficiency due to lower pumping loses.

Engine experiments were carried out in order to show the effects of lean dual fuel operation on engine performance and combustion. Table 5-30 shows the engine operating parameters for dual fuel part load condition. A fixed duration diesel pilot injection was used to provide ignition and the engine load was only controlled by varying the amount of injected LPG. Operating the engine with λ=2.5 resulted to 60% lower load than that of λ=1 operation. Subsequently pilot SOI was varied from 5 to 25 degrees before TDC whilst adjusting LPG fuelling, with the aim of demonstrating the effect of SOI for constant λ.

Operating parameters	
Engine speed [rpm]	1000
SOI pilot [deg]	variable
Pilot duration[μs]	95
λ	2.5
Injection pulses	1 pilot +78% LPG (all cases)
EGR rate	0%

Table 5-28 Engine operating parameters for dual fuel part load operation

Table 5-30 shows the effects of SOI on dual fuel engine various operating parameters for λ=2.5. Engine IMEP is 60% lower than the IMEP for stoichiometric operation. The small variation is mainly due to the continuous LPG adjustment at every SOI in order to maintain λ. ISFC has increased at part load operation. This is the result of the leaner mixture reducing the flame temperature of LPG and consequently lowering the flame speed. Due to the lower flame speed of the premixture, there is an increased tendency to combustion abnormality which is evident on the increased COV. Notwithstanding this, the average fuel conversion efficiency for dual fuel operation at part load is 34% which is near the best thermal efficiency of a typical gasoline engine

NOx emissions measured for 9, 15 and 21 pilot SOI are very low at part load due to the reduced combustion temperatures showing a tendency to increase whilst retarding pilot SOI.

Figure 5.72 and Figure 5.73 show the ROHR profiles and Figure 5.74 and Figure 5.75 the burning rate curves for dual fuel part load operation. The start of the combustion is shifted and the ignition delay is almost constant when SOI is advanced from 5 to 15 degrees before TDC. The combustion duration is also constant with small fluctuations within this region.

Ignition delay increased significantly when SOI was advanced beyond 15 degrees but without shifting the start of the combustion. Combustion duration and COV increase markedly at 25 SOI due to the abnormal combustion.

The best engine operation is achieved when SOI is between 17-19 degrees BTDC. IMEP increased whilst ISFC reduced resulting to higher fuel conversion efficiency. The main reason is the higher burning rates.

An early pilot injection increased the ignition delay but reduces ROHR .

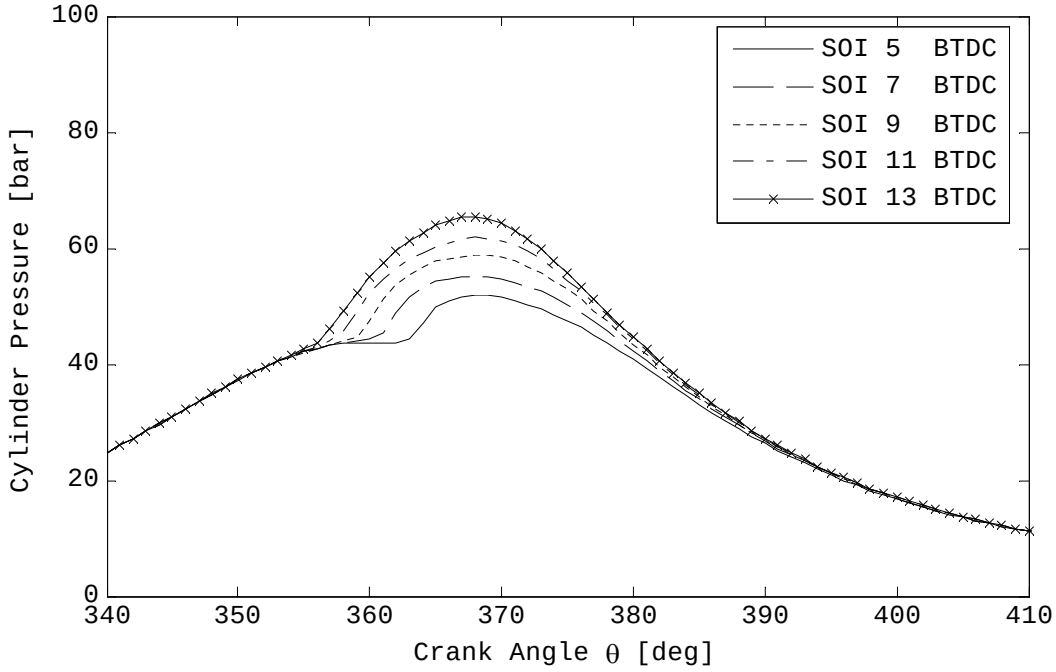

Figure 5.68 Dual fuel part load cylinder pressure histories

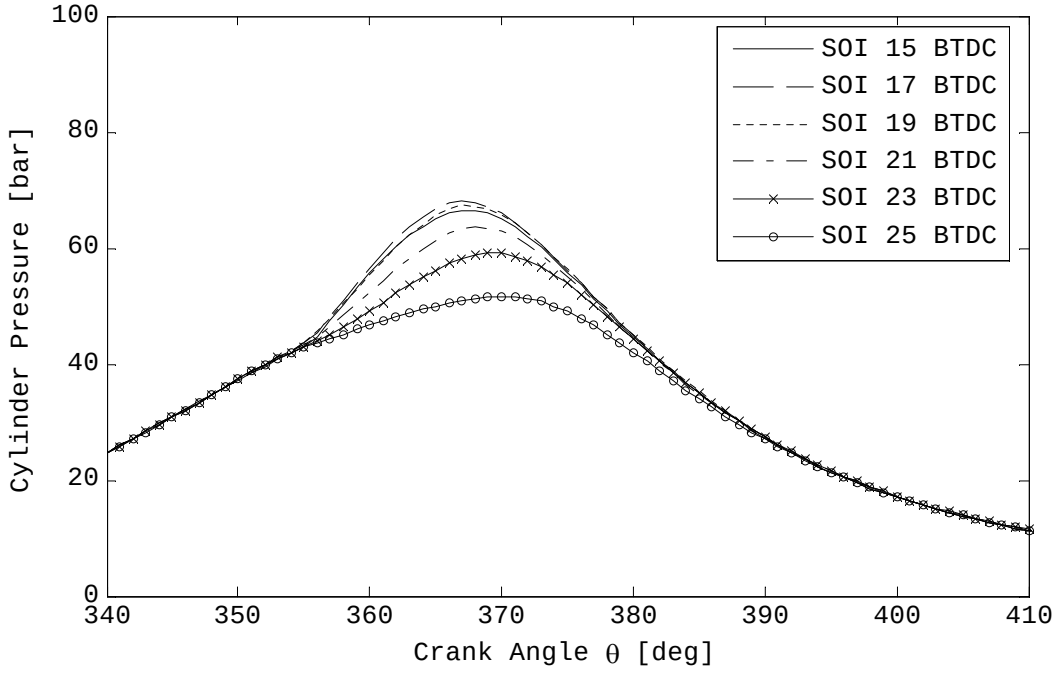

Figure 5.69 Dual fuel part load cylinder pressure histories

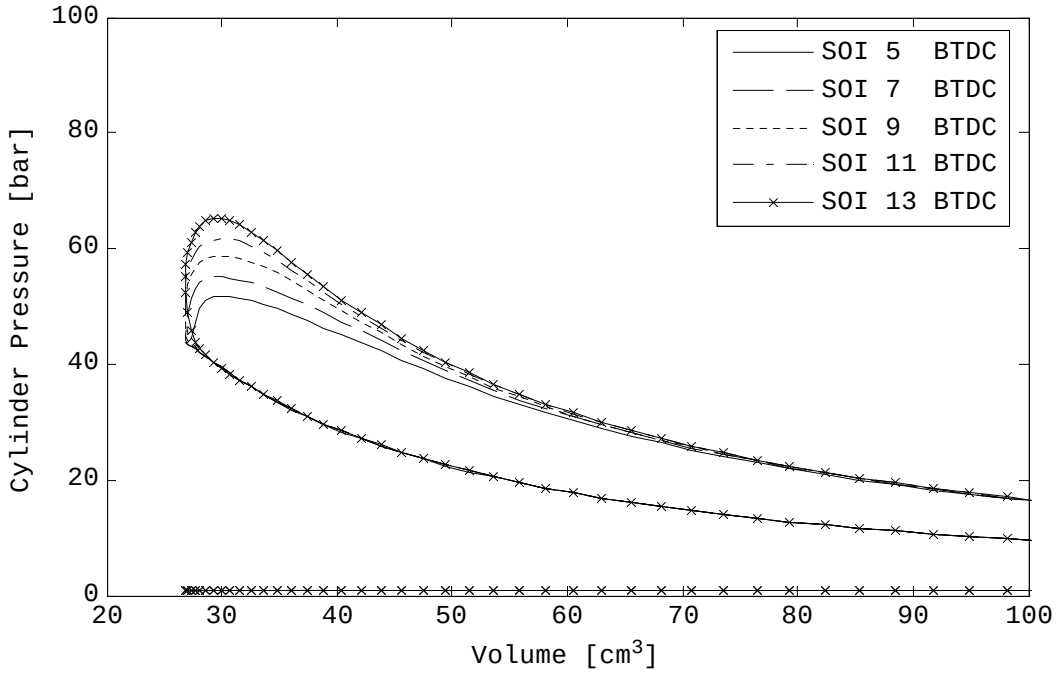

Figure 5.70 Dual fuel part load PV diagrams

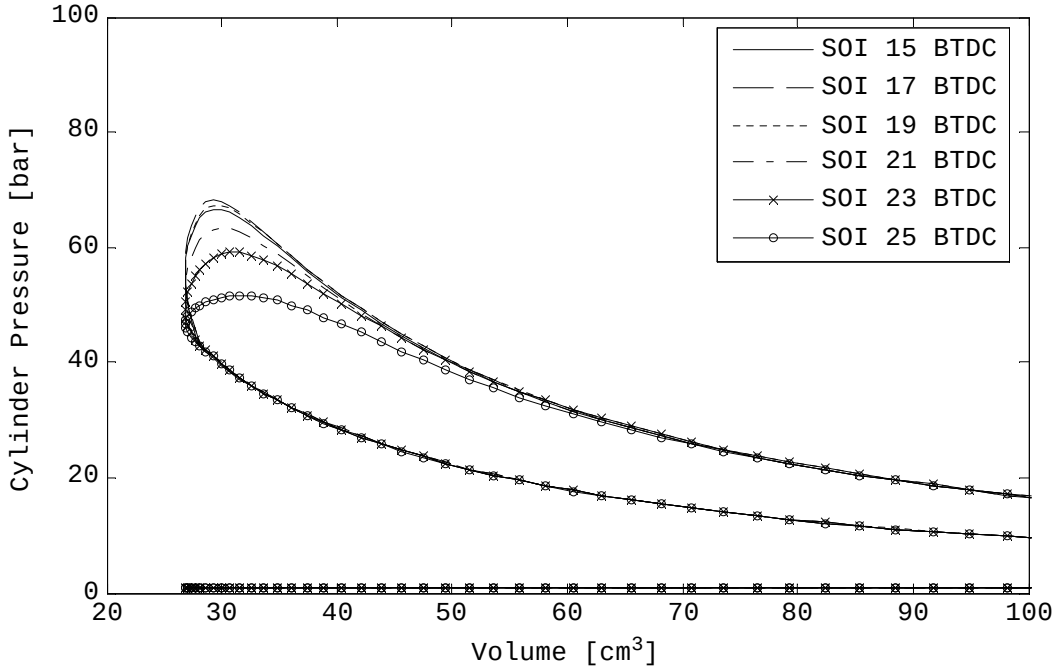

Figure 5.71 Dual fuel part load PV diagrams

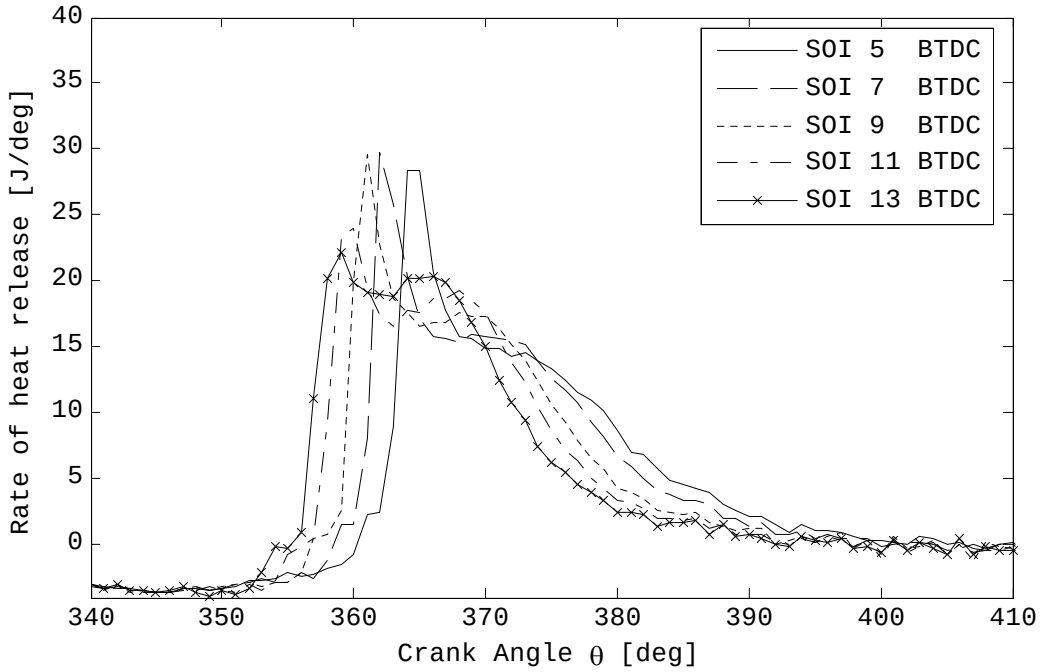

Figure 5.72 Dual fuel part load ROHR profiles

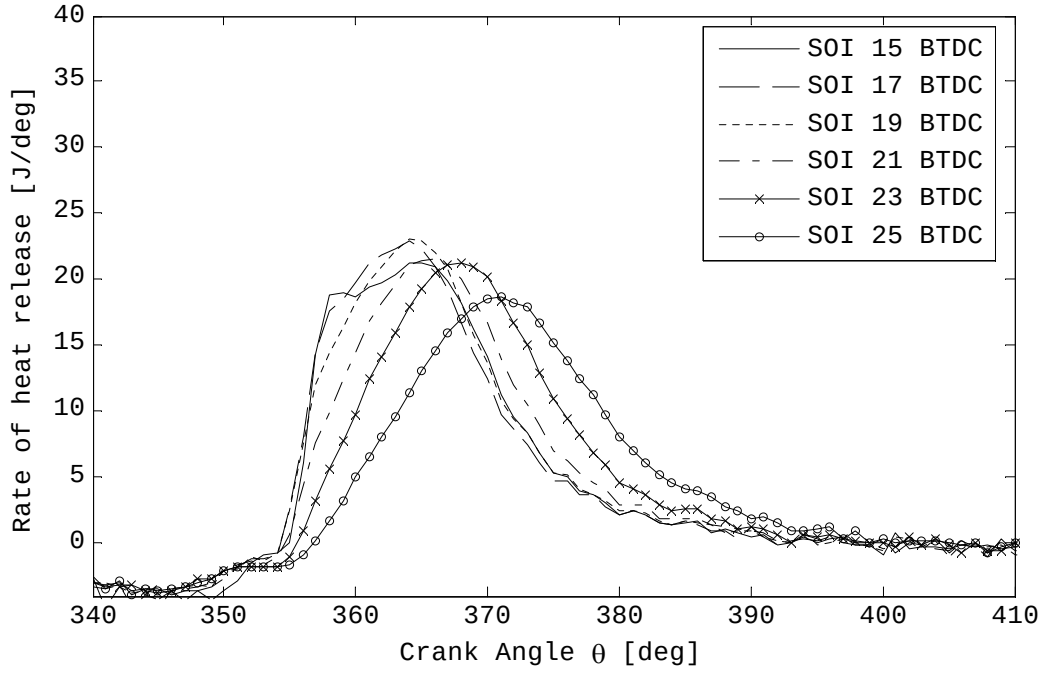

Figure 5.73 Dual fuel part load ROHR profiles

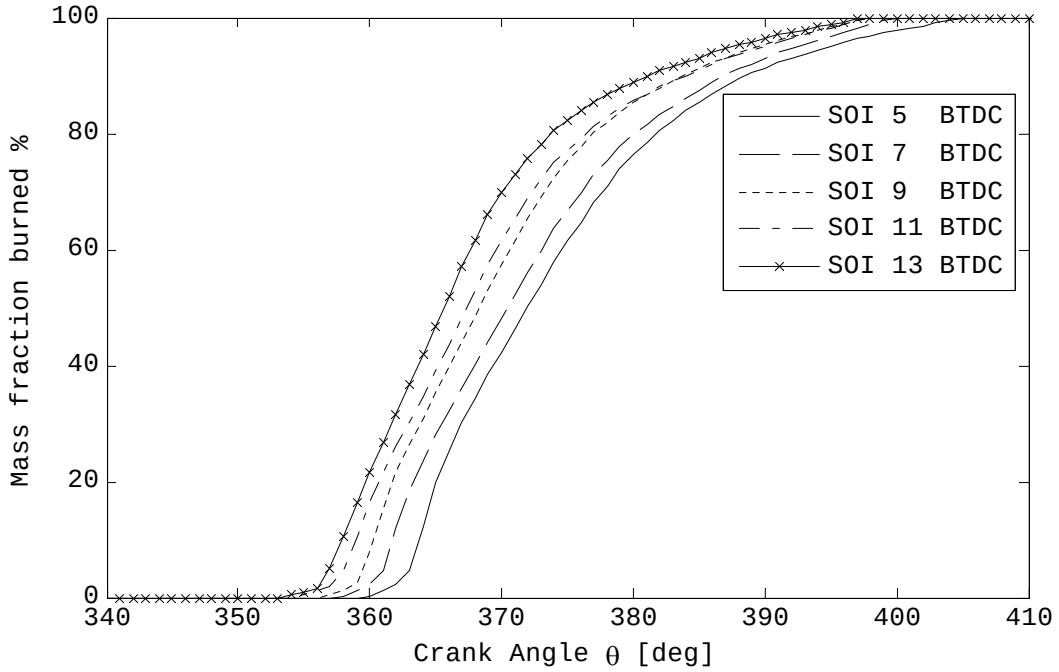

Figure 5.74 Dual fuel part load MFB curves

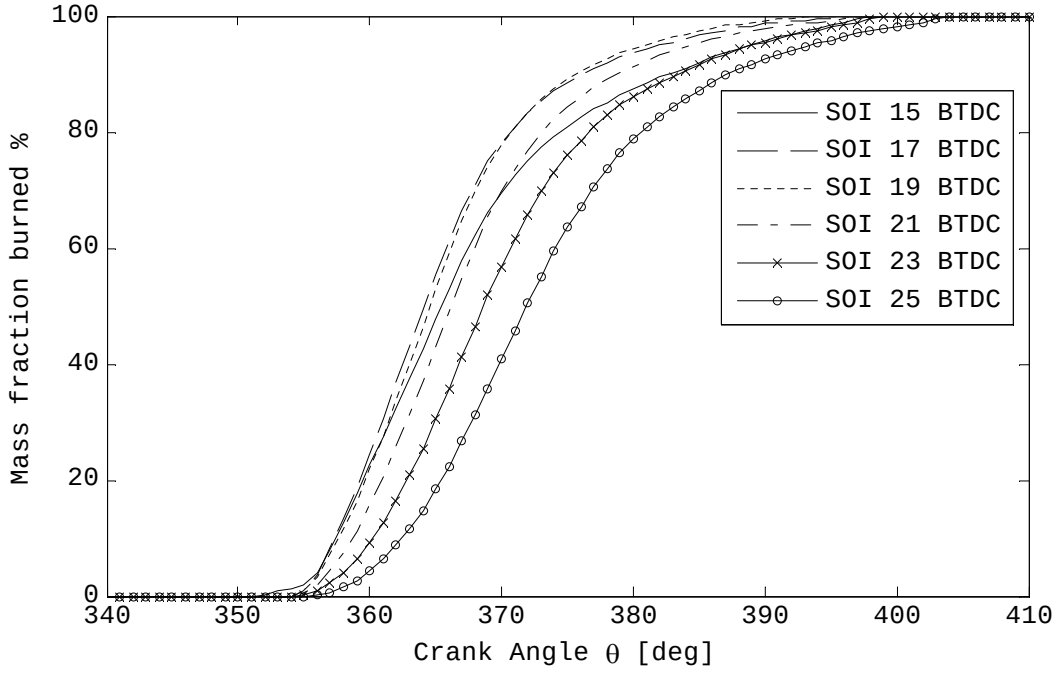

Figure 5.75 Dual fuel part load MFB curves

SOI CA (BTDC)	5	7	9	11	13	15	17	19	21	23	25
SOI [CA]	355	353	351	349	347	345	343	341	339	337	335
SOC [CA]	359	357	356	354	353	351	354	354	354	354	355
Comb duration [deg]	46	43	42	44	45	47	44	41	45	46	50
Mass fraction burned 02%	3	3	3	3	3	4	1	1	2	3	3
Mass fraction burned 05%	4	4	3	4	4	5	2	2	3	4	5
Mass fraction burned 10%	5	5	4	5	5	6	3	4	5	6	7
Mass fraction burned 50%	13	13	12	13	13	14	10	11	12	15	17
Mass fraction burned 90%	30	30	28	30	28	32	22	22	25	29	32
Mass fraction burned 95%	36	35	33	36	35	38	28	27	31	35	39

Table 5-29 Effect of pilot SOI on par load dual fuel operation

SOI CA (BTDC)	5	7	9	11	13	15	17	19	21	23	25
IMEP [bar]	3.2	3.4	3.5	3.6	3.7	3.7	3.8	3.8	3.7	3.7	3.4
ISFC [g/KWh]	250	239	232	225	220	218	216	214	221	221	239
COV [%]	3.6	3.9	3	2.1	2.2	2.8	2.9	2.9	3.2	4.7	7.3
NOx [ppm]			130			128			122		
Visible smoke	no	no	no	no	no	no	no	no	no	no	no
Knock	no	no	no	no	no	no	no	no	no	no	no
η_t [%]	31	32	33	34	35	35	36	36	35	35	32
η_v [%]	85	85	85	85	85	85	85	85	85	85	85

Table 5-30 Part load dual fuel operation performance parameter

6 CONCLUSIONS

Thesis Main contributions

An efficient dual fuel engine operating on a unique combination of high pressure diesel and liquid phase propane that is highly controllable was developed.

Engine experiments showed that diesel pilot injection can be used to ignite a larger amount of premixed LPG on a high compression ratio diesel engine and also that it can be highly controllable.

Diesel operation

- A pilot injection results in an increase of thermodynamic conditions within the combustion chamber. Pilot injection significantly minimises combustion noise by reducing the amount of fuel injected during the diesel combustion delay period. This effectively reduces the premixed combustion duration from which combustion knock is generated.

- Apart from reducing combustion noise, pilot injection helps reducing NOx by lowering combustion peak temperatures and also improves significantly the engine's cold start capability.

- Supplying up to 90 Volts to the injector solenoid for the first 20μs of the pilot energising time enables rapid solenoid operation. This boost voltage significantly reduces pilot injection duration and improves injection repetition.

- The minimum dwell time between pilot and main is limited by the injector hydraulic and electric solenoid performance. Therefore a long duration pilot strategy is more common for solenoid injectors fitted on high speed engines where opening and closing response becomes an issue particularly at high engine speeds. However, long duration pilots are likely to increase engine BSFC due to the inevitably higher amount of heat release occurring before TDC. On the other hand using short pilot durations combined with short dwell times, precise combustion control can be achieved but at the same time good shot-to-shot injection stability is limited by the injector solenoid and needle design.

- On in-production engines using solenoid injectors the dwell times between consecutive injections cannot be reduced below a minimum threshold because of

electronic/hydraulic response time. With the advent of the new piezoelectric injectors this limitation can be stretched.

- Below certain pilot duration, the fuel injected quantity is too small to influence the main combustion and combustion noise starts. On the other hand a long pilot duration results to similar high noise levels as a single main injection and this would additionally increase engine BSFC

- The start of combustion (SOC) is directly depended to SOI timing. Advancing the SOI increases the combustion duration whilst retarding SOI increases the combustion burning rates which increases engine's thermal efficiency.

- Splitting the main injection, the rate of injection can be precisely controlled leading to a more progressive combustion. This results to a lower rate of heat release which consequently reduces combustion temperatures and therefore NOx.

- By using split injection the fuel is less likely to penetrate against the cylinder wall and more likely to settle in the within the piston bowl. This would result in lower HC emissions.

- Using a variable injector nozzle, the injection rate control would be possible but this technology is not yet available at the time.

- EGR increases ignition delay and shifts the location of the start of the combustion due to the dilution effect. The longer ignition delay causes more fuel to burn in the premixed phase resulting to a slightly higher ROHR. Despite this small increase in ROHR, NOx is still low due to the EGR flow reducing the peak combustion temperature.

- Combining EGR with split injection can significantly reduce NOx emissions. Split injection can be used to control the number of premixed-phase combustion events whilst EGR to control the duration of premixed phase.

Dual fuel operation

- The diesel pilot ignition concept was explored and the results show that it is probably the best method to provide ignition of LPG on a high compression ratio engines. There are two main reasons for this. First, the majority of modern diesel engines use common rail systems and therefore diesel pilot is readily available.

Second, if a conventional automotive spark ignition system is to be used, more than 50 KV will be required to generate spark across the electrodes for an average turbocharged diesel engine due to its high compression pressures. Although this can be solved by using stronger ignition coils, the higher brake up voltage across the electrodes causes sparkplug fouling and premature failure. This is also a current problem concerning the highly boosted downsized engines which needs further development.

- The ignition delay of dual fuel engine is longer than that of diesel, mainly due to the LPG charge cooling effect reducing the in cylinder temperature. Owing to the larger latent heat of vaporization LPG evaporates rapidly causing a great in-cylinder temperature drop and thus extends pilot ignition delay. The higher the amount of injected LPG the longer the ignition delay.

- An early pilot SOI increases the ignition delay leading to engine misfire due to diesel pilot dilution on LPG. This is due to the longer residence of injected pilot into the cooled LPG charge before autoignition conditions occur in the combustion chamber.

- Engine misfire when retarding the pilot SOI is the result of excessive in-cylinder temperature drop from the late LPG charge evaporation. This indicates that under normal operation, charge cooling effect continues during combustion.

- Dual fuel operation experimental results showed that the amount of injected LPG has a strong effect on diesel pilot SOC. Combustion delay is relatively small for low to medium LPG quantities but it increases markedly with higher LPG percentages. Therefore the charge cooling effect increases with the amount of LPG injected.

- Results readily show that the injection timing has a significant effect on the cycle pressure time history and the hence on the combustion performance of the engine. It is reassuring to note that the engine operating under the diesel pilot ignition concept can be readily controlled using injection timing alone.

- Although pilot injection is properly injected through each hole over the cylinder peripheral, spray fluctuation becomes larger than that seen in conventional diesel engines due to a small amount of injection.

- Dual fuel stoichiometric operation with 92% LPG can be achieved on a throttle-less dCi engine using EGR. Better results can be achieved if EGR is combined with diesel spit injection. This can increase engine toque at low engine speeds.

- Stoichiometric dual fuel operation is clearly a better way to burn LPG than the usual spark ignited gaseous injection way even in a non-optimised engine. The significantly higher IMEP allows potential for engine downsizing.

- At part load the dual fuel ISFC is higher than that of diesel. This is the result of the leaner mixture reducing the flame temperature of LPG and consequently lowering the flame speed. Due to the lower flame speed of the premixture, there is also an increased tendency to combustion abnormality. Part load operation can be improved by increasing diesel pilot injection.

7 RECOMENDATIONS-FUTURE WORK

Combustion Visualisation techniques are used very often to investigate combustion phenomena. The combustion visualisation involves mainly high-speed photography of the combustion process. Combining the analysis of cylinder pressure data with combustion photographs helps to establish a better descriptive model of the compression-ignition process.

At the outset of this thesis, it was decided to develop an endoscope based imaging system to perform direct combustion photography. The main motivation was to correlate combustion images with heat release profiles in order get a better understanding on the ignition of the premixture form a diesel pilot injection delivered from a multihole injector.

A flexible boresope was obtained and a light source was constructed. This particular borescosope consist of an optical fibre inside flexible plastic cable and an image eyepiece focusing lens set Figure 7.1 . Inside the flexible cable there is the core fibre which transits the image surrounded by a bundle of other optical fibres which used to transmit light for illumination purposes. The diameter of the optical fiber is 1.5 mm. The borescope can be used for direct viewing or it can be attached to a camera by the means of a special adaptor.

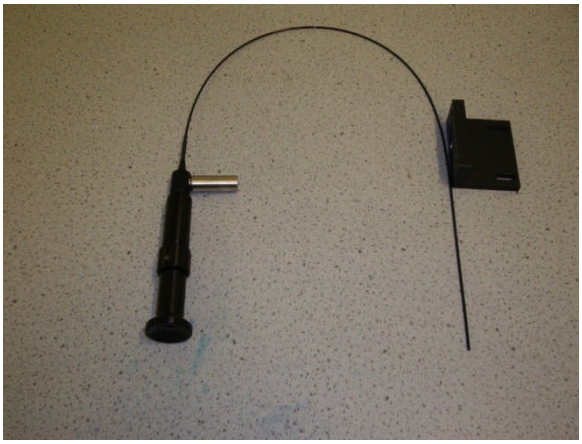

Figure 7.1 Flexible borescope

Provision was made on the new cylinder head to accommodate the borescope. A special dummy plug was fabricated to replace the borescope when it is not used. Also a method of cooling the borescope tip was proposed and designed.

The end

REFERENCES

A Helmantel, J. S. (2003). Visualization of the effects of post injection and swirl on the combsution process of a passenger car common rail DI diesel engine. *ASME* .

Adatia, A. (2006). *Experimental Investigation of Diesel HCCI Using a Ricardo E6 Single Cylinder Engine* . Cranfield University.

Agarwal, A., & Assanis, D. (2000). Multidimensional modeling of ignition, combustion and Nitric oxides formation in direct injection natural gas engine. *SAE* .

Amorese, C., De Matthaeis, S., De Mitchele, O., & Satriano, A. The gaseous fuel option: LPG and CNG. *Proceedings of international conference on Vehicle alternative fuels and environmental protection.* Doublin: 2004.

Atlantic Consulting (2009). LPG Carbon Footprint Relative to Other Fuels. A Scientific Review. Retrieved October 2009 form http://www.exceptionalenergy.com.

Bauer, H. (2004). *Diesel-Engine Management.* Plochingen: Robert Bosch GmbH.

Bilcan, A, Le Corre, O, Tazerout, M, Ramesh, A, Ganesan, S. Characterization of the LPG-diesel, dual-fuel combustion. *SAE Technical Paper Series, 2001-28-0036.* 2001.

Boisen, P. (July 2002). Pathways to alternative fuels into future. *Proceedings of international conference on vehicle alternative fuels and environmental protection.* The Netherlands.

Bosch, R. (2002). *Diesel engine management 2nd edition.* SAE inernational.

Boyer. (1949). Status of dual fuel engine development. *SAE 296* .

Campbell, A. S. (1979). *Thermodynamic Analysis of Combustion Engines.* New York Chichester Brisbane Torondo: John Wiley & Sons.

Challen, B., & Baranescu, R. (1999). *Diesel engine reference book second edition.* Butterworth.

Chen, Z , Konno, M, Goto, S. Study on homogenous premixed charge CI engine fuelled with LPG. *JSAE Review, v 22, n 3, p 265-270.* 2001.

Crouse, W. (1970). *Automotive Engine Design.* McGraw-Hill.

Epping, K., Aceves, S., Bechtold, R., & Dec, J. (2002). The potential of HCCI combsution for high efficiecy and low emissions. *SAE* .

Gokhale, R. (2004). Hybrid technology: future of automobiles. *Proceeding of international conference on vehicle alternative fuels and environmental protection.*

Greenhalgh, D. (2002, March). Combustion in piston engines. *Cranfield Automotive MSc course* . Cranfield.

Gunner, R. (2006). Injector control unit design. *R2G2 Controls Ltd* . Cranfield Bedfordhsire.

Harrison, M. F. (2002). Engine thermofluids Volume 3 Page 9. *Notes to accompany the MSc course* . Cranfield University.

Heywood, J. B. (1988). *Internal Combustion Engine Fundamentals.* United States: McGraw-Hill.

Hitache, C. (2006). *MSc Thesis 'Experimental Investigation of Diesel HCCI using a Ricardo E6 Single cylinder engine'.* Bedfordshire: Cranfield University.

Ishida, M., Tagai, T., Ueki, H., & Sakaguchi, D. (2004). Comparison of combustion characteristics between natural gas and methanol in a dual fuel diesel engine . *Proceedings of international conference on vehicle alternative fuels and environmetal protection.*

Ishida, M., Ueki, H., Sakaguchi, D., & Imaji. (2004). Simultaneous reduction on NOx and Smoke by port injection of methanol/water blend in a DI diesel engine. *Proceedings of 15th international combustion engine symposim (international) paper N09935202.*

J.Shao, Y. (2002). Digital imaging based analysis and characterisation of diesel sprays. *Fuel injection systems.* One birdcage walk, westminster, London: IMECHE.

Jermy, M., Harrison, M., Vuorenkoski, A., Kaparis, E., & Macarthney, M. (2004). Overcoming power loss in LPG/Propane and CNG conversions of vehicle engines. *Proceedings of international conference on vehicle alternative fuels and environmetal protection.*

Kajitani, S., Chen, Z., Kommo, M., & Rhee, K. (1997). Engine performance and exhaust characteristics of DI diesel engine oerated with DME. *SAE* .

Ladommatos, N., & Zhao, H. (2001). *Engine Combustion instrumentation and diagnostics.* US: SAE International.

Lilly, L. (1986). *Diesel engines Reference Book.* London: Butterworths.

Mitsubushi. (2003, April). *Mitsubishi motors*. Retrieved 2003, from www.mitsubishi-motors.co.jp

N. Ladommatos, S. .. (1998). Effects of EGR on heat release in diesel combustion. *SAE* .

Plynt, M., & Martyr, A. (1999). *Engine Testing* (Second ed.). Butterworth Heineman.

Rassweiler, G., & Withrow, L. (1938). Motion Pictures of Engine Flames Correlated with Pressure Cards. *SAE Journal transactions volume 42 paper no 5* , 185-204.

Ricardo. (2002, April). *Diesel passenger car and light commercial vehicle markets in Western Europe.* Retrieved April 2003, from Ricardo: http://www.ricardo.com

Ricardo, H. R. (1968). *The High-Speed Internal Combustion Engine.* London & Glasgow: Blackie & Son Limited.

Richard Ehleskog, R. L. (2007). Effect of Multiple Injections on Engine-out Emissions Levels Including Particulate Mass from an HSDI Diesel Engine. *SAE* .

Robert Bosch GmbH. (2001). *Bosch Sensors.* Robert Bosch GmbH Automotive Aftermarket.

Stone, R. (1999). *Introduction to internal combsution engines 3rd edition.* Macmillan Press Ltd.

Stone, R. Armitage, I. (1987). *Comparison of methods for the calculation of mass fraction burnt from engine pressure time diagrams.* Proc. Inst. Mech. Engrs. Volume 201, Part D

Sugiyama, K, Kajiwara, M, Iwami, M, Mori, M, Oguma, M, Kinoshita, K, Goto, S. *Performance and emissions of a DI diesel engine operated with LPG and cetane-enhancing additives*. SAE Technical Paper Series, 2003-01-1920. 2003.

Taylor. (1999). *The internal combsution engine in theory and practice volume two.* 1999: The MIT press.

Theodoridis, E. (2003). *Diesel/LPG Combustion Studies.* Mechanical Engineering. Cranfield: Cranfield University.

vcacarfueldata. (2003, 03 25). Retrieved from vcacarfueldata: http://www.vcacarfueldata.org.uk

Vouorenkoski, A. K. (2004). *Development of a Liquid Phase LPG MPI Conversion System.* Cranfield: Cranfield University.

www.transportenergy.org.uk. (2004). Retrieved from www.transportenergy.org.uk: www.transportenergy.org.uk

APPENDIX